Systematic interaction mapping reveals novel modifiers of neurodegenerative disease processes

D i s s e r t a t i o n

zur Erlangung des akademischen Grades

d o c t o r r e r u m n a t u r a l i u m

(Dr. rer. nat.)

im Fach Biologie

eingereicht an der

Mathematisch-Naturwissenschaftlichen Fakultät I

der Humboldt-Universität zu Berlin

von

M.Sc. Jenny Russ

Präsident der Humboldt-Universität zu Berlin

Prof. Dr. Jan-Hendrik Olbertz

Dekan der Mathematisch-Naturwissenschaftlichen Fakultät I

Prof. Stefan Hecht, Ph.D.

Gutachter/in: 1. Prof. Dr. Hanspeter Herzel

2. Prof. Dr. Erich Wanker

3. Prof. Dr. Thomas Sommer

Tag der mündlichen Prüfung: 12. September 2012

Abstract

Neurodegenerative diseases (NDs) such as Alzheimer's disease (AD), Parkinson's disease (PD) or amyotrophic lateral sclerosis (ALS) are progressive brain disorders characterized by the accumulation of insoluble protein aggregates in neuronal cells or the extracellular space of patient brains.

To elucidate potential common pathological mechanisms in different NDs, I created comprehensive interaction networks for various known and predicted neurodegenerative disease proteins (NDPs). I identified 18,663 protein-protein interactions (PPIs) for 449 bioinformatically selected wild-type target proteins and 22 mutant variants of 11 known NDPs by using an automated yeast two-hybrid (Y2H) system. The functional analysis of the interaction partners of corresponding wild-type and mutant NDPs revealed strong differences in the case of all 11 NDPs and especially for the ALS protein TDP-43. The identified PPIs were used to generate networks for individual NDs such as AD or PD and to identify proteins that are connected to multiple NDPs. For example, I found that five neurodegenerative diseases are connected by four proteins (APP, ZMAT2, ZNF179 and IQSEC1) that link known NDPs such as huntingtin, TDP-43, parkin, ataxin-1 and SOD1. Analysis of publicly available gene expression data suggested that the mRNA expression of the four proteins is abnormally altered in brains of ND patients. Moreover, the knock-down of IQSEC1, ZNF179 or ZMAT2 aggravates pathogenic disease mechanisms such as aggregation of mutant huntingtin or TDP-43 as well as hyperphosphorylation of tau. Additionally, I identified 22 modifiers of TDP-43 aggregation, which are members in 7 protein complexes. These complexes were predicted based on combined data from PPI as well as siRNA screenings. Finally, I found that the proteins HDAC1, pRB, HP1, BRG1 and c-MYC, which form one of the predicted complexes, influence TDP-43 aggregation by altering its mRNA expression.

Keywords: neurodegenerative diseases, protein-protein interactions, modifiers, aggregation, toxicity, TDP-43

Zusammenfassung

Neurodegenerative Erkrankungen (NDs) wie Alzheimer (AD), Parkinson (PD), und amyotrophe lateral Sklerose (ALS) sind Hirnerkrankungen, die durch unlösliche Proteinaggregate in Neuronen oder im Extrazellularraum charakterisiert sind.

In dieser Arbeit habe ich für verschiede bekannte und vorhergesagte neurodegenerative Krankheitsproteine (NDPs) Proteininteraktionsnetzwerke erstellt, um mögliche gemeinsame Krankheitsmechanismen genauer zu studieren. Mit Hilfe eines automatisierten Hefe-Zwei-Hybrid-Systems (Y2H) konnte ich 18.663 Protein-Protein-Interaktionen (PPIs) für 449 wildtyp und 22 mutierte Proteine identifizieren. Eine genaue funktionelle Analyse der Interaktionspartner von korrespondierenden wildtyp und mutierten Proteinen ergab deutliche Unterschiede zum einen im Fall von allen untersuchten Proteinen und insbesondere im Fall vom ALS Krankheitsprotein TDP-43. Die identifizierten PPIs wurden außerdem verwendet um krankheitsspezifische Netzwerke zu erstellen und um Proteine zu identifizieren, die mit mehreren NDPs verbunden sind. Ich habe auf diese Weise vier Proteine (APP, IQSEC1, ZNF179 und ZMAT2) gefunden, die mit bekannten NDPs with Huntingtin, TDP-43, Parkin und Ataxin-1 interagieren und so fünf verschiedene NDs miteinander verbinden. Die Reduktion der mRNA Expression von IQSEC1, ZNF179 oder ZMAT2 mit Hilfe von siRNA führte zu einer Verstärkung von pathogenen Mechanismen wie der Aggregation von mutiertem Huntingtin und TDP-43 sowie der Hyperphosphorylierung des Proteins Tau. Außerdem habe ich 22 Proteine entdeckt, die die Aggregation von TDP-43 deutlich verändern und außerdem Mitglieder in sieben vorhergesagten Proteinkomplexen sind. Die Proteinkomplexe habe ich durch Kombination von Interaktionsdaten und Daten eines siRNA Screenings vorhergesagt. Zusätzlich habe ich herausgefunden, dass die Proteine eines vorhergesagten Komplexes, nämlich HDAC1, pRB, HP1, BRG1 und c-MYC, die Aggregation von TDP-43 durch Veränderung von dessen Genexpression beeinflussen.

Schlagwörter: neurodegenerative Erkrankungen, Protein-Protein Interaktionen, Aggregation, Toxizität, TDP-43

Für Margerate und Angie,
deren Kampf um ihr Leben mich jeden Tag neu inspiriert und
die mir gezeigt haben jedes Hindernis mit einem Lächeln zu überwinden

Danksagung

Zuerst möchte ich Prof. Dr. Erich Wanker für die Themenstellung und besonders für die Unterstützung bei der Ideenfindung um wieder neue Aspekte aus unserem riesigen Netzwerk zu zaubern. Dank ihm bin ich zu einer reiferen und selbstständigen Wissenschaftlerin geworden bin, die ohne viele Schwierigkeiten in die weite Welt hinausziehen kann.

Ganz herzlich bedanke ich mich auch bei meinen Kollegen im Labor ohne deren Hilfe ich nie so viel geschafft hätte und ohne die es im Labor echt langweilig gewesen wäre. Mein Dank gilt vor allem Kirstin Rau und Martina Zenkner nicht nur in Sachen Laborarbeit, sondern besonders was lange Diskussionen, tolle Kinoabende und aufregendes Eishockey angeht. Ich danke auch Alexandra Redel dafür, dass sie mich in „ihrem“ Labor so gut aufgenommen hat und mal wieder einen Plan hatte, wenn ich nicht so genau wusste, wie ein Experiment jetzt am Besten von statten geht. In diesem Zusammenhang möchte ich auch Angeli Möller und Katja Mühlenberg für ihre Unterstützung vor und während des Schreibens meiner Doktorarbeit danken.

Besonders Danken möchte ich auch Maliha Shah. Dank ihr kann ich jetzt jeden Frust und Stress einfach davonlaufen und habe auch kein Problem bei einem Wettkampf im Schlussfeld ins Ziel zu kommen, denn schließlich ist der Weg das Ziel. Ich hatte viel Spaß dabei mit dir die schönsten Ecken Europas zu erkunden und schätze dich als eine meiner besten Freundinnen.

Außerdem danke ich meinem Bruder für stundenlange Gespräche am Telefon über Gott und die Welt, aber doch meistens über Computer und andere technische Geräte. Ich verdanke ihm meine Liebe zu Mathematik, Informatik und Science Fiction, ohne die diese Arbeit niemals entstanden wäre.

Ganz besonders danken möchte ich natürlich auch meinen Eltern, besonders für ihre jahrelange Unterstützung aller Art und dass sie mir die Freiheit und Möglichkeit gegeben haben, schon ganz früh die Welt zu erkunden. Dank euch bin ich zu dem Mensch geworden, der ich heute bin, und habe meine Liebe für die Wissenschaft entdeckt.

Besonderen Dank gilt auch meiner großen Liebe Patrick, für sein Verständnis, das Aushalten meiner kleinen Vulkanausbrüche, aufbauende Worte während aller Krisenzeiten, die tollen Kurzreisen um mal wieder Stress abzubauen und dass er mich auffängt, wenn ich es brauche.

Contents

List of Figures

List of Tables

Abbreviations

AD	Alzheimer’s disease
Aβ	amyloid-β
ALS	Amyotrophic lateral sclerosis
AICD	APP intracellular C-terminal domain
Co-IP	co-immunoprecipitation
CTF	C-terminal fragment
FTLD	frontotemporal lobar degeneration
GO	Gene Ontology
HD	Huntington’s disease
ND	neurodegenerative disease
NDP	neurodegenerative disease protein
PD	Parkinson’s disease
PPI	protein-protein interaction
ROS	reactive oxygen species
SCA	spinocerebellar ataxia
SDS-PAGE	sodium dodecyl sulphate polyacrylamide gel electrophoresis
UPS	ubiquitin-proteasome system
Y2H	yeast two-hybrid

1 Introduction

1.1 Neurodegenerative diseases

1.1.1 Common pathogenic characteristics and molecular mechanisms of neurodegenerative diseases

Neurodegenerative diseases (NDs) are conditions, which are characterized by a profound reduction in the size and volume of the human brain due to the death of neurons in specific brain regions that are typical for each disease (Table 1) [1]. NDs progress gradually and become symptomatic only when the neuronal dysfunction and nerve cell loss exceeds a certain threshold [1]. Therefore, the actual brain degeneration may precede the clinical symptoms by many years.

The large group of NDs includes diseases such as Alzheimer's disease (AD), amyotrophic lateral sclerosis (ALS), Huntington's disease (HD), Parkinson's disease (PD) and spinocerebellar ataxias (SCAs). Some of these diseases share symptoms such as memory loss (AD, PD and HD) and movement-related disturbances (ALS, HD, PD and SCAs) and all of them are finally fatal [1]. Mutations in about 100 neurodegenerative disease proteins (NDPs) cause familial forms of NDs [2-6]. The mechanisms by which the different mutations induce disease are largely unknown. In some diseases, such as HD and SCAs, a family history of the disease can be ascertained in almost every case [5], whereas in others, such as AD [6, 7], PD [8, 9] and ALS [2], about 1-10% of all cases are inherited. NDs share other common features: all disorders appear late in life and their pathology is characterized by neuronal loss and synaptic abnormalities [1]. Another hallmark of NDs is the accumulation of misfolded proteins (Table 1), which results in the formation of toxic protein aggregates [10-12]. Additionally, neurodegenerative disorders share other common molecular mechanisms, such as mitochondrial dysfunction and oxidative stress, neuronal apoptosis and impaired protein homeostasis, which will be further elucidated in the following sections.

Table 1: Overview of neurodegenerative diseases

Disease	Affected brain regions	Aggregating proteins	Type of protein deposits
Alzheimer's disease (AD)	Cerebral cortex, hippocampus	Amyloid-β (Aβ), tau	Extracellular plaques, intracellular tangles
Amyotrophic lateral sclerosis (ALS)	Spinal cord, motor cortex, brain stem	TDP-43, SOD1, FUS	Intracellular cytoplasmic inclusions
Huntington's disease (HD)	Striatum, cerebral cortex	Huntingtin	Intracellular nuclear inclusions
Parkinson's disease (PD)	Substantia nigra	α-synuclein	Intracellular cytoplasmic inclusions (Lewy bodies)
Spinocerebellar ataxias (SCAs)	Cerebellum	Ataxin-1, ataxin-2 ataxin-3, ataxin-7, …	Intracellular nuclear or cytoplasmic inclusions

Protein aggregation in neurodegenerative diseases

The accumulation of insoluble protein aggregates in different brain regions is a pathological hallmark of a large number of NDs (Table 1). Protein aggregation can result from a mutation in a NDP (e.g. huntingtin, TDP-43 or α-synuclein [13-15]), a genetic alteration that causes an elevation in the amounts of a normal protein (e.g. duplication of the *SNCA* gene encoding α-synuclein [16]), or can occur in the absence of genetic alterations, e.g. triggered by aging [17]. Evidence from a variety of sources supports the hypothesis that protein aggregation is critical for neurodegeneration in various NDs: (1) genetics – genes linked to familial forms of NDs often encode aggregation-prone protein [13-15]; (2) animal models – over-production of aggregating proteins produces disease-associated phenotypes [18]; (3) biophysics – disease-associated

mutations promote *in vitro* aggregation [19-21]; and (4) mathematical modelling – rates of cell death as well as disease progression are consistent with a nucleation-dependent aggregation process [22-24].

Although large proteinaceous aggregates (inclusion bodies) in patient brains has been recognized as a typical feature of NDs for many years, it is still under discussion whether these structures are the primary toxic species [17]. The determination of the neuropathological link between protein aggregation and disease is exacerbated by a poor correlation between the aggregate load in the brain and the severity of clinical symptoms [25-28]. Moreover, protein aggregates can be found in brains from healthy individuals [29]. Thus, there is increasing evidence that inclusion bodies might represent an end-stage manifestation of a multistep aggregation process [30]. Misfolded monomeric proteins, oligomers or protofibrils, which develop before inclusion bodies are detectable, might cause cellular toxicity [30].

Each neurodegenerative disease is associated with the aggregation of certain proteins such as huntingtin in HD or TDP-43 in sporadic ALS and in many familial ALS cases (Table 1). However, certain proteins were found to be aggregated in several NDs, indicating that different NDs share common or at least overlapping molecular mechanisms. One example is the microtubule-associated protein tau, whose aggregates can be found in patients with AD, PD and frontal temporal dementia with parkinsonism linked to chromosome 17 (FTDP-17) [31-34]. Moreover, mutations in tau are associated with FTDP-17 [33]. Another example is the protein α-synuclein, which is the main component of Lewy bodies found in brains of patients with PD or dementia with Lewy bodies [35] and was also discovered in extracellular plaques of AD patients [36]. Furthermore, aggregation of TDP-43 occurs in ALS and frontotemporal lobar degeneration (FTLD) patients [37, 38], AD patients [39], patients with PD and dementia with Lewy bodies [40], HD patients [41] as well as SCA patients [42].

Mitochondrial dysfunction, oxidative stress and neuronal apoptosis

Involvement of mitochondria is likely to be an important common theme in NDs, as mitochondria are key regulators of cell survival and death [43] and several NDPs have been found to interact with mitochondria. Net production of reactive oxygen species (ROS), which results in oxidative stress, is another mechanism by which mitochondria contribute to NDs. Mitochondria contain multiple electron carriers capable of producing ROS as well as an extensive network of antioxidant defences [44]. Mitochondrial insults, including oxidative damage by ROS, can thus cause an imbalance between ROS production and removal, resulting in net ROS production [44]. Oxidative stress can lead to DNA damage and cell death [44].

Mitochondrial dysfunction and oxidative damage is e.g. implicated in the pathogenesis of AD. Oxidative damage occurs early in the AD brain, before the onset of plaque formation [45]. Moreover, hydrogen peroxide treatment increased intracellular amyloid-β (Aβ) peptide levels [46], the main component of extracellular plaques [6], indicating that oxidative stress is causally linked to AD. Oxidative stress also activates signaling pathways that increase expression of β-secretase, which results in increased Aβ production, and increases aberrant phosphorylation of tau [47, 48]. Furtermore, Aβ has been shown to interact directly with the mitochondrial matrix protein ABAD and disruption of this interaction results in a reduction of Aβ-induced apoptosis and the generation of free-radicals in neurons [49]. Presenilin and all the other components of the γ-secretase complex have also been localized to mitochondria, where they form an active γ-secretase complex [50].

Many genes, whose mutations cause familial PD, also indicate that mitochondrial dysfunction is critical for disease pathogenesis. For example α-synuclein is found in degenerating mitochondria from mice over-producing A53T α-synuclein and over-expression of α-synuclein impairs mitochondrial function and increases oxidative stress [51, 52]. The E3 ubiquitin ligase parkin can

associate with the outer mitochondrial membrane, where it prevents cytochrome c release and caspase activation, which could induce apoptosis [53]. This protective effect is abrogated by parkin mutations and by proteasome inhibitors [53]. Moreover, parkin and PINK1 act together in the quality control of mitochondria by inducing mitophagy (autophagy-based degradation of damaged mitochondria) [54].

In both sporadic and familial ALS, postmortem spinal cord samples show abnormalities in mitochondrial structure, number and localization [55]. Additionally, mutant variants of the protein Cu^{2+}/Zn^{2+} superoxide dismutase 1 (SOD1), which are responsible for ~20% of familial ALS cases, have been shown to interact in a mutant-specific manner with the mitochondrial protein Bcl-2 and thus inhibit its anti-apoptotic functions [56]. Over-expression of SOD1_G93A in mice results in mitochondrial degeneration, which precedes motor neuron death, suggesting that mitochondrial abnormalities trigger the onset of ALS [57]. Moreover, mutant SOD1 promotes aberrant ROS production, which results in oxidative damage of mitochondrial lipids and proteins as well as impaired respiration and ATP synthesis [58].

Several lines of evidence demonstrate the involvement of mitochondrial dysfunction in HD. Biochemical studies show decreased activities of the mitochondrial complexes II and III in the human HD brain [59]. In striatal cells obtained from mutant huntingtin knock-in mouse embryos, mitochondrial respiration and ATP production are significantly impaired [60]. Mutant huntingtin associates with the outer mitochondrial membrane and increases sensitivity to calcium-induced cytochrome c release [61]. Moreover, mutant hungtingtin also translocates to the nucleus, where it binds and increases the level and transcriptional activity of p53 [62]. p53 activates the pro-apoptotic protein BAX, either directly or by increasing expression of BH3-only Bcl-2 family members NOXA and PUMA [63].

Impaired protein homeostasis in neurodegenerative diseases

Several lines of experimental evidence indicate that a disturbance of protein homeostasis contributes to the pathogenesis in various neurodegenerative diseases [64]. Different protein homeostasis mechanisms maintain appropriate protein concentration levels, protein folding, protein interactions and protein localization [65]. These mechanisms include molecular chaperones, the ubiquitin-proteasome system (UPS) and autophagy.

As neurons are terminally differentiated, post-mitotic cell types, it has been suggested that they are especially susceptible to the cumulative effects of misfolded proteins as they are unable to reduce the load of toxic intermediates through consecutive rounds of mitosis [66]. Therefore, the capacity of molecular chaperones to reduce misfolded proteins by refolding is essential for maintaining neuronal integrity [67]. Over-expression of chaperones such as heat-shock proteins (Hsp70 and Hsp40) has been shown to decrease toxicity induced by Aβ peptides, mutant huntingtin and mutant α-synuclein [68-70]. Moreover, protein aggregates found in ND patients were shown to colocalize with molecular chaperones [71-74]. This sequestration could lead to widespread dysfunction of protein homeostasis as chaperones associated with insoluble protein aggregates might not be available for refolding of other cellular proteins [75].

The UPS is one of the major pathways that targets impaired and misfolded proteins for destruction and recycling [76-79]. Ubiquitination is the targeting process for the elimination of unfolded or misfolded proteins via the UPS. It occurs through a series of enzymatic reactions involving ubiquitin-activating enzymes (E1), ubiquitin-conjugating enzymes (E2) and ubiquitin protein ligases (E3) [78]. E3 ligases catalyze the final addition of ubiquitin molecules to lysine residues of damaged target proteins [78]. This provides the signal for its removal and degradation by the 26S proteasome [80, 81]. In addition, E4 is a new ubiquitination enzyme responsible for multiubiquitin chain assembly [82].

The UPS has been implicated in each of the major neurodegenerative diseases. The deposition of ubiquitin-tagged proteins in many NDs implies a lowered capacity of cells to degrade misfolded proteins [37, 38, 83-85]. The E3 ubiquitin ligase parkin for example contributes to the clearance of α-synuclein and Aβ peptides, and thereby reverses toxicity (mitochondrial dysfunction and proteasome inhibition) induced by α-synuclein and Aβ [86, 87]. CHIP, in collaboration with Hsp70 and Hsp90, polyubiquitinates a number of misfolded proteins and thereby enhances cell survival. These include gene products with expanded polyglutamine tracts responsible for HD and SCAs [88, 89], tau [90], mutant SOD1 [91] as well as α-synuclein [92]. Moreover, several studies suggested that intracellular Aβ peptides and α-synuclein protofibrils inhibit the proteasome activity [93, 94], indicating that dysfunction of the UPS contributes to NDs.

Autophagy is another important cellular process, which is responsible for the degradation of aggregated proteins. Moreover, activation of autophagy may be protective in some NDs by enhancing the removal of toxic protein aggregates [95]. Targeting autophagy with rapamycin, which induces autophagy through the inhibition of the mTOR pathway, decreases the deposition of abnormal protein aggregates and alleviates disease progression in animal models of HD and PD [96, 97]. Several studies provided evidence that autophagy is impaired in NDs. A recent study revealed aberrant cargo recognition in cellular and mouse models of HD [98]. Mutant huntingtin over-expression also resulted in an elevated autophagosome formation [96, 99]. Autophagy deregulation was initially linked to AD where autophagic vesicles were found to accumulate in brains of AD patients [100, 101]. Autophagy was induced after Aβ over-production and in APP/PS1 transgenic mice [101-103]. Moreover, strong evidence indicates that Aβ is generated in vesicles during autophagy, suggesting that autophagy activation in AD brains may exacerbate AD pathogenesis by increasing Aβ levels [101, 104]. Additionally, clearance of autophagic vesicles is impaired in AD brains [105]. PD is also strongly linked to

autophagy. α-Synuclein e.g. was found to be degraded by macroautophagy and chaperone-mediated autophagy (CMA) [106, 107]. Over-expression of mutant α-synuclein inhibits CMA [108, 109], while over-expression of the wild-type protein is associated with macroautophagy inhibition [110]. Defects in autophagy are also implicated in ALS. Increasing evidence suggests that defects in autophagic flux or in specific autophagy-regulatory processes, rather than induction, contributes to motor neuron degeneration in ALS [111]. Treatment of SOD1_G93A transgenic mice with rapamycin inactivates the mTOR pathway but fails to reduce the level of mutant SOD1 aggregates [112]. Moreover, mutant SOD1 can inhibit the autophagic process and can lead to defective clearance [113]. Finally, TDP-43 has been implicated in the transcriptional regulation of proteins central for autophagy [114]. Depletion of TDP-43 causes autophagy impairment and results in the accumulation of polyubiquitinates proteins [114].

1.1.2 Alzheimer's disease

Pathogenesis

Alzheimer's disease (AD) is the most common form of dementia [115]. Clinically AD is characterized by progressive cognitive impairment, loss of memory and abnormal behaviour [115]. AD generally affects people over the age of 65 [115]. However, around 5% of AD patients show a much earlier disease onset (40-50 years old), most of which are familial cases [115]. Mutations in APP, presenilin 1 and presenilin 2 are associated with familial cases of AD [116-119]. Extracellular plaques consisting mainly of Aβ peptides (produced from APP) [120] and intracellular neurofibrillary tangles consisting largely of hyperphosphorylated tau [121] are the major histopathological hallmarks of AD. Besides the aggregation of Aβ and tau polypeptides, numerous other structural and functional alterations occur, including inflammatory responses and oxidative stress [122-124]. The consequences of all the pathological changes, including the effects of the Aβ

and tau pathologies, is severe neuronal and synaptic dysfunction as well as neuronal loss in the cerebral cortex and the hippocampus [125].

APP processing and Aβ generation

Aβ is produced from the amyloid precursor protein (APP) by endoproteolysis [125]. APP can be cleaved by different enzymes or enzyme complexes termed α-, β- and γ-secretases resulting in the production of different truncated peptides (Figure 1) [125]. Three enzymes with α-secretase activity have been identified: ADAM9, ADAM10 and ADAM17 [126]. BACE1 was discovered as the β-secretase enzyme [127]. The γ-secretase was found to be a complex of enzymes composed of presenilin 1 or 2, nicastrin, APH1 (anterior pharynx defective) and PEN2 (presenilin enhancer 2).

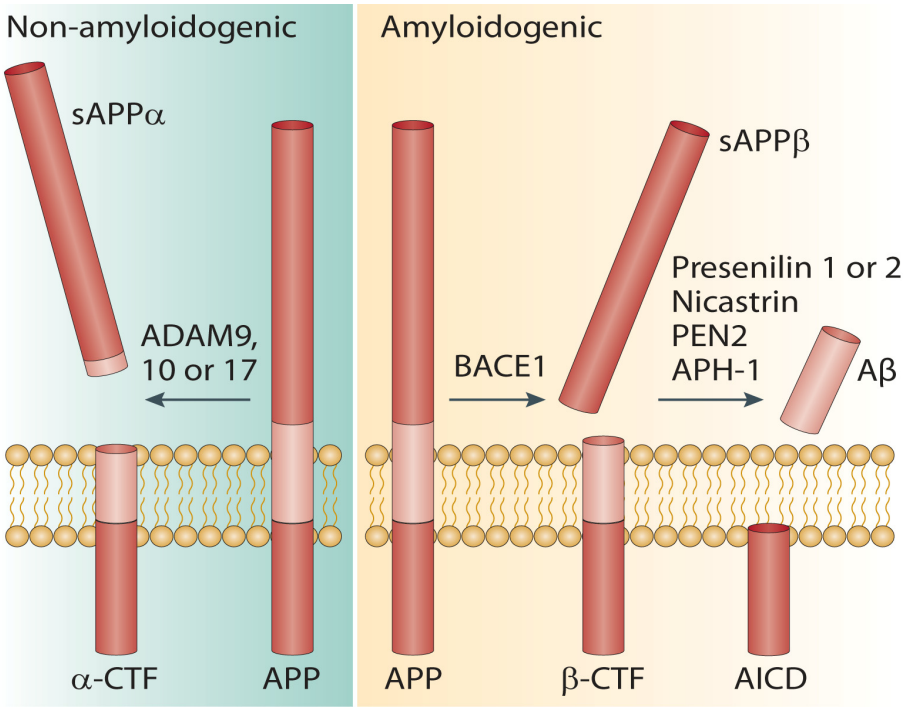

Figure 1: Overview of APP processing (adapted from [125]). AICD – APP intracellular domain; CTF – C-terminal fragment; sAPP – soluble APP N-terminal fragment; APH-1 – anterior pharynx defective 1 protein; PEN2 – presenilin enhancer 2 protein.

The cleavage and processing of APP can be devided into a non-amyloidogenic and an amyloidogenic pathway. In the prevalent non-amyloidogenic pathway, APP is cleaved by the α-secretase at a position 83 amino acids from the carboxy (C) terminus, producing a large amino (N)-terminal ectodomain (sAPPα), which is secreted into the extracellular space [128]. The resulting C-terminal fragment (α-CTF) is retained in the membrane and subsequently cleaved by the γ-secretase, producing the APP intracellular domain (AICD) and a short peptide called p3 [129]. Importantly, cleavage by the α-secretase occurs within the Aβ region, thereby inhibiting formation of Aβ. Moreover, α-secretase cleavage occurs mainly at the plasma membrane, while β-cleavage is mainly found in endosomes or the trans-Golgi network [130].

The amyloidogenic pathway is an alternative cleavage pathway for APP, which leads to Aβ peptide generation. The initial proteolysis is mediated by the β-secretase at a position located 99 amino acids from the C-terminus [125]. This results in the release of sAPPβ into the extracellular space and leaves the 99-amino-acid β-CTF within the membrane [125]. Subsequent cleavage of this fragment (between residues 38 and 43) by the γ-secretase liberates aggregation-prone Aβ peptides [125]. Most of the Aβ peptides that are produced are 40 residues in length (Aβ40), whereas a small proportion (~10%) have a length of 42 residues (Aβ42) [125]. The Aβ42 variant is more hydrophobic and more prone to fibril formation than Aβ40 [20], and it is this longer peptide that is also the predominant isoform found in amyloid plaques [131].

Tau pathology in AD

Neurofibrillary tangles (NFTs) have been identified as a major pathological hallmark in AD brains [121]. However, the structural and functional relevance of NFTs for AD pathogenesis is not completely understood. The microtubule-associate protein tau is the major component of NFTs [121]. Tau promotes

microtubule assembly, stabilizes microtubules, and affects the dynamics of microtubules in neurons [132].

Increasing evidence suggests that hyperphosphorylated tau protein is critically involved in AD pathogenesis, particularly impairing axonal transport of APP and organelles such as mitochondria in neurons [133, 134]. Furthermore, N-terminal tau fragments are thought to cause mitochondrial dysfunction and synaptic damage in AD model systems [135, 136]. Recent reports have demonstrated that Aβ-induced oxidative stress is a critical factor for hyperphosphorylation of tau in AD neurons [137-139]. Phosphorylation of tau is regulated by several kinases, including GSK3β and Cdk5, both of which are activated by extracellular Aβ [140, 141]. Tau is cleaved by GSK3β, caspase-3, caspase-9 and calpain, which can be activated by soluble Aβ species in cell model systems [142, 143]. Moreover, it appears that tau might be an important downstream mediator of Aβ toxicity [130]. Triple transgenic mice with mutant APP, presenilin 1 and tau proteins develop Aβ deposition prior to the appearance of NFTs [144]. Additionally, reducing Aβ levels prevents tau pathology and abrogates spatial memory problems in AD models [145]. Finally, when AD transgenic mice that over-express APP are crossed with mice lacking tau, no detioration in spatial memory function is seen despite the accumulation of Aβ [146].

1.1.3 Amyotrophic lateral sclerosis

Clinical symptoms and neuropathology

Amyotrophic lateral sclerosis (ALS) is considered to be the most common adult-onset motor neuron disease (MND). It is a progressive disorder that involves selective degeneration of both upper and lower motor neurons in the motor cortex, brainstem and spinal cord [147]. Disease progression is characterized by muscle atrophy, spasticity and weakness [147]. Paralysis of the respiratory

muscles is usually fatal within 1-5 years after disease onset [147]. Up to 10% of ALS patients have familial ALS (FALS) [147]. FALS is usually inherited in an autosomal dominant manner, although there are rare cases of autosomal recessive and X-linked disease [2]. FALS is associated with mutations in 13 genes including *SOD1*, *TARDBP* (encodes TDP-43) and *FUS* (for an overview see [2]). About 15-20% of ALS patients also meet the criteria of frontotemporal lobar degeneration (FTLD), which is characterized by behavioural and cognitive impairments [148]. Moreover, ~15% of FTLD patients develop symptoms of MND [148], indicating that ALS and FTLD are part of a broader disease spectrum [149]. Histopathologically sporadic and familial ALS is mainly characterized by cytoplasmic ubiquitin-positive TDP-43 inclusions [37, 38]. In contrast, patients with FALS that are caused by mutations in SOD1, FUS and optineurin contain mainly insoluble SOD1, FUS and optineurin protein aggregates [150-153].

TDP-43 protein and ALS pathogenesis

The TAR DNA binding protein (TDP-43) is encoded by the *TARDBP* gene on chromosome 1. TDP-43 is a 414 amino acid protein that can shuttle between the nucleus and the cytoplasm due to the presence of a nuclear localization signal (NLS) and a nuclear export signal (NES; Figure 2) [154]. It comprises two RNA recognition motifs (RRMs) that allow binding to nucleic acids [154]. TDP-43 also contains a C-terminal glycine-rich domain that is important for protein-protein interactions (Figure 2) [154]. Most of the identified mutations associated with familial ALS and/or FTLD lie in the C-terminal region [154]. However, to date it is still unclear why these mutations cause ALS and/or FTLD. However, animal models that over-express wild-type or mutant TDP-43 show neurotoxicity, which is dependent on the expression level of the disease protein [155]. Recent reports indicate that neurotoxicity is dependent on the RNA binding capacity and the intracellular localization of TDP-43 [156]. TDP-43 inclusions have also been reported to occur in various forms of neurodegenerative diseases including AD [39], PD and dementia with Lewy

bodies [40] and HD [41]. Finally, TDP-43 has been found to be involved in different steps of gene expression including transcription, mRNA splicing, mRNA transport and translation [157]. These findings suggest that altered RNA processing might be an important aspect in the pathogenesis of ALS and other neurodegenerative diseases.

Figure 2: Domain structure of TDP-43. NLS – nuclear localization signal; NES – nuclear export signal; RRM – RNA recognition motif.

Aggregated TDP-43 is ubiquitinated and hyperphosphorylated in brains of ALS and FTLD patients [37, 38]. In particular, phosphorylation at Ser409/410 is a specific feature of neuropathological inclusions [158, 159]. Additionally, TDP-43 is cleaved by caspase 3 into C-terminal fragments of different size (25 kDa or 35 kDa) [160]. Interestingly, lack of normal nuclear TDP-43 localization is consistently observed in inclusion-bearing tissues [37, 38]. Together these data suggest that, in addition to a toxic gain-of-function suggested by the aggregation of TDP-43, a loss of nuclear functions might contribute to the disease pathogenesis in ALS. Indeed among the mRNAs, whose levels or processing is affected by TDP-43, are molecules that encode proteins, which are related to neuronal function and development or which have been implicated in neurological diseases [161-163]. RNAs, whose levels are mostly depleted by reduction of TDP-43, are derived from genes with the longest introns (average size >100 kb) and that encode proteins involved in synaptic activity [161-163]. Since genes with very long introns are preferentially expressed in the nervous system, they could be the reason for the selective vulnerability observed in ALS patients [161-163]. TDP-43 also regulates the expression as well as the splicing of several disease-related pre-mRNAs including those encoding, FUS, progranulin, tau, parkin, huntingtin and different

ataxins [161-163]. TDP-43 was also shown to bind its own mRNA and thereby regulates its own expression by promoting mRNA instability [161-164].

1.2 Protein-protein interaction studies for neurodegenerative disease proteins

In this section I will give an overview over published protein-protein interaction (PPI) studies. These studies provide valuable insights into the function of neurodegenerative disease proteins (NDPs) and can substantially increase our understanding of disease mechanisms. However, previous investigations have mainly focused on single disease proteins and have created focused PPI networks for individual diseases or disease processes. Therefore, a better understanding of common neurodegenerative disease mechanisms, requires a more comprehensive identification of PPIs for multiple NDPs.

1.2.1 Single protein interaction studies

One strategy to assess possible biological and pathological functions of neurodegenerative disease proteins is to identify interacting proteins for NDPs using yeast two-hybrid (Y2H) or affinity purification methods. The first published studies mainly discovered single interactions for example between the APP C-terminal domain and the G_0 protein [165], Fe65 [166] or X11 [167]. More systematic interaction studies identified large sets of novel interaction partners for huntingtin. Goehler *et al.* for example found 165 new interaction partners for huntingtin with Y2H screens, which resulted in the functional annotation of 16 previously uncharacterized proteins and the discovery of GIT1, which functions as an enhancer of huntingtin aggregation [168]. In contrast, Kaltenbach *et al.* identified 234 high-confidence huntingtin associated proteins with Y2H (104 PPIs) and affinity purification (130 PPIs) methods [169]. Moreover, this study discovered a new association between huntingtin and components of the vesicle secretion apparatus such as Stx1A, NAPA, CACNA2D1 and SNAP25 [169]. Additionally, 48 of 60 tested proteins modified mutant huntingtin-induced

cytotoxicity in a *Drosophila* model [169], indicating that PPI data sets contain a large fraction of proteins that function as aggregation modulators. Two recent studies identified a large set of TDP-43 interactors, which are involved in transcriptional regulation, mRNA processing, translation, microRNA processing and DNA repair, indicating that TDP-43 plays a role in those biological processes [170, 171].

Interaction studies focussing on single NDPs also provided strong evidence that mutant NDPs have distinct interaction partners compared to the wild-type proteins and provide insights into disease mechanisms. The disease-causing polyglutamine expansion for example altered the interactions of huntingtin with HAP1/p150^{Glued} complexes as well as numerous transcription factors (e.g Sp1 and TBP), leading to their functional impairment [172-179]. Additionally, perturbed interactions between mutant ataxin-1 and transcription factors such as LANP, PQBP1, Gfi-1, SMRT, Boat and Sp1 might exert the deleterious effects of mutant ataxin-1 on transcriptional regulation. Moreover, a mutant polyglutamine tract in ataxin-1 clearly alters the interaction preference of the protein in neuronal cells [180, 181]. It was found that mutant ataxin-1 preferentially forms a complex with the protein RBM17, which might contribute to the SCA1 disease phenotype by a gain-of-function mechanism, whereas wild-type ataxin-1 is present in a capicua-containing complex [180, 181]. When ataxin-1 is mutated the formation of abnormal RBM17-ataxin-1 complexes in patient brains might disrupt cellular functions and cause disease [180, 181].

1.2.2 Protein-protein interaction studies for multiple NDPs

Previously, two studies have been reported that describe the identification of PPIs for multiple NDPs. Lim *et al.* identified 770 mostly novel interactions for 54 proteins involved in 23 inherited ataxias [182]. Many ataxia-causing proteins share interaction partners, indicating that different diseases are caused by common disease mechanisms [182]. This study established that systematic interaction mapping is a valuable tool to elucidate the pathogenic mechanisms

of NDs [182]. The second study focused on mutant proteins that cause AD or potentially alter disease pathogenesis [183]. Additionally, 44 proteins encoded by candidate susceptibility genes were screened for interactions [183]. The identified interactions suggested new mechanistic details underlying AD: the authors found for example an interaction between APOE and presenilin 1, indicating that APOE might regulate the function of presenilin 1 [183]. Moreover, this study suggests that the protein PDCD4 might be a neuronal death regulator and that the protein ECSIT provides a connection between oxidative stress, inflammation and mitochondrial dysfunction in AD [183].

1.2.3 Studies analyzing PPI networks for proteins causing several different neurodegenerative diseases

Previously, two studies were published that focused on the analysis of literature-based interaction networks for NDPs associated with different NDs. One of these studies compared the PPIs of 13 proteins, whose mutations cause one of six investigated NDs (AD, PD, ALS, HD, dentatorubral-pallidoluysian atrophy (DRPLA) and prion disease) [184]. Their main objective was to utilize the available PPI networks to better understand the common molecular principles of NDs [184]. Based on the available literature data they were able to identify 19 proteins that link 2-4 different NDPs [184]. However, using the available data one protein (caspase-8) was found that interacted with known NDPs associated with four diseases (AD, HD, DRPLA or prion disease) [184], indicating that further interaction studies are necessary to identify new connections between different NDs. A second, very recent study explored literature-based interactions for proteins associated with PD, AD, multiple sclerosis, rheumatoid arthritis or type 1 diabetes [185]. They found a strong correlation between AD and type 1 diabetes in terms of shared interactomes and functional annotations [185], supporting the view that these diseases might have overlapping disease mechanisms. Biological evidence indeed indicates that dysregulation of insulin metabolism might affect Aβ accumulation and degradation [186-188], substantiating the results from the interaction studies.

1.3 Aims of the thesis

Cellular functions are mediated through complex assemblies of proteins that are linked through physical interactions. Knowledge about interactions that connect proteins helps us understand the normal functions of proteins as well as the underlying molecular basis of disease processes. Therefore, one major aim of my thesis was the generation of PPI networks for known wild-type and mutant NDPs as well as proteins involved in neurodegenerative disease processes using the yeast-two hybrid system. Additionally, I wanted to identify disease-relevant interactions by comparing interaction partners of wild-type and mutant NDPs. I also aimed to discover proteins that play a role in multiple neurodegenerative diseases such as Alzheimer's disease, Huntington's disease and amyotrophic lateral sclerosis. This might give insights into common neurodegenerative disease processes and lead to the discovery of drug targets that are relevant in multiple NDs. Finally, I seeked to identify novel TDP-43 aggregation and toxicity modifiers using a network modelling approach by combining data from PPI screenings and systematic, cell-based siRNA experiments.

2 Results

2.1 Generating protein-protein interaction networks for neurodegenerative diseases using an automated yeast two-hybrid system

Neurodegenerative diseases (NDs) are characterized by the progressive loss of neurons and have several pathological mechanisms in common. However, mechanistic details remain elusive. As protein-protein interaction (PPI) networks are important resources for unravelling disease mechanisms, I created a comprehensive PPI network connecting a large number of already known neurodegenerative disease proteins (NDPs) involved in different NDs. In this chapter the target selection, the protein-protein interaction (PPI) screen, the confidence scoring of yeast two-hybrid (Y2H) PPIs and the validation of interactions in mammalian cells are presented.

2.1.1 Prediction of 3,711 neurodegenerative disease-related target genes

In the past decade several studies have used bioinformatics and/or high-throughput experimental techniques to generate ND-related protein interaction networks in order to elucidate disease mechanisms [168, 180, 182, 189]. However, to this date a comprehensive PPI network connecting known NDPs involved in different NDs has not been generated.

To create a first comprehensive PPI network for various NDs, all human protein-coding genes were prioritized according to their connection to NDs. The prioritization of genes was done in close collaboration with Dr. Jean-Fred Fontaine (Andrade lab, MDC Berlin-Buch). Several manual or automated analysis steps were performed, which utilized data from publications about NDs as well as ND-related processes and public databases (

Table **2**). The data included among others high-throughput experimental data sets, genomic and drug data as well as MEDLINE abstracts.

Table 2: Data sets used to prioritize genes according to their relatedness to NDs.

Data set	Analyses methods	Description
Core1	Manual	Disease genes for which mutations that cause disease (AD, HD, PD, ALS, SCA1 or SCA3) have been identified
Core2	Manual	Genes related to NDs by genetic studies from the OMIM database
Modulator1	Manual	Genes associated with NDs based on available literature data
Modulator2	Manual	Known genetic modulators of toxicity and aggregation of known NDPs such as huntingtin, α-synuclein and SOD1
HTT	Manual	HTT interacting proteins identified in high-throughput experiments
Orthologs	Manual	Modifier genes from model organisms that influence protein aggregation or toxicity of known NDPs
Linkage	Automated	Candidate genes situated in ND-related chromosomal regions identified in linkage studies in which no gene could be linked to the studied disease
Textmining1	Automated	Text mining-based analysis of MEDLINE abstracts for genes involved in ND processes (AD, HD, PD, ALS and SCA)
EST	Automated	Observed ESTs in tissues of the nervous system
Expression	Automated	Differentially expressed genes in brains of AD, PD and HD; microarray data sets
Drugbank	Automated	Extraction of known drug targets from DrugBank
DrugSE	Automated	Prediction of ND-related drug targets by side effect similarity
TextDrugs	Automated	Data mining-based identification of ND-related drug targets
Textmining2	Automated	Text mining-based analysis of MEDLINE abstracts for genes that play a role in protein aggregation

Data set	Analyses methods	Description
MaxUS	Automated	Published interaction partners of selected proteins from the UniHI database; selection of the top 20 predicted interactors of Core1 and Core2 proteins from the STRING database
Aging	Automated	Genes differentially expressed in aged normal human brains compared to younger brains; microarray data set

Each analyzed gene, which could be associated with any one of the different data sets, obtained a score depending on the associated data set (see 4.2.5.1). The score for each data set was defined by assessing the relation of each set to ND processes. Therefore, known ND genes (Core1) were assigned a very high score, while known drug targets from DrugBank were assigned a very low score, as there is no direct relation to NDs (Table 14). Combining the single scores obtained for each human protein-coding gene into a single score (see section 4.2.5.1) revealed a list of 3,711 genes with score $\geq$ 100, which are potentially involved in ND processes. The higher the score the stronger is the association of the gene to ND processes.

A functional enrichment analysis of the 3,711 predicted genes that are associated with various ND processes in comparison to the human genome supported the feasibility of the prioritization method. I found that ~10% of the predicted genes are known to play a direct role in ND processes, compared to just 5% in the human genome (Figure 3). Additionally, genes involved in processes such as apoptosis, protein folding, synaptic transmission and RNA splicing, which are altered in NDs, were enriched with this data filtering strategy (Figure 3).

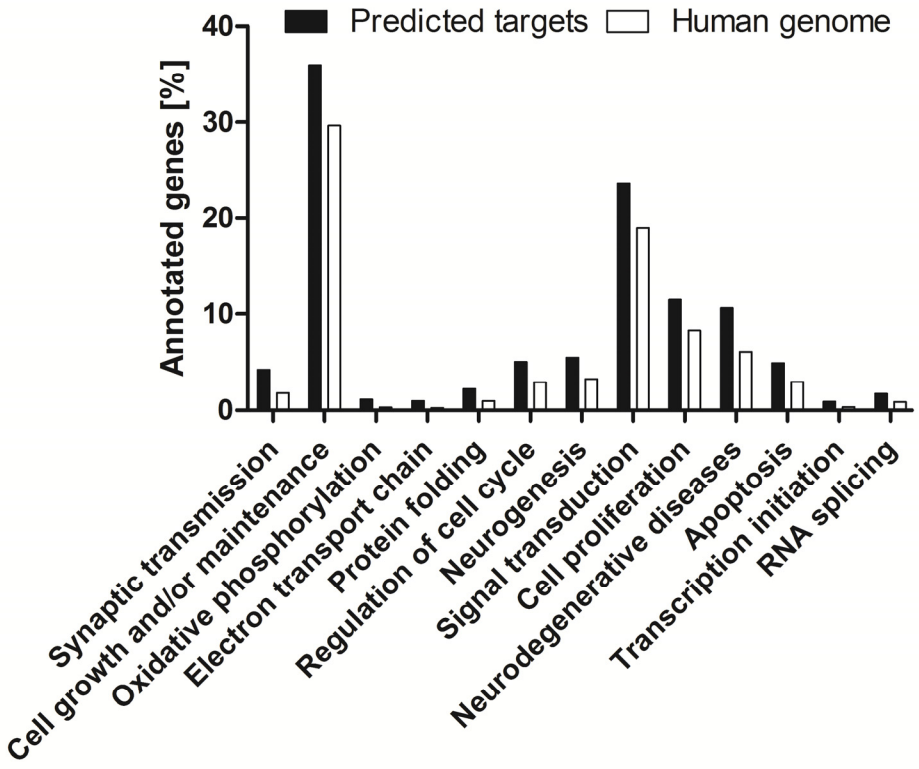

Figure 3: Functional enrichment analysis for the 3,711 predicted target genes potentially involved in NDs. Over-represented GO terms and KEGG pathways in comparison to the human genome were identified with the program EASE. Only categories with Bonferroni-adjusted p-value < 0.5 were considered.

2.1.2 Analysis of genes selected for systematic interaction screens

From the list of 3,711 ND-related genes, the top 655 protein-coding genes with score ≥ 310 were selected for systematic interaction screens using an automated yeast two-hybrid (Y2H) method [190]. The selection covered 83 known ND genes (e.g. *SNCA*, *MAPT*, *APP*, *HTT*, *ATXN1* and *SOD1*) involved in several NDs such as Parkinson's disease (PD), Alzheimer's disease (AD), Huntington's disease (HD), different types of spinocerebellar ataxia (SCA) and amyotrophic lateral sclerosis (ALS). In addition, 171 (26.1%) other disease genes and 50 (7.6%) predicted risk factors or susceptibility genes for NDs (e.g. *APOE*, *CLU*, and *GBA*) were among the selected genes (Figure 4A). Furthermore, 35.6% (233 genes) of the 655 selected genes are known drug

targets and 14.4% (94 genes) of the selected genes are known modulators of aggregation or toxicity induced by NDPs (e.g. α-synuclein and huntingtin). Finally, 57 (8.7%) genes were predicted to encode proteins whose homologs form insoluble protein aggregates with age in *Caenorhabditis elegans* (*C. elegans*). The complete list of selected target genes for interaction studies can be found in the Appendix (5.1).

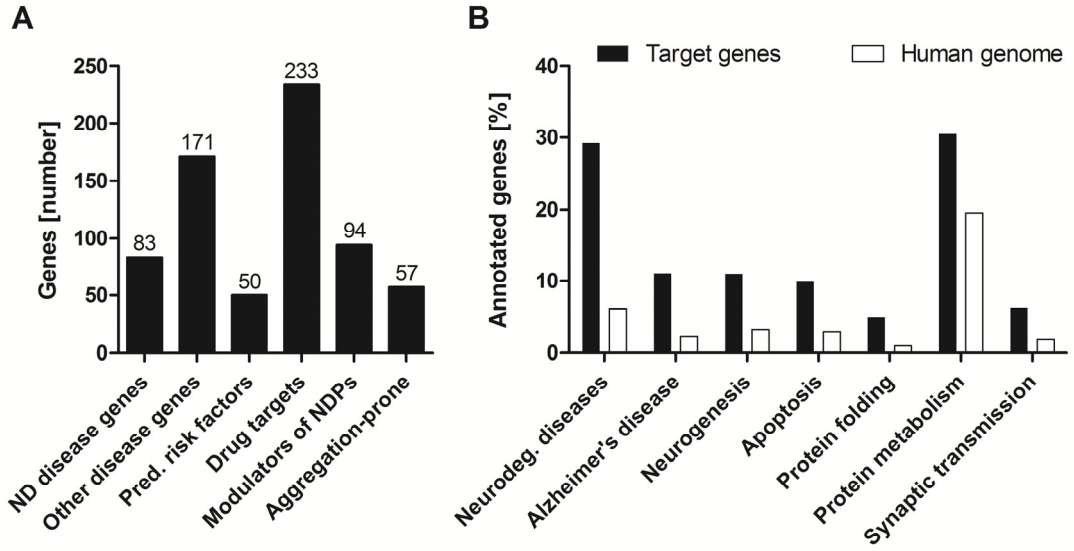

Figure 4: Bioinformatics analysis of selected target genes. (A) Annotation of target genes as disease genes, risk factors, known drug targets, modulators and homologs of aggregation-prone proteins. (B) Functional enrichment analysis with the program EASE. Only GO terms or KEGG pathways with Bonferroni-adjusted p-value < 0.5 were considered.

When the 655 selected genes were analyzed for over-represented Gene Ontology (GO) terms and KEGG pathways (Figure 4B) a significant enrichment of the KEGG pathways “Neurodegenerative disease” and “Alzheimer’s disease” (~30% and ~11% respectively) was observed compared to the human genome (~6% and ~2% respectively). This supports the view that a large number of the selected genes play a direct role in neurodegenerative disease processes. Additionally, proteins with specific functions that are altered in ND processes, such as apoptosis, protein folding or protein metabolism, were enriched among the selected genes (Figure 4B). Other more neuronal function-related terms

(neurogenesis and synaptic transmission) were also significantly enriched, indicating that many of the selected genes have a functional role in neurons.

2.1.3 Selection of mutant variants for yeast two-hybrid screens

Neurodegenerative diseases occur mainly sporadically, but in rare cases mutations in different disease genes such as *APP* in AD and *SNCA* in PD cause familial forms of the diseases [191-193]. Exceptions are disorders that are caused by a pathogenic extension of polyglutamine stretches, such as HD, which are purely genetic [194]. The main difference between sporadic and familial diseases is an earlier onset in familial forms [195], so that certain molecular changes might be more pronounced in those cases. Therefore protein-protein interactions of mutant proteins might give insights into disease mechanisms, which cannot be revealed when only wild-type proteins are screened for interactions. Thus, I generated 22 mutant variants of 11 known ND genes that cause familial AD, ALS, HD and PD (Table 3).

I produced two mutant variants of α-synuclein (A30P and E46K) that cause autosomal dominant Parkinson's disease (PD) and Lewy body dementia with parkinsionism, respectively [14, 196]. They were selected for systematic interaction screening, because they both increase the aggregation propensity of α-synuclein [197, 198]. Mutations in the E3 ubiquitin ligase parkin (*PARK2*) are associated with autosomal recessive juvenile PD [199]. The selected mutation Q311STOP results in the expression of a truncated parkin protein that lacks ubiquitin ligase activity, which is thought to be responsible for the development of juvenile PD [200, 201]. Mutations in the LRRK2 gene are one of the most common causes of genetically inherited PD [202]. As full-length LRRK2 protein (app. 250 kDa) is to large for Y2H interaction screens, only the wild-type WD40 repeat domain, which mediates protein-protein interactions [203], and a mutant variant of this domain (G2385A) were chosen for interaction screens [204]. Earlier studies have demonstrated that LRRK2 variants with a G2385A mutation are more toxic than the wild-type protein and efficiently induce apoptosis [205].

Expansion of polyglutamine (polyQ) repeats in a diverse set of proteins is associated with different types of spinocerebellar ataxias (SCAs) and Huntington's disease (HD). Mutant ATXN1 alleles (encoding mutant ataxin-1 protein with an extended polyQ tract) contain pure repeat tracts consisting of 41 or more CAG repeats (encoding glutamines) and are associated with SCA1 [206, 207]. Detailed analysis of ataxin-1 protein-protein interactions revealed that the polyQ expansion inhibits the function of native protein complexes containing ataxin-1 and causes SCA1 neuropathology [180] and therefore one mutant (Q79) was selected for Y2H screens. In patients diagnosed with SCA3 or Machado-Joseph disease CAG expansions of 41 or more were identified in the ATXN3 gene encoding the ataxin-3 protein [208]. Ataxin-3 mutations, such as the selected mutation (Q73), enhance mitochondrial-mediated cell death [209]. Abnormal expansion of a polyglutamine tract in the N-terminus of huntingtin causes HD [13, 194] and induces cytotoxicity which leads to the death of neurons [210, 211]. I screened several N-terminal huntingtin fragments of different lengths with pathogenic polyQ tracts of different sizes (Table 3).

The three selected mutant versions of SOD1 (A4V, G85R, and G93A) are associated with familial amyotrophic lateral sclerosis (FALS) [212, 213]. The A4V mutation is the most frequent mutation of SOD1 identified in FALS patients [212, 214]. Aggregation and cytotoxicity of the SOD1_G85R mutation were well characterized in transgenic mice [215, 216]. Similarly, it was shown in several models that the SOD1_G93A mutation leads to the death of neurons by an enhanced capacity to generate free radicals [217, 218]. The selected TDP-43 mutations Q331K (associated with sporadic ALS) and M337V (associated with FALS) were previously shown to promote aggregation and toxicity of TDP-43 [15, 219]. The selected mutation in FUS (R521C) was one of the first detected mutations in FUS associated with FALS [150, 153]. Transgenic rats overexpressing this mutant also develop ALS phenotypes [220].

Table 3: Mutant proteins selected for Y2H screens. Abbreviations: PD – Parkinson's disease; SCA - spinocerebellar ataxia; HD – Huntington's disease; ALS – amyotrophic lateral sclerosis; AD - Alzheimer's disease.

Protein	Gene symbol	Mutations	Disease	References
α-Synuclein	SNCA	A30P, E46K	PD	Kruger et al. (1998) [14]; Zarranz et al. (2004) [196]
Parkin	PARK2	Q311STOP	PD	Hattori et al. (1998) [200]
Leucin-rich repeat kinase 2	LRRK2	G2385A	PD	Mata et al. (2005) [204]
Ataxin-1	ATXN1	Q79	SCA1	Orr et al. (1993) [207], Banfi et al. (1994) [206]
Ataxin-3	ATXN3	Q73	SCA3	Kawaguchi et al. (1994) [208]
Huntingtin	HTT	Q49, Q51, Q68, Q73, Q79, Q80	HD	Duyao et al. (1993) [13]
Superoxide dismutase 1	SOD1	A4V, G85R, G93A	ALS	Deng et al. (1993) [212], Rosen et al. (1993) [213]
TAR DNA binding protein (TDP-43)	TARDBP	Q331K, M337V	ALS	Sreedharan et al. (2008) [15]
Fused in sarcoma	FUS	R521C	ALS	Kwiatkowski et al. (2009) [150]
Amyloid precursor protein	APP	K670N/M671L	AD	Mullan et al. (1992) [118]
Presenilin 1	PSEN1	A431E	AD	Yescas et al. (2006) [221], Murrell et al. (2006) [222]

Mutations in APP and presenilin 1 are associated with familial Alzheimer's disease (AD) [118, 221, 222]. The selected APP mutation (K670N/M671L) leads to an 6-8 times increased Aβ production [223-226], whereas the selected presenilin 1 mutation (A431E) modulates γ-secretase cleavage site preference, which leads to an increased production of Aβ42 [227].

2.1.4 Identification of protein-protein interactions with the Y2H method

As described above the top 655 genes predicted to be involved in neurodegenerative diseases (NDs) were initially selected for systematic interaction screens. For Y2H screens available bait (522) and prey (15,863) cDNAs were cloned into Gateway™ compatible Y2H screening vectors pBTM116-D9 (baits) and pACT4-DM (preys) and transformed into *MATa* and *MATα* yeast strains, respectively. Baits were systematically tested for autoactivity in the Y2H system, i.e. the ability to activate a reporter gene without an interaction partner. This was essential as the Y2H system is based on the reconstitution of a transcription factor. Initiation of transcription, due to latent reporter gene activation activity is present in ~5% of all proteins [228]. In the end, 108 genes were excluded and 414 non-autoactivating genes were selected for Y2H screens. Briefly, in the used automated Y2H system interacting proteins activate the *HIS3* and *URA3* reporter genes, which enable the cells to grow on selective agar plates without histidin and uracil. Additionally, lacZ reporter gene activation was monitored in β-galactosidase assays. For systematic interaction mapping, 16 non-autoactivating baits were pooled and mated with one of the available preys. This was followed by a retest, in which all interacting preys were tested against each individual pool member (an exemplary result is shown in Figure 5A). The initial screens were performed in quadruplicates (cut-offs for retest: ≥3x growth or ≥2x growth and ≥1x *lacZ* positive), and the retests were done in quintuplicates. In total, 449 wild-type and 22 mutant proteins (baits) were screened for interactions against a library of 15,863 proteins (preys), i.e. more than 7.4 million protein pairs were tested for interactions. Finally, 18,663 protein-protein interactions (PPIs) connecting 3,728 proteins were identified, of

which 16,353 PPIs involved only wild-type proteins and 2,310 PPIs involved mutant proteins. The identified interactions can be combined into a network by considering the interactions as edges and the connected proteins as nodes. This revealed one giant network of 18,662 interactions between 3,726 proteins and a single isolated network of two proteins (Figure 5B)[1].

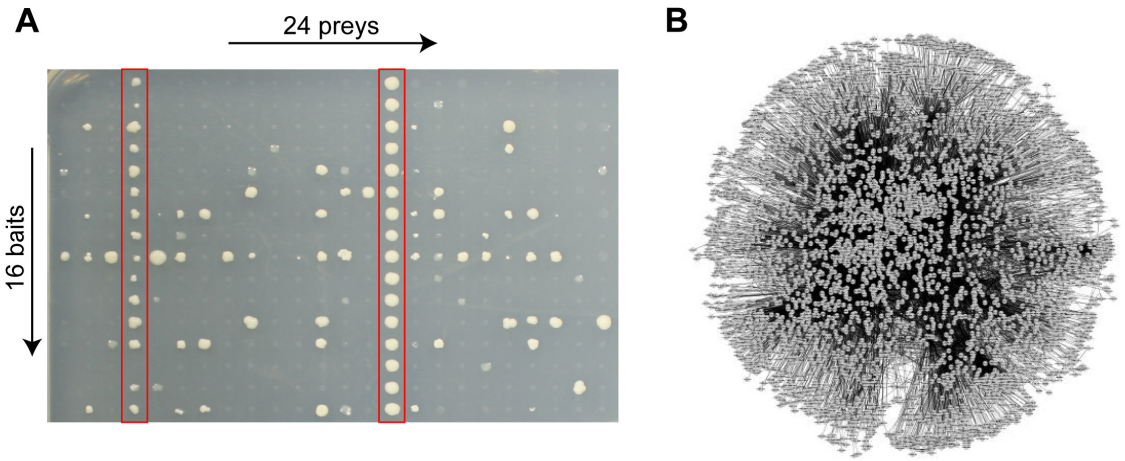

Figure 5: A PPI network for proteins involved ND process identified by automated Y2H screens. (A) A representative picture of results obtained in retest experiments, where the identified interaction partners are tested against the single bait proteins of each pool. In this case 2 of the 24 tested prey proteins were probably autoactive (marked with red boxes), because they interacted with a majority of the tested bait proteins. (B) Graphical representation of the identified Y2H network. In total, 18,663 interactions (edges) connect 3,728 proteins (nodes).

Structural analysis of the resulting neurodegenerative disease network of 18,663 PPIs with the NetworkAnalyzer plugin of Cytoscape revealed an average shortest path length between any two proteins of 3.41 interactions (Figure 6A) [229]. This means that the presented network is highly connected and fulfils the small world property [230], a characteristic feature of many

[1] The table with the identified interactions can be found online: http://141.80.164.19/y2h_network/ppi_search.php. The web page is currently password protected. The password can be requested from me (jennyruss@gmx.de).

networks such as the scientific collaboration networks [231] and several PPI networks [190, 232]. In the network each protein has about 10 interaction partners on average, which supports the observation that it is a high-density network. Additionally, I analyzed whether the network is scale-free by determining the degree distribution of the proteins in the network [233]. As expected for scale-free networks, the analysis showed a slow, power-law-related decrease for the network proteins (Figure 6B). Networks that are characterized by a power-law degree distribution are highly non-uniform: most of the nodes have only a few links, while a few nodes have very large number of links (so called hubs), which hold the other nodes together [233]. Additionally, I found that the network contains 200 hub-proteins with more than 30 interaction partners and 1,030 proteins with just one interaction partner. A scale-free network is assumed to be more robust against random perturbations [234]. It is also interesting to identify regions in the network where proteins form cluster [233]. To assess this network characteristic, the average clustering coefficients for each protein were calculated. In my network with proteins potentially involved in NDs the clustering coefficients decrease with an increasing number of interaction partners of a protein (Figure 6C), which suggests a hierarchical network architecture [235]. This supports the previously published observation, that protein networks have two levels of organization: level 1 - the global organization by hub-proteins and level 2 - local organization modules represented by protein clusters, which are connected by hubs [190]. Finally, I also analyzed the extent to which the proteins in the network share interaction partners with other nodes, which is displayed by the topological coefficient (TC) for each protein in the network. In the identified PPI network the TC decreases with an increasing number of interaction partners (Figure 6D), showing that hub-proteins only share few interaction partners. This indicates that the hub-proteins are distributed throughout the network and do not cluster together.

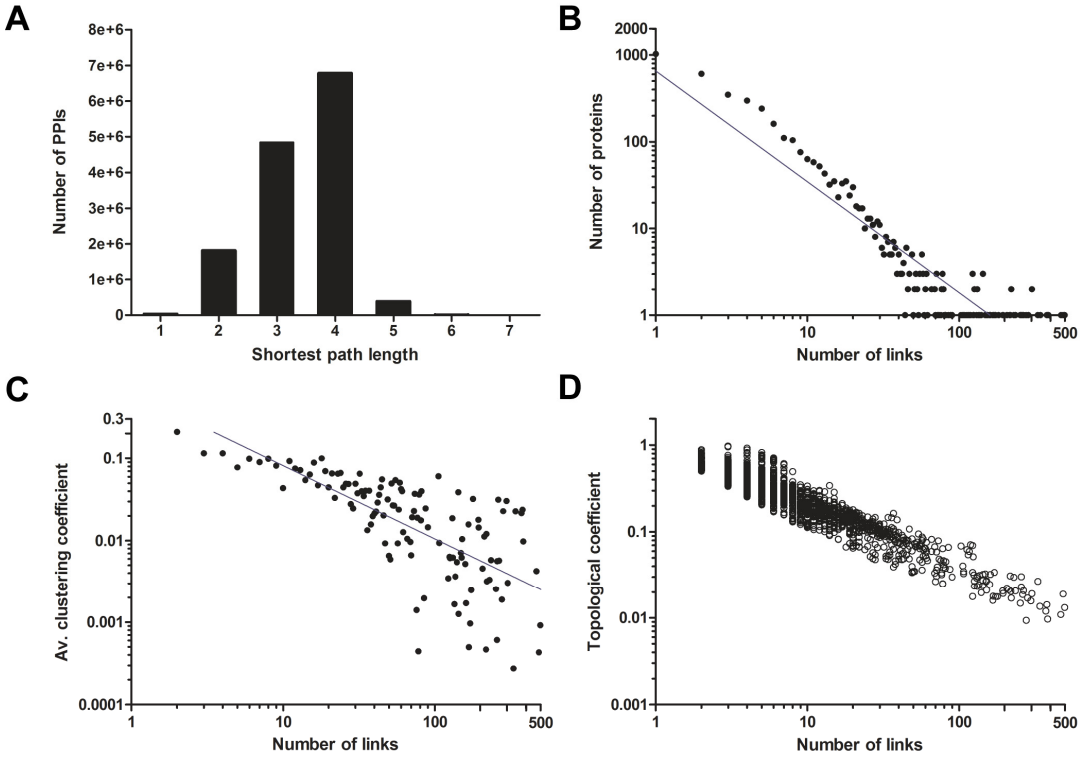

Figure 6: Structural properties of the Y2H PPI network were examined with the NetworkAnalyzer plugin of Cytoscape [229, 236]. (A) Distribution of the shortest path length between pairs of proteins in the Y2H network. On average, any two proteins in the network are connected via 3.41 links. (B) Degree distribution of the network proteins. Number of proteins with a given link x in the network approximates a power law ($y=651.78*x^{-1.265}$). (C) Degree distribution of the clustering coefficients of the network proteins. The average clustering coefficient of all nodes approximates a power law ($y = 0.592*x^{-0.872}$). (D) Distribution of the topological coefficients of the network proteins.

2.1.5 Predicting high confidence Y2H interactions

To score the confidence of experimentally derived Y2H interactions a machine learning based method was developed (together with M. Schaefer, Andrade lab MDC Berlin-Buch). The method is a support vector machine (SVM) based approach to obtain a comprehensive PPI score, which reflects the confidence of each individual interaction and combines five individual sub-scores. As described in the Methods section (4.2.5.2) the five sub-scores included Gene Ontology semantic similarity, complementarity of protein domains, co-

expression of genes/proteins, number of orthologous interactions and network distance of proteins. The SVM decision function was used to categorize each interaction into two classes – high confidence (HC) and lower confidence (LC).

Using the established scoring system 5,967 (32.5%) of all 18,663 PPIs were predicted to be HC interactions, whereas 12,595 (67.5%) were LC PPIs (Figure 7). Homodimers could not be scored and accounted 101 interactions. In the data set of HC PPIs 803 (13.2%) were identified as previously published interactions, while in the LC PPI set only 7% (886) published PPIs were found (Figure 7). This indicates that the established scoring system is of good quality and enriches known interactions in the HC PPI data set. The analysis also revealed that the interaction screens detected 10.1% (1,719 PPIs) of all previously published interactions with the selected bait proteins (17,005 PPIs - which were identified with diverse methods). However, focusing on Y2H data 44.7% (3,849 PPIs) of the previously published interactions were identified with this approach.

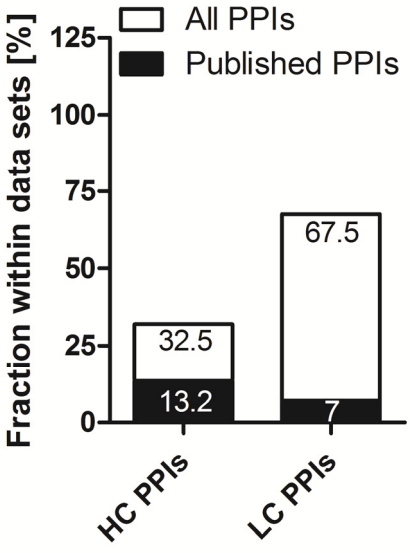

Figure 7: Prediction of high confidence (HC) and lower confidence (LC) PPIs. 32% of all identified PPIs were HC interactions, whereas 67.5% were LC PPIs. In comparison to the identified LC PPIs (7% previously published), almost twice as many HC PPIs were previously published (13.2%).

2.1.6 Validation of Y2H interactions in mammalian cells with LUMIER

The LUMIER assay was adapted for high-throughput validation of Y2H interactions (Figure 40) [237, 238]. Briefly, each protein-coding cDNA was shuttled into two mammalian expression vectors (pPA-Reni-DM and pFireV5-DM). Then, protein A (PA)-Renilla luciferase (RL)-tagged fusion proteins were co-produced with firefly luciferase (FL)-tagged putatively interacting proteins in HEK293 cells. After 48 h protein complexes were co-immunoprecipitated from cell extracts in IgG-coated 384-well plates. After several washing steps interactions between bait (PA-RL fusion proteins) and prey proteins (FL fusion proteins) were monitored by quantification of firefly luciferase activity. The LUMIER assay was performed in both orientations (either protein immobilized) with triplicates of each. An interaction was accepted as positive if at least in one orientation two of the three repetitions were positive. As described in section 4.2.2.5 three protein pairs (A) PA-RL-X + FL-Y, (B) PA-RL + FL-Y and (C) PA-RL-X + FL were individually co-produced in HEK293 cells to investigate the interaction between proteins X and Y. R-op and R-ob binding ratios were obtained by dividing the firefly luminescence activity measured in sample A by activities found in samples B (R-op) and C (R-ob). R-op and R-ob binding ratios of >1.5 were determined as threshold for reliable, specific protein-protein interactions.

In a first step, the adapted LUMIER assay was tested using 83 well described protein-protein interactions from a “Golden positive set”, which were found in more than one peer-reviewed publication [239, 240]. It was possible to detect 70 of these PPIs as positives in this assay, resulting in a validation rate of 84.3%. The result suggests that the established LUMIER assay works well for the validation of PPIs.

Next, the adapted LUMIER assay was used to validate a representative subset of interactions from the Y2H screen. The interactions taken for validation were selected by the following priorities: PPIs of targets for which wild-type and

mutant constructs had been screened in the Y2H assay were validated with first priority, followed by interactions of known important disease proteins and risk factors of neurodegenerative diseases. Based on these criteria 1,341 PPIs were tested in the modified LUMIER assay (561 HC PPIs / 780 LC PPIs), which covered 8.1% (HC: 10.8% / LC: 6.9%) of the identified Y2H interactions (Figure 8). The average validation rate for the tested interactions in the LUMIER assay was 48%. Finally, I assessed the quality of the confidence scoring system using the LUMIER validation results. 321 PPIs (57.2%) of the HC PPI data set were successfully validated, whereas only 323 LC PPIs (41.4%) were reproduced with the LUMIER assay (Figure 8). Therefore, the validation rate is significantly higher for HC than for LC interactions ($p < 0.0001$, Fisher's exact test).

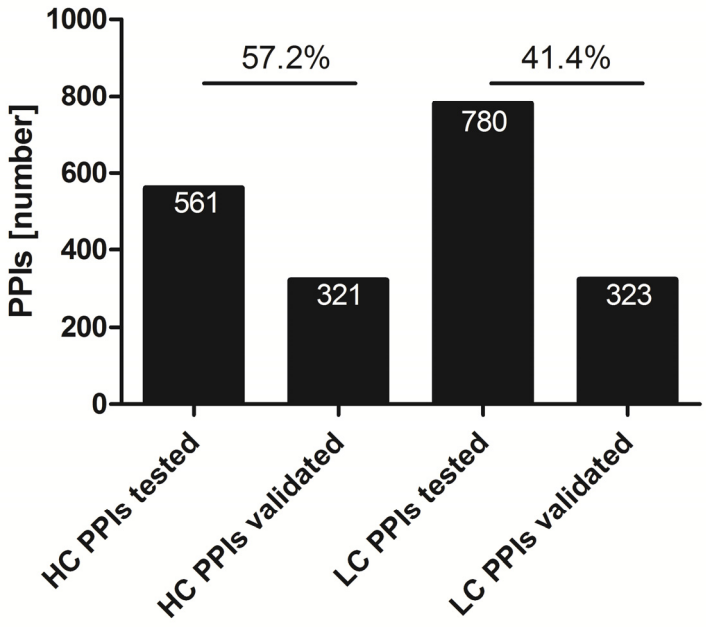

Figure 8: Validation of identified Y2H interactions with a modified LUMIER assay. The number of validated PPIs among the tested HC interactions (57.2%) was significantly higher than for the LC PPIs ($p < 0.0001$, Fisher's exact test).

As described above a large set of Y2H interactions was validated with the LUMIER assay in HEK293 cells. Next, I specifically analyzed the LUMIER data obtained with different variants of TDP-43. TDP-43 is the main component of ubiquitinated aggregates in sporadic and familial ALS as well as in some cases

of FTLD [37, 38]. Moreover, mutations in TDP-43 cause familial ALS and FTLD [154]. In case of TDP-43, 108 interactions (80 HC PPIs, 28 LC PPIs) were tested with the LUMIER assay and 80 PPIs (74.1%; HC: 65 (81.3%); LC: 15 (53.6%)) could be validated (Figure 9). Interestingly, the validation rate for the two ALS-causing mutant variants of TDP-43 (Q331K: 26 of 27 (96.3%); M337V: 10 of 11 (90.9%)) was significantly higher ($p < 0.0001$, Fisher's exact tests) than for wild-type TDP-43 (44 of 70 (62.9%)). This suggests that the interactions of the two mutants might be stronger or less transient than the interactions of wild-type TDP-43.

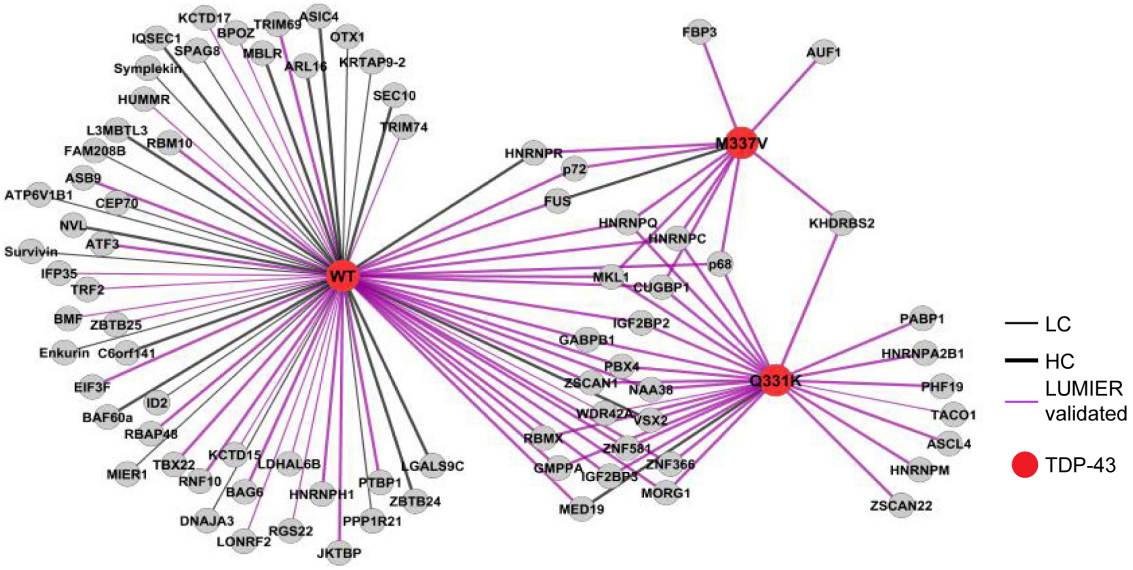

Figure 9: Validation of TDP-43 interactions with the LUMIER assay. The shown network contains 108 tested PPIs for wild-type (WT) TDP-43 and mutant TDP-43 (Q331K and M337V). The validated interactions are shown as violet lines. Abbreviations: HC – high confidence PPIs; LC – lower confidence PPIs.

2.1.7 PHF19 specifically interacts with mutant TDP-43 in mammalian cells

In the previous section I described that the adapted LUMIER assay works very well for the validation of PPIs identified in automated Y2H screenings. Next, I took advantage of the LUMIER assay to identify wild-type or mutant specific TDP-43 interactions in mammalian cells. I specifically analyzed TDP-43 interactions, because a large set of TDP-43 Y2H interactions could be validated

with the LUMIER assay and it was shown previously that the ALS protein FUS interacts more strongly with mutant TDP-43 [171]. For that, I tested a set of 40 high confidence (HC) Y2H interactions of TDP-43, in the LUMIER assay with wild-type (wt) and mutant variants of the TDP-43 protein (Q331K and M337V). In the first experiment 8 mutant/wt-specific PPIs were identified for TDP-43 (hnRNP Q, PHF19, GMPPA, ZNF581, NAA38, PCGF6, TRIM69 and MED19) with this approach. To further validate these results the LUMIER experiment was repeated with the 8 identified interactions (Figure 10). Just the interactions detected as specific in both experiments were accepted as specific for the wild-type or mutant protein. Seven proteins either interacted with all three variants of TDP-43 (hnRNP Q, NAA38 and TRIM69) or with wild-type TDP-43 and with one of the two mutants (Q331K: GMPPA, ZNF581 and PCGF6; M337V: MED19). In contrast, the PHD finger protein PHF19 specifically interacted with TDP-43_Q331K and TDP-43_M337V but not with wild-type TDP-43 (Figure 10A).In the Y2H screen PHF19 was also seen to specifically interact with the mutant TDP-43_Q331K. PHF19 was previously shown to interact with two components (EZH2 and EED) of the chromatin-remodelling complex PRC2, which is required for transcriptional repression [241]. Therefore, PHF19 might regulate the function of this protein complex and the interaction with mutant TDP-43 might disrupts the function of the PRC2 complex.

Analysis of the Renilla and firefly luminescence before co-immunoprecipitation (input) revealed that both bait (Renilla luciferase-tagged wild-type and mutant TDP-43) and prey proteins (firefly luciferase-tagged PHF19) were produced at similar levels in HEK293 cells during the LUMIER assay (Figure 10B). These results ensure that the interaction between wild-type TDP-43 and PHF19 was not identified because one of the proteins was not produced, but because the two proteins do not interact.

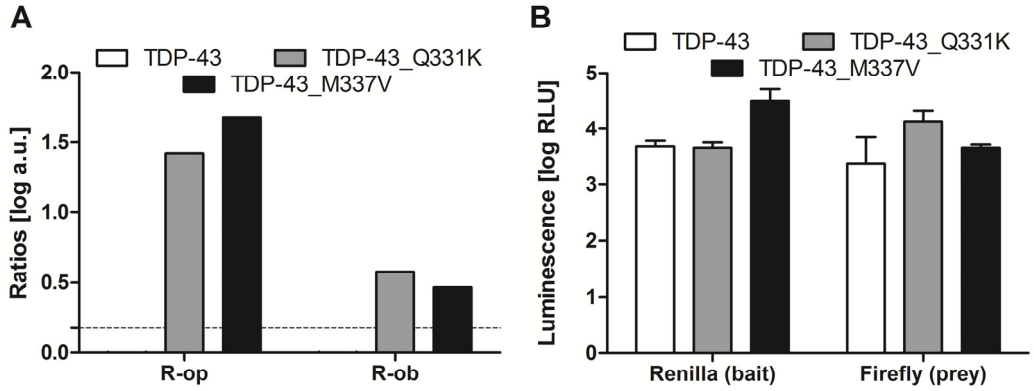

Figure 10: PHF19 specifically interacts with mutant TDP-43 in mammalian cells. (A) Mean log(R-op) and log(R-ob) values for the tested interactions between the three forms of TDP-43 and PHF19 are shown. PHF19 specifically interacts with TDP-43_Q331K and TDP-43_M337V (R-op and R-ob < log(1.5) in case of wild-type TDP-43). (B) Bait and prey proteins were produced at similar levels in HEK293 cells. Production was estimated by measuring Renilla and firefly luminescence. Error bars indicate standard deviation (n = 3).

2.1.8 Validation of high-confidence TDP-43 interactions by co-immunoprecipitation experiments

Four LUMIER validated HC interactions of wild-type TDP-43 (FUS, IGF2BP2, RbAp48, and NAA38) were further investigated with co-immunoprecipitation (Co-IP) experiments. The Co-IP experiments were based on endogenous proteins and were performed using the neuroblastoma cell line SH-SY5Y. Proteins were selected for Co-IPs when they were expressed in the human brain (The Human Protein Atlas [242]) and when an antibody was available.

Co-IPs of endogenous proteins were performed by incubating fresh SH-SY5Y cell lysates first with specific antibodies for 3 h and then additionally with protein G-coated Dynabeads® for 1 h (for more details see section 4.2.2.7). PPIs were then analyzed by SDS-PAGE and Western blotting. The interaction of TDP-43 and the hnRNP protein FUS (Figure 11) was used as a positive control. FUS, like TDP-43, is an ALS and FTLD disease protein [150, 153]. Its interaction with TDP-43 was first identified with a mass spectrometry-based method (SILAC-TAP) and validated among others by endogenous Co-IPs from HeLa cells [171].

In this study, it was possible to validate the interaction between TDP-43 and the insulin growth factor-II mRNA-binding protein family member IGF2BP2 (Figure 11). This interaction was also previously detected by SILAC-TAP but was not verified with other methods [171]. Additionally, I validated the newly identified interaction between TDP-43 and RbAp48, a Mi-2/nucleosome remodelling and deacetylase (NuRD) complex member, by Co-IPs (Figure 11) [243, 244]. The Mi-2/NuRD protein complex is implicated in chromatin remodelling and transcriptional repression, supporting the hypothesis that TDP-43 plays a functional role in transcriptional regulation and chromatin remodelling. Finally, the interaction of TDP-43 and NAA38 was not successfully validated here as the protein was not detectable in SH-SY5Y cells.

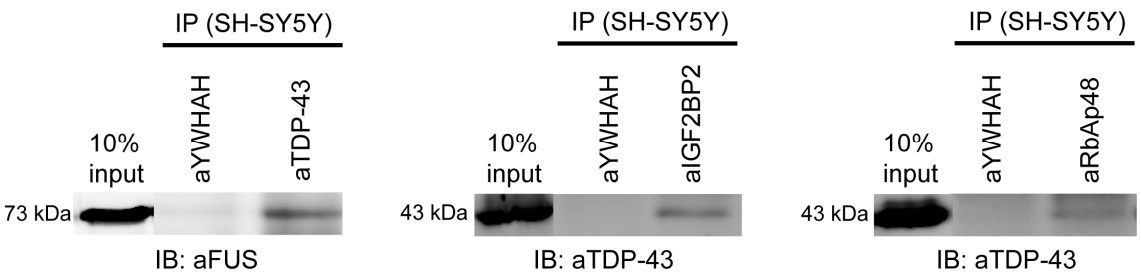

Figure 11: Validation of the interactions between TDP-43 and FUS (anti-FUS), IGF2BP2 (anti-TDP-43) and RbAp48 (anti-TDP-43) by co-immunoprecipitation of endogenous proteins. Immunoprecipitations (IPs) from SH-SY5Y cell lysates were performed with antibodies against TDP-43, IGF2BP2, RbAp48 and 14-3-3-eta (YWHAH; control antibody). Immunoblotting (IB) was performed with antibodies against FUS and TDP-43.

2.2 Bioinformatic analyses of high confidence PPI networks for neurodegenerative diseases

The high confidence (HC) interactions described in the previous chapter provide a basis for more detailed investigation into the biological relevance of the identified interactions. Therefore, the analyses described in this chapter focuses primarily on HC protein-protein interactions (PPIs). This chapter includes a comparison of wild-type and mutant HC PPI networks with a specific focus on

TDP-43 and the identification of four proteins that link five different neurodegenerative diseases (AD, ALS, HD, PD and SCA1) to each other.

2.2.1 Comparison of the wild-type and mutant Y2H PPI networks

As described in section 2.1.5 the interactions identified with the Y2H system were devided into two groups: high confidence (HC) and lower confidence (LC) PPIs. A comparison of the interactions that have been detected with mutant or wild-type baits revealed similar rates of HC interactions (wild-type PPIs: 38.2% (788 PPIs); mutant PPIs: 39.0% (567 PPIs); Figure 12A). However, I found that the rate of published interactions in these data sets is slightly higher for mutant interactions than for wild-type interactions. As expected a higher number of previously identified interactions were identified in the data sets of both wild-type and mutant HC interactions compared to LC interactions. This readily confirms the analysis shown in Figure 7, which did not differentiate between wild-type and mutant Y2H PPIs. Thus, this analysis indicates that both wild-type and mutant bait proteins produce Y2H interaction data of very similar quality.

Next, I analyzed whether the wild-type and mutant bait proteins reveal overlapping Y2H HC PPI data sets (Figure 12B). I found that 78% (442 PPIs) of the mutant PPIs were also identified with wild-type bait proteins, indicating that most prey proteins can be identified with both wild-type and mutant bait proteins. However, 145 PPIs (22%) were exclusively detected with mutant baits and 366 PPIs (43.9%) with wild-type baits, indicating that wild-type baits detect a significantly higher number of interactions than mutant NDPs ($p = 0.0015$, Fisher's exact test). This suggests mutations in NDPs more likely cause a disease phenotype by a loss-of-function rather than a gain-of-function mechanism.

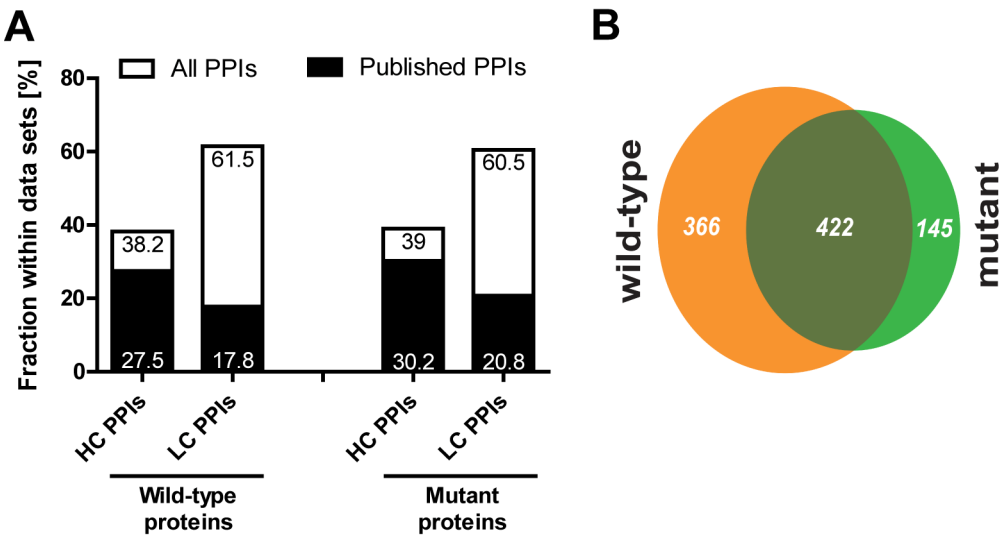

Figure 12: Comparison of Y2H interaction networks generated with wild-type and mutant NDPs. (A) The rate of high confidence (HC) interactions was comparable among the corresponding wild-type and mutant PPIs and the number of published interactions was markedly higher among the HC interactions for both wild-type and mutant PPI networks. (B) 78% of the mutant HC interactions overlapped with the corresponding wild-type interactions. The rate of wild-type specific interactions (43.9%) was significantly higher than the rate of mutant specific interactions (22%). Abbreviations: LC – lower confidence; wt – wild-type.

The analysis of HC Y2H PPIs above strongly indicates that wild-type and mutant NDPs yield overlapping but also unique interaction partners (Figure 12). To gain further insight into disease mechanisms, subnetworks for specific NDPs were analyzed in more detail. Initially, the number of wild-type and mutant PPIs of each NDP was ascertained (independent of the number of mutants screened). The results are summarized in Table 4. Interestingly, for most of the mutant proteins fewer interaction partners were identified than for the corresponding wild-type proteins (e.g. APP and parkin). Exceptions were the proteins α-synuclein and ataxin-1, suggesting that mutations in these two proteins cause disease by a gain-of-function rather than a loss-of-function mechanism. In all cases, more than 50% of interactions were shared by both the mutant and wild-type forms of a protein. The proteins FUS (36.4%) and α-synuclein (35.1%) showed the highest rate of mutant specific interactions, whereas no mutant specific interactors could be identified for presenilin 1,

LRRK2 and ataxin-3. In contrast, the number of wild-type specific interactions ranged from 14.5% for ataxin-1 to 85.7% for ataxin-3 and therefore varied widely for different individual NDPs.

Table 4: Number of HC wild-type, mutant and overlapping PPIs for each NDP identified with the Y2H system. In brackets the rates of wild-type-specific, mutant-specific and mutant interactions overlapping with corresponding wild-type PPIs are shown.

Disease	Protein	Wild-type PPIs	Mutant PPIs	Overlapping PPIs
AD	APP	166 (64.5%)	74 (20.3%)	59 (79.7%)
AD	Presenilin 1	11 (54.6%)	5 (0%)	5 (100%)
ALS	FUS	11 (36.4%)	11 (36.4%)	7 (63.6%)
ALS	SOD1	26 (23.1%)	23 (13%)	20 (87%)
ALS	TDP-43	95 (34.7%)	78 (20.5%)	62 (79.5%)
HD	Huntingtin	227 (35.7%)	173 (15.6%)	146 (84.4%)
PD	LRRK2	2 (50%)	1 (0%)	1 (100%)
PD	Parkin	73 (74%)	26 (26.9%)	19 (73.1%)
PD	α-synuclein	66 (27.3%)	74 (35.1%)	48 (64.9%)
SCA1	Ataxin-1	83 (14.5%)	98 (27.5%)	71 (72.5%)
SCA3	Ataxin-3	28 (85.7%)	4 (0%)	4 (100%)

For some of the NDPs several variants with point mutations were screened for protein-protein interactions. This included α-synuclein, SOD1 and TDP-43. A detailed analysis of TDP-43 interaction partners follows in the next section.

As described in section 2.1.3 the two mutant variants A30P and E46K of α-synuclein were screened for interactions in addition to the wild-type protein. In total 66 interactions were identified for the wild-type protein, whereas 68 PPIs were found with the A30P variant and only 19 PPIs were detected for α-synuclein E46K (Figure 13A). The fact that very different numbers of interaction

partners were identified with mutant and wild-type α-synuclein proteins, which also very likely have different cellular functions, is in agreement with previous reports indicating that different mutant α-synuclein variants might cause different forms of synucleinopathies (A30P: Parkinson's disease and E46K: Lewy body dementia with parkinsonism [14, 196]). I suggest that based on the identified interaction partners that the A30P mutation might cause a gain-of-function phenotype, while the E46K mutation might lead to a loss-of-function phenotype.

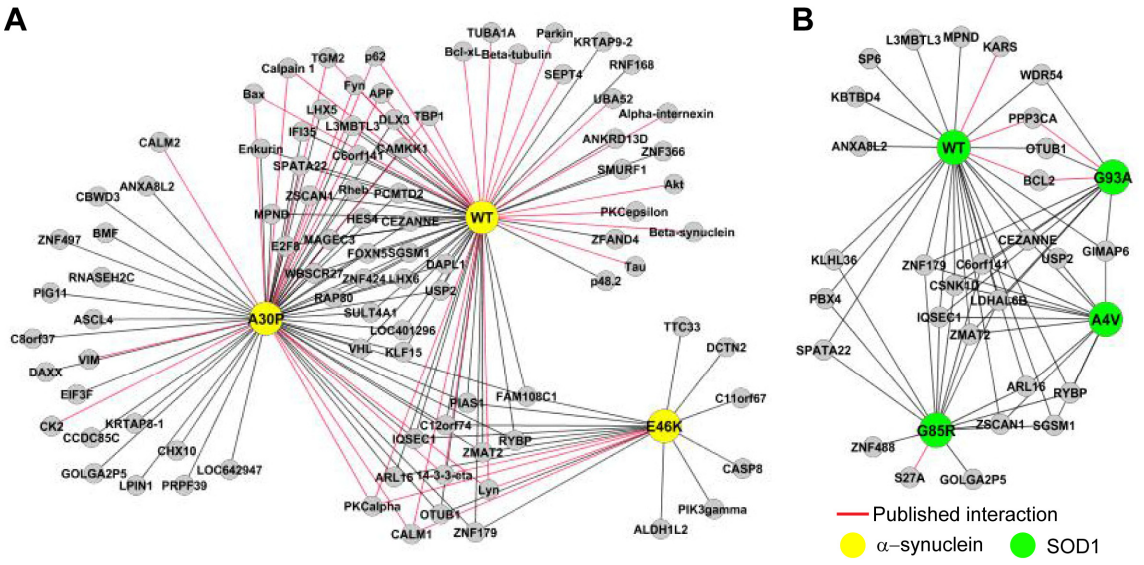

Figure 13: Interactions identified for wild-type and mutant variants of (A) α-synuclein and (B) SOD1. In both cases the different mutations lead to alterations in terms of interaction partners. Abbreviation: WT – wild-type.

In comparison to the wild-type SOD1 protein (26 PPIs) fewer interactions could be identified for all three selected SOD1 mutants (A4V (13 PPIs), G85R (16 PPIs) and G93A (11 PPIs)) as shown in Figure 13B. Interestingly, mutant specific PPIs could only be detected for the G85R variant (18.8% (3 PPIs)) and just six wild-type specific PPIs were found in total for SOD1. This indicates that the three SOD1 mutations lead to a loss-of-function phenotype in terms of protein-protein interactions.

2.2.2 Identification of functionally distinct interaction partners for wild-type and mutant neurodegenerative disease proteins

Next, the HC Y2H networks generated for wild-type and mutant NDPs were investigated for enrichment of protein and/or pathways that are abnormally altered in patients with NDs. A GO term enrichment analysis (only biological process categories were considered) was performed with the Cytoscape plugin BinGO for the two networks and the results are depicted in Figure 14. I found that GO terms with disease relevance (e.g. cell death, transcription and RNA splicing) were found to be significantly enriched among the HC interactors of mutant NDPs compared to HC interactors of wild-type proteins, indicating that abnormal interactions between mutant NDPs and proteins involved in key cellular processes might contribute to the disease phenotype in NDs (Figure 14). The statistical significance of this analysis was evaluated with Fisher's exact tests. GO terms related to transcription and protein production like "regulation of transcription" ($p < 0.0001$), "RNA splicing" ($p < 0.0001$), and "mRNA stabilization" ($p = 0.0239$) as well as cell death related terms such as "regulation of programmed cell death" ($p = 0.0032$), "cell death" ($p = 0.017$), and "apoptotic mitochondrial changes" ($p = 0.0494$) were significantly enriched in the PPI data set, which was obtained with mutant NDPs. In addition, neuronal development related terms (e.g. "neurogenesis" ($p = 0.0099$) and "regulation of NS development" ($p = 0.0067$)) and other functional categories which are not immediately related to neurodegenerative diseases like "intracellular signaling" ($p < 0.0001$) and "DNA repair" ($p < 0.0001$) were also enriched among the mutant protein interactors. These results indicate that mutations in NDPs such as TDP-43, α-synuclein, SOD1 or APP yield HC Y2H PPI networks that are functionally different to networks that are obtained with wild-type NDPs.

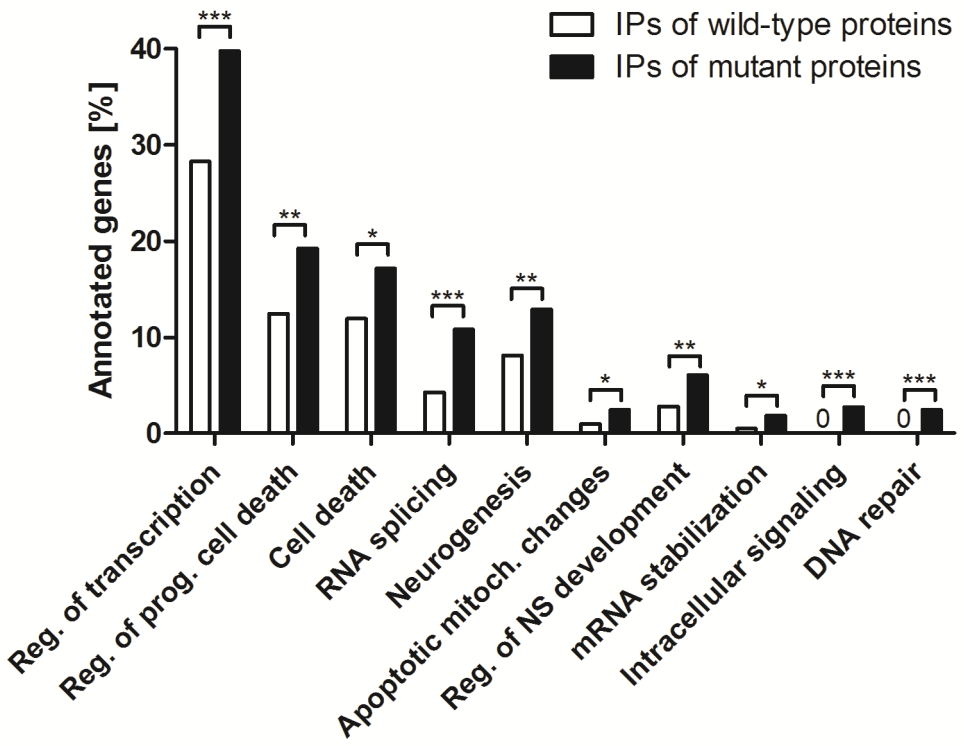

Figure 14: Functional enrichment analysis of wild-type and mutant HC PPI networks. Biological process-related over-represented GO terms were identified with the Cytoscape plugin BinGO in both networks and significance of enrichment was assessed by Fisher's exact tests (*p < 0.05; **p-value < 0.01; ***p-value < 0.001). Abbreviations: IPs – interaction partners.

Along with wild-type TDP-43, two disease-causing mutants (Q331K and M337V) were screened for interactions using the Y2H system. In total, 96 high confidence PPIs were detected for wild-type TDP-43. In comparison, fewer interactions were found for the mutant proteins (Q331K: 71 PPIs; M337V: 23 PPIs; see Figure 15A). The strong difference in number of interactions for the two mutants compared to wild-type TDP-43 suggests a loss-of-function phenotype. Moreover, the lower number of PPIs identified with the M337V mutant compared to the Q331K mutant seems to be in agreement with the fact that the Q331K mutation is associated with sporadic ALS, whereas the M337V mutation is associated with familial ALS [15]. No such agreement could be found when considering the aggregation propensity or the toxicity of the two mutant variants as it was shown that TDP-43_Q331K consistently forms more

aggregates and is more toxic to yeast cells than the TDP-43_M337V protein [219]. Additionally, significantly more wild-type specific interactions (34.4% (33 PPIs)) could be identified than mutant specific ones (Q331K: 18.3% (13 PPIs; p = 0.0151, Fisher's exact test); M337V: 17.4% (4 PPIs; p = 0.009, Fisher's exact test)).

When comparing the functional annotations (Gene Ontology and literature information) of the interactors of wild-type TDP-43 with those of the two mutants, it is apparent that significantly more of the wild-type interactors play a role in protein degradation (14 PPIs (14.7%, wild-type), while only a few proteins with such a cellular function were detected with the mutant variants (Q331K: 2 PPIs, 2.8%; M337V: 1 PPI, 4%; shown in Figure 15). This suggests that the degradation of the mutant proteins might be disturbed in ALS patients, which might lead to increased protein aggregation, which is a characteristic feature in patients [37, 38]. Indeed, previous studies showed that ALS-associated mutations in TDP-43 increase its stability [171]. In contrast the percentage of proteins associated with a function in transcription was very similar for the interactors of the three proteins (wild-type: 30.5% (29 PPIs); Q331K: 36.6% (26 PPIs); M337V: 26.1% (6 PPIs); Figure 15). This indicates that the function of TDP-43 as transcriptional regulator is not disturbed by the mutations.

Finally, I found that in comparison to the wild-type protein and the Q331K mutant a significantly higher fraction of TDP-43_M337V interactors were associated with RNA processing (wild-type: 26.3% (25 PPIs); Q331K: 26.8% (19 PPIs); M337V: 56.5% (13 PPIs); see Figure 15). As TDP-43 is known to be involved in RNA processing, these results suggest that the function of TDP-43 in RNA processing might be disturbed in case of the M337V mutant protein.

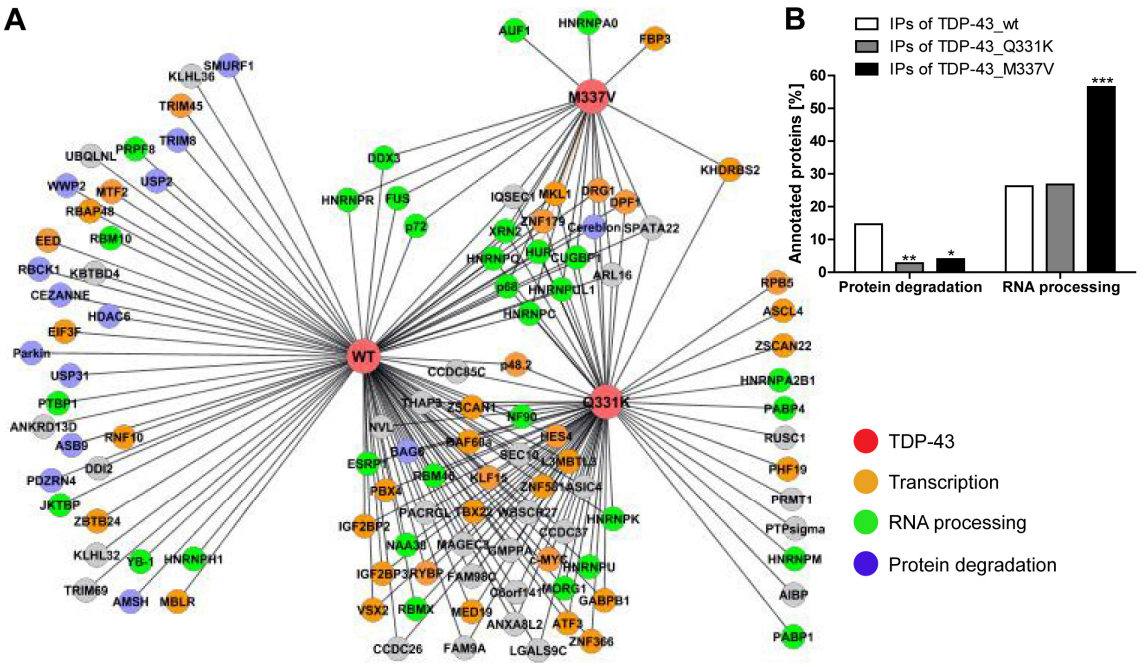

Figure 15: Identification of HC PPIs for wild-type and mutant TDP-43 proteins. (A) Network of HC interactions generated with wild-type (WT) TDP-43, TDP-43_Q331K and TDP-43_M337V proteins as baits. The interactors were functionally annotated according to Gene Ontology and literature information and the functions were summarized to three main groups (transcription, RNA processing and protein degradation). (B) The fraction of interaction partners (IPs) with a function in protein degradation is significantly higher for wild-type proteins than for mutant TDP-43 proteins. In comparison, significantly more IPs involved in RNA processing were found for TDP-43_M337V than for wild-type TDP-43 or the mutant variant Q331K. The significance was assessed by Fisher's exact tests (*p < 0.05; **p < 0.01; *** p < 0.001).

2.2.3 Connecting neurodegenerative disease proteins via common HC interaction partners

One of the main objectives in this study was to utilize comprehensive PPI networks to identify new proteins that play a role in different NDs. Therefore, ND-specific PPI networks for Huntington's disease (HD; 254 PPIs), spinocerebellar ataxia type I (SCA1; 112 PPIs), Parkinson's disease (PD; 218 PPIs), amyotrophic lateral sclerosis (ALS; 201 PPIs), and Alzheimer's disease (AD; 201 PPIs) were generated using the available HC Y2H interactions (Figure 16). In this study the term "common interaction partner of neurodegenerative disease proteins (NDPs)" was defined as a protein that associates with different NDPs and

thereby might link the disease processes in different NDs. By filtering all five ND-specific networks for interaction partners of NDPs found in all five networks, I identified four proteins (APP, IQSEC1, ZNF179 and ZMAT2) connected all five NDs (Figure 16). The interactions of the four proteins with wild-type and mutant NDPs are summarized in Appendix 5.2.

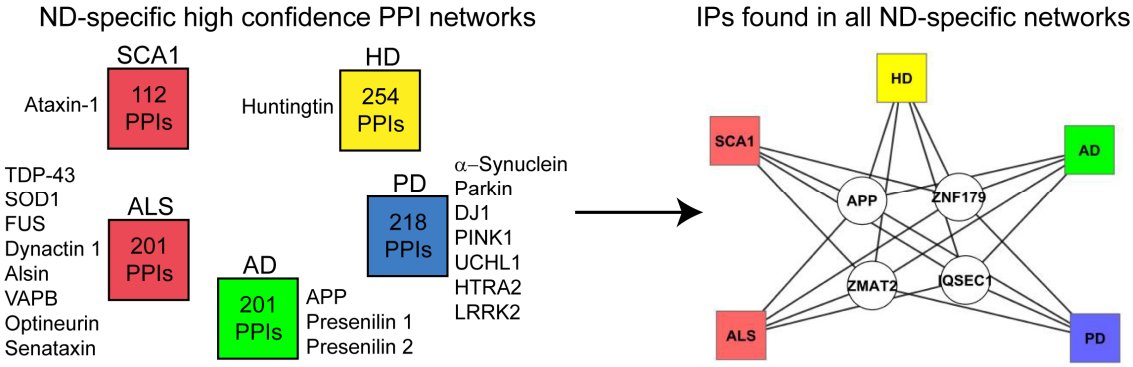

Figure 16: APP, IQSEC1, ZNF179 and ZMAT2 connect five different neurodegenerative diseases. Five ND-specific HC PPI networks were generated from HC PPIs identified with the listed NDPs. The networks were filtered for interaction partners (IPs) of NDPs common to all five networks. This resulted in the depicted protein-disease network.

The amyloid precursor protein APP is involved in synaptic formation as well as repair and APP expression is upregulated during neuronal differentiation and after neural injury [130, 245]. Roles in cell signalling, long-term potentiation, and cell adhesion have also been proposed for APP [246]. The ARF-GEP$_{100}$ protein (IQSEC1) is involved in signal transduction. It is a guanine nucleotide exchange factor that promotes binding of GTP to the ADP ribosylation factor protein ARF6 [247]. IQSEC1, by activation of ARF6, is therefore involved in the control of processes such as endocytosis of plasma membrane proteins, E-cadherin recycling and actin cytoskeleton remodelling [248]. ZNF179 is a RING finger protein, which is highly expressed in the brain [249]. ZNF179 is assumed to be involved in transcriptional regulation [250], but the function is not well described. The function of the zinc finger matrin-type 2 protein (ZMAT2) is unknown. But the zinc finger of matrin-type proteins were previously found to be involved in RNA

splicing suggesting that ZMAT2 might also be involved in this process [251, 252].

To investigate whether the four proteins APP, IQSEC1, ZNF179 and ZMAT2 indeed play a role in several NDs, I analyzed their mRNA expression in PD, HD and AD patient brains from previously published data collected by NextBio Research (Figure 17) [253-258]. Strikingly, I found that all four proteins are significantly down-regulated in the caudate nucleus of HD patients compared to controls. Similarly, three of these proteins (APP, IQSEC1 and ZMAT2) were found to be abnormally down-regulated in the substantia nigra of PD patients and the hippocampus of AD patients (IQSEC1, ZNF179 and ZMAT2). In contrast, an up-regulation of APP was observed in AD brains compared to controls, confirming previously published results [259]. These results indicate that the four proteins indeed seem to play a role in the pathogenesis of several neurodegenerative diseases and are a good starting point for further investigations.

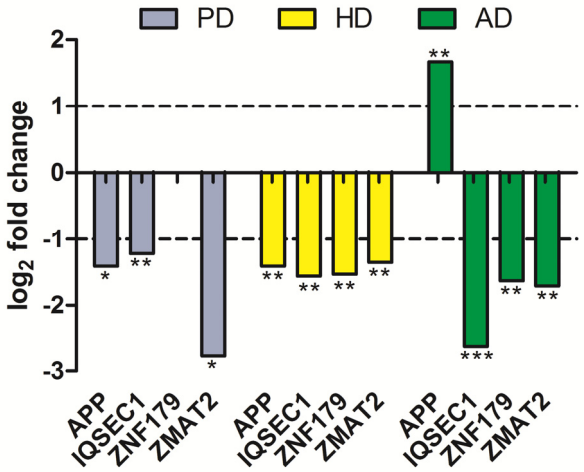

Figure 17: mRNA expression of APP, IQSEC1, ZNF179 and ZMAT2 is dysregulated in PD, HD and AD patient brains. The analysis was based on gene expression data available from NextBio Research (*p < 0.05; **p < 0.01; ***p < 0.001; Student's t-test) [254]. In case of ZNF179 no data was available from PD patient brains.

2.3 Investigating the functional role of IQSEC1, ZNF179 and ZMAT2 in neurodegenerative disease processes

In the previous chapter I described that APP, IQSEC1, ZNF179 and ZMAT2 interact with different NDPs that as mutant variants cause familial AD, ALS, HD, PD or SCA1. In the following chapter I investigated the role of IQSEC1, ZNF179 and ZMAT2 in ND processes such as protein aggregation and Aβ production. I focus on the three proteins because to date nothing is known about them in relation to NDs. All the experiments were performed in the AD cell model SH-SY5Y_APP695, which stably over-expresses APP695. This was done to have the same cell model in all experiments.

2.3.1 Knock-down of IQSEC1, ZNF179 and ZMAT2 alters the mRNA expression of several neurodegenerative disease proteins

As I explained in section 2.2.3, ZNF179 and ZMAT2 most likely play a functional role in transcriptional regulation. Moreover, gene expression changes can directly cause neurodegenerative diseases, as shown for the duplication of the *SNCA* gene, which causes increased α-synuclein protein levels in neurons and leads to autosomal dominant PD [16, 260]. Therefore, transcriptional regulation in general might be an important mechanism in neurodegenerative disease processes. Thus, it would be very interesting to know whether IQSEC1, ZNF179 and ZMAT2 that were identified by interaction network filtering (Figure 16) influence the expression of known ND genes in a neuronal cell model.

In order to analyze the effect of the three proteins IQSEC1, ZNF179 and ZMAT2 on the expression of the genes *HTT*, *ATXN1*, *TARDBP*, *APP*, *SNCA* and *PARK2*, they were knocked-down in the neuronal cell line SH-SY5Y_APP695. This to some extend recapitulates the situation in patient brains, because previous investigations indicate that expression of these genes is abnormally down-regulated in brains of PD, HD and AD patients (see Figure 17). Total RNA was isolated from the cells 72 h after transfection with siRNA pools and mRNA

levels were assessed by qRT-PCR after cDNA synthesis. In addition to the mRNA levels of the six known disease genes (*HTT*, *ATXN1*, *TARDBP*, *APP*, *SNCA* and *PARK2*) the mRNA levels of IQSEC1, ZNF179 and ZMAT2 were determined to quantify the knock-down effeciency. The qRT-PCR data was evaluated with the comparative CT method (see section 4.2.1.10). The data was first normalized to the housekeeping gene ACTB (β-actin) and then compared to the reference sample transfected with non-targeting control siRNA. Significance was assessed by Student's t-tests.

Knock-down of IQSEC1 resulted in a significantly increased expression of the genes *HTT*, *TARDBP*, *SNCA* and *PARK2* (Figure 18) in the SH-SY5Y_APP695 cell model, while IQSEC1 was down-regulated by about 78% through the siRNA treatment (Figure 18). In contrast, I found that knock-down of ZNF179 (mRNA expression reduced by 68%) significantly reduced *HTT*, *ATXN1*, *TARDBP* and *SNCA* mRNA expression. *APP* expression was also slightly reduced by ZNF179 siRNA treatment, whereas *PARK2* mRNA levels were slightly increased. Interestingly, the treatment of the samples with siRNA targeting ZMAT2 significantly enhanced the mRNA expression of all six disease genes (*HTT*, *ATXN1*, *TARDBP*, *APP*, *SNCA* and *PARK2*), while the mRNA level of ZMAT2 was decreased by 43%. In summary, these results indicate that the knock-down of IQSEC1, ZNF179 and ZMAT2 indeed changes the expression of known ND genes such as *HTT*, *SNCA* or *PARK2*. This suggests that the three proteins, which were identified by interaction network filtering, play a role in transcriptional regulation of several ND genes.

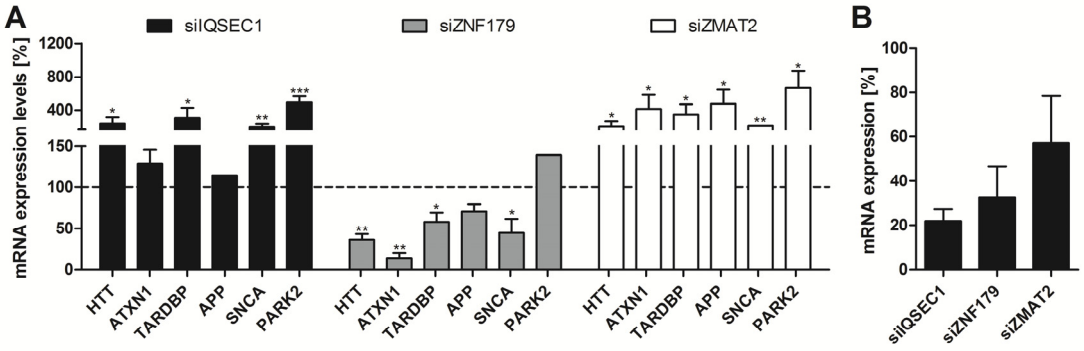

Figure 18: mRNA expression analysis of known ND genes after knock-down of IQSEC, ZNF179 and ZMAT2. (A) Treatment of SH-SY5Y_APP695 cells with IQSEC1, ZNF179 and ZMAT2 siRNA pools altered mRNA expression of ND genes (*p < 0.05; **p < 0.01; ***p < 0.001; n = 3; Student's t-test). Knock-down of ZNF179 mainly reduced expression of ND genes, whereas knock-down of IQSEC1 and ZMAT2 predominantly increased mRNA expression of ND genes. (B) mRNA expression of IQSEC1, ZNF179 and ZMAT2 after treatment with siRNA pools. siRNA treatment resulted in a knock-down efficiency of 40-80%. In both graphs error bars indicate SD values.

2.3.2 Silencing of IQSEC1, ZNF179 and ZMAT2 increases huntingtin, ataxin-1 and TDP-43 aggregation

Previous studies indicate that the NDPs huntingtin (*HTT*), ataxin-1 (*ATXN1*) and TDP-43 (*TARDBP*) form insoluble protein aggregates in Huntington's disease (HD), spinocerebellar ataxia type 1 (SCA1) and amyotrophic lateral sclerosis (ALS), respectively (see section 2.1.3). Moreover, experimental evidence was obtained that protein aggregation in patient brains and disease model systems is connected with neuronal dysfunction and toxicity [261-263]. Therefore, I analyzed the effect of IQSEC1, ZNF179 and ZMAT2 knock-down on mutant huntingtin (EYFP-HTTEx1Q79), mutant ataxin-1 (EYFP-ATXN1Q79) and wild-type TDP-43 (EYFP-TDP-43) aggregation in a mammalian cell model system. For this purpose, SH-SY5Y_APP695 cells were co-transfected with EYFP-HTTEx1Q79, EYFP-ATXN1Q79 or EYFP-TDP-43 encoding plasmid vectors and siRNA pools targeting IQSEC1, ZNF179 or ZMAT2. After 72 h of incubation the cells were fixed and aggregation of the corresponding NDPs was assessed using high content fluorescence imaging (see 4.2.3.5). Only cells with an EYFP

signal were considered and results were normalized to cells transfected with non-targeting control siRNA. The significance of changes in aggregation was assessed by Student's t-tests. The knock-down of all three proteins significantly increased aggregation of huntingtin, ataxin-1 and TDP-43 (Figure 19). These results provide strong evidence that the proteins IQSEC1, ZNF179 and ZMAT2 are potential modifiers of ND processes, which likely influence aggregation of huntingtin, ataxin-1 and TDP-43 in HD, SCA1 and ALS.

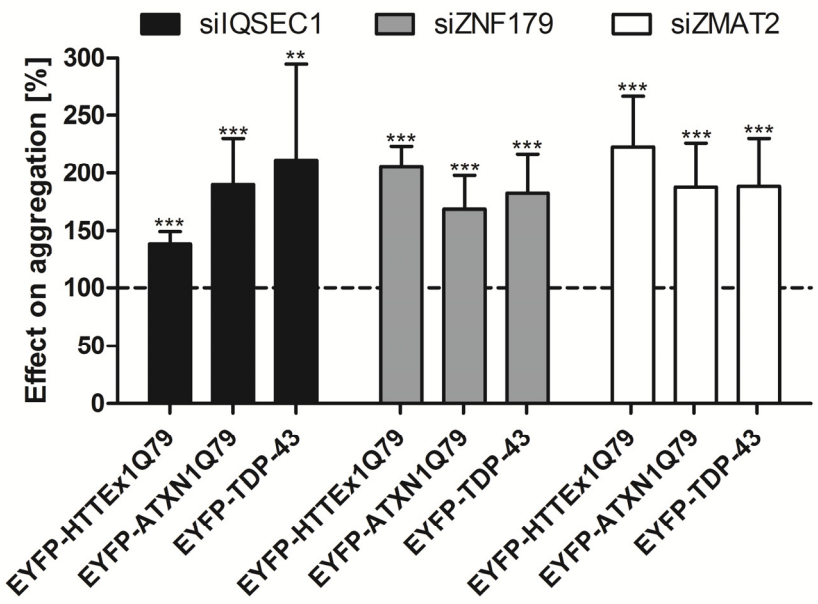

Figure 19: Silencing of endogenous IQSEC1, ZNF179 and ZMAT enhances huntingtin, ataxin-1 and TDP-43 aggregation. SH-SY5Y_APP695 cells were co-transfected with siIQSEC1, siZNF179, siZMAT2 or with siNTC together with plasmid vectors encoding EYFP-HTTEx1Q79, EYFP-ATXN1Q79 or EYFP-TDP-43. The cells were incubated for 72 h and aggregation was quantified using high content fluorescence imaging. The IQSEC1, ZNF179 and ZMAT2 knock-down resulted in a ~1.5-2-fold increase of huntingtin, ataxin-1 or TDP-43 aggregation (**p < 0.01; ***p < 0.001; n = 9; Student's t-test). The values are shown as mean+SD.

2.3.3 Knock-down of endogenous IQSEC1, ZNF179 and ZMAT2 influences Alzheimer's disease-related pathogenic mechanisms

The results presented in the previous section suggest that the proteins IQSEC1, ZNF179 and ZMAT2 might play a role in the pathogenesis of three different neurodegenerative diseases (NDs). As the mRNA expression of the three genes

was significantly altered in Alzheimer's disease (AD) brains (Figure 17) and knock-down of ZMAT2 significantly increased APP mRNA expression, the three proteins might also play a role in AD. Aβ peptides in the brains of AD patients are known to form toxic oligomeric structures and plaques [6] as well as trigger the assembly of neurofibrillary tangles, which consist of the hyperphosphorylated microtubule-associated tau protein [121, 264]. APP is a critical factor in the pathogenesis of AD, as APP undergoes post-translational processing to generate amyloid-β (Aβ) peptides [115, 130]. Therefore, I next tested the effects of IQSEC1, ZNF179 and ZMAT2 knock-down on Aβ production and the expression of total as well as of hyperphosphorylated tau.

Extracellular levels of Aβ40 and Aβ42 released from SH-SY5Y_APP695 cells into the medium were measured using an Aβ ELISA kit (Meso Scale Discovery) in order to assess the effect of siRNA treatment on APP processing. Briefly, 72 h post-transfection with siRNA pools, medium samples were collected and prepared for the Aβ ELISA according to the manufacturer's instruction. The measured raw data was normalized to the number of cells in each sample. The concentrations of the Aβ peptides were calculated from a standard curve (established with a dilution series of both peptides) and compared to cells transfected with non-targeting control siRNA. The Aβ42/Aβ40 ratio was calculated from the values of single peptides. This analysis was performed, because it is known from patients with familial AD that mutations in disease genes such as presenilin 1 influence the ratio of Aβ42/Aβ40 peptides and cause a shift towards Aβ42 in patient brains [265]. Here, I found that the knock-down of IQSEC1, ZNF179 and ZMAT2 significantly decreased extracellular Aβ40 levels (IQSEC1: -55%; ZNF179: -50%; ZMAT2: -78%; Figure 20). However, I also observed that the knock-down of the three genes either had no significant effect on Aβ42 levels (siIQSEC1) or significantly increased the extracellular levels of Aβ42 (ZNF179: +28.6% and ZMAT2: +43.4%). This gave rise to an significantly increased Aβ42/Aβ40 ratios in case of IQSEC1 (~3-fold) and

ZMAT2 (~6-fold) and an almost significant rise of the ratio in case of ZNF179 depletion (+170%). In summary, this analysis shows that the knock-down of IQSEC1, ZNF179 and ZMAT2 influence the production of Aβ peptides, resulting in the production of more aggregation-prone Aβ42 peptides [20, 131, 266]. This is in agreement with the finding that knock-down of these three genes results in an increased huntingtin, ataxin-1 and TDP-43. Thus, reduced expression of the three proteins in patient brains might influence pathogenesis in different NDs.

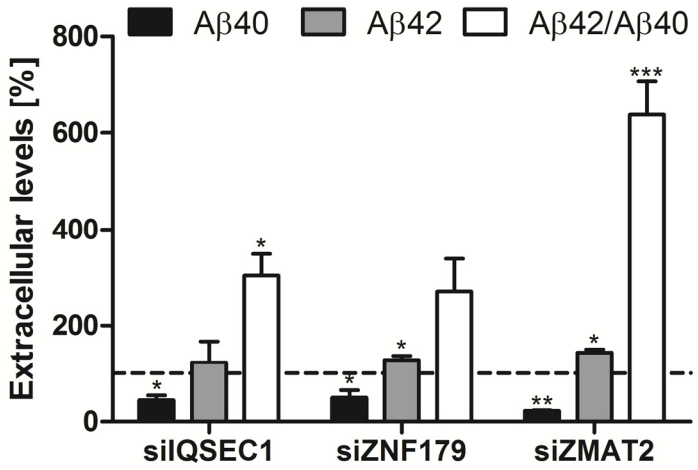

Figure 20: Quantificiation of extracellular Aβ peptide levels after silencing of IQSEC1, ZNF179 and ZMAT2 in SH-SY5Y_APP695 cells. 72 h after transfection with siRNAs the concentration of the Aβ peptides was measured in the cell culture medium using an Aβ ELISA kit. The ratio of Aβ42 to Aβ40 peptides was altered upon siRNA treatment, because the levels of Aβ40 decreased and the Aβ42 levels were increased (IQSEC1, ZNF179 and ZMAT2). The significance in comparison to samples treated with non-targeting control siRNA was assessed by Student's t-tests (n = 3; *p < 0.05; **p < 0.01; ***p < 0.001) and the columns represent mean+SD values.

Next, I studied the effects of IQSEC1, ZNF179 and ZMAT2 silencing on the expression of tau and hyperphosphorylated tau proteins. Protein expression was analysed by SDS-PAGE and Western blotting 72 h post-transfection with siRNA pools targeting the four proteins. As a control I used non-targeting control siRNA. The Western blot signal intensities were quantified by 2D densitometry (AIDA software, raytest Isotopenmessgeräte GmbH). The quantified signals of

the analyzed proteins were normalized to the corresponding signals of β-actin. All forms of the endogenous tau protein (phosphorylated and non-phosphorylated) were visualized with the K9JA polyclonal antibody against human tau (1:1,000, Dako) in order to determine the total amount of tau. The so called paired helical filaments (PHFs) are a major component of the neurofibrillary tangles and that are composed of tau in a hyper-phosphorylated state [267]. Hyperphosphorylated tau was visualized with the monoclonal anti-PHF-tau antibody AT8 (1:100; Thermo Scientific), which specifically detects PHF-tau doubly phosphorylated at Ser202 and Thr205 [268]. In Figure 21 it is shown that the knock-down of IQSEC1, ZNF179 and ZMAT2 led to a significant increase of total tau in the SH-SY5Y_APP695 cell model. The silencing of IQSEC1 and ZNF179 also significantly increased the amount of hyperphosporylated tau protein. However, this effect was less pronounced compared to the effect on total tau protein production. These results indicate that decreased expression of IQSEC1, ZNF179 and ZMAT2 not only influence APP processing and Aβ peptide production but also affect tau production and phosphorylation.

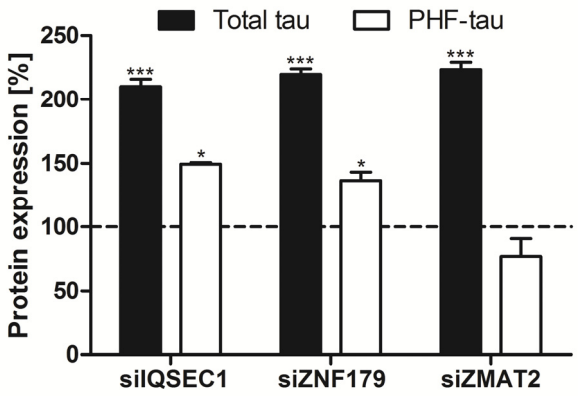

Figure 21: Analysis of total and hyperphosphorylated tau protein levels in SH-SY5Y_APP695 cells upon IQSEC1, ZNF179 or ZMAT2 knock-down. Total and hyperphosphorylated PHF tau was quantified in relation to signals from cells treated with non-targeting control siRNA, followed by signal normalization to β-actin levels. The knock-down of IQSEC1, ZNF179 and ZMAT2 significantly increased the expression of total tau. In addition, knock-down of IQSEC1 and ZNF179 also enhanced the levels of hyperphosphorylated PHF-tau protein (*$p < 0.05$; **$p < 0.01$; ***$p < 0.001$; $n = 3$; Student's t-test). Error bars represent SD values.

In summary, the results from the different cell-based assays suggest that the proteins IQSEC1, ZNF179 and ZMAT2 might play an important role in the pathogenesis of several neurodegenerative diseases such as AD, HD and ALS.

2.4 The identification of TDP-43 aggregation modifiers with siRNA experiments

In the following chapter I present how protein-protein interaction data and data from a large-scale siRNA screen can be used in combination to predict protein aggregation modifiers. A FRET-based aggregation assay was developed for the initial siRNA screen to quantify TDP-43 aggregation. Moreover, I generated a more aggregation-prone C-terminal fragment of TDP-43 (TDP-43_CT). Finally, the predicted protein aggregation modifiers were analyzed by focussed knock-down experiments in the human neuroblastoma cell line SH-EP. In the end I identified five proteins that regulate expression of TDP-43.

2.4.1 Generating a C-terminal TDP-43 fragment (TDP-43_CT) and the development of a FRET-based TDP-43 aggregation assay

Several studies have shown that TDP-43 is the major component of the predominantly cytoplasmic inclusions observed in ALS and FTLD patients with ubiquitin-positive inclusions (FTLD-U) [37, 38]. Moreover, there is evidence that TDP-43 is intrinsically aggregation-prone [219]. Normally, TDP-43 is mainly localized to the nucleus, but cytoplasmic aggregation in neurons leads to a substantial loss of nuclear TDP-43, suggesting that its redistribution to the cytoplasm is critical for disease pathogenesis [38]. In addition, pathologic TDP-43 is characterized by ubiquitination, phosphorylation and proteolytic cleavage, which generates C-terminal fragments [38]. C-terminal fragments of 25 kDa and 35 kDa are probably produced by caspase 3 cleavage [160]. Moreover, the 25 kDa fragment is associated with an enhanced aggregation potential and toxicity in yeast and mammalian cells [269, 270]. Therefore, I generated a C-terminal

fragment of TDP-43 (amino acids 219-414; TDP-43_CT) resembling the 25 kDa C-terminal fragment for PCR amplification using full-length TDP-43 as template (see Materials and Methods). The domain structure of TDP-43 and the generated fragment TDP-43_CT used in the following experiments is shown in Figure 22. TDP-43_CT does not contain a nuclear localization signal (NLS) and is therefore retained in the cytoplasm.

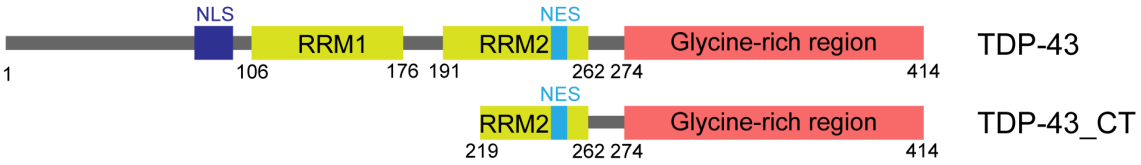

Figure 22: The domain structure of full-length TDP-43 and of the C-terminal fragment TDP-43_CT. Full-length TDP-43 contains two RNA recognition motifs (RRM1 and RRM2), which are flanked by the N-terminal and C-terminal tail. The C-terminal tail contains a glycine-rich region known to mediate protein-protein interactions. The second RRM contains a nuclear export signal (NES), whereas the N-terminal region habors the nuclear localization signal (NLS). TDP-43_CT includes most of the second RRM domain and the glycine-rich region of the C-terminus.

Mammalian cell expression vectors were generated encoding full-length TDP-43 and TDP-43_CT tagged with enhanced cyan fluorescent protein or enhanced yellow fluorescent protein (CFP-TDP-43, CFP-TDP-43_CT, YFP-TDP-43 and YFP-TDP-43_CT). As a first step I analyzed the production of the four proteins in HEK293 cells by SDS-PAGE and immunoblotting. Transient expression of the fusion proteins resulted in an increased level of full-length TDP-43 compared to the C-terminal fragment TDP-43_CT (Figure 23A). This could be probably due to the increased aggregation propensity and toxicity of the truncated TDP-43_CT fragment. Thus, I investigated the aggregation propensity of TDP-43_CT and full-length TDP-43 in HEK293 cells by fluorescence microscopy. TDP-43_CT formed large amounts of cytoplasmic aggregates of different sizes within 24 h (Figure 23B), whereas full-length TDP-43 only showed very small numbers of aggregates at this time point (not shown).

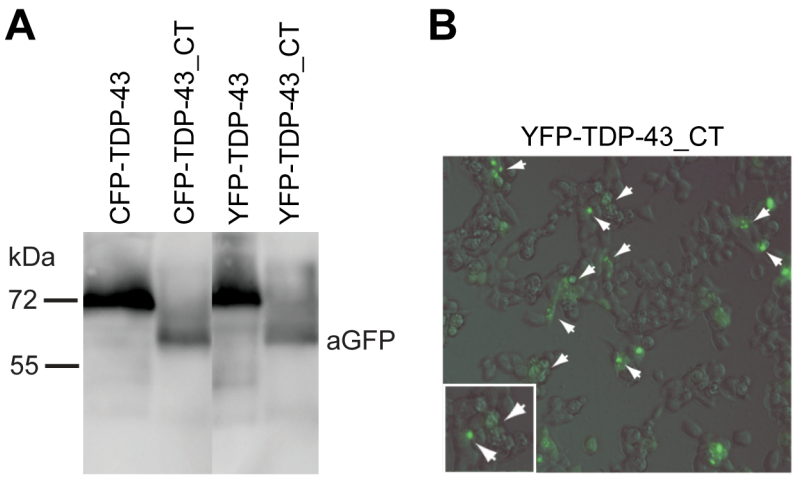

Figure 23: Expression of CFP-TDP-43, YFP-TDP-43, CFP-TDP-43_CT and YFP-TDP-43_CT in HEK293 cells. (A) 48 h after transfection cell extracts were prepared and 30 µg of total protein was separated by SDS-PAGE and analyzed by Western blotting. The proteins were detected using the anti-GFP antibody (1:1,000). (B) 24 h after transfection the expression and aggregation of YFP-TDP-43_CT was analyzed by fluorescence microscopy. YFP-TDP-43_CT formed cytoplasmic aggregates of different sizes (marked with arrows).

Next, I established a high-throughput aggregation assay based on fluorescence resonance energy transfer (FRET) to identify modifiers of TDP-43 aggregation. The assay was initially developed to quantify polyglutamine protein aggregation [271] and was performed as described in section 4.2.3.6. In proof-of-principle experiments the aggregation of full-length TDP-43 and the generated C-terminal fragment was analyzed with the developed assay and compared to results obtained with cells transfected with empty YFP and CFP vectors. Briefly, HEK293 cells were co-transfected with the corresponding expression vectors encoding either CFP and YFP fusion proteins or only CFP and YFP. Due to the aggregation of the fusion proteins, the light emitted by CFP (donor; excitation at 436 nm) is able to excite the YFP acceptor resulting in fluorescence at 530 nm [271]. YFP fluorescence (excitation 485 nm, emission 530 nm), CFP fluorescence (excitation 436 nm, emission 485 nm), as well as the FRET signal (excitation 436 nm, emission 530 nm) were measured in the Infinite M200 plate reader (Tecan) 72 h after transfection. I found that the NET-FRET signals were significantly increased for full-length TDP-43 (497.1%) and TDP-43_CT

(629.8%) compared to the vector control (Figure 24), indicating that both proteins form aggregates in mammalian cells. The higher signal for TDP-43_CT compared to the full-length protein suggests that indeed TDP-43_CT has a higher aggregation propensity than TDP-43. This is the reason why TDP-43_CT was chosen for the initial high-throughput screen to identify TDP-43 aggregation modifiers.

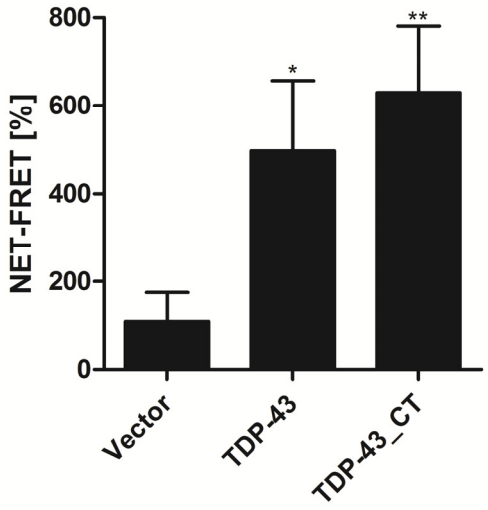

Figure 24: Development of a FRET-based aggregation assay to quantify TDP-43 aggregation. NET-FRET signals for HEK293 cells co-transfected with vectors encoding YFP and CFP, YFP-TDP-43 and CFP-TDP-43 as well as YFP-TDP-43_CT and CFP-TDP-43_CT. The NET-FRET signals for TDP-43 and TDP-43_CT were significantly higher than for the vector control, showing that the two proteins strongly aggregated in HEK293 cells (*$p < 0.05$; **$p < 0.01$; $n = 3$; Student's t-test). Error bars represent means+SD.

2.4.2 Identification of TDP-43 aggregation modifiers from a set of computationally predicted ND-related genes

One of the main objectives in this study was to identify protein aggregation modifiers using the generated Y2H protein-protein interaction data. Therefore, I systematically analysed a set of 1,134 computationally predicted ND-related genes in knock-down experiments in HEK293 cells using the established FRET-based TDP-43 aggregation assay. The FRET assays were performed with the C-terminal fragment of TDP-43 (TDP-43_CT) as described in the previous section. This fragment lacks the nuclear localization signal of full-length TDP-43

(Figure 22) and therefore rapidly forms small and large cytoplasmic aggregates in mammalian cells (Figure 23B). The siRNA screen was performed in collaboration with the Boutros laboratory at the DKFZ. The method is described in more detail in section 4.2.3.6. The targets selected for the RNAi screen were the 1,143 top scoring genes taken from the list of 3,711 predicted neurodegenerative disease (ND)-related genes (see section 2.1.1). The knock-down gene set completely covered the genes selected for the Y2H screens. The screened genes contained 111 ND genes, 239 other disease genes and 48 predicted risk factors or susceptibility genes for NDs (Figure 25A). Additionally, the screened siRNAs also covered 368 drug targets, 166 previously published modulators of protein aggregation or toxicity, as well as 103 aggregation-prone proteins. In the siRNA screen I identified 191 proteins which significantly affected TDP-43_CT aggregation. Among these proteins 43 enhanced whereas 148 suppressed TDP-43_CT aggregation.

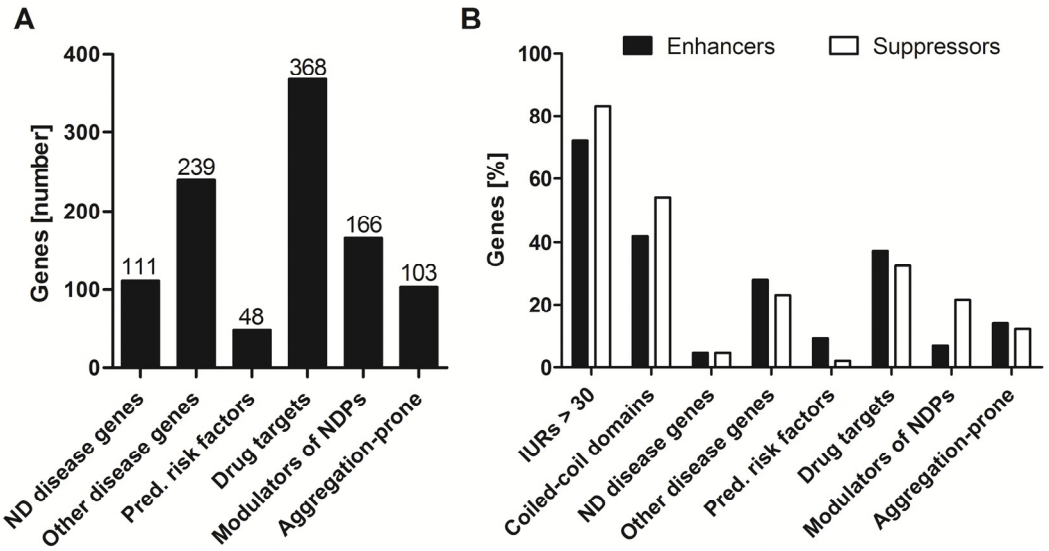

Figure 25: Bioinformatics analysis of target genes selected for siRNA screens and the identified TDP-43 aggregation modifiers. (A) Number of target genes annotated as disease genes, risk factors, drug targets, modulators of ND protein aggregation or toxicity and genes encoding aggregation-prone proteins. (B) Percentage of identified enhancers and suppressors annotated as genes encoding proteins with intrinsically unstructured regions (IURs) and coiled-coil domains as well as the other annotations mentioned in (A).

Among the identified modifiers I found a high percentage of proteins with internally unstructured regions (IURs; >70%) as well as coiled-coil (CC) domains (>40%). When I compare enhancers (E) and supressors (S) of TDP-43 aggregation, I observed fewer genes, which encode proteins with IURs (E: 72.1% (31); S: 83.1% (123)) and with CC domains (E: 41.9% (18); S: 54.1% (80)) among the enhancers (Figure 25B). The set of genes with aggregation enhancing effect contained significantly more predicted risk factors (9.3% (4); p = 0.0267, Fisher's exact test) in comparison to the aggregation suppressors (2.0% (3)). The opposite was observed for the known modulators of ND protein aggregation or toxicity (E: 7.0% (3); S: 21.6% (32); p = 0.0132, Fisher's exact test). The relative numbers of known ND genes (E: 4.7% (2); S: 4.7% (7)), other disease genes (E: 27.9% (12); S: 23.0% (34)), drug targets (E: 37.2% (16); S: 32.4% (48)), and aggregation-prone homologs in *C. elegans* (E: 14.0% (6); S: 12.2% (18)) were almost comparable.

2.4.3 Prediction of protein complexes that alter aggregation of full-length TDP-43

In the previous chapter I described how I identified 191 proteins that significantly influence the aggregation of TDP-43_CT in HEK293 cells. Next, I combined the siRNA data with PPI data to predict highly connected protein complexes that are linked to TDP-43. In summary, this means that I created a PPI network, which consists of Y2H interactions enriched for TDP-43 interaction partners as well as the 191 TDP-43 aggregation modifiers, which were identified in siRNA screens, and their interaction partners. The resulting network consisted of 7,951 PPIs connecting 4,315 proteins. Next, I predicted 37 protein complexes, defined as highly connected clusters of proteins, with the program Cfinder [272]. Finally, I selected 7 protein complexes, which in total contain 33 proteins, for follow-up siRNA experiments in the human neuroblastoma cell line SH-EP (Figure 26). The selection of complexes was based on two criteria: a) at least one of the interactions in a complex must have been found by Y2H screening and b) the TDP-43 protein must be part of the complex or directly

connected to a predicted protein complex member (Figure 26). I functionally annotated each complex according to the known functions of the complex members (Figure 26). For the annotation of proteins in the complexes available Gene Ontology or literature information was utilized. Three complexes (1, 3 and 7) are likely involved in transcription, four complexes (2, 4, 5 and 7) in protein degradation, and two complexes have a function in RNA processing (3 and 6). In addition, protein complexes involved in apoptosis (4 and 7), and signal transduction (5 and 6) have been predicted. Proteins in complex 2 are also very likely involved in regulation of the cell cycle and proteins in complex 4 potentially function in transport processes.

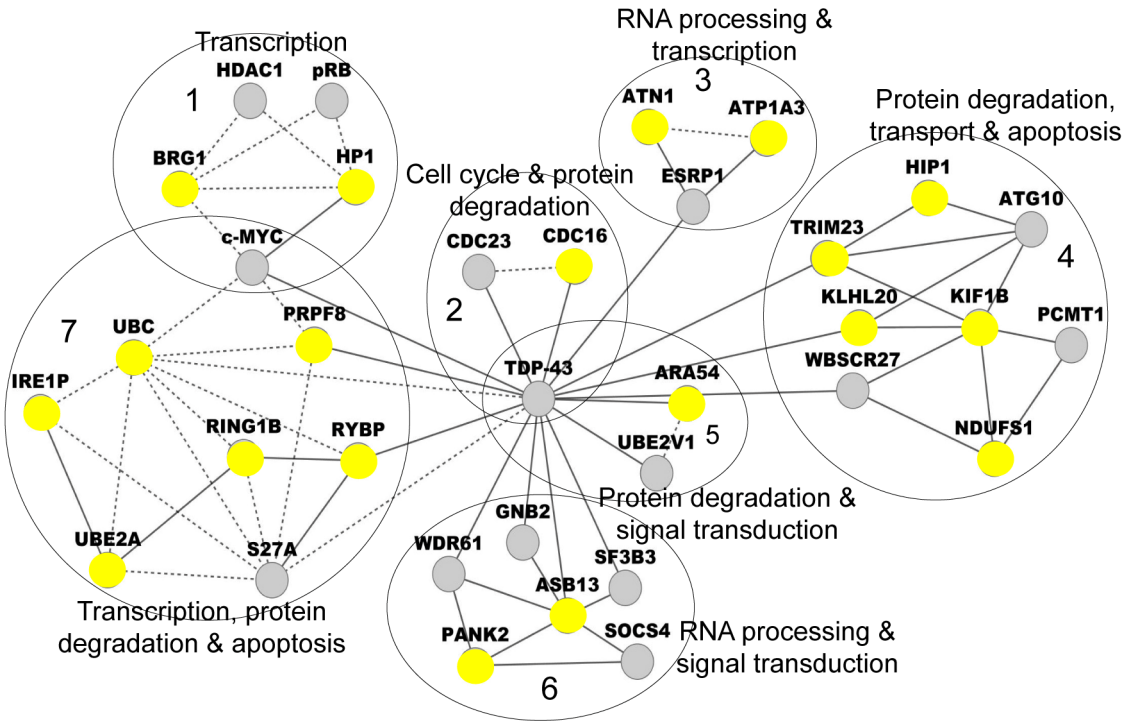

Figure 26: Predicted protein complexes selected for validation experiments by combination of data from siRNA screens and PPI studies. Members of each complex are encircled and each complex is functionally annotated according to GO and literature information. Y2H interactions identified in this study are marked with solid lines, whereas literature-based interactions are depicted by dotted lines. The proteins which were identified as aggregation modifiers of TDP-43_CT in the initial siRNA screen are depicted as yellow nodes.

2.4.4 The discovery of protein complexes that affect TDP-43 aggregation in cell-based assays

A large fraction of the proteins in the computationally predicted protein complexes (17 of the 33 complex members) are modifiers of TDP-43 aggregation that were identified in the previous siRNA screens in HEK293 cells (Figure 26). Next, I investigated whether the 33 computationally predicted complex members influence aggregation of full-length TDP-43 in the SH-EP neuroblastoma cell line. SH-EP cells were co-transfected with 150 ng YFP-TDP-43 and a selected siRNA pool (100 nM total). The over-production of YFP-TDP-43 was analyzed by SDS-PAGE and immunoblotting using an anti-TDP-43 antibody (Figure 27A). Additionally, Figure 27B shows that YFP-TDP-43 protein forms cytoplasmic aggregates in SH-EP cells after 48 h, which is a prerequisite for the identification of modifier proteins.

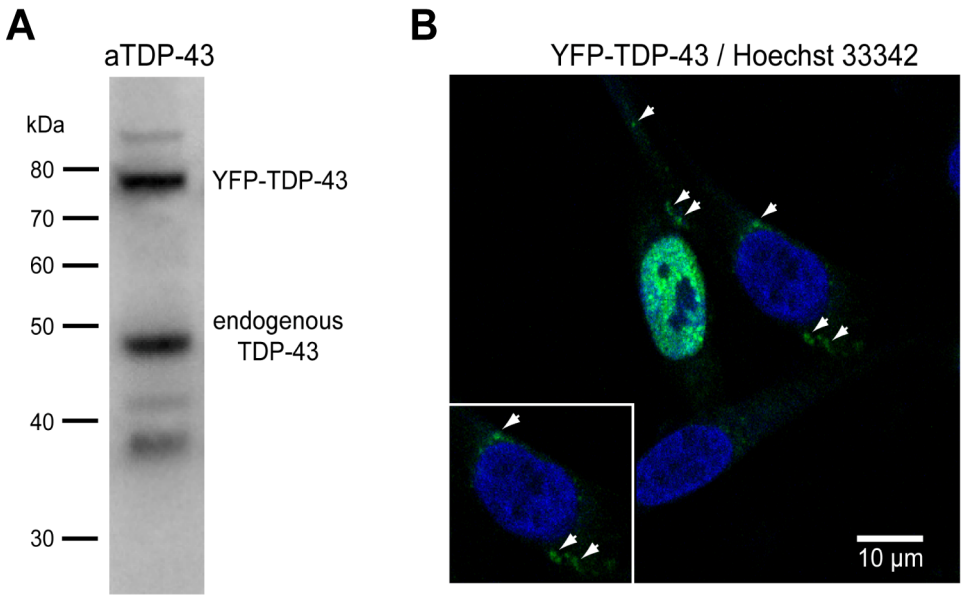

Figure 27: Overproduction of YFP-TDP-43 in the neuroblastoma cell line SH-EP. (A) Analysis of SH-EP cell extracts by SDS-PAGE and Western blotting. The used anti-TDP-43 antibody (1:1,000) recognized YFP-TDP-43 (~78 kDa) as well as endogenous TDP-43 (~48 kDa). (B) YFP-TDP-43 formed cytoplasmic aggregates (green dots marked with arrows) in SH-EP cells. Aggregates were detected with confocal microscopy. The nuclei were stained with Hoechst 33342 (blue).

The effects of siRNA-based knock-downs on TDP-43 aggregation were assessed after 72 h by high content fluorescence imaging using a Cellomics^{TM} microscope. Modifiers were accepted as hits, if their knock-down significantly altered TDP-43 aggregation in three independent experiments (each performed in triplicates). The significance was assessed with Student's t-tests in comparison to non-targeting control siRNA. The results for each complex member are shown in Figure 28. Using this approach, I identified 10 genes whose knock-down significantly enhanced TDP-43 aggregation, whereas knock-down of 12 genes showed the opposite effect. On the level of the predicted complexes I found that all members of complex 1 and 2 significantly altered TDP-43 aggregation in this cell model. Interestingly, the knock-down of the direct interaction partners of TDP-43 in these two complexes (c-MYC, CDC23 and CDC16) increased protein aggregation, whereas knock-down of the indirect interaction partners (BRG1, HDAC1, pRB and HP1) reduced TDP-43 aggregation. For the other five complexes only some of the predicted members significantly influenced aggregation of TDP-43. Interestingly, 11 of the 17 aggregation modifiers (64.7%) identified in the initial large-scale screen in HEK293 cells could also be identified as TDP-43 aggregation modifiers in SH-EP cells. Moreover, I found that 22 of 33 (66.7%) predicted complex members influence TDP-43 aggregation in SH-EP cells. In the initial large-scale screen only 16.8% (191 modifiers of 1,134) of the tested genes significantly altered TDP-43 aggregation in HEK293 cells. This indicates that the combination of siRNA and PPI data as well as the prediction of complexes from PPI networks is a valid and very successful approach to identify modifiers of aggregation-prone NDPs.

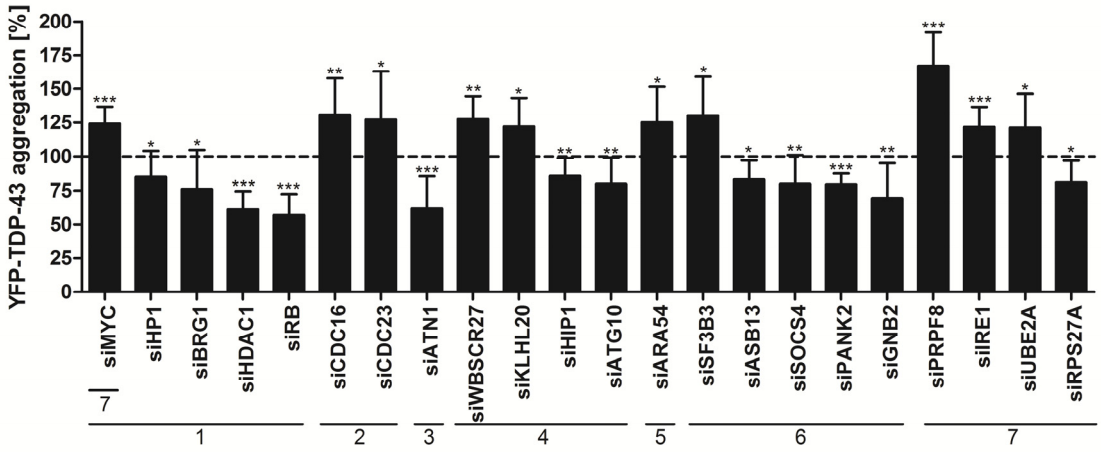

Figure 28: Effects of potential modifier proteins on YFP-TDP-43 aggregation monitored by high content fluorescence imaging. 33 potential modifiers that form seven protein complexes were tested by siRNA experiments in SH-EP cells. The results for 22 hits are shown. They were identified in three independent experiments are summarized here and are sorted according to their complex membership. The knock-down of 10 proteins significantly increased aggregation in comparison to non-targeting control siRNA, whereas 12 proteins significantly reduced aggregation of TDP-43 upon siRNA knock-down (*$p < 0.05$; **$p < 0.01$; ***$p < 0.001$; $n = 9$; Student's t-tests). Error bars represent means+SD.

Next, I randomly selected nine TDP-43 aggregation modifier genes and quantified their expression after siRNA treatment for 72 h by qRT-PCR (Figure 29). The generated results were first normalized to the mRNA levels of the endogenous control ACTB (β-actin) and then compared to results of cells treated with non-targeting control siRNA. The knock-down efficiency was found to be between 40% (HDAC1) and 95% (RB) in these cell-based assays.

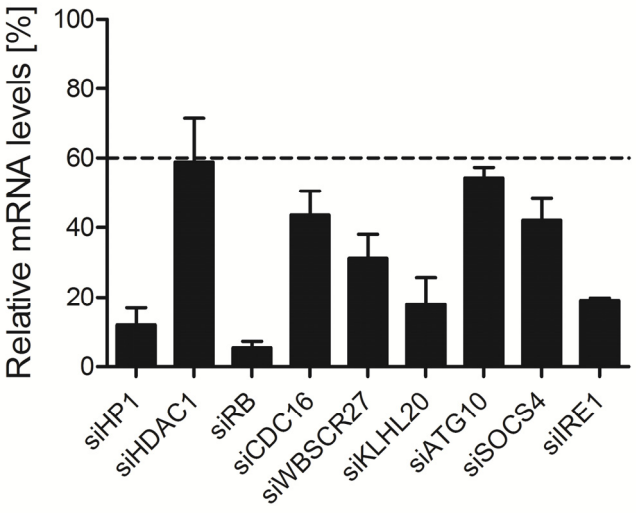

Figure 29: Quantification of relative mRNA levels after siRNA knock-down of selected target genes in SH-EP cells. The mRNA levels were quantified by qRT-PCR, normalized to the mRNA levels of ACTB and compared to results obtained with non-targeting control siRNA. A knock-down efficiency between 40% and 95% was observed for selected target genes.

2.4.5 Knock-down of complex 1 members alters TDP-43-induced cytotoxicity and TDP-43 mRNA expression

Complex 1, which consists of the proteins c-MYC, BRG1, HDAC1, pRB and HP1 (Figure 26), was selected for further, more detailed experiments. All proteins in this complex are known to function in transcriptional regulation [273-280], suggesting that they might also influence the expression of TDP-43 in SH-EP cells.

First I analyzed whether knock-down of the complex 1 members influences TDP-43-induced cytotoxicity in SH-EP cells. Toxicity was measured 72 h after siRNA treatment using a caspase 3/7 activity assay. The treatment of SH-EP cells with siRNA pools targeting MYC, RB, HDAC1 and HP1 significantly decreased TDP-43-induced toxicity in SH-EP cells (siMYC: -17.4%; siRB: -28.2%; siHDAC1: -23.5%; siHP1: -11.4%). In contrast, knock-down of BRG1 did not significantly alter TDP-43-induced cytotoxicity.

Next, the four identified TDP-43 toxicity modifiers were also tested for their effect on cytotoxicity in the absence of the disease protein. I found that the

knock-down of MYC significantly reduced the cytotoxicity in SH-EP cells in the absence of TDP-43, indicating that this effect is not dependent on the expression of the disease protein. However, a TDP-43 dependent toxicity effect was observed for the proteins pRB, HDAC1 or HP1, indicating that they are specific modifiers of TDP-43-induced cytotoxicity.

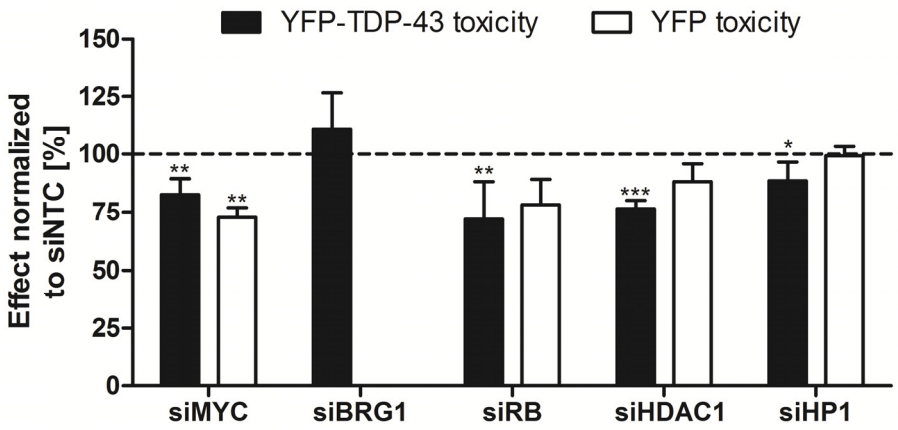

Figure 30: Knock-down of complex 1 members significantly influences the toxicity of aggregation-prone TDP-43 in SH-EP cells. The knock-down of the genes RB, HDAC1 and HP1 specifically reduced TDP-43-induced toxicity. In contrast, knock-down of MYC shows an unspecific toxicity effect. Cytotoxicity was monitored with caspase 3/7 activity assays. The significance was assessed by Student's t-tests and comparison to non-targeting control siRNA (siNTC; *p < 0.05; **p < 0.01; ***p < 0.001; n = 9). Error bars represent means+SD.

As I described above all five proteins in complex 1 are known to be involved in transcriptional regulation. The proto-oncogene c-MYC can either activate or repress gene transcription. It is thought to regulate transcription by recruiting several co-factors to target genes that possess the capability to alter the chromatin structure by acetylating core histones as well as transcriptional regulators [281, 282]. MYC also activates all three RNA polymerases [283]. BRG1, pRB, HDAC1 and HP1 mediate transcriptional regulation directly, mainly by chromatin remodelling [274, 276, 277, 279, 280]. BRG1, pRB and HDAC1 for example form a protein complex that regulates CREST-mediated transcription primary cortical neurons [278]. This suggested that the proteins might influence the expression of TDP-43 and thereby modify its aggregation and toxicity.

Therefore, I quantified the amount of TDP-43 mRNA in SH-EP cells upon knock-down of the five complex members by qRT-PCR (Figure 31). The treatment of SH-EP cells with a MYC-specific siRNA pool dramatically increased TDP-43 mRNA levels (~5 times), suggesting that increased TDP-43 aggregation in SH-EP cells is caused by increased production of the disease protein. In contrast, the knock-down of BRG1, RB, HDAC1 and HP1 caused a dramatic decrease of TDP-43 mRNA levels (e.g. more than 90% in case of BRG1, RB and HDAC1), indicating that these proteins function as enhancers of TDP-43 mRNA expression. Thus, these results suggest that siRNA-mediated knock-down of pRB, HDAC1 and HP1 expression most likely reduces TDP-43 aggregation and toxicity in SH-EP cells because expression of TDP-43 is diminished.

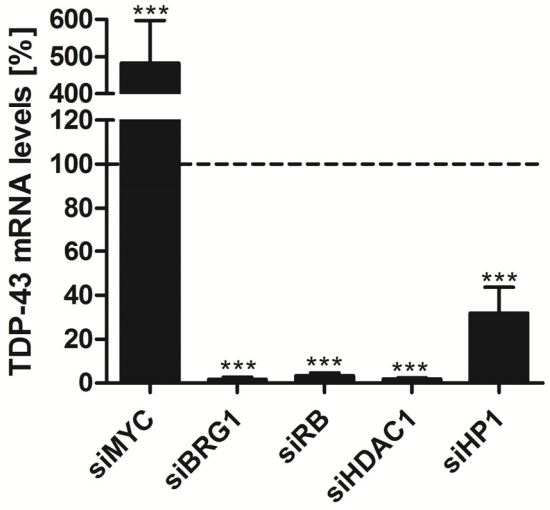

Figure 31: Knock-down of complex 1 members MYC, BRG1, RB, HDAC1 and HP1 changes TDP-43 mRNA expression in SH-EP cells. TDP-43 mRNA levels were quantified by RT-PCR, normalized to mRNA levels of ACTB and compared to results from cells treated with non-targeting control siRNA. The knock-down of MYC significantly increased the expression of TDP-43, whereas BRG1, RB, HDAC1 and HP1 siRNA treatments significantly reduced TDP-43 expression (***$p < 0.001$; $n = 3$; Student's t-tests). Error bars represent means+SD.

Finally, I investigated the knock-down of the target proteins HP1, c-MYC, BRG1 and HDAC1 by SDS-PAGE and immunoblotting (Figure 32). I found that the levels of the target proteins are indeed reduced in cells that are treated with specific siRNAs, confirming the results obtained by qRT-PCR (Figure 29).

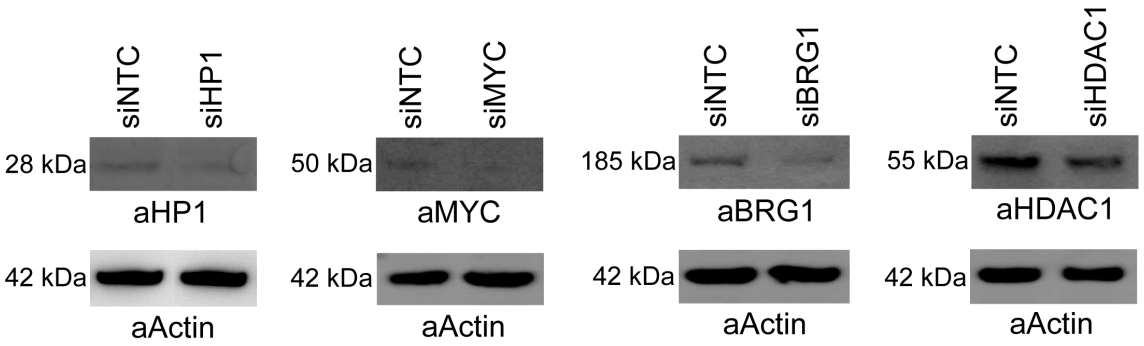

Figure 32: Analysis of target protein expression by SDS-PAGE and immunoblotting. Protein levels were reduced by treatment with HP1, MYC, BRG1 and HDAC1 siRNAs. 30 µg of total protein prepared from SH-EP cells was analyzed by SDS-PAGE and Western blotting. The endogenous proteins were detected using anti-HP1, anti-MYC, anti-BRG1 and anti-HDAC1 antibodies. Actin was used as a loading control.

2.4.6 TDP-43 aggregation and toxicity is specifically influenced by HDAC1 but not by HDAC2 or HDAC6

Finally, I tested whether the effect of HDAC1 on TDP-43 aggregation and toxicity is specific or if related histone deacetylases also influence misfolding and toxicity of the disease protein. I selected HDAC2, a type I histone deacetylase like HDAC1 with similar functions [284], and HDAC6, a type IIB histone deacetylase, which is associated with aggresomes formation and influences the degradation of misfolded proteins for these experiments [285-287]. Silencing of the genes in TDP-43 expressing SH-EP cells revealed that knock-down of HDAC2 and HDAC6 significantly increased aggregation of TDP-43, while knock-down of HDAC1 showed the opposite effect (Figure 33). These results indicate that HDAC1 is a specific regulator of TDP-43 aggregation and toxicity.

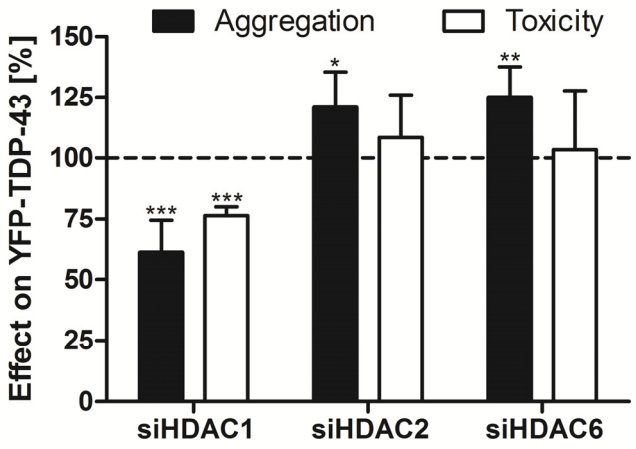

Figure 33: Silencing of HDAC1 specifically decreased the aggregation and toxicity of TDP-43. SHEP cells were co-transfected with YFP-TDP-43 and siRNA pools targeting the selected HDACs or the non-targeting control. Aggregation was analyzed by high content fluorescence imaging and toxicity was assessed by caspase 3/7 activity assays. The significance was determent by comparison to non-targeting control siRNA samples (*p < 0.05; **p < 0.01; ***p < 0.001; n = 9; Student's t-tests). The error bars represent means+SD.

Finally, the knock-down of HDAC2 and HDAC6 in SH-EP cells was assessed by SDS-PAGE and Western blotting (Figure 34). I found that the HDAC2 and HDAC6 protein production levels were reduced upon treatment with specific siRNAs for 72 h, indicating that the effects obtained with HDAC2 and HDAC6 siRNAs was based on reduced production of the two proteins.

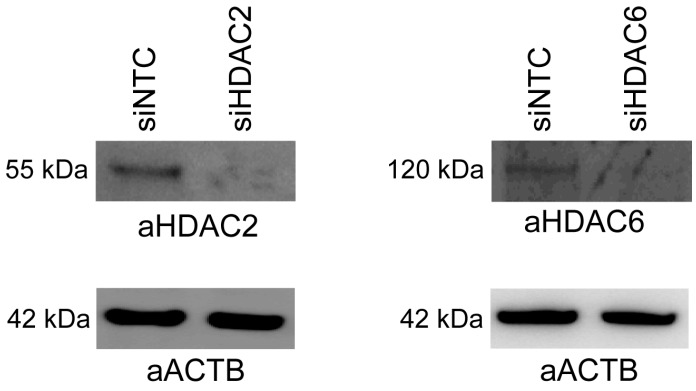

Figure 34: siRNA-mediated gene silencing of reduced the protein expression of HDAC2 and HDAC6 in SH-EP cells. The same amounts of total protein (30 µg) prepared from SH-EP cells were analyzed by SDS-PAGE and Western blotting. Endogenous proteins were detected using anti-HDAC2 and anti-HDAC6 antibodies. Actin was used as a loading control.

3 Discussion

3.1 Systematic interaction mapping for neurodegenerative disease proteins

Neurodegenerative diseases (NDs) are characterized by a progressive loss of neurons in motor, sensory, or cognitive systems [1]. The diseases share symptoms including memory-loss, lack of mobility and are finally fatal [1]. The pathogenesis of NDs, such as Huntington's disease (HD), Alzheimer's disease (AD), and Parkinson's disease (PD), has been linked to inappropriate processing and elimination of misfolded proteins [1]. The accumulation of misfolded proteins results in the formation of toxic protein aggregates [1, 288, 289], which are a characteristic feature of all NDs. These diseases are increasingly found to share other common molecular characteristics. For instance, mechanisms that would normally process and remove misfolded proteins, including the ubiquitin-proteasome system (UPS) [290, 291], autophagy [292] and chaperone-mediated protein refolding [293, 294], are impaired. In addition, it has been shown that toxicity in cell and animal models of NDs can be decreased using the similar strategies. For example, over-expression of heat-shock proteins has been shown to decrease toxicity induced by mutant huntingtin (HD), amyloid-β (AD) and mutant α-synuclein (PD) [68-70]. Furthermore, caspase inhibitors decrease both mutant huntingtin and mutant SOD1 (ALS) toxicity [295, 296].

These findings suggest that common therapeutic targets can be identified for some or even all NDs. Therefore, a comprehensive approach to understand these diseases in relation to each other may uncover new information that single-disease studies cannot provide. One powerful approach for inferring common disease mechanisms is to systematically identify protein-protein interactions (PPIs). To this day experimental based interaction studies for neurodegenerative disease proteins (NDPs) focused either on single proteins or specific diseases. Single protein interaction studies provided evidence that for

example TDP-43 is involved in microRNA processing and DNA repair processes [170, 171], while the disease protein huntingtin is associated with components of the vesicle secretion apparatus [169]. Moreover, such interaction studies also identified several new modifiers of mutant huntingtin-induced cytotoxicity [168, 169]. Disease-centered studies discovered common processes and pathways as well as new candidate genes for inherited ataxias [182]. Similarly, a comprehensive PPI study for multiple NDPs covering several neurodegenerative diseases might identify common disease processes.

Here, I created a comprehensive PPI network, which interconnects several known NDPs, using the yeast-two hybrid method. In total 449 wild-type and 22 mutant proteins predicted to cause NDs or to be related to NDs were systematically screened for interactions against a library of 15,863 human proteins. 57 of the 449 screened proteins are known NDPs, including for example huntingtin, α-synuclein and the amyloid precursor protein (APP). The yeast-two hybrid screen produced a network of 18,663 interactions connecting 3,728 proteins. This is the first PPI network of this scale that links multiple known NDPs and thereby connects several neurodegenerative diseases.

3.2 Wild-type and mutant neurodegenerative disease proteins have distinct interaction partners

The yeast-two hybrid screen performed in this study identified 2,310 protein-protein interactions for 22 mutant NDPs (see section 2.1.3 for a detailed description of the selected mutants). Detailed analyses on the functional level revealed significant differences between the interaction partners of mutant and wild-type NDPs. I for example found that among the interacting proteins of mutant NDPs are significantly more proteins that are involved in transcriptional regulation than among the interaction partners of wild-type NDPs (see section 2.2.2). This result clearly supports previous findings of other groups, indicating that transcriptional dysregulation contributes to the pathogenesis in NDs.

Transcriptional dysregulation mediated by mutant ataxin-1 for example is an important feature of SCA1 pathogenesis. Perturbed interactions between expanded ataxin-1 and transcription factors such as LANP, PQBP1, Gfi-1, SMRT, Boat and Sp1 are believed to exert the deleterious effects of expanded ataxin-1 [297-302]. Similarly, aberrant PPIs of huntingtin mediate neurotoxicity in HD. Polyglutamine expansion alters the interactions of huntingtin with HAP1/p150^{Glued} complexes as well as numerous transcription factors (e.g. Sp1, CBP and TBP), leading to their functional impairment [172-179].

Interestingly, the functional analysis of the interaction partners of wild-type TDP-43, TDP-43_Q331K and TDP-43_M337V delivered no evidence that transcription regulation is altered in ALS. However, I found that more interaction partners of wild-type TDP-43 play a functional role in protein degradation than the interaction partners of the two mutant proteins TDP-43_Q331K and TDP-43_M337V. This result suggests that ALS-causing mutations in TDP-43 might disrupt or inhibit their degradation upon misfolding, which might result in an increased protein aggregation. This hypothesis is supported by publications showing that disease-causing mutations in TDP-43 increase the propensity of TDP-43 to spontaneously assemble into insoluble protein aggregates [171, 219, 303, 304]. Moreover, over-expression of mutant TDP-43 in mice, rats or *C. elegans* causes progressive locomotor defects and paralysis reminiscent of ALS [155, 305-307]. In theses models aggregates of ubiquitinated TDP-43 accumulate in motor neurons, suggesting that dysfunction of intracellular protein degradation systems could be important for disease pathogenesis [155, 305-307]. Additionally, recent studies show that the inhibition of either the ubiquitin-proteasome system or autophagy increases TDP-43 aggregation [308, 309]. Consistantly, induction or enhancement of autophagy by rapamycin or trehalose treatment is associated with reduced TDP-43 accumulation [310, 311].

I found that SMURF1, an E3 ubiquitin ligase, is one of the proteins, which specifically interacted with wild-type but not with mutant TDP-43. Interestingly, a recent study showed that another SMURF protein - SMURF2 - co-aggregates

with TDP-43 as well as the adaptor protein p62 and the autophagy marker LC3 [309, 312, 313]. This suggests that SMURF1 might also be located in TDP-43 aggregates and is involved in the UPS-mediated degradation of wild-type TDP-43 (Figure 35A).

Another very interesting protein, which specifically interacted with wild-type TDP-43 in the Y2H screen, is HDAC6. This protein was previously shown to regulate aggresome formation in response to misfolded protein stress [314]. It has been proposed that aggresome formation is a specific and active cellular response to cope with excessive levels of misfolded and aggregated proteins [315]. In support of this hypothesis, components of proteasomes and molecular chaperones were found to be actively recruited to aggresomes [315, 316]. Aggresomes and Lewy bodies, which are found in neurons affected by Parkinson's disease, share similar biochemical and morphological characteristics [317]. Therefore, aggresomes might be also important in the pathogenesis of other neurodegenerative diseases. Disruption of dynein motor function prevented aggresome formation, which indicated that dynein collects and transports aggregated proteins from the cytoplasm to the aggresome for degradation [318, 319]. HDAC6 was shown to bind polyubiquitinated misfolded proteins and dynein motors [314]. Thus, HDAC6 most likely recruits misfolded proteins to dynein motors for transport to aggresomes [314]. It was also shown that HDAC6 expression is regulated by TDP-43. Knock-down of TDP-43 significantly reduced HDAC6 mRNA as well as protein levels and resulted in increased cell death in mutant ataxin-3 over-producing cells [285, 320, 321]. Moreover, TDP-43 specifically binds to HDAC6 mRNA [285, 320, 321]. In this study I identified a protein-protein interaction between TDP-43 and HDAC6, which suggests that there are further mechanisms on the protein level involved, which will have to be explored in more detail in the future (Figure 35B). The interaction of TDP-43 and HDAC6 could for example depend on polyubiquitination of TDP-43, which would mean that HDAC6 targets TDP-43 for aggresome-dependent degradation.

Another protein that was found to specifically interact with wild-type TDP-43 in Y2H assays was AMSH, a deubiquitination enzyme that participates in endosomal sorting (Figure 35C) [322]. AMSH impairment results in missorted ubiquitinated cargoes *in vitro* and in severe neurodegeneration *in vivo* [323]. Moreover, according to a recent study AMSH plays an important role in the degradation of ubiquitinated proteins in the central nervous system and AMSH deficiency leads to TDP-43 accumulation in glial cells [324]. All these results indicate that SMURF1, AMSH and HDAC6 are involved in the degradation of TDP-43. As these proteins do not interact with the two mutant TDP-43 variants (TDP-43_Q331K and TDP-43_M337V), it can be concluded that the ALS-causing mutations disturb these interactions and probably also the degradation of the mutant proteins. Future experiments will have to be conducted to show whether for example SMURF1 indeed ubiquitinates TDP-43 and whether there are differences in ubiquitination when comparing wild-type and mutant TDP-43.

In addition to wild-type specific interaction partners I also identified proteins that specifically interacted with a mutant form of TDP-43. One of them is the arginine methyltransferase PRMT1, which specifically interacted with TDP-43_Q331K. Previous studies provided evidence that PRMT1 plays a role in pathogenic mechanisms relevant for amyotrophic lateral sclerosis (ALS). PRMT1 regulates the nuclear-cytoplasmic shuttling of FUS, another ALS disease protein, by protein arginine methylation [325]. Depletion of PRMT1 reduces the ability of FUS mutants to localize to the cytoplasm and form insoluble aggregates [325]. Similarly, PRMT1 might also influence the transport of TDP-43 to the cytoplasm. In contrast to FUS, TDP-43 does not contain a GAR motif and therefore might only be methylated at a few single arginine residues by PRMT1. Protein arginine methylation does not only influence nuclear-cytoplasmic shuttling, it also dramatically affects transcription and RNA processing [326]. Thus, TDP-43 and PRMT1 might act in concert to regulate the transcription or RNA processing of common targets in neuronal cells (Figure 35D). These results require further experiments to validate the specificity of the interaction. Moreover, it needs to

be studied whether PRMT1 binding to TDP-43 causes arginine methylation and influences the toxicity of the disease protein in mammalian cells.

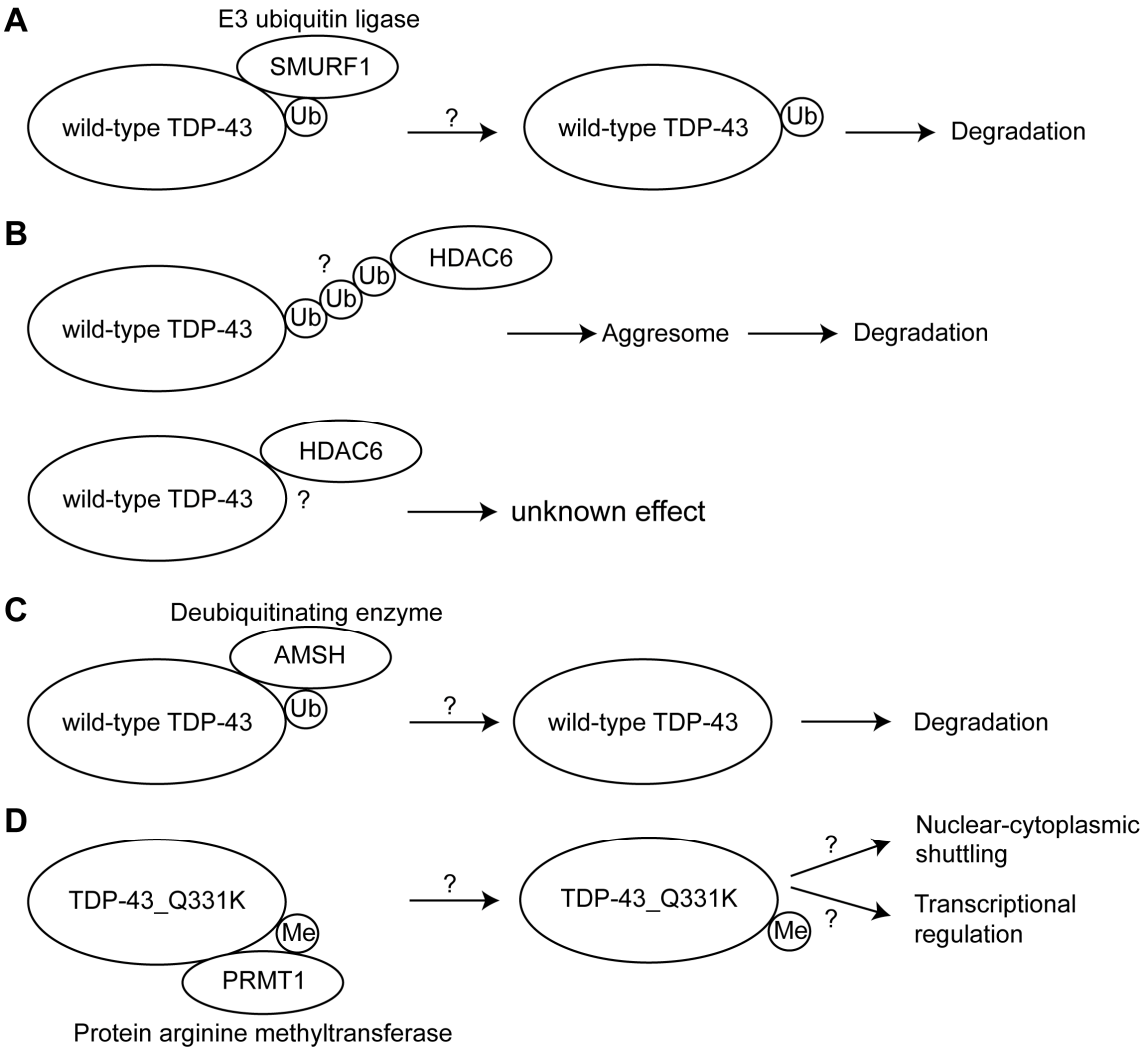

Figure 35: Possible consequences of wild-type- or mutant-specific TDP-43 protein-protein interactions (PPIs). (A) The interaction of wild-type TDP-43 with SMURF1 might result in the ubiquitination of TDP-43, which would mark the protein for degradation by the proteasome. (B) If the PPI between HDAC6 and wild-type TDP-43 is polyubiquitination dependent, TDP-43 can be transported to aggresomes by dynein and subsequently degraded by autophagy. It is also possible that the interaction of HDAC6 with TDP-43 is independent on TDP-43 ubiquitination. (C) The deubiquitinating enzyme AMSH might deubiquitinate wild-type TDP-43, which would result in its degradation by an unknown mechanism. (D) The mutant protein TDP-43_Q331K interacted with the protein arginine methyltransferase PRMT1, which might result in the methylation of arginine residues of TDP-43. Methylation of TDP-43 might influence its nuclear-cytoplasmic shuttling ability or its function as transcriptional regulator.

3.3 IQSEC1, ZNF179 and ZMAT2 influence the pathogenic mechanisms of several neurodegenerative diseases

I identified APP, IQSEC1, ZNF179 and ZMAT2 as common interactors of different neurodegenerative disease proteins (NDPs), whose mutations cause Alzheimer's disease (AD), amyotrophic lateral sclerosis (ALS), Parkinson's disease (PD), Huntington's disease (HD) and spinocerebellar ataxia type 1 (SCA1). The results described in section 2.3 of this thesis provide evidence that IQSEC1, ZNF179 and ZMAT2 play an important role in multiple NDs. Depletion of these three proteins in human neuroblastoma cells for example increased abnormal protein aggregation of the disease proteins huntingtin, mutant ataxin-1 and TDP-43 (see section 2.3.2). Moreover, the knock-down of IQSEC1, ZNF179 and ZMAT2 also in cell models dramatically influenced Aβ peptide production, a key event in AD pathogenesis [20, 131, 266]. Finally, I found that silencing of these three disease-connecting proteins significantly increased the total levels of tau protein as well of hyper-phosphorylated tau in cell assays. Hyper-phosphorylated tau is the major component of neurofibrillary tangles, which are intraneuronal aggregates commonly found in AD patient brains [267]. It could be shown in this study that the three disease-connecting proteins are mainly down-regulated in HD, PD and AD patient brains (see section 2.2.3). This finding in combination with my other observations implies that IQSEC1, ZNF179 and ZMAT2 are critical for maintaining neuronal function. Thus, neurodegeneration could be promoted by a progressive depletion of these four proteins in patient brains (Figure 36).

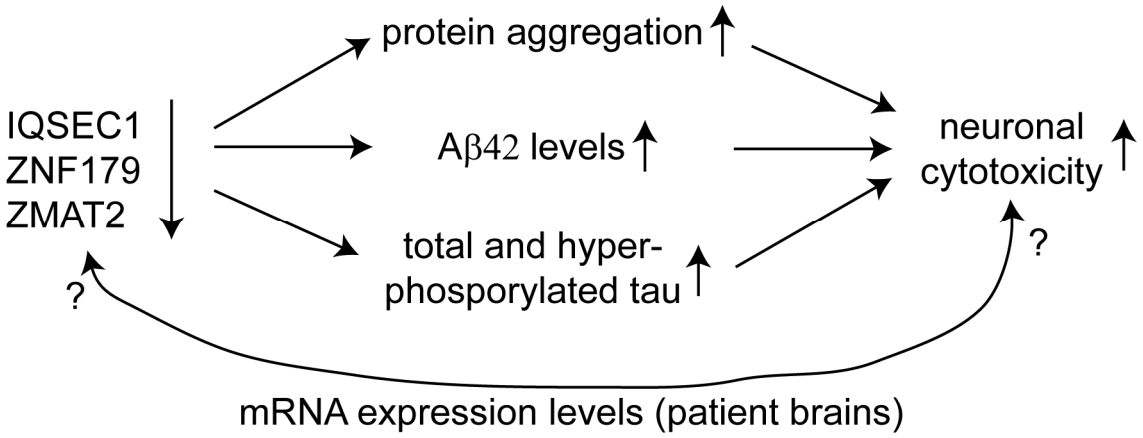

Figure 36: Depletion of IQSEC, ZNF179 and ZMAT2 results in increased pathogenic neurodegenerative disease mechanisms. Exacerbated pathogenic mechanisms such as increased protein aggregation of NDPs result in increased neuronal cytotoxicity. ND patient brains are characterized by widespread cell death as well as mRNA down-regulation of the three proteins. Therefore, neurodegeneration might be the reason or the observed reduction in mRNA levels of the three disease-connecting proteins, which then would further increase pathogenic disease mechanisms, and causes progressing neuronal cytotoxicity.

To this day none of the three proteins had been implied to play a role in neurodegenerative diseases. In fact, ZNF179 and ZMAT have never been associated with neurodegenerative diseases. Moreover, there is not much known about these two proteins in general. ZNF179 is a RING finger protein, which is highly expressed in brain tissue and is possibly involved in transcriptional regulation during nervous system development [249, 250]. Many proteins with a RING finger domain play critical roles in the ubiquitin-proteasome system (UPS) [327-329], indicating that ZNF179 might also be a member of the UPS. The function of ZMAT2 is not well described, but its zinc finger domain of matrin type suggests that it is probably involved in RNA splicing [251, 252]. Indeed knock-down of ZMAT2 resulted in significantly up-regulated mRNA expression levels of huntingtin, ataxin-1, TDP-43, APP, α-synuclein and parkin. Further experiments will be necessary to clarify functional roles of ZNF179 and ZMAT2 in mammalian cells.

IQSEC1, also known as ARF-GEP$_{100}$, is a guanine nucleotide exchange factor that promotes binding of GTP to the ADP ribosylation factor protein ARF6 (a small G protein) [247]. IQSEC1 is involved in controlling endocytosis of plasma membrane proteins, E-cadherin recycling and actin cytoskeleton remodelling via activation of the ARF6 protein [248]. ARF6 was also shown to control APP processing by influencing the endosomal sorting of the β-secretase BACE1 protein (Figure 37) [330]. ARF6-Q67L, which lacks GTP hydrolysis activity, blocked the delivery of BACE1 to early endosomes, indicating that GTP hydrolysis of ARF6 is required for endosomal sorting of BACE1 [330]. ARF6-Q67L co-expression with mutant APP resulted in a marked decrease of Aβ peptides [330]. Thus, IQSEC1 is essential for the activation of ARF6 and knock-down of this protein should coincide with a decreased activity of ARF6, which in turn might explain the reduced amount of Aβ peptides observed after IQSEC1 silencing. The increase in aggregation of huntingtin, ataxin-1 and TDP-43 as well as the marked rise in tau protein expression upon IQSEC1 knock-down could also be explained by another regulatory mechanism involving ARF6 – autophagosome formation (Figure 37) [331]. It is known that the over-expression of the ARF6_Q67L mutant blocks the formation of early autophagic structures [331]. The knock-down of IQSEC1 might have similar effects in mammalian cells which could result in the accumulation of misfolded proteins, because protein degradation by autophagy might be disturbed due to reduced activation of ARF6. In order to obtain support for this hypothesis, autophagosome formation upon IQSEC1 depletion needs to be analyzed with biochemical and cell biological methods.

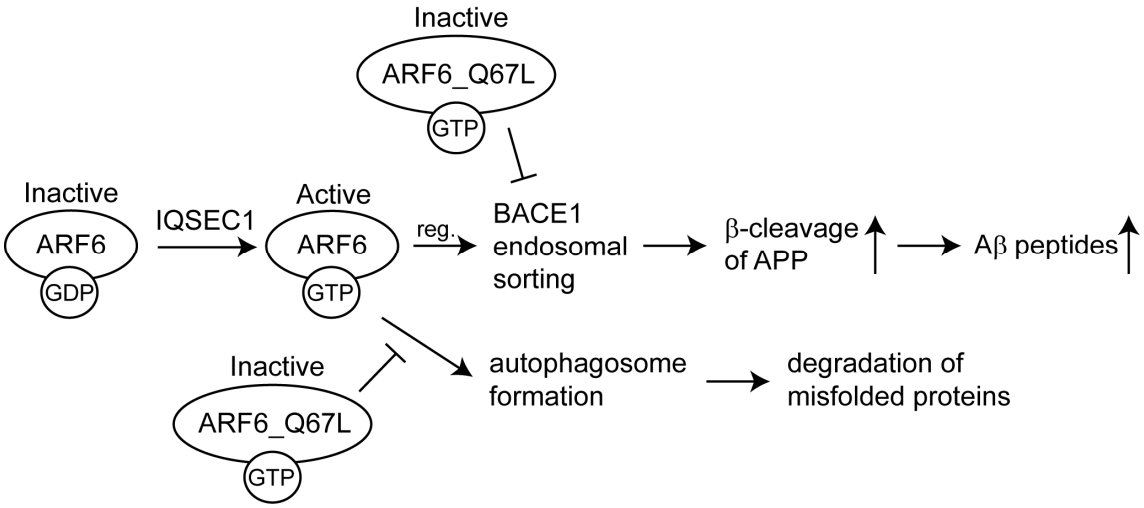

Figure 37: IQSEC1 regulates ARF6 activation and thereby likely regulates BACE1 endosomal sorting and autophagosome formation. Depletion of IQSEC1 could alter BACE1 endosomal sorting resulting in decreased APP cleavage and Aβ production. The knock-down of IQSEC1 might also decrease autophagosome formation, which could result in the accumulation of misfolded proteins. Both observations were made with the inactive GTP hydrolysis mutant ARF6_Q67L indicating that active ARF6 is critical in both processes [330, 331].

3.4 Identification of a protein complex that modulates TDP-43 aggregation

One of the aims of this thesis was the identification of protein aggregation modifiers using the available Y2H protein-protein interaction data. During the last decade a large number of proteins., that modify aggregation or cytotoxicity of NDPs such as huntingtin, ataxin-1 and SOD1 were discovered by genome-wide screens in model organisms like yeast, worm or fly [169, 332-337]. The results obtained in model organisms do not always reflect the situation in mammalian cells. A recent study for example reported that knock-down of human genes led to the opposite effect on huntingtin aggregation than the knock-down of their *C. elegans* homologs [338]. Therefore, I performed all siRNA screens in human cells. For the initial large-scale screen I used HEK293 cells, which are well suited for high-throughput experiments because of their easy handling. The second, more focused screen, which was performed in

order to identify protein complexes that modulate TDP-43 aggregation was conducted in the neuroblastoma cell line SH-EP to have a more appropriate neuronal cell model.

In this thesis I focused on the analysis of TDP-43 aggregation modifiers. TDP-43 is the main component of aggregates found in ALS and FTLD-U patients [37]. Moreover, patients with AD, Lewy body dementia, HD and SCA were also shown to exhibit TDP-43 inclusions [37, 39, 41, 42]. To this date only in one study modifiers of TDP-43-induced cytotoxicity have been reported [339]. It was shown that over-production of the yeast ataxin-2 homolog Pbp1 enhanced TDP-43 toxicity. Moreover, ataxin-2 with intermediate length polyglutamine expansions was found to increase the risk to develop ALS [339]. These results indicate that the identification of further TDP-43 aggregation or toxicity modifiers is a feasible strategy to increase our understanding of the pathomechanism in ALS. Here, I identified 22 proteins that significantly altered TDP-43 aggregation in cell-based assays (10 enhancers and 12 suppressors; see section 2.4.4). These proteins are members of seven predicted protein complexes (see section 2.4.3). In this study a protein complex was defined as a set of highly connected proteins within a protein-protein interaction (PPI) network. The employed PPI network for *in situ* complex prediction consisted of Y2H-based and previously published interactions for TDP-43 and the 191 TDP-43 aggregation modifiers, which were identified with an in the initial FRET-based siRNA screen in HEK293 cells (see section 2.4.2).

Most of the 22 identified TDP-43 aggregation modifiers according to available Gene Ontology data are either involved in transcriptional regulation (c-MYC, HP1, BRG1, HDAC1, pRB, ATN1 and IRE1) or protein degradation (KLHL20, ATG10, CDC16, CDC23, ARA54, UBE2A and S27A). The other proteins play a role in signal transduction (ASB13, SOCS4 and GNB2), RNA splicing (SF3B3 and PRPF8), protein transport (HIP1) or co-enzyme synthesis in mitochondria (WBSCR27 and PANK2). All proteins in complex 1 (c-MYC, HP1, BRG1, HDAC1 and pRB) are involved in transcriptional regulation [274, 276, 277, 279-

282] and knock-down of each complex member significantly altered TDP-43 aggregation. Depletion of c-MYC enhanced aggregation, whereas knock-down of HP1, BRG1, HDAC1 and pRB reduced TDP-43 aggregation. Additionally, silencing of pRB, HDAC1 and HP1 significantly decreased TDP-43-induced cytotoxicity. Due their known role as transcriptional regulators I hypothesized that the five proteins in complex 1 might also modify TDP-43 expression. Indeed I found that knock-down of c-MYC significantly increased mRNA levels of endogenous TDP-43, while silencing of HP1, HDAC1, BRG1 and pRB reduced TDP-43 mRNA expression. This is the first time that a functionally connected group of regulators of TDP-43 expression were identified.

Disruption of protein homeostasis (proteostasis) is thought to play a key role in pathogenic mechanisms of neurodegenerative diseases [64]. Proteostasis is the ability of a cell to maintain appropriate protein concentration levels, protein folding, protein interactions and protein localization [65]. Mechanisms contributing to maintain proteostasis have been observed at all levels of the protein production cycle: from gene transcription regulation to protein folding and transport of the folded protein molecules to their appropriate cellular localization [65]. A very important regulatory step of protein production exists at the RNA processing stage. RNA-binding proteins (RBPs) like TDP-43 regulate all aspects of this pathway by influencing different steps in the mRNA life-cycle: capping and polyadenylation, splicing, editing, stability, export, transport and localization [340]. Because of their importance, the expression of RBPs is tightly regulated by the ceullular regulatory machinery. In case of TDP-43 depletion and enhancement of protein levels is toxic for cells and results in phenotypes reminiscent of ALS or FTLD [155, 341-345]. Recently, it has been reported that TDP-43 can regulate its own protein levels by binding to its mRNA in the 3'-UTR region (Figure 38) [164]. It was shown that the TDP-43 autoregulatory mechanism is based on a negative feedback loop [164]. When TDP-43 nuclear levels rise, increased binding of the protein to the 3'-UTR promotes mRNA instability and this is related to exosome-mediated degradation of TDP-43

mRNA [164]. When TDP-43 levels drop below the natural threshold, increased mRNA stability and lower exosome degradation cause TDP-43 levels to rise again [164].

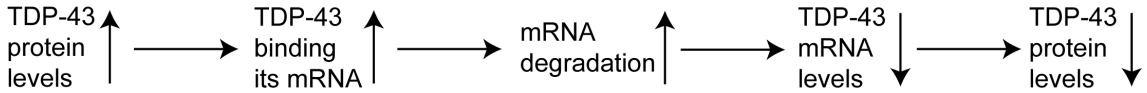

Figure 38: TDP-43 auto-regulates its own mRNA levels through a negative feedback loop. The auto-regulatory mechanism is caused by binding of TDP-43 to the 3'-UTR of its own mRNAs, which promotes RNA instability and exosome-mediated mRNA degradation.

TDP-43 aggregation occurs in the cytoplasm and is often accompanied by nuclear clearance of the protein [37, 38]. I obtained similar results, when YFP-TDP-43 was over-produced in SH-EP cells (Figure 27). Depletion of TDP-43 from the nucleus as a result of its aggregation in the cytoplasm might cause a disturbance of the TDP-43 auto-regulation mechanism. Uncontrolled TDP-43 expression levels could yield even more TDP-43 aggregates by an increased production of mRNA and subsequently of more protein. These aggregates would then serve as a seed by recruiting more TDP-43 protein to inclusion bodies [19], causing both a loss- and gain-of-function phenotype [346]. Increased sequestration of TDP-43 into aggregates in the cytoplasm would thus lead to a major increase in TDP-43 production by an attempt of the cell to overcome eventual loss-of-function effects in the nucleus [347]. With regard to the disturbed auto-regulation of TDP-43, two studies have found increased mRNA levels in the brain of FTLD patients [348, 349] and TDP-43 protein expression was increased by a nucleotide substitution in the 3'-UTR region of TDP-43 identified in FTLD patients [350].

My studies in cell model systems indicate that silencing of BRG1, pRB, HDAC1 or HP1 dramatically decreases TDP-43 expression levels (Figure 39A). This could be based on direct regulation of *TARDBP* gene transcription or on altered expression of proteins that play a role in the auto-regulatory mechanism of TDP-43 expression such as exosome components (Figure 39A). All four proteins are mainly involved in transcriptional repression [276, 351-354]. This

suggests that down-regulation of the four proteins should result in increased TDP-43 expression, if they would directly influence its gene expression. As the mRNA levels of TDP-43 were decreased after knock-down of BRG1, pRB, HDAC1 and HP1, it suggests that they probably do not directly influence TDP-43 expression. Therefore silencing of BRG1, pRB, HDAC1 and HP1 might restores or strengthens the auto-regulatory mechanism of TDP-43 expression, resulting in the observed decrease in TDP-43 mRNA expression. If the auto-regulatory mechanism of TDP-43 expression is restored, increased protein levels of TDP-43 (e.g. because of over-production of exogeneous TDP-43 (in my siRNA experiments in the form of YFP-TDP-43)) would result in increased exosome-mediated endogenous TDP-43 mRNA degradation and therefore lead to reduced TDP-43 mRNA levels [164].

In comparison to the proteins BRG1, pRB, HDAC1 or HP1 knock-down of c-MYC had the opposite effect on TDP-43 mRNA expression and YFP-TDP-43 aggregation (Figure 39B). c-MYC is known to repress or activate gene expression [281-283]. If c-MYC directly represses TDP-43 expression, knock-down of MYC would result in increased endogenous TDP-43 expression, which indeed was the case in my experiments (Figure 39B). However, MYC silencing could also inhibit the auto-regulatory mechanism of TDP-43 and thereby increase TDP-43 expression (Figure 39B). Therefore, further experiments are necessary to clarify how c-MYC, BRG1, pRB, HDAC1 and HP1 regulate the expression of TDP-43.

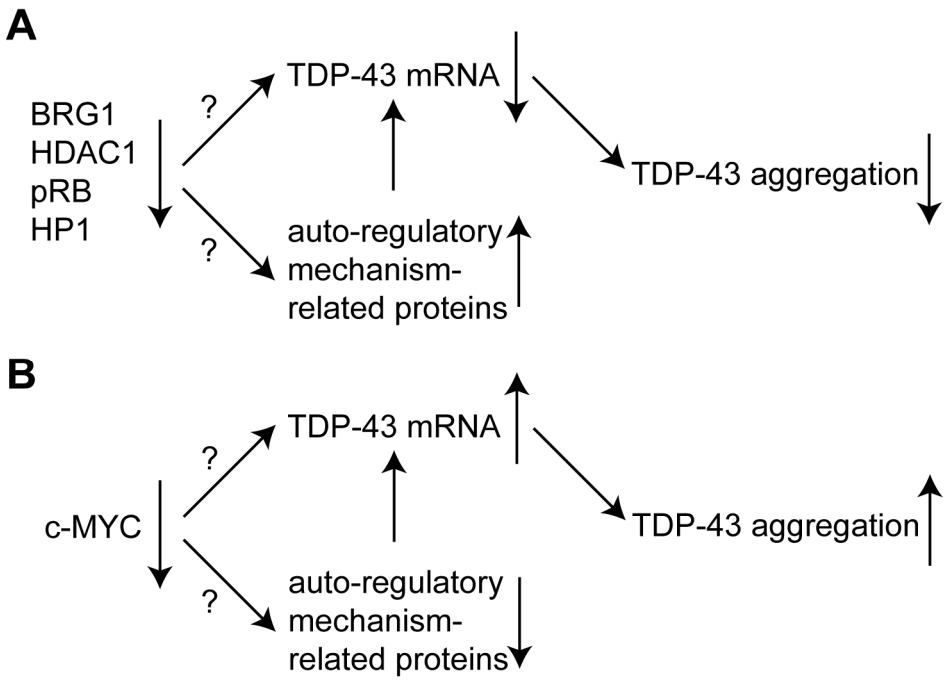

Figure 39: Silencing of BRG1, HDAC1, pRB, HP1 and c-MYC influenced TDP-43 mRNA expression as well as TDP-43 protein aggregation. (A) BRG1, HDAC1, pRB and HP1 mRNA depletion reduced TDP-43 mRNA expression either directly or by altering the expression of proteins that are involved in the auto-regulatory mechanism of TDP-43 mRNA expression such as exosome components. Decreased TDP-43 mRNA levels most likely resulted in reduced TDP-43 aggregation (B) In contrast, the depletion of c-MYC had the opposite effect. Knock-down of this gene increased TDP-43 mRNA levels either directly or indirectly, which results in increased protein synthesis and TDP-43 aggregation.

3.5 Outlook

In order to further elucidate mechanism how the proteins IQSEC1, ZNF179 and ZMAT2 influence the toxicity and aggregation of NDPs such as TDP-43 or huntingtin additional experiments are necessary. First of all, it is necessary to assess the effects of the knock-down of these three proteins on α-synuclein and parkin induced cytotoxicity in a neuronal cell line or primary neurons. In this study I obtained evidence that mRNA expression of IQSEC1, ZNF179 and ZMAT2 is altered in PD brains, suggesting that these proteins might also

influence the synthesis and function of the proteins α-synuclein and parkin (SNCA and PARK2) that play a key role in the pathogenesis of PD. Furthermore, it would be interesting to learn whether silencing of the three proteins also influences the cytotoxicity induced by other NDPs such as huntingtin or TDP-43. In case of huntingtin a suitable model would be a rat PC12 cell line, which stably expresses a toxic HTTEx1Q103-GFP fusion protein [355]. The human neuroblastoma cell line SH-EP (established as a model for TDP-43 toxicity in this thesis) or the mouse motor neuron-like cell line NSC-34 [356] are suitable models to assess TDP-43 cytotoxicity. Another important aspect for further experiments is to elucidate the functions for ZNF179 and ZMAT2 in disease model systems, because there is not much known about the cellular function of these two proteins. Additionally, it would be interesting to show whether knock-down of IQSEC1 alters BACE1 endosomal sorting and inhibits autophagosome formation. This was shown for inactive ARF6_Q67L, but also needs to be investigated for IQSEC1 [330, 331].

The results in this thesis indicate that BRG1, HP1, HDAC1, pRB and c-MYC regulate TDP-43 expression and subsequently also affect TDP-43 aggregation. The experiments in this could not clearly elucidate how these five proteins regulate the expression of the *TARDBP* gene. Therefore, additional experiments need to be conducted to establish whether these proteins directly bind to the *TARDBP* gene. This can be done by chromatin immunoprecipitation (ChIP) experiments [357]. Furthermore, by determining the acetylation status of histones that bin to the regulatory sequences of the *TARDBP* gene it should be possible to determine whether the gene is silenced upon knock-down of any of the five proteins. Additionally, TDP-43 mRNA expression also needs to be assessed after knock-down of the five proteins in the absence of YFP-TDP-43 over-expression, as over-production of exogeneous TDP-43 might influence endogenous TDP-43 expression because of the auto-regulatory mechanism controlling TDP-43 expression.

4 Materials and Methods

4.1 Materials

4.1.1 Bacterial strains

Mach1™ T1R — *E. coli/* F- Φ80*lac*ZΔM15 Δ*lac*X74 *hsd*R(rK-, mK+)Δ*rec*A1398 *end*A1 *ton*A (Invitrogen), recommended strain for use with the Gateway® Cloning System.

4.1.2 Yeast strains

L40ccua — *MATa his3Δ200 trp1-901 leu2-3, 112 LYS2::(lexAop)$_4$-HIS3 ura3::(lexAop)$_8$-lacZ ADE2::(lexAop)$_8$-URA3 GAL4 gal80 can1 cyh2 [168]*

L40ccα — *MATα his3Δ200 trp1-910 leu2-3, 112 ade2 LYS2::(lexAop)$_4$-HIS3 URA3::(lexAop)$_8$-lacZ GAL4 gal80 can1 cyh2 [168]*

4.1.3 Cell lines

SH-EP — Human neuroblastoma cell line derived from SK-N-SH cells;adherent epithelial-like cells growing as monolayer [358] (Prof.Dr. M. Schwab, DKFZ [359])

HEK293 — Human embryonal kidney cell line; adherent fibroblastoid cells growing as monolayer (DSMZ, Deutsche Sammlung für Mikroorganismen und Zellkulturen GmbH)

SH-SY5Y — Human neuroblastoma cell line derived from SK-N-SH cells and sub-cloned via SH-SY5 and SH-SY [358] (DSMZ, Deutsche Sammlung für Mikroorganismen und Zellkulturen GmbH)

SH-SY5Y_ APP695 — Human neuroblastoma cell line stably transfected with APP695 (kindly provided by Prof. Dr. Willnow, MDC)

4.1.4 Plasmid vectors

<u>pBTM116-D9</u>

Characteristics	Y2H bait vector, *2μ* plasmid, Gateway® cloning
Size	8,206 bp
Promoter	pADH1

Tag	LexA DNA-binding domain
Auxotrophic marker	*TRP1*
Resistance	AmpR
Reference	Stelzl *et al.* 2005 [190]

pACT4-DM

Characteristics	Y2H prey vector, *2µ* plasmid, Gateway® cloning
Size	9,444 bp
Promoter	pADH1
Tag	*GAL4* activation domain
Auxotrophic marker	*LEU2*
Resistance	AmpR
Reference	Grelle *et al.* 2006 [360]

pPA-Reni-DM

Characteristics	Expression vector for mammalian cells, Gateway® cloning
Size	8,404 bp
Promoter	CMV
Tag	Protein A-Renilla luciferase
Resistance	AmpR
Reference	Palidwor *et al.* 2009 [238]

pFireV5-DM

Characteristics	Expression vector for mammalian cells, Gateway® cloning
Size	8,828 bp
Promoter	CMV
Tag	Firefly luciferase-V5
Resistance	AmpR
Reference	Palidwor *et al.* 2009 [238]

pdECFP-Amp

Characteristics	Expression vector for mammalian cells, Gateway® cloning
Size	6,195 bp
Promoter	CMV
Tag	Enhanced cyan fluorescent protein (ECFP)
Resistance	AmpR
Reference	Simpson *et al.* 2000 [361]

pdEYFP-Amp

Characteristics	Expression vector for mammalian cells, Gateway® cloning
Size	6,157 bp
Promoter	CMV
Tag	Enhanced yellow fluorescent protein (EYFP)
Resistance	AmpR
Reference	ImaGenes GmbH

pDONR221

Characteristics	Entry vector of the Gateway® cloning system
Size	4,470 bp
Resistance	KanR
Reference	Invitrogen

4.1.5 Microbiological media and buffers

100x Ade	2 g/l adenine
1000x Ampicillin stock	100 mg/ml dissolved in 50% ethanol, stored at -20°C
AttoPhos™ buffer	50 mM Tris-HCl pH 9.0, 500 mM NaCl, 1 mM $MgCl_2$
AttoPhos™ reagent	10 mM AttoPhos™ reagent dissolved in 100 mM Tris-HCl pH 9.0
1% BSA	Bovine serum albumin was dissolved in 1x PBS to a final concentration of 1% (w/v)
Carbonate buffer	70 mM $NaHCO_3$, 30 mM Na_2CO_3, pH 9.6

10x DNA sample buffer	0.42% bromophenol blue, 0.42% xylene cyanol, 25% ficoll type 400, dissolved in distilled water, stored at -20°C
100x His	2 g/l histidine
1000x Kanamycin stock	25 mg/ml dissolved in distilled water, stored at -20°C
100x Leu	10 g/l leucine
LUMIER lysis buffer	50 mM HEPES, 150 mM NaCl, 10% glycerine, 0.1% NP-40, 20 mM NaF, 1.5 mM $MgCl_2$, 1 mM EDTA, 25 U/ml benzonase, 1 mM PMSF and 1x protease inhibitor
Lysis buffer for mammalian cells	50 mM Tris-HCl pH 8.8, 100 mM NaCl, 5 mM $MgCl_2$, 1% NP-40, 1 mM EDTA, stored at 4°C; add protease inhibitors (Complete™ final concentration: 1x, 1 mM PMSF) and 25 U/ml benzonase before use
LB (Luria Bertani) medium	10 g/l Bacto Peptone, 5 g/l yeast extract, 10 g/l NaCl, pH 7.2
25x Protease inhibitors	One tablet of Complete™ protease inhibitor (Roche) dissolved in 2 ml distilled water, stored at -20°C
10x PBS	80 g NaCl, 2g KCl, 14.4 g Na_2HPO_4, 2.4 g KH_2PO_4 to 1 l with distilled water
1x PBS-T	1x PBS, 0.05% Tween® 20
4% PFA	4 g of paraformaldehyde dissolved in 100 ml PBS and heated at 50°C for 5 min to reach a clear solution, stored at -20°C
PMSF	100 mM PMSF dissolved in isopropanol, stored at -20°C
10% resolving gel	3.3 ml of 30% acrylamide, 2.5 ml of 1.5 M Tris-HCl(pH 8.8), 100 µl of 10% SDS, 4.05 ml ddH_2O, 100 µl of 10% APS and 10 µl TEMED
4% stacking gel	0.65 ml of 30% acrylamide, 1.25 ml of 0.5 M Tris-HCl (pH 6.8), 50 µl 10% SDS, 3.05 ml ddH_2O, 50 µl of 10% APS and 10 µl TEMED
SD medium	6.7 g/l yeast nitrogen base, 20 g/l glucose, 10 ml 100x amino acid stock solution (amino acid dependent on auxotrophic markers of yeast strain used)
4x SDS loading buffer	200 mM Tris-HCl pH 6.8, 400 mM DTT, 8% SDS, 4 mg/ml bromophenol blue, 40% glycerol, store at -20°C
1x SDS running buffer	1x WB buffer, 0.1% SDS

5% skimmed milk	Skimmed milk powder was dissolved in TBS-T to a final concentration of 3% (w/v)
S.O.C. medium	2% tryptone, 0.5% yeast extract, 10 mM NaCl, 2.5 mM KCl, 10 mM $MgCl_2$, 10 mM $MgSO_4$, 20 mM glucose
TBE	89 mM Tris base, 89 mM boric acid, 2 mM EDTA (pH 8.0)
TBS	20 mM Tris-HCl pH 7.5, 150 mM NaCl
TBS-T	20 mM Tris-HCl pH 7.5, 150 mM NaCl, 0.05% Tween® 20
TE buffer	10 mM Tris-HCl (pH 8.0), 1 mM EDTA
100x Trp	2 g/l tryptophane
100x Ura	2 g/l uracil
10x WB buffer	30 g/l Tris, 144 g/l glycin
Western blot buffer	1x WB buffer, 10% ethanol
YPD medium	10 g/l yeast extract, 20 g/l bacto peptone, 20 g/l glucose

4.1.6 Media and supplements for mammalian cell culture

Dulbecco's modified Eagle medium (DMEM) with 4.5 g/l D-glucose, sodium pyruvate, without L-glutamine	Gibco
Dulbecco's modified Eagle medium (DMEM) with 1 g/l D-glucose, L-glutamine, sodium pyruvate	Gibco
0.5% Trypsin and 0.53 mM Na-EDTA in Hanks' B.S.S.	Gibco
Fetal calf serum (FCS) from E.G. approved countries	Gibco
Dulbecco's phosphate buffered saline (D-PBS) without calcium and magnesium	Gibco
L-glutamine	Gibco
Penicillin G (10,000 units/ml) and Streptomycin sulphate (10,000 µg/ml) in 0.85% saline	Gibco
MEM Non Essential Amino Acids (100x)	Gibco
Hygromycin B (100 mg/ml)	Invitrogen
Opti-MEM®	Gibco

4.1.7 PCR primers for entry clone synthesis

TDP-43_CT_attB1:
5'-GGG GAC AAG TTT GTA CAA AAA AGC AGG CTG GGC CAC CAT GGT CTT CAT CCC CAA GCC A-3'
TARDBP_reverse_attB2:
5'-GGG GAC CAC TTT GTA CAA GAA AGC TGG GTG CTA CAT TCC CCA GCC AGA AGA CTT AGA-3'

The oligonucleotides were synthesized by metabion international AG in quantities of 40 nmol and were purified by desalting. Primers were resolved in nuclease-free water and used in PCR reactions at 100 µM concentrations.

4.1.8 siRNAs

ON-TARGETplus SMARTpool siRNAs were purchased from Dharmacon siRNA Technologies (Thermo Scientific) in a quantity of 5 nmol and were resolved to a concentration of 20 µM in RNAse-free water. The non-targeting control siRNA No. 4 (NTC; Thermo Scientific) was used as negative control and siGLO Red (fluorescence tag DY-547) was used as transfection control. Ambion *Silencer*® Select siRNAs (Life Technologies) were a kind gift of Prof. Dr. Michael Boutros (DKFZ, Heidelberg).

Table 5: siRNA target sequences

Name	Company	Target mRNA sequences
ARA54	Ambion	GAUCUGAUGUAGACCAAGA GGAUGCAAUUUCUUAAGGA CAAUGACCCUGGUUCACCA
ASB13	Ambion	GUGUGAGGCUUCUUAUUGA CGAGUACUACGAAAAGACA GUGCUUCGAGUACUACGAA
ATG10	Ambion	GAAUCUACCUCUGAGUUAU CAAUAAGAAUGUCAACUAU CAACAGAUAGGUGAUAGUU
ATN1	Ambion	CCUUAUUCAUCCUCUAGUA GCAAGAUGCUAUCCAUGCA GGCGGAGCCUUAAUGAUGA
ATP1A3	Ambion	CCGUGAAGCUGAUGCGUGA GGGUUUGACCCACAGCAAA CGGACAAAUUGGUCAAUGA

Name	Company	Target mRNA sequences
BACE1	Ambion	GCAUCACCAUCCUUCCGCA AGACGACUGUUACAAGUUU GCAUGAUCAUUGGAGGUAU
BRG1	Ambion	GUAGCUCCGAGGUCUGAUA GGAAUACCUCAAUAGCAUU GGCUUGAUGGAACCACGAA
CDC16	Ambion	GCUGUAUAUUGGAUUAGAA GGAACGAGGUAACAGUUGA CACGAAAACUGGACAAAUU
CDC23	Ambion	CUUGGUGCCUGGACACUAA GACCCUUACAGGAUUGAAA GAUUGAUAAAUAUCGUGUA
ESRP1	Dharmacon	AGUCAGGGCACGAGGUUUA GGACAGCAUUGCCCUAUUA CAAUGAUUUCAGAGCCUUA CCCGGUAUAUUGAGGUUUA
GNB2	Ambion	GGGUUUUGCUGGACACAGU AGACCUUCAUCGGCCAUGA GGGAUUCCAUGUGCCGACA
HDAC1	Ambion	CUAUGGUCUCUACCGAAAA CCGGUCAUGUCCAAAGUAA CCAAUAUGACUAACCAGAA
HDAC2	Ambion	CUACGACGGUGAUAUUGGA GGCAGAUAUUUAAGCCUAU GGGUUGUUUCAAUCUAACA
HDAC6	Ambion	CCGUGAGAGUUCCAACUUU CAGUUUAUCUGCAUCCGAA GGAGGGUCCUUAUCGUAGA
HIP1	Ambion	GAGCCUGUCUGAGAUAGAA GCAAAUCACAGAUCGAAGA CCACUUAAUUGAGCGACUA
HP1	Ambion	ACCUGGUUCUUGCAAAAGA GCAGAGCAAUGAUAUCGCU GGAGCACAAUACUUGGGAA

Name	Company	Target mRNA sequences
IRE1	Ambion	CCUGCGCUAUCUGACCUUC CAGGACAUCUGGUAUGUUA GAAACUUCCUUUUACCAUC
IQSEC1	Dharmacon	GAGCAGAUAUCAAAGUGUU CGGAAGAAAUUCACCGAUG GGACUCGCCUGCCUUUAGC CGAGAAAUCUUCCUGUUCA
KIF1B	Ambion	GCAAUGCUGUUAUCAAUGA GGAAAAUCUUAUACAAUGA CGAAGAUCCCUGUUUUGCA
KLHL20	Ambion	GAUGGAUCCUCUUAUCUCA GGAUCCUCUUAUCUCAAUA GCUUCUAUGAGUACCAGAA
MYC	Ambion	GAGCUAAAACGGAGCUUUU AGACCUUCAUCAAAAACAU ACAGCCCACUGGUCCUCAA
NDUFS1	Ambion	CUCCUAAUCUUGUUCGAUA CCAUAGCUGAUGUUAUUCU GGGUUGGAAUAUCCUAACA
PANK2	Ambion	GCAUAUGCUUUGGAUUAUU GGACGGUCACAGUGCUAUU GAGCGACUUUGAUCACCAU
PIMT	Ambion	CAAUCUCCGCAAAAAUGGA GGAUUCUCCACAAUCAAUA CCCACUAUGCAAAAUGUAA
PRPF8	Ambion	GCAGAUACAUUGAUCGCAU GGACAUGAACCAUACGAAU CCCUACAUGUGAACAACGA
RB	Ambion	GCGUGUAAAUUCUACUGCA GGAUAGCAAAACAACUAGA CCAGUACCAAAGUUGAUAA
RING1B	Ambion	GGAGUGUUUACAUCGUUUU CAAACGGACCAAAACAUCU GGCUAGAGCUUGAUAAUAA

Name	Company	Target mRNA sequences
RPS27A	Ambion	GUACUUUGUCUGACUACAA CCUCGGAUACGAUAGAAAA GGACGUACUUUGUCUGACU
RYBP	Ambion	CAAAGACCAGCGAAACAAA GAAACAGUGCUGAAGCCUU GCAUCUGCGAUGUGAGGAA
SF3B3	Ambion	CAACCUUAUUAUCAUUGAA CGUCUAUACUUACAAGCUU GUUUCAUCUGGGUUCGCUA
SOCS4	Ambion	GAAGUUAUCUUGGUCAAAA GGAUGGUCAGCUAAAACGA CAGUGAAUGGUAUAGAGAA
TRIM23	Ambion	CCCAUUUGAUCGACAAGUA GGGUCGUUACGUUAGGAUU CUCUAGCUGAUAAACCUCA
UBC	Ambion	GGUUGAUCUUUGCCGGAAA GUGAAGACCCUGACUGGUA GCAAAUCUUCGUGAAGACA
UBE2A	Ambion	CCAGGAGAACAAACGGGAA GAACAAACGGGAAUAUGAA GGAUGAACCCAAUCCCAAU
UEV1A	Ambion	UGGAGUAAAUAGUUCUAAU GAAUUCAUAUAGCAUCAAA AGUAAAUAGUUCUAAUGGA
WBSCR27	Dharmacon	CAAUGCGAUACCUGAGCUA CGGACUACGACCAGGAUGU CGUCCAACCUUCAAUACAA UACCGAAAGUGGAAGGCGA
WDR61	Dharmacon	GAUCAGGUCUGGGGAGUAA CGUCUUUGGGACUUGGAAA CAAAGAGAAUGUACGGAUU AGGAACUCAUGUCGGGAAA
ZMAT2	Dharmacon	CGAGAAGAGGCUCACGGAA AGGAAAAGGCCAAAGCGUA GGAUAUUACUGCAAUGUCU CUGAGGAGGACUUGACAUU

Name	Company	Target mRNA sequences
ZNF179	Dharmacon	AAACAGAGCUUCAUGGGAA GAACCAAGGCCAUGCAAGC AUACAGACCUGGACUAUCU AGAGGGAGUUCGAGGAGUA

4.1.9 Quantitative real-time PCR assays

TaqMan® Gene Expression Assays with FAM or VIC as dye label were purchased from Applied Biosystems (Life Technologies).

Table 6: TaqMan® Gene Expression Assays

Gene symbol	TaqMan® accession	Assay function	Dye label
ACTB	Hs99999903_m1	Housekeeping gene	FAM or VIC
APP	Hs01552283_m1	Target transcript	FAM
ATG10	Hs00919719_m1	Target transcript	FAM
ATXN1	Hs00165656_m1	Target transcript	FAM
CBX5	Hs01127577_m1	Target transcript	FAM
CDC16	Hs00187430_m1	Target transcript	FAM
HDAC1	Hs02621185_s1	Target transcript	FAM
HTT	Hs00918174_m1	Target transcript	FAM
IRE1	Hs00176385_m1	Target transcript	FAM
IQSEC1	Hs00208333_m1	Target transcript	FAM
KLHL20	Hs00976200_m1	Target transcript	FAM
PARK2	Hs01038318_m1	Target transcript	FAM
RB	Hs01078066_m1	Target transcript	FAM
SNCA	Hs01103383_m1	Target transcript	FAM
SOCS4	Hs00328404_s1	Target transcript	FAM

Gene symbol	TaqMan® accession	Assay function	Dye label
TARDBP	Hs00606522_m1	Target transcript	FAM
WBSCR27	Hs00381185_m1	Target transcript	FAM
ZMAT2	Hs00291823_m1	Target transcript	FAM
ZNF179	Hs00246644_m1	Target transcript	FAM

4.1.10 Antibodies

Antibodies were used for immunoblotting (IB), immunofluorescence (IF) and immunoprecipitation (IP). For IPs 1.6 µg of each antibody was used.

Table 7: Primary antibodies

Antibody	Species	Dilution	Supplier
Anti-Actin	Mouse	1:2,000 (IB)	Abcam
Anti-BRG1	Rabbit	1:2,000 (IB)	ProteinTech
Anti-FUS	Rabbit	1:2,000 (IB)	ProteinTech
Anti-GFP	Mouse	1:1,000 (IB)	Abgent
Anti-HDAC1	Rabbit	1:800 (IB)	ProteinTech
Anti-HDAC2	Rabbit	1:2,000 (IB)	ProteinTech
Anti-HDAC6	Rabbit	1:1,000 (IB)	ProteinTech
Anti-HP1	Rabbit	1:800 (IB)	ProteinTech
Anti-IGF2BP2	Rabbit		ProteinTech
Anti-MYC	Rabbit	1:1,000 (IB)	ProteinTech
Anti-RBBP4	Rabbit		Abcam
Anti-Human Tau	Rabbit	1:1,000 (IB)	Dako
Anti-PHF-tau (AT8)	Mouse	1:100 (IB)	Thermo Scientific
Anti-TDP-43	Rabbit	1:1,500 (IB)	ProteinTech

Antibody	Species	Dilution	Supplier
Anti-YWHAH	Rabbit		ProteinTech
Gamma globulin	Sheep		Jackson Immunoresearch

Table 8: Secondary antibodies

Antibody	Conjugate	Species	Dilution	Supplier
Anti-mouse IgG	Alkaline phosphatase	Goat	1:10,000	Sigma
Anti-rabbit IgG	Alkaline phosphatase	Goat	1:10,000	Sigma
Anti-mouse IgG	Peroxidase	Goat	1:2,000	Sigma
Anti-rabbit IgG	Peroxidase	Goat	1:2,000	Sigma
Anti-sheep IgG		Rabbit		Jackson Immunoresearch

4.1.11 Enzymes, proteins, markers and DNA

BP Clonase enzyme mix	Invitrogen
Benchmark prestained protein ladder	Invitrogen
Benzonase purity grade II	Merck
BSA 10 mg/ml	NEB
BsrGI restriction enzyme	NEB
Herrings sperm carrier DNA	Clontech
1 kb DNA ladder	Invitrogen
LR Clonase enzyme mix	Invitrogen
PageRuler Prestained Protein Ladder	Thermo Scientific
Phusion HF Master Mix	NEB
Proteinase K	Sigma

4.1.12 Kits

Apo-ONE® homogenous caspase-3/7 assay	Promega
BCA Protein assay reagent	Pierce
Dharmafect 1 transfection reagent	Dharmacon
Dharmafect Duo transfection reagent	Dharmacon
Dual-Glo™ Luciferase Assay System	Promega
Duolink In Situ Red Starter kit	Olink Bioscience
Human/Rodent Abeta 3-Plex Ultra-Sensitive Kit	Meso Scale Discovery
Lipofectamine 2000	Invitrogen
Plasmid Mini kit	Qiagen
QIAquick gel extraction kit	Qiagen
QIAshredder homogenizer columns	Qiagen
Quick blunting kit	NEB
RNAeasy Mini kit	Qiagen
RevertAid H Minus First Strand cDNA Synthesis kit	Fermentas
TaqMan® Universal PCR Master Mix	Applied Biosystems
TransIT transfection reagent	Mirrus
Western Lightning ECL	Perkin Elmer

4.1.13 Chemicals and consumables

3MM Whatman filter paper	Whatman
Agarose	Invitrogen
Ammoniumpersulfate (APS)	BioRad
Ampicillin-trihydrate	Sigma-Aldrich
Blot absorbent filter paper	BioRad
Bovine serum albumin, fraction V	Merck
Bromophenol blue	Merck
Cell culture dishes	BD Falcon
Cellulose acetate membrane 0.2 µm	Schleicher & Schuell
Complete protease inhibitor cocktail	Roche
Cover slips (round)	BD Biosciences
Dithiothreitol (DTT)	Serva
Dimethylsulfoxide (DMSO)	Sigma-Aldrich

Dynabeads® Protein G for Immunoprecipitation	Invitrogen
Ethidium bromide solution 10 mg/ml	Sigma-Aldrich
Ethylenediamine tetraacetic acid (EDTA)	Merck
Filter paper GB005	Schleicher & Schuell
Glycerol	Merck
High density nylon membranes	Micron Separations Inc.
Hoechst 33342	Biovision
Kanamycin A monosulfate	Sigma-Aldrich
MicroAmp Optical 96-well reaction plate	Applied Biosystems
MicroAmp Optical Adhesive film	Applied Biosystems
NP-40 (IGEPAL CA 630)	Sigma-Aldrich
NuPAGE® MES SDS Running Buffer	Invitrogen
NuPAGE® Novex 4-12% Bis-Tris Gel 1.0 mm, 10/15 well	Invitrogen
Protran BA 83 nitrocellulose membrane	Schleicher & Schuell
O-phenanthroline	Merck Chemicals
Para-formaldehyde	Sigma-Aldrich
Phenylmethylsulfonylfuoride (PMSF)	Sigma-Aldrich
Polyoxyethylensorbitan-Monolaureat Tween20	Sigma-Aldrich
P-t-Octylphenyl-polyoxyehtylen Triton X-100	Sigma-Aldrich
QTray	Molecular Devices
Restriction digest buffer 2	NEB
RNAse Zap	Carl Roth
Sodium glycinate	Sigma-Aldrich
TEMED	Life Technologies
TrypanBlue solution (0.4%)	Sigma-Aldrich
X-Gal (5-bromo-4-chloro-3-indolyl-β-D-galactopyranosid)	Promega

All other chemicals, salts, buffer substances, solvent, acids and bases were from Carl Roth GmbH.

4.1.14 Laboratory equipment

7500 Real-time PCR system	Applied Biosystems
Arrayscan VTI HCS reader (Cellomics)	Thermo Scientific
Bio imaging system for agarose gels	Gene Genius

C1000™ thermal cycler	BioRad
Centrifuge 5417C / 5430 / 5810R	Eppendorf
Cryo 1C freezing container	Nalgene
Image reader LAS-3000	Fujifilm
Infinite M200 plate reader	Tecan
Infinite M1000 plate reader	Tecan
NanoDrop 8000 Photometer	Peqlab
Pipetting robots	Biomek
Polyacrylamide gel electrophoresis apparatus, Criterion system	BioRad
Photometer Ultraspec 3000	Amersham Biosciences
PTC-200 gradient cycler	MJ Research
Rearraying pipetting robot	Tecan
SECTOR® Imager 6000	Meso Scale Discovery
Semi-dry Western blotting apparatus	BioRad
Spotting robot	KBiosystems
Thermomixer comfort	Eppendorf
TW8 water bath	Julabo
XCell SureLock™ Mini-Cell Electrophoresis System	Invitrogen

4.2 Methods

4.2.1 Molecular biology based methods

4.2.1.1 Creation of new Gateway®-compatible entry clones

Gateway®-compatible entry clones of TDP-43_CT was created by adding *attB* recombination sites to TDP-43 cDNA constructs in a PCR reaction using appropriate primers described in section 4.1.7.1. The cDNA construct was a kind gift of Prof. Dr. C. Shaw. The components of the PCR reaction and the PCR program are described in Table 9 and Table 10.

Table 9: Composition of the PCR reaction to create entry clones

Component	Volume (µl)
Water	21 µl
2x Phusion HF master mix	25 µl
Primer 1 (10 µM)	1 µl
Primer 2 (10 µM)	1 µl
Template DNA (15 ng)	2 µl

Table 10: PCR program to create entry clones

Cycle step	Temperature	Time	Cycles
Initial denaturation	98°C	30 s	1
Denaturation	98°C	10 s	
Annealing	55°C	30 s	35
Extension	72°C	3 min	
Final extension	72°C	5 min	1
	4°C	hold	

PCR products were purified by DNA gel electrophoresis (Section 4.2.1.7) and the app. fragments were extracted from agarose gels with the QIAquick gel extraction kit (Qiagen) according to the manufacturer's instructions. The purified PCR products were cloned into the vector pDONR221 by performing BP reactions for 2 h at 25°C. The BP reactions had the following composition:

5 µl purified PCR fragment

2 µl BP clonase mix II

2 µl 1x TE

1 µl pDONR221 (75 ng/µl)

After that the cloning reaction mix was transformed into chemically competent *Escherichia coli* (*E.* coli) Mach1-T1R cells (Section 4.2.1.3). After growing single clones over night, plasmid DNA was prepped (Section 4.2.1.4). Correctness of the constructs was checked by restriction digest with *BsrGI* (Section 4.2.1.6).

4.2.1.2 Shuttling of cDNA constructs into expression vectors

cDNA constructs taken from our entry clone library or self-made entry clones were shuttled into expression vectors using the Gateway® technology (Invitrogen). The following reactions were incubated over night at room temperature according to the shuttling protocol of the manufacturer:

1 µl entry clone DNA (~100 ng/µl)

1 µl expression vector (75 ng/µl)

1 µl LR clonase mix II

2 µl 1x TE

After the incubation the shuttling mixture was transformed into chemically competent *E. coli* Mach1-T1R according to the following section (4.2.1.3). After growing single clones over night and preparing the plasmid DNA from them using the protocol in section 4.2.1.4, the correctness of the expression constructs was controlled by restriction digest with *BsrGI* (Section 4.2.1.6).

4.2.1.3 Chemical transformation of *E. coli*

For the transformation of chemically competent Mach1-T1R *E. coli* cells with plasmid DNA, the BP reaction mix (10 µl) or the shuttling reaction mix (5 µl) were added to 10 µl of competent Mach1-T1R cells and incubated on ice for 30 min followed by a heat-shock for 45 s at 42°C. Next, the cells were cooled on ice for 5 min, mixed with 100 µl S:O.C. medium without antibiotics and then incubated at 37°C with shaking for 1 h. Finally, the cells were plated onto LB-agar plates with the corresponding antibiotics and were grown at 37°C over night.

4.2.1.4 Plasmid preparation from *E. coli*

For amplification of plasmid DNA, LB medium supplemented with the appropriate antibiotics was inoculated with single *E. coli* colonies and the cells were grown over night at 37°C in an incubator-shaker (250 rpm). The cells were harvested by centrifugation (5 min at 4,000 rpm (Centrifuge 5810 R (Eppendorf)) and the plasmid DNA was purified using the Qiagen Plasmid Mini kit according to the manufacturer's instructions.

4.2.1.5 Determination of DNA and RNA concentration

The concentration of nucleic acids was determined by measuring the absorbance of the purified DNA or RNA in aqueous solution at 260 nm (A260) and 280 nm (A280) in a NanoDrop spectrophotometer (Thermo Scientific). A260 readings of 1.0 are equivalent to 50 µg/ml double-stranded DNA or 40 µg/ml single-stranded RNA. The A260/A280 ratio is used to assess DNA and RNA purity and a ratio of 1.8 to 2.1 indicates a high purify of the DNA or RNA sample.

4.2.1.6 Restriction digest of DNA with *BsrGI*

The restriction digest of the plasmid DNA samples with the enzyme *BsrGI* was performed in restriction digest buffer 2 according to the following recipe:

7.8 µl ddH_2O

1 µl 10x restriction buffer 2

2 µl DNA (~ 100 ng/µl)

0.1 µl BSA (10 mg/ml)

0.1 µl enzyme *BsrGI* (10,000 U/ml)

The reactions were incubated at 37°C for 2 h and then stopped by adding 10x DNA sample buffer. The samples were analysed by electrophoresis on agarose gels (Section 4.2.1.7).

4.2.1.7 DNA electrophoresis

For the separation of DNA fragments and PCR products mixed with 10x DNA sample buffer were loaded onto 1% (w/v) TBE agarose gels and separated by applying 80 V for

30 min. The agarose gels contained 0.5 g/ml ethidium bromide to visualize the DNA after separation under ultra violet (UV) light (Bio imaging system for agarose gels (Gene Genius)). 1x TBE was used as running buffer.

4.2.1.8 RNA isolation from mammalian cells

Total RNA from mammalian cells was extracted and purified using the RNeasy Mini Kit following the manufacturer's instructions. To disrupt the cells, cell pellets were resuspended in the lysis buffer provided with the kit and homogenized by centrifugation through QIAshredder columns. Total RNA within the homogenate was purified from contaminants by applying the homogenates supplemented with 70% ethanol to RNeasy spin columns. The total RNA was eluted from RNeasy spin columns with 30 µl RNase-free water. The concentration of the total RNA preparations was determined using a spectrophotomer as described in section 4.2.1.5.

4.2.1.9 First strand cDNA synthesis by reverse transcription

The retroviral enzyme reverse transcriptase is used to transcribe RNA into complementary DNA (cDNA). Such as other polymerases this specific RNA-dependent DNA polymerase needs an oligonucleotide bound to the RNA which serves as starting point for the strand complementation. For the transcription of total RNA oligo-$(dT)_{18}$ primers (Fermentas) were used, which recognize the poly-A tail of eukaryotic mRNA. 150-800 ng of total RNA (depending on the initial RNA concentration of the samples from one experiment) were transcribed into cDNA with the RevertAid™ H Minus First Strand cDNA Synthesis Kit (Fermentas) according to the manufacturer's protocol.

4.2.1.10 Quantitative real-time PCR (qRT-PCR)

The quantitative real-time polymerase chain reaction (qRT-PCR) is a highly sensitive technique to simultaneously amplify and quantify a DNA target sequence, based on the principle of a standard PCR [362]. The DNA quantification occurs by fluorescence measurement after each PCR cycle. For fluorescence detection the PCR products can be labelled with fluorescent dyes such as SYBR® green, which unspecifically intercalate into DNA double-strands, or with sequence-specific fluorescent probes (TaqMan probes) that carry a fluorophore (reporter) at their 5'-end and a quencher of fluorescence at the 3'-end of the probe. The close proximity of the reporter to the quencher prevents detection of its fluorescence; breakdown of the probe by the 5' to 3'

exonuclease activity of the Taq polymerase breaks the reporter-quencher proximity and thus allows unquenched emission of fluorescence, which can be detected after excitation with a laser [363]. The intensity of the fluorescence signal is directly proportional to the amount of amplified double-stranded PCR product and therefore increases over time with each PCR cycle.

cDNA obtained from the reverse transcription of total RNA (150-800 ng; same concentration for each sample in the experiment) diluted 1:500 in nuclease-free water was used as template in the qRT-PCR reactions. For detection of the target cDNA purchased primer/probe mixes, specific for human mRNAs (FAM-labelled) were used (see section 4.1.9 and Table 6). As endogenous control for normalization of the relative mRNA levels to the amount of total RNA the TaqMan ACTB Endogenous Control Assay (FAM-labelled for single experiments and VIC-labelled for multiplex experiments) was used. All qRT-PCR reactions were performed with 2-3 biological replicates and 2-4 technical replicates as single experiments to measure knock-down effects after siRNA treatment (detection of target and endogenous control cDNA in different wells) or as multiplex experiments to analyse expression of TARDBP, APP, HTT, ATXN1, SNCA or PARK2 (detection of TDP-43 or APP and ACTB cDNA within the same well). The composition of the real-time PCR reactions is shown below in Table 11 and Table 12.

Table 11: Components of single qRT-PCR reactions

Component	**Volume**
cDNA template (dilution 1:500)	2 µl
TaqMan Gene Expression Assay (20x) or TaqMan Endogenous Control Assay	1 µl
TaqMan Universal PCR Master Mix (2x)	10 µl
Nuclease-free water	7 µl
Final volume	20 µl

Table 12: Components of a multiplexed qRT-PCR reaction

Component	Volume
cDNA template (dilution 1:500)	2 µl
TaqMan Gene Expression Assay (20x)	1 µl
TaqMan Endogenous Control Assay (20x)	1 µl
TaqMan Universal PCR Master Mix (2x)	10 µl
Nuclease-free water	6 µl
Final volume	20 µl

All qRT-PCR reactions were performed in the 7500 Real-Time PCR System (Applied Biosystems) using the following amplification program:

Table 13: qRT-PCR amplification program

Temperature	Time	Cycles
50°C	15 min	1
95°C	2 min	1
95°C	15 s	
60°C	45 s	50

The qRT-PCR data were analyzed using the comparative cycle time (CT) method. The CT value corresponds to the PCR cycle in which the measured fluorescence intensity in each sample overcomes the background signal for the first time. The more target cDNA is present in the sample the earlier the threshold will be exceeded, resulting in a small cycle number and a low CT value. The CT value of each sample was normalized to the CT value of the endogenous control ACTB by calculating their difference in cycle time (ΔCT) with the following formula:

$$\Delta CT = CT_{target} - CT_{endogenous\ control}$$

$\Delta\Delta$CT values were obtained by finding the difference between the samples of interest and the control samples (treated with non-targeting control (NTC) siRNA) by calculating:

$$\Delta\Delta CT = \Delta CT_{sample} - \Delta CT_{NTC}$$

The fold change was calculated as $FC = 2^{-\Delta\Delta CT}$ for negative $\Delta\Delta CT$ values and as $FC = 1/2^{-\Delta\Delta CT}$ for positive $\Delta\Delta CT$ values. The knock-down effect in percent was calculated as $KD = (1 - 2^{-\Delta\Delta CT})*100$.

4.2.2 Protein biochemistry based methods

4.2.2.1 Determination of protein concentrations

The concentration of proteins in aqueous solution was determined with the bicinchoninic acid (BCA) protein assay (Pierce). The BCA method is based on the reduction of Cu^{+2} to Cu^{+1} by proteins in an alkaline solution. The binding of BCA to Cu^{+1} results in a purple-colored product that absorbs at 562 nm. The amount of product formed is dependent upon the amount of protein in the sample. The absorption of the samples was compared to a BSA standard curve, based on a BSA dilution series, to determine the exact concentration of each sample.

4.2.2.2 SDS-polyacrylamide gel electrophoresis (SDS-PAGE)

SDS-PAGE is a technique used to separate proteins according to their molecular mass relatively independent to their individual charge and was carried out according to Laemmli [364]. In brief, proteins are exposed to the anionic detergent sodium dodecyl sulphate (SDS) before and during gel electrophoresis. SDS denatures proteins, causing multimeric proteins to dissociate into their subunits, and all polypeptide chains are forced into extended conformations with similar charge-mass ratios. SDS treatment therefore eliminates the effects of differences in shape so that chain length, which reflects mass, is the sole determinant of the migration rate of proteins in SDS-PAGE. Additionally, DTT can be used to denature disulfide-linked tertiary structures. Hence, all samples were mixed with 4x SDS-loading buffer (8% SDS) supplemented with 200 mM DTT and were heat denatured for 5 min at 99°C. SDS-PAGE was performed with self-cast gels made up of 4% (stacking gel) plus 10% (resolving gel) polyacrylamide gels or with pre-cast NuPAGE® Novex 4-12% Bis-Tris gels (Invitrogen). As a marker for protein size, Benchmark™ Prestained Protein Ladder (Invitrogen) or PageRuler™ Prestained Protein Ladder (Thermo Scientific) was taken. The gels were run at 125 V in either 1x SDS running buffer for 1.5 h (self-cast gels) or in 1x NuPAGE® MES SDS running buffer for 40 min (pre-cast gels).

4.2.2.3 Western Blotting

Following the separation by SDS-PAGE the proteins were transferred onto nitrocellulose membranes (Schleicher and Schuell) to immobilize the proteins and to visualize them by immonstaining. The transfer was performed in the semi-dry transblot apparatus (BioRad) at 20 V for 1.5 h. Subsequently the membranes were blocked in 5% skimmed milk solution for 1 h at room temperature. The membranes were then incubated with the desired primary antibody over night (Table 7), washed three times with 1x TBS-T and in a second step incubated with the corresponding secondary antibody conjugated to either alkaline phosphatise or horseradish peroxidise (Table 8) for 1 h. After washing the membranes three times in 1x TBS-T and three times in 1x TBS, the proteins were detected either by fluorescence measurement under 460 nm UV-light (AttoPhos; Europa Bioproducts) or by chemiluminescence detection as recommended by the manufacturer (Western Lightning^{TM}, PerkinElmer) measurement in the LAS3000 image reader (Fuji).

4.2.2.4 Total protein staining with Ponceau-S

After blotting, the nitrocellulose membranes were quickly rinsed with distilled water and incubated in Ponceau-S solution (Sigma-Aldrich) for a few seconds. Subsequently, the membranes were washed with distilled water to remove background staining and to allow visual inspection of the blots. The dye was removed completely by incubating the blots in distilled water for 20 min.

4.2.2.5 Luminescence-based mammalian interactome mapping technology (LUMIER)

The LUMIER assay is a highly sensitive method to validate and to detect protein-protein interactions [237]. For LUMIER assays protein A (PA)-Renilla luciferase (RL)-tagged fusion proteins were co-produced with firefly luciferase (FL)-tagged putatively interacting proteins in HEK293 cells. After 48 h protein complexes were co-immunoprecipitated from cell extracts (lysed with LUMIER lysis buffer) with IgG-coated 384-well microtiter plates (BD Falcon). By several washing steps with 1x PBS-T weakly bound endogeneous cellular proteins are removed from the complex. Interactions between bait (PA-RL fusion proteins) and prey proteins (FL fusion proteins) were monitored by quantification of firefly luciferase activities [238]. Quantification of Renilla

luciferase activity was used to confirm that PA-RL-tagged bait proteins are successfully immunoprecipitated from cell extracts. To detect Renilla and firefly luciferase-based luminescence in samples with fusion proteins the Dual-glo Luciferase kit (Promega) was used. Bioluminescence was quantified in a luminescence plate reader (TECAN Infinite M1000). For each interaction both PA-RL and FL interaction fusion combinations were tested.

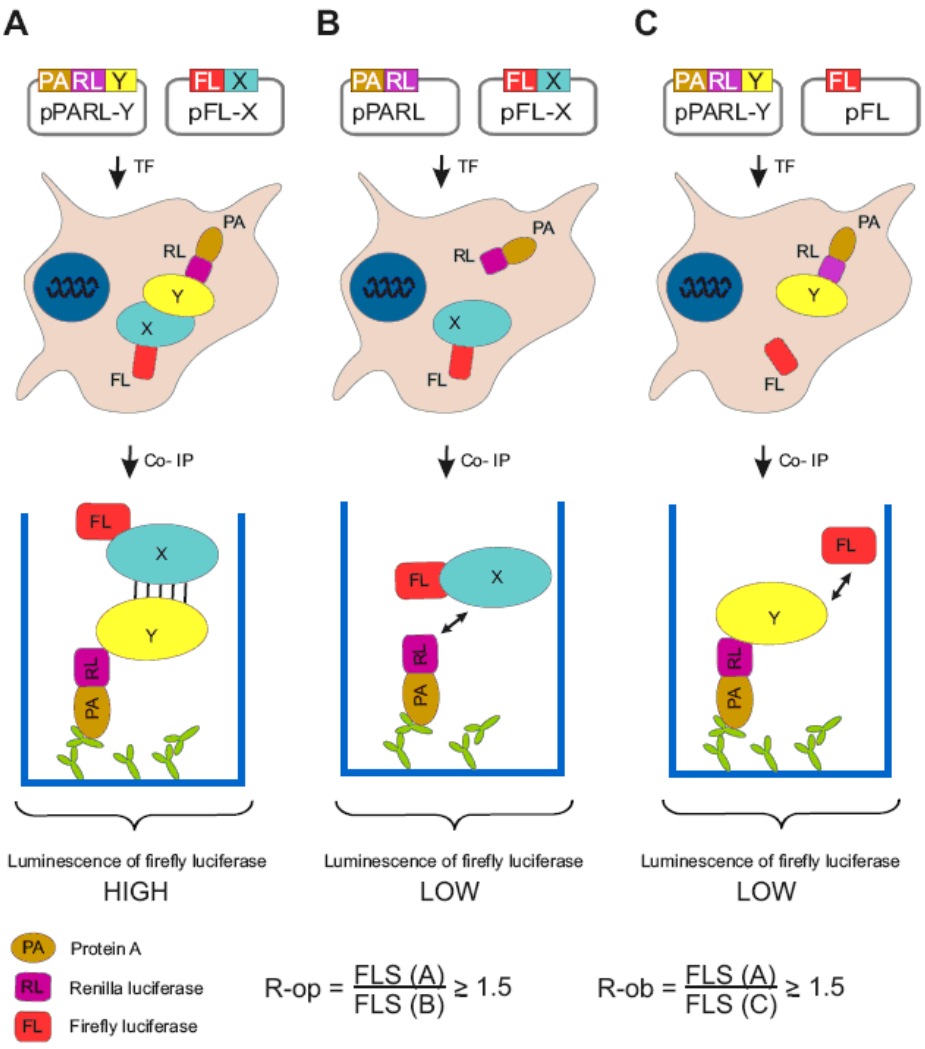

Figure 40: Overview of the LUMIER assay.

For each protein pair tested (interaction between selected bait and prey proteins) three different parallel co-immunoprecipitation experiments (Figure 40, Co-IPs A-C) were performed in HEK293 cells, in order to assess the specificity of an interaction. To

investigate the interaction between proteins X and Y the protein pairs (A) PA-RL-X + FL-Y, (B) PA-RL + FL-Y and (C) PA-RL-X + FL were individually co-produced in HEK293 cells. The proteins PA-RL (fusions of protein A and Renilla luciferase) and FL (firefly luciferase) in experiments B and C were used as controls to examine background protein binding. The resulting protein complexes in Co-IPs A-C were systematically analyzed by quantification of firefly luciferase activity. R-op and R-ob binding ratios were obtained by dividing the firefly luminescence activity measured in sample A by activities found in samples B and C. These controls allow assessing the protein interaction specificity. Low R-op values are an indication for unspecific prey protein interactions, while low R-ob values indicate unspecific bait protein interactions. Based on empirical studies with a set of well-characterized positive and negative interaction pairs, R-op and R-ob binding ratios of 1.5 were determined as threshold for reliable, specific protein-protein interactions.

4.2.2.6 IgG coating of the LUMIER assay plates

The 384-well microtiter plates for the LUMIER assay were IgG coated using 50 µl coating buffer (10 µg/ml sheep gamma globulin in carbonate buffer) per well. The plates with the coating buffer were agitated at 200 rpm for 3 h at room temperature. After that, the wells were blocked for 1 h with 100 µl blocking buffer (1% (w/v) BSA in carbonate buffer) per well with agitation. The wells were washed three times for 5 min with 1x TBS-T with agitation, and coated with the affinity matrix by adding 50 µl capture solution (3.3 µg/ml rabbit anti-sheep IgG in carbonate buffer) per well. The affinity matrix coating step was done at least over night at 4°C with agitation in a humid atmosphere. Finally, the plates were washed three times for 5 min with 1x TBS-T before being used for the assay.

4.2.2.7 Co-immunoprecipitation (Co-IP) from cell lysates

For co-immunoprecipitation of endogenous proteins from mammalian cells (SH-SY5Y and SH-SY5Y_APP695), 500 µg protein from fresh cell lysates in 500 µl LUMIER lysis buffer was incubated with 1.6 µg of a specific antibody against the protein to be immunoprecipitated or against 14-3-3-eta (YWHAH) as control for 3 h at 4°C on a rotating wheel (50 rpm). Next, 30 µl of Protein G-coated Dynabeads® were added to the cell lysate-antibody mixtures and the samples were incubated for 1 h at 4°C on a rotating wheel (50 rpm). Following the binding, samples were washed three times with

1x PBS-T under rotation (5 rotations each) at room temperature. For elution 2x SDS-loading buffer was added to the beads and the samples were heat denatured at 99°C for 5 min, followed by SDS-PAGE and Western Blotting.

4.2.2.8 Aβ ELISA

To analyze the effect of siRNA treatment or protein over-production on extracellular levels of Aβ40 and Aβ42 peptides, the Aβ ELISA kit "Human/Rodent Abeta 3-Plex Ultra-Sensitive Kit" (Meso Scale Discovery) was used. SH-SY5Y_APP695 cells were transfected with siRNA (30 nM; knock-down experiments), with plasmid DNA (400 ng; over-expression experiments) or with both siRNA and plasmid DNA (rescue experiment) in 96-well plates and incubated for 72 h. Next, 50 µl of the cell culture medium was removed from each sample well and treated with 50 mM O-phenanthrolin (1 mM final concentration) to inhibit peptidases present in the cell culture medium. The cells were fixed with 4% para-formaldehyde and the nuclei were stained with Hoechst 33342 (4 µg/ml). The medium samples, the Aβ standards (delivered with the kit) for the calculation of the standard curve and the ELISA plates were prepared according to the manufacturer's instructions and the ELISA plates were read in the SI6000 (Meso Scale Discovery). The number of cells and protein aggregates in case of over-expression experiments were assessed by high content screening using the Arrayscan VTI HCS reader (Thermo Scientific).

4.2.3 Methods in cell biology

4.2.3.1 Cultivation of mammalian cells

SH-EP cells were cultured in Dulbecco's modified Eagle medium (DMEM) with 4.5 g/l D-glucose, L-glutamine, sodium pyruvate supplemented with 10% fetal calf serum (FCS), 100 U/ml penicillin and 100 µg/ml streptomycin at 37°C and 5% CO_2. Cells were grown up to 90% confluence and split down to 10% confluence. Briefly, the culture medium was removed; cells were washed with 5 ml D-PBS and detached from the flask by incubation with 0.5% (w/v) trypsin / 1 mM EDTA at room temperature for 2 min. Then, cells were resuspended in 20 ml pre-warmed culture medium and diluted into fresh 150 cm² culture flasks.

SH-SY5Y cells were grown in DMEM with L-glutamine, 1 g/l D-glucose, sodium pyruvate supplemented with 15% FCS, 1% non-essential amino acids, 100 U/ml

penicillin and 100 µg/ml streptomycin at 37°C and 5% CO_2. Cells were split down when they reached 80-90% confluence as described above and diluted into a fresh cell culture flask.

SH-SY5Y_APP695 cells were grown in the same medium as SH-SY5Y cells and were split down as SH-SY5Y cells. The medium was supplemented with hygromycin B (60 µl per 20 ml medium) to maintain the stable expression of APP695.

HEK293 cells were cultured in DMEM with 1 g/l D-glucose, L-glutamine, supplemented with 100 U/ml penicillin and 100 µg/ml streptomycin at 37°C and 5% CO_2. Cells were grown up to 90% and were split down to 10% confluence as described for SH-EP cells.

4.2.3.2 Long-term storage of mammalian cells

Cells were grown to 90% confluence in 150 cm² culture flasks. After removing the medium, cells were washed and detached by trypsination as described above and pelleted by centrifugation at 1,500 rpm for 5 min. Subsequently, cells were resuspended in 1 ml of fetal calf serum supplemented with 10% DMSO. Cells were then slowly cooled down to -80°C in a cryo-tube over night. Finally, the tubes were transferred to the liquid nitrogen tank for long term storage.

4.2.3.3 Determination of the cell number by TrypanBlue staining

TrypanBlue is an acidic dye, which binds to cellular proteins. In dead cells the cell membrane is permeabilized which allows the dye to enter the cytosol resulting in a blue cell staining. Cells which are alive cannot be stained and appear bright under the microscope. Because of the blue color one can easily distinguish between living and dead cells. To determine the number of living cells within a population a Neubauer counting chamber was used. 10 µl of cell suspension was mixed with 90 µl TrypanBlue staining solution (0.4%), applied to the counting chamber and the living cells were counted in each of the 4 large counting squares. The number of viable cells (cells/ml) is calculated according to the formula:

$$Total\ cell\ number = \frac{number\ of\ counted\ cells}{4} \times 8 \times 10^4$$

4.2.3.4 Transient transfection of mammalian cells

In all cases siRNA, expression vectors or transfection reagent were diluted in the appropriate amount of Opti-MEM®.

HEK293 cells

FRET assay-based RNAi screens were performed in 384-well plates using pools of three synthetically produced siRNAs purchased from Ambion. 4,000 HEK293 cells per well were reverse transfected with siRNA pools (200 nM in total) with Dharmafect 1 according to the manufacturer's instructions, i.e. cell suspensions were seeded on top of the siRNA-transfection reagent mixtures. The cells were incubated for 24 h at 37°C and 5% CO_2. Then, the cells were co-transfected each with 10 ng of the EYFP-TDP-43_CT and with 10 ng of the ECFP-TDP-43_CT expression vectors using the TransIT transfection reagent according to the manufacturer's instructions. The samples were further incubated for 48 h at 37°C and 5% CO_2.

FRET assays for assessment of TDP-43 aggregation were established by co-transfecting HEK293 cells with 100 ng of the EYFP and ECFP expression vectors, with 100 ng of the EYFP-TDP-43 and ECFP-TDP-43 expression vectors or with 100 ng of the EYFP-TDP-43_CT and EYFP-TDP-43_CT expression vectors using Lipofectamine 2000 (25 µl per 1 ml medium). Here, 16,000 cells per well were seeded one day before transfection in 96-well plates and the cells were incubated for 48 h after transfection at 37°C and 5% CO_2.

For expression tests HEK293 cells seeded in 96-well plates (24 h before transfection) were transfected with EYFP-TDP-43, ECFP-TDP-43, EYFP-TDP-43_CT or ECFP-TDP-43_CT expression vectors using Lipofectamine 2000 (25 µl per 1 ml medium) and incubated for 48 h at 37°C and 5% CO_2.

SH-EP cells

RNAi experiments were performed using pools of three (Ambion) or four (Dharmacon) synthetically produced siRNAs. For the RNAi screen SH-EP cells were reversely transfected with pools of siRNA (100 nM in total) and 150 ng of EYFP-TDP-43 expression vector using Dharmafect Duo as transfection reagent in 96-well plates (aggregation and toxicity; 8,000 cells per well; 0.375 µl / well Dharmafect Duo) or 24-well plates (qRT-PCR, Western Blots and laser scanning microscopy; 40,000 cells per

well; 1.875 µl / well Dharmafect Duo). The samples were incubated for 72 h at 37°C and 5% CO_2.

SH-SY5Y cells and SH-SY5Y_APP695 cells

For siRNA and over-expression experiments, SH-SY5Y_APP695 cells were seeded into 96-well plates (12,000 cells / well) or into 24-well plates (60,000 cells / well) using medium supplemented with hygromycin B (3 µl / ml medium). After incubating the cells at 37°C and 5% CO_2 for 24 h, the medium was exchanged by 50 µl (96-well) or 250 µl (24-well) of medium without antibiotics. The cells were then transfected with pools of siRNA (30 nM in total) or 400 ng EYFP fusion protein expression vectors using Lipofectamine 2000 (0.8 µl per well (96-well) or 4 µl per well (24-well)) in 50 µl or 250 µl Opti-MEM®. After 24 h of incubation at 37°C and 5% CO_2, the medium was replaced by fresh medium without antibiotics and the cells were further incubated for another 48 h under the same conditions.

SH-SY5Y cells were similarly transfected except that the medium of the freshly seeded cells was not supplemented with hygromycin B.

4.2.3.5 Quantification of protein aggregation by high content fluorescence imaging

Modulators of protein aggregate formation were tested in SH-EP cells. Cells were reversely co-transfected with 150 ng EYFP-TDP-43 and siRNA pools (100 nM in total) in black 96-well plates with transparent bottom (BD Falcon). 72 h after transfection cells were fixed with 4% para-formaldehyde and DNA was stained with Hoechst 33342 (1:2,500). The cell culture plates were then placed into a high content screening (HCS) cell analysis system (Arrayscan VTI). HCS is defined as the automation of high-content cell biological investigation of arrayed cells including the key operations of image acquisition, archiving, processing and analysis, and cellular knowledge mining [365]. ‘High content’ is used to refer to processes that are defined spatially and temporally in the context of the structural and functional integrity of each individual cell within an array of cells [365]. Nuclei were identified by Hoechst fluorescence, cell dimensions were fitted using the ArrayScan VTI software (Thermo Scientific). EYFP-TDP-43 over-production (total intensity within each cell) and aggregation (mean intensity of spots,

mean size of spots and mean number of spots per cell) was quantified by YFP fluorescence. Only cells with YFP fluorescence signals were analyzed and the fluorescence signals were normalized Automatedally to the number of YFP transfected cells. Each one of three independent experiments performed was done in triplicate (i.e. 9 data points).

Similarly, high content fluorescence imaging was used to quantify the number of SH-SY5Y_APP695 cells (based on Hoechst fluorescence), which were transfected with 30 nM siRNA pools or 400 ng EYFP expression plasmids, fixed with 4% para-formaldehyde and stained with Hoechst 33342 after 72 h incubation at 37°C and 5% CO_2. In case of cells transfected with EYFP expression plasmids the aggregation of the EYFP fusion proteins was assessed as described for SH-EP cells above. Each experiment was performed in triplicates.

4.2.3.6 A cell-based FRET assay to quantify TDP-43 aggregation

The FRET (Förster resonance energy transfer) method was used to analyse the effect of siRNA-based protein knock-down on aggregation of TDP-43_CT in high throughput in HEK293 cells. For monitoring the aggregation, HEK293 cells are first transfected with siRNA pools (200 nM in total) and 24 h later co-transfected with 10 ng of EYFP-TDP-43_CT expression plasmids and 10 ng of ECFP-TDP-43_CT expression plasmids in 384-well plates (“Sample”). Moreover, other cells were transfected with ECFP-TDP-43_CT expression plasmids and β-galactosidase expression plasmids (“ECFP-Control”) or EYFP-TDP-43_CT and β-galactosidase expression plasmids (“EYFP-Control”) as controls for background fluorescence. The ECFP can be excited at 436 nm and emits light at 485 nm, while EYFP can be excited at 485 nm and the fluorescence signal will be detected at 530 nm. When the donor (ECFP) and acceptor (EYFP) are in close proximity (1-10 nm) due to the aggregation of the fusion proteins, the emitted light from the donor at 485 nm is able to excite the acceptor which results in fluorescence emission at 530 nm. EYFP fluorescence (excitation 485 nm, emission 530 nm), ECFP fluorescence (excitation 436 nm, emission 485 nm), as well as the FRET signal (excitation 436 nm, emission 530 nm) were measured in the Infinite M200 plate reader (Tecan) 48 h after plasmid transfection. To assess the effect of protein knock-down on TDP-43_CT aggregation a corrected FRET signal (NET-FRET) was calculated using the following formula:

$$NET - FRET =$$
$$FRET_{Sample} - \left(\frac{FRET_{ECFP-Control}}{CFP_{ECFP-Control}} \times CFP_{Sample}\right) - \left(\frac{FRET_{EYFP-Control}}{YFP_{EYFP-Control}} \times YFP_{Sample}\right)$$

Each experiment was performed in duplicates.

4.2.3.7 Caspase 3/7 activation assays

Caspase activity was measured in black 96-well plates with transparent bottom, using biochemical assays monitoring the activity of caspases 3/7. For that the Apo-ONE™ Homogenous Caspase-3/7 Assay (Promega) was used according to the manufacturer's instructions. The assay buffer rapidly lyses mammalian cells and the caspase substrate Z-DEVD-R110 present in the solution can be cleaved by active caspases 3 and 7, revealing a fluorescent group whose emission at 521 nm can be detected after excitation at 499 nm in a fluorescent plate reader. For detection of the signals in SH-EP cells under screening conditions a volume of 100 µl Apo-ONE™ Homogenous Caspase-3/7 Assay was added to 100 µl cells in medium and the caspase activity signals were monitored over a time span of 5 h, measuring the fluorescence every 5 min in the Infinite M200 plate reader (Tecan).

4.2.3.8 Confocal microscopy

SH-EP cells were seeded on cover slips in 24-well cell culture plates (40,000 cells/well) and transfected with cDNA encoding YFP-TDP-43 (450 ng) using Dharmafect Duo transfection reagent. 72 h after transfection cells were fixed with 4% para-formaldehyde, stained with Hoechst 33342 (1:2,500 in PBS) and mounted with ProLong® Gold antifade reagent. TDP-43 over-production and aggregation was monitored by YFP fluorescence. Images were recorded using a Leica SP2 confocal microscope.

4.2.4 Yeast-specific molecular biological methods

Yeast cells were generally cultivated at 30°C.

4.2.4.1 Transformation of plasmid DNA into yeast cells using the lithium acetate method

Yeast strains to be transformed were incubated over night in 2 ml liquid YPD medium and then transferred into 28 ml fresh YPD medium. The culture was incubated (30°C; 250 rpm) until the cells reached an OD_{600} of 0.4 to 0.6. After centrifugation at 2,000 rpm for 5 min, the pellet was washed with 10 ml 1x TE, resuspended in 1 ml mix I (1 ml lithium acetate (1 M), 5 ml sorbitol (2 M), 0.5 ml TE (10x) and 3.5 ml ddH_2O) and incubated for 10 min to 1 h at room temperature. Each transformation sample was composed of 40 µl competent yeast cells (in mix I), 0.5 µg of plasmid DNA, 5 µg Hering's sperm carrier DNA and 230 µl mix II (1.5 ml lithium acetate (1 M), 1.5 ml TE (10x), 10 ml PEG 3350 (60% w/v) and 2 ml ddH_2O). The samples were carefully mixed and incubated for 30 min at 30°C. After adding 30 µl of DMSO to each sample, a heat shock was performed at 42°C for 7 min. After that, the samples were plated on selective medium and were incubated for 3-5 days at 30°C.

4.2.4.2 Yeast two-hybrid (Y2H) assays

Shortly after invention of the yeast two-hybrid system (Y2H) [366], it was adapted for library screens (Figure 41). The proteins of interest are provided as plasmid-encoded recombinant fusion proteins. The bait proteins are fused to a DNA-binding domain (DBD) of the bacterial transcription factor LexA (encoded in the vector pBTM116-D9). The prey proteins are tagged by the activation domain (AD) of *GAL4*. A physical interaction between of the bait and prey protein leads to the reconstitution of a transcription factor and thus to the activation of reporter genes such as *HIS3* and *URA3* (Figure 41). This allows the yeast to grow on minimal medium lacking the app. amino acids (SDIV (-Leu, -Trp, -Ura, -His)), whereas this is not the case for non-interacting protein pairs.

To create a prey matrix for interaction mating, the *MAT*α yeast strain L40ccα was individually transformed with pACT4-DM-based plasmids encoding prey proteins. The resulting yeast prey clones were arrayed in 384-well microtiter plates. cDNAs encoding the bait proteins (see Section 5.1) were shuttled into the yeast expression vector

pBTM116-D9 and the resulting plasmids were transformed into the *MATa* yeast strain L40ccua. Activation of the reporter genes *HIS3*, *URA3* and lacZ in auto-activation tests as a result of the production of bait proteins was tested systematically. Only non-auto-active constructs were taken for interaction mating assays with prey proteins [190].

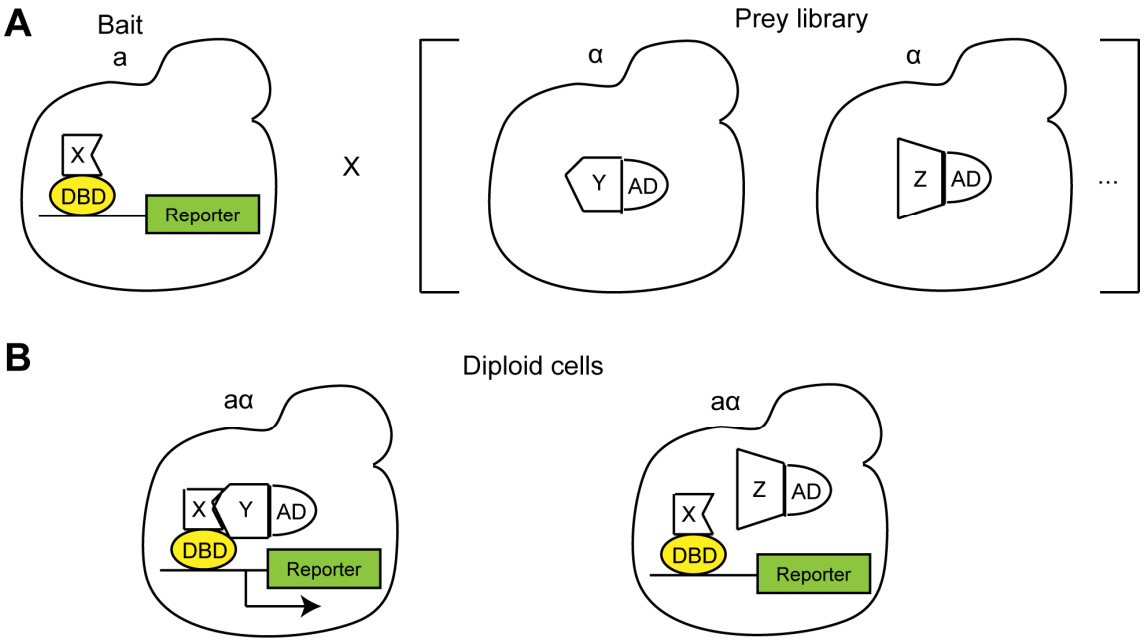

Figure 41: The yeast two-hybrid principle. (A) Haploid yeast cells of mating type *a* are transformed with a bait plasmid and those of mating type *α* with prey plasmids. A single bait strain is mated with a prey library. (B) Resulting diploids carry the genetic material of mated haploids. Interacting fusion proteins activate expression of reporter genes which assures survival on minimal medium that lacks certain amino acids (diploid on the left); diploids with non-interacting proteins cannot grow (diploid on the right). Abbreviations: DBD – DNA-binding domain, AD – activation domain.

Liquid cultures of *MAT*α yeast strains (preys) were replicated in 384-well microtiter plates using a pipetting robot (Tecan, Freedom EVOware®) and then mixed with bait producing *MATa* strains. For interaction mating, yeast mixtures were transferred onto YPD agar plates (QTrays) using a spotting robot (K4, KBiosystems) and were incubated for 48 h at 30°C. After mating, clones were Automatedally picked from agar plates and transferred into 384-well microtiter plates containing SDII (-Leu, -Trp, +Ura, +His) liquid medium and from there they were spotted onto SDII (-Leu, -Trp, +Ura, +His) agar to select for diploid yeasts carrying both bait and prey vectors. After incubation for 48 h at 30°C, diploid yeast clones were spotted onto SDIV (-Leu, -Trp,

-Ura, -His) agar to detect positive protein-protein interactions as well as on high density nylon membranes on top of SDIV agar plates for the LacZ assay. In the LacZ assay β-galactosidase is produced only in growing cells in which bait and prey proteins interact. After incubation for 3-4 days at 30°C, grown colonies were fractured with liquid nitrogen (2 min) and β-galactosidase activity was detected with X-Gal substrate (2-8 h at 37°C). Digital images were taken from agar plates as well as from high density nylon membranes for Visual Grid software (GPC Biotech) assisted result digitalization. The automated Y2H screen was done in 4 repetitions.

4.2.5 Bioinformatics-based methods of analysis

4.2.5.1 Prediction of neurodegenerative disease-related target genes

Prioritization of target genes

Several manual and automated methods were applied in order to prioritize human protein-coding genes to their relation to neurodegenerative diseases. Methods were based on manual selections from the literature, analysis of high-throughput experimental data sets, data mining of genomic and drug data, and text mining of MEDLINE abstracts. The methods were mainly focused on the five following diseases: Alzheimer's disease (AD), Huntington's disease (HD), Parkinson's disease (PD), amyotrophic lateral sclerosis (ALS), and spinocerebellar ataxia 1 (SCA1). Each method *m* was used to score a gene *g* with a sub-score R_{mg} between 0 (not selected or no predicted relation) and 1 (high confidence selection or prediction):

$$R_{mg} \in [0,1]$$

An overall gene score S_g was computed as a weighted sum of the method sub-score as:

$$S_g = \sum_m W_m \times R_{mg}$$

where a method weight W_m was defined as shown in Table 14.

Table 14: Weights of each data set used to predict ND-related target genes

Data set	Weight
Core1	1,000
Core2	1,000
Modifier1	500
Modifier2	250
HTT	100
Orthologs	50
Linkage	100
Textmining1	200
EST	50
Expression	200
Drugbank	50
DrugSE	1,000
TextDrugs	200
Textmining2	200
MaxUS	250
Aging	200

Scaling of P-values

When a method m was used to analyze a high-throughput data set of size *N* (e.g. the total number of probes of a microarray data set) and returned a P-value, the sub-score R_{mg} of gene *g* was defined as:

$$R_{mg} = \frac{\min\left(-\log_{10}(P-value), -\log_{10}\left(\frac{C}{N}\right)\right)}{-\log_{10}\left(\frac{C}{N}\right)}$$

where C = 10^{-30} for method Textmining2 and C = 0.05 for methods Textmining1, Expression, TextDrugs and Aging.

Methods for the prioritization of ND-related target genes

In the following section I give an overview over the different data sets used for the prioritization of ND-related target genes. The different data sets were used to prioritize all human protein-coding genes.

Core1: 7 neurodegenerative disease-causing genes known to be related to AD, HD, PD, ALS and SCA1 (sub-score = 1 if selected, 0 otherwise) were manually selected from the literature.

The Core2 data set was a manual ranking of genes genetically related to NDs from the OMIM database (sub-score = 1 if strongly related, 0.75 if related, 0.5 if moderately related, 0.3 if selected, and 0 otherwise).

The Modifier1 data set was based on manual selection from the literature of genes with mutations associated with NDs (sub-score = 1 if selected, 0 otherwise).

The Modifier2 data set was based on manual selection from the literature of genes known to be disease modulators (sub-score = 1 if selected, 0 otherwise).

The HTT method selected HTT-interacting proteins from a study using high-throughput Y2H screenings and affinity pull down followed by mass spectrometry experiments. The HTT sub-score was set to 1 if the gene was listed in the related article [169], 0 otherwise.

The Orthologs method selected genes based on several studies of HD and SCA modulators in human or animal models (mouse, *S. cerevisae*, *Drosophila melanogaster* and *C. elegans*). From a set of selected articles (Table 15), relevant genes were extracted and Automatedally matched to the human orthologs using the HomoloGene database. Additionally targets were extracted by a manual bibliographic analysis. Genes were collected from publications published until 2006. Modifiers from genome-wide studies to single gene studies were included. The sub-score is set to 1 if the gene was relevant, listed in the articles, and if it has a human ortholog. The sub-scores were equal to 0 otherwise.

Table 15: Studies used to identify known modulators in human or animal models.

Pubmed ID	Reference	Disease	Model
11081516	Fernandez-Funez et al. (2000), Nature 408(6808): 101-6	SCA1	Drosophila
15254017	Ghosh and Feany (2004), Hum Mol Genet. 13(18): 2011-8	SCA1, SCA3, HD, PD, AD	Drosophila
17984172	Branco et al. (2008), Hum Mol Genet. 17(3): 376-90	SCA1, HD	Drosophila
17953484	Bilen J, Bonini NM. (2007), PLoS Genet, 3(10):1950-64.	SCA3	Drosophila
17500595	Kaltenbach et al. (2007), PLoS Genet, 3(5): e82	HD	Drosophila
15806102	Giorgini et al. (2005), Nat Genet, 37(5): 526-31	HD	S. cerevisae
14657499	Willingham et al. (2003), Science, 302(5651): 1769-72	HD, PD	S. cerevisae
16794039	Cooper et al. (2006), Science, 313(5785): 324-8	PD	S. cerevisae
15084750	Nollen et al. (2004), PNAS, 101(17): 6403-8	HD	C. elegans
16469881	Gidalevitz et al. (2006), Science, 311(5766): 1471-4	HD	C. elegans
10624951	Cummings et al. (1999), Neuron, 24: 879-892	SCA1	Mouse
11448943	Cummings et al. (2001), Hum Mol Genet, 1511-1518	SCA1	Mouse
11741393	Shahbazian et al. (2001), Neurobiol. Dis., 8: 974-981	SCA1	Mouse
9635424	Warrick et al. (1998), Cell, 93: 939-949	SCA3	Drosophila
16525503	Boeddrich et al. (2006), EMBO J, 25: 1547	SCA3	Drosophila
12486229	Faber et al. (2002), PNAS, 99: 17131	HD	C. elegans

Pubmed ID	Reference	Disease	Model
11607033	Steffan et al. (2001), Nature, 413: 739-743	HD	Drosophila
16980958	Kitamura et al. (2006), Nature Cell Biology, 8: 1163	HD	Mammalian cells
10710314	Kazemi-Esfariani and Benzer (2002), Science, 1837	HD	Drosophila
12122205	Morley et al. (2002), PNAS, 99: 10417-10422	HD	C. elegans

The Linkage method was based on a set of gene predictions for AD, HD, PD, and ALS using the G2D tool [367]. G2D evaluated genes in the chromosomal region where the disease was mapped, prioritized them for a possible relation to the disease based on the phenotype of the disorder or their similarity to an already known related gene. If a phenotype was linked to several loci, known or inferred interactions between proteins from two loci were also taken.

The Textmining1 method used information from the MEDLINE database to select genes related to AD, HD, PD, ALS and SCA1. An analysis of the links between the genes and the scientific abstracts can define the potential disease genes by checking if the articles mainly relate to the disease. The topic of each article is defined by its annotated MeSH terms. By linking the MEDLINE and the Entrez Gene databases it was possible to highlight the genes potentially involved in each disease. Over-representation of a disease in gene annotations was evaluated by a Fisher's exact test. For instance, the APP gene (GeneID = 351) was linked to 680 articles, including 325 about Alzheimer's disease (P-value = 6.892E-12). As no MeSH term was specifically dedicated to SCA1, a more general term was used to produce the results, e.g. "spinocerebellar ataxias". The sub-score was a scaling of the returned P-value between 0 and 1. We selected P-values below 0.005. The score equals 1 means that topics of articles related to a specific gene over-represented in at least one of the five NDs (AD, HD, PD, ALS and SCA1) with very high confidence. A score of 0 means no over-representation.

The EST method was based on an EST database to obtain evidence for gene expression in tissues from the nervous system. I used the GenBank database to select ESTs annotated to be expressed in the nervous system. EST tissue annotations were matched to relevant MeSH terms. I used all MeSH headers and synonymous terms which depend on “Nervous System” (MeSH term ID = A08) in the hierarchy. Assignment of ESTs to genes was done by similarity search (BLAT) on the human genome (GoldenPath). Only hits with high score and percentage of identity (BLAT score/qSize $\geq$ 95 and pid $\geq$ 95%) were selected. The sub-score was set to 1 when ESTs were selected, 0 otherwise.

The Expression method was based on publically available microarray data sets of ND-related human samples (Table 16). Each data set was background corrected with GCRMA and normalized by quantile scaling to extract differentially expressed genes between healthy controls and ND patients. There was no SCA1-related data set available in the NCBI GEO database. The score was a scaling of the minimal P-value between 0 and 1. I selected P-values below 0.005. A score of 1 means that a gene was considered differentially expressed with very high confidence, whereas a score of 0 means no differential expression.

Table 16: Publicly available microarray data sets from the NCBI GEO database

NCBI GEO ID	Pubmed ID	Samples	Disease	Origin of samples
GSE4757	16242812	20	AD	Brain, entorhinal cortex
GDS2601	16979800	28	AD	Peripheral blood, mononuclear cells
GDS2519	17215369	105	PD	Whole blood
GDS810	14769913	31	AD	Brain, hippocampal CA1 region
GDS2821	17571925	25	PD	Brain, substantia nigra
GSE4595	17233347	20	ALS	Brain, motor cortex
GDS412	14645737	11	ALS	Spinal cord, gray matter
GDS1331 and GDS1332	16043692	31	HD	Peripheral blood

The Drugbank method was based on the DrugBank database [368], which is a bioinformatics and chemoinformatics resource that combines detailed drug data with comprehensive drug target information. At the time of download, the database contained app. 4,800 drug entries including more than 1,350 FDA-approved small molecules, 123 FDA-approved biotech (protein/peptide) drugs, 71 nutraceuticals and ~3,243 experimental drugs. Additionally, more than 2,500 non-redundant protein sequences (i.e. drug targets) are linked to these FDA approved drug entries. For each gene, I have set a list of drugs which target the gene. The specificity of each drug decreases with its number of targets. Each drug related to a gene was scored as follows:

$$Drug\ specificity = \frac{1}{\sqrt{number\ of\ known\ gene\ targets}}$$

Then, the final gene score was the maximum of observed scores of its related drugs. Low scores denoted weakly specific drugs, and high scores denoted very specific drugs.

The DrugSE method derived a probability for two drugs to share a protein target using side effect similarity, integrated with their structural (2D) similarity [369]. It allows to reliably predict target sharing also for dissimilar drugs. It is known that the sequence similarity of the known targets of two drugs and the chemical similarity of drugs are molecular features that can be exploited to predict whether they share a target. The more similar the known targets of two drugs are the higher is the probability that they bind to the same protein. Similarly, the more similar two drugs are structurally the more likely is it that they bind to the same protein. Based on the scores (reliability that a drug is involved in one of the neurodegenerative diseases) the putatively involved genes were chosen. The sub-score was the maximal observed for each gene with the drugs. Scores were between 0 and 1. Scores were multiplied by the drug specificity (as defined in the Drugbank method).

The TextDrugs method aimed to define a list of drugs related to NDs for each human gene by using text mining of MEDLINE abstracts. First, known drugs were scored for their association to a neurodegenerative disease by using MeSH terms. These scores were multiplied by the corresponding drug specificities. Then, by using DrugBank to identify drug targets, for each human protein-coding gene a list of ND-related drugs

was set. Additionally, a list of known ND drugs and related targets were used to select further targets (Table 17). The best drug-ND associations were first evaluated and selected by Fisher's exact tests (P-values < 0.005). P-values were scaled from 0 (no association) to 1 (strong association). Scores were multiplied by the drug specificity. Then, the final gene score was the maximum of observed scores of its related ND drugs.

Table 17: Known neurodegenerative disease-related drugs

Disease	Drug	DrugBank ID
AD	Memantine	4054
AD	Donepezil	3152
AD	Galantamine	3449
AD	Rivastigmine	5077
PD	Levodopa	836
PD	Carbidopa	2563
PD	Benserazide	2327
PD	Tolcapone	4659569
PD	Entacapone	4659568
PD	Bromocriptine	2443
PD	Pergolide	4745
PD	Pramipexole	4885
PD	Ropinirole	5095
PD	Cabergoline	2512
PD	Apomorphine	2215
PD	Lisuride	3938
PD	Salegiline	5195
PD	Rasagiline	122316
ALS	Riluzole	5070

The Textmining2 method used the Génie text mining algorithm to predict human protein-coding genes related to protein aggregation [370]. The training set was composed of abstracts related to protein aggregation from a PubMed query and compared to the rest of MEDLINE. The sub-score was a scaling of the P-value between 0 and 1. I selected 992 genes with at least one hit in its abstract list. Uncorrected P-values ranged from 10^{-5} to 15.5^{-158}. A score equals to 1 stood for very high confidence, whereas a score of 0 meant no over-representation.

The MaxUS method was based on genes derived with the Core1 and Core2 method and used the UniHI database to find interacting proteins and the STRING database to find functionally related genes [371-374]. The UniHI database was downloaded and the human genes were processed. Genes showing direct interactions with one or several Core1 or Core2 genes received the highest scores. A search in STRING was made for each Core1 gene and the 20 best candidates to be functionally related were selected for each gene. Text mining data was excluded and only Core2 genes with sub-score ≥ 0.5 were used. 462 genes were mapped to unique Entrez GeneIDs. The overall score was the maximum between UniHI and STRING scores. The UniHI gene score took into account the number of related direct and indirect interactors within the Core1 and Core2 gene lists, and the STRING score depended on the number of interactors (Table 18 and Table 19).

Table 18: Sub-scores for the interactors of Core1 and Core2 genes derived from the UniHI database.

Direct interactors	Shortest path	Gene distribution	Cummulative distribution	Score
≥5	1	83	83	1.0
4	1	82	165	0.91
3	1	211	376	0.82
2	1	510	886	0.73
1	1	1,581	2,467	0.64
0	2	8,252	10,719	0.0
0	3	1,698	12,417	0.0
0	≥4	12,703	25,120	0.0

Table 19: Sub-score for interactions derived from the STRING databse

Number of interactors	Score
4	1.0
3	1.0
2	0.82
1	0.64

The Aging method was based on genes differentially expressed between young (age ≤ 42 years) and older (age ≥ 73 years) individuals from a gene list provided in a published study [375]. The method was used because the main risk factor to develop NDs is aging. Post-mortem samples from the frontal cortex of 30 individuals ranging in age from 26 to 106 were analysed using Affymetrix microarrays. The sub-score was a mapping of the provided p-values. A score of 1 was a p-value equal to 0 and a score of 0.8 was a p-value equal to 0.01. Score 0 stood for no differential expression.

4.2.5.2 Scoring of Y2H-based protein-protein interactions

To assign confidence scores to Y2H derived protein-protein interactions, several commonly used sources of evidence were integrated into an overall score:

1. **Gene Ontology (GO) semantic similarity.** FunSimMat scores were retrieved for each protein pair via the provided web service [376]. Only the GO categories “biological process” and “cellular component” were considered.

2. **Complementarity of protein domains.** The number of potentially interacting domains of each protein pair were counted as indicated by the database DOMINE (version 2.0) [377, 378].

3. **Co-expression.** Co-expression of two proteins was assessed by calculating their topological overlap values in the GeneAtlas gene expression data set (16,742 genes in 79 mainly normal tissue samples) [379] by weighted gene co-expression network analysis (WGCNA) using the WGCNA package of the statistical environment R [380, 381]. The topological overlap of two genes reflects their

relative interconnectedness based on the level of concordance between gene expression profiles (calculated by Pearson rank correlation).

4. **Number of orthologous interactions.** The number of species in which orthologous pairs of proteins were observed to interact were retrieved from the database HomoMINT (release date: March 5, 2009) [382], I2D (release date: January 7, 2010) [383] and the data set from *Lehner and Fraser (2004)* [384].

5. **Network distance.** Two features were extracted from a large integrated network of known PPIs: the length of the shortest path between the two proteins and the number of edge-disjoint paths connecting them.

To capture non-linear relations between the different features, a support vector machine (SVM) was used to predict whether a measured interaction was a true or a false positive one. The library LIBSVM (Library for Support Vector Machines) was used to train an SVM to distinguish a known high-confidence PPI set (I selected the top 4,203 interactions from a large integrated PPI network [385]) from an equally sized random interaction set. I used a RBF kernel and performed a grid search in combination with five-fold cross validation to determine the optimal hyperparameters (the kernel's parameter γ and the soft margin parameter C). I found C = 0.5 and γ = 2 to perform best, showing an area under the ROC (Receiver Operating Characteristic) curve of 0.86. Missing values were replaced by the feature-specific median values of the training data in the training and experimental set. All features were scaled to the interval [-1,1]. The SVM decision function was used to categorize each interaction into two classes: high confidence (HC) and lower confidence (LC). The boundary of 0.1 was chosen arbitrarily.

4.2.5.3 Computational analysis of PPI networks

The software platform Cytoscape was used to visualize and analyze PPI networks [236]. To calculate network topology parameters including the diameter of the network, the average number of neighbours, the number of connected pairs of nodes, node degree, average clustering coefficients, and shortest path length the Cytoscape plugin "NetworkAnalyzer" was applied [229]. The Cytoscape plugin "BiNGO" and the tool "EASE" were deployed to identify over-represented Gene Ontology terms (BiNGO and EASE) and KEGG pathways (EASE) among a list of genes in comparison to the human

genome [386, 387]. BiNGO performs hypergeometric tests, whereas EASE calculates Fisher exact probabilities. I only considered categories with adjusted p-values < 0.05 (adjusted with the Bonferroni method) as statistically significant.

For the prediction of coiled-coil domains (CC) in amino acid sequences of modifier proteins the COILS program was used [388]. Only high probability CC sequences (0.8-1) were considered.

Intrinsically unstructured regions (IURs) of size greater than 30 were predicted with the program FoldIndex© using the default settings [389].

Neurodegenerative disease genes and other disease genes were identified by manual search of the OMIM database (http://omim.org) and of information found in GeneCards [390]. Similarly, genetic risk factors or susceptibility genes for neurodegenerative diseases were predicted by manual search of the OMIM database. Additionally, genetic modifiers associated to Alzheimer's disease were obtained from the AlzGene database [391].

Genes were defined as drug targets if they could be mapped to entries in the DrugBank database [368, 392].

In a recent proteomics study, it was shown that, with age, several hundred proteins become insoluble in the multicellular organism *C. elegans* [393]. To identify aggregation-prone proteins encoded by the analyzed genes, the genes were mapped to their homologues in *C. elegans* using the HomoloGene database and then I compared them to the list of *C. elegans* proteins mentioned above.

To identify known modulators of neurodegenerative disease protein (NDP) aggregation or toxicity among a list of genes, the genes were mapped to a list of 705 human genes, whose homologues altered NDP aggregation or toxicity in one of 21 large-scale studies in model organisms (Table 20). The model organism genes were mapped to the human genes using the HomoloGene database or using the information provided in the publications.

Table 20: Studies in model organisms which identified modifiers of NDP-induced aggregation or toxicity

Reference	Model organism	NDPs studied
Bilen et al. (2007), PLoS Genetics, 3(10), 1950-1964.	Drosophila melanogaster	Ataxin 3
Blard et al. (2007), Hum. Mol. Genetics, 16(5), 555-566	Drosophila melanogaster	Ataxin 3, Tau
Branco et al. (2008), Hum. Mol. Genetics, 17(3), 376-390	Drosophila melanogaster	Ataxin 1, ataxin 3, huntingtin
Cooper et al. (2006), Science, 313(5785), 324-328	S. cerevisae	α-synuclein
Doumanis et al. (2009), PLoS One, 4(9), e7275	Drosophila melanogaster	Huntingtin
Fernandez-Funez et al. (2000), Nature, 408(6808), 101-106	Drosophila melanogaster	Ataxin 1
Ghosh and Feany (2004), Hum. Mol. Genetics, 13(18), 2011-2018	Drosophila melanogaster	Ataxin 1 ataxin 3, polyglutamine
Giorgini et al. (2005), Nature Genetics, 37(5), 526-531	S. cerevisae	Huntingtin
Gitler et al. (2009), Nature Genetics, 41(3), 308-315	S. cerevisae	α-synuclein
Hamamichi et al. (2008), PNAS, 105(2), 728-733	C. elegans	α-synuclein
Kaltenbach et al. (2007), PLoS Genetics, 3(5), e82	Drosophila melanogaster	Huntingtin
Kraemer et al. (2006), Hum. Mol. Genetics, 15(9), 1483-1496	C. elegans	Tau
Kuwahara et al. (2008), Hum. Mol. Genetics, 17(19), 2997-3009	C. elegans	α-synuclein
Latouche et al. (2007), J Neurosci, 27(10), 2483-2492	Drosophila melanogaster	Ataxin 7

Reference	Model organism	NDPs studied
Nollen et al. (2004), PNAS, 101(17), 6403-6408	C. elegans	Polyglutamine
Shulman and Feany (2003), Genetics, 165(3), 1233-1242	Drosophila melanogaster	Tau
Van Ham et al. (2008), PLoS Genetics, 4(3), e1000027	C. elegans	α-synuclein
Wang et al. (2009), PLoS Genetics, 5(1), e1000350	C. elegans	SOD1
Willingham et al. (2003), Science, 302(5651), 1769-1772	S. cerevisae	Huntingtin, α-synuclein
Yeger-Lotem et al. (2009), Nature Genetics, 41(3), 316-323	S. cerevisae	α-synuclein
Zhang et al. (2010), Genetics, 184(4), 1165-1179	Drosophila melanogaster	Huntingtin

5 Appendix

5.1 Genes selected for systematic interaction screens

GeneID	Gene Symbol	Gene name	Score	ND gene	Other disease gene	Pred. Risk factor	Drug target	Modulators of NDPs	Aggregation-prone	Interactions found
6622	SNCA	synuclein, alpha (non A4 component of amyloid precursor)	2302.5	x			x			231
4137	MAPT	microtubule-associated protein tau	2227.9	x		x				6
351	APP	amyloid beta (A4) precursor protein	2200	x						429
3064	HTT	huntingtin	2177.5	x						955
6310	ATXN1	ataxin 1	2173.5	x						367
5071	PARK2	parkinson protein 2, E3 ubiquitin protein ligase (parkin)	2132.5	x						187
6647	SOD1	superoxide dismutase 1, soluble	2110	x						95
5663	PSEN1	presenilin 1	2103.3	x						27
11315	PARK7	parkinson protein 7	2075.9	x			x	x	x	20
9627	SNCAIP	synuclein, alpha interacting protein	2029.2			x				n.s.
5664	PSEN2	presenilin 2 (Alzheimer disease 4)	2006.2	x						36
7345	UCHL1	ubiquitin carboxyl-terminal esterase L1 (ubiquitin thiolesterase)	1974.2	x		x				42
6311	ATXN2	ataxin 2	1960	x		x		x		13
65018	PINK1	PTEN induced putative kinase 1	1956.4	x				x		11
5428	POLG	polymerase (DNA directed), gamma	1910	x						n.s.
1312	COMT	catechol-O-methyltransferase	1895				x			18
348	APOE	apolipoprotein E	1870.9		x	x	x			36
120892	LRRK2	leucine-rich repeat kinase 2	1798.6	x		x				8
23064	SETX	senataxin	1711.9	x						4
6908	TBP	TATA box binding protein	1705.5	x		x				n.s.

GeneID	Gene Symbol	Gene name	Score	ND gene	Other disease gene	Pred. Risk factor	Drug target	Modulators of NDPs	Aggregation-prone	Interactions found
23435	TARDBP	TAR DNA binding protein	1693.3	x		x				256
1639	DCTN1	dynactin 1	1658	x		x				67
9217	VAPB	VAMP (vesicle-associated membrane protein)-associated protein B and C	1653.4	x						5
43	ACHE	acetylcholinesterase	1610.5				x			n.s.
1813	DRD2	dopamine receptor D2	1577.5		x	x	x			n.s.
4744	NEFH	neurofilament, heavy polypeptide	1525.5			x		x		1
4929	NR4A2	nuclear receptor subfamily 4, group A, member 2	1500							n.s.
57679	ALS2	amyotrophic lateral sclerosis 2 (juvenile)	1500	x						10
2	A2M	alpha-2-macroglobulin	1482.8			x	x			54
773	CACNA1A	calcium channel, voltage-dependent, P/Q type, alpha 1A subunit	1460	x			x			n.s.
1814	DRD3	dopamine receptor D3	1428.3				x			0
116443	GRIN3A	glutamate receptor, ionotropic, N-methyl-D-aspartate 3A	1402				x			n.s.
5582	PRKCG	protein kinase C, gamma	1391.5	x						5
2903	GRIN2A	glutamate receptor, ionotropic, N-methyl D-aspartate 2A	1383.4			x	x			n.s.
2904	GRIN2B	glutamate receptor, ionotropic, N-methyl D-aspartate 2B	1380.7			x	x			n.s.
1812	DRD1	dopamine receptor D1	1368.6				x			n.s.
27429	HTRA2	HtrA serine peptidase 2	1357.3	x		x				69
5621	PRNP	prion protein	1330	x			x			2
150	ADRA2A	adrenergic, alpha-2A-, receptor	1314.4				x			n.s.
57053	CHRNA10	cholinergic receptor, nicotinic, alpha 10 (neuronal)	1300				x			n.s.
1135	CHRNA2	cholinergic receptor, nicotinic, alpha 2 (neuronal)	1290		x		x			n.s.
6712	SPTBN2	spectrin, beta, non-	1286.6	x						n.s

GeneID	Gene Symbol	Gene name	Score	ND gene	Other disease gene	Pred. Risk factor	Drug target	Modulators of NDPs	Aggregation-prone	Interactions found
		erythrocytic 2								.
3357	HTR2B	5-hydroxytryptamine (serotonin) receptor 2B, G protein-coupled	1285.5				x			0
26281	FGF20	fibroblast growth factor 20	1284.2							n.s.
1128	CHRM1	cholinergic receptor, muscarinic 1	1256.4				x			1
6314	ATXN7	ataxin 7	1250	x						n.s.
6653	SORL1	sortilin-related receptor, L(DLR class) A repeats containing	1250			x				1
1129	CHRM2	cholinergic receptor, muscarinic 2	1231.8				x			0
8973	CHRNA6	cholinergic receptor, nicotinic, alpha 6 (neuronal)	1227.7							n.s.
2670	GFAP	glial fibrillary acidic protein	1196.5	x				x		164
2907	GRINA	glutamate receptor, ionotropic, N-methyl D-aspartate-associated protein 1 (glutamate binding)	1195.7							n.s.
1145	CHRNE	cholinergic receptor, nicotinic, epsilon (muscle)	1182		x					n.s.
56652	C10orf2	chromosome 10 open reading frame 2	1182	x						0
1815	DRD4	dopamine receptor D4	1173.5		x	x	x			6
5630	PRPH	peripherin	1173.3			x				46
6336	SCN10A	sodium channel, voltage-gated, type X, alpha subunit	1140				x			n.s.
1621	DBH	dopamine beta-hydroxylase (dopamine beta-monooxygenase)	1135.8		x		x			17
3358	HTR2C	5-hydroxytryptamine (serotonin) receptor 2C, G protein-coupled	1104.4				x			n.s.
323	APBB2	amyloid beta (A4) precursor protein-binding, family B, member 2	1097.3	x						103
26058	GIGYF2	GRB10 interacting GYF protein 2	1085	x						n.s.

GeneID	Gene Symbol	Gene name	Score	ND gene	Other disease gene	Pred. Risk factor	Drug target	Modulators of NDPs	Aggregation-prone	Interactions found
590	BCHE	butyrylcholinesterase	1062			x	x			0
4846	NOS3	nitric oxide synthase 3 (endothelial cell)	1055.8			x	x			42
2521	FUS	fused in sarcoma	1050	x						31
4729	NDUFV2	NADH dehydrogenase (ubiquinone) flavoprotein 2, 24kDa	1038.7		x	x	x			84
25814	ATXN10	ataxin 10	1000	x						40
57338	JPH3	junctophilin 3	1000	x						221
126	ADH1C	alcohol dehydrogenase 1C (class I), gamma polypeptide	993			x	x			0
25978	CHMP2B	charged multivesicular body protein 2B	982.8	x						n.s.
23345	SYNE1	spectrin repeat containing, nuclear envelope 1	982.5	x						n.s.
54822	TRPM7	transient receptor potential cation channel, subfamily M, member 7	981.2			x				n.s.
1816	DRD5	dopamine receptor D5	968.3		x		x			n.s.
2896	GRN	granulin	959.9	x						270
5521	PPP2R2B	protein phosphatase 2, regulatory subunit B, beta	959.5	x						n.s.
3708	ITPR1	inositol 1,4,5-trisphosphate receptor, type 1	956.5	x				x		n.s.
4747	NEFL	neurofilament, light polypeptide	955.5		x					103
1356	CP	ceruloplasmin (ferroxidase)	952.3	x			x			n.s.
2861	GPR37	G protein-coupled receptor 37 (endothelin receptor type B-like)	940.3							16
642	BLMH	bleomycin hydrolase	928.7			x				5
283	ANG	angiogenin, ribonuclease, RNase A family, 5	921.6	x			x			n.s.
4311	MME	membrane metallo-endopeptidase	918.9				x			0
55775	TDP1	tyrosyl-DNA phosphodiesterase 1	910	x						13

GeneID	Gene Symbol	Gene name	Score	ND gene	Other disease gene	Pred. Risk factor	Drug target	Modulators of NDPs	Aggregation-prone	Interactions found
1636	ACE	angiotensin I converting enzyme (peptidyl-dipeptidase A) 1	906.2		x	x	x			n.s.
1020	CDK5	cyclin-dependent kinase 5	902.9				x			7
3748	KCNC3	potassium voltage-gated channel, Shaw-related subfamily, member 3	895.6	x						n.s.
146057	TTBK2	tau tubulin kinase 2	890.6	x				x		3
146	ADRA1D	adrenergic, alpha-1D-, receptor	887.5				x			n.s.
2534	FYN	FYN oncogene related to SRC, FGR, YES	865.1				x			3
815	CAMK2A	calcium/calmodulin-dependent protein kinase II alpha	862.5							6
4353	MPO	myeloperoxidase	857.4			x	x			1
6620	SNCB	synuclein, beta	851.7	x						5
5328	PLAU	plasminogen activator, urokinase	849.1			x	x			n.s.
2932	GSK3B	glycogen synthase kinase 3 beta	843.1			x	x	x		n.s.
596	BCL2	B-cell CLL/lymphoma 2	835.2				x			n.s.
836	CASP3	caspase 3, apoptosis-related cysteine peptidase	835.1				x			1
3356	HTR2A	5-hydroxytryptamine (serotonin) receptor 2A, G protein-coupled	834.7				x			0
26353	HSPB8	heat shock 22kDa protein 8	817.2		x					n.s.
7052	TGM2	transglutaminase 2 (C polypeptide, protein-glutamine-gamma-glutamyltransferase)	813.4				x			14
5413	SEPT5	septin 5	812.4							8
4128	MAOA	monoamine oxidase A	803		x		x			1
3312	HSPA8	heat shock 70kDa protein 8	790.2					x	x	0
322	APBB1	amyloid beta (A4) precursor protein-binding, family B, member 1 (Fe65)	787.5			x				7

GeneID	Gene Symbol	Gene name	Score	ND gene	Other disease gene	Pred. Risk factor	Drug target	Modulators of NDPs	Aggregation-prone	Interactions found
6532	SLC6A4	solute carrier family 6 (neurotransmitter transporter, serotonin), member 4	783.8		x		x			n.s.
4035	LRP1	low density lipoprotein receptor-related protein 1	782.7			x	x			2
3553	IL1B	interleukin 1, beta	779		x	x	x			n.s.
26994	RNF11	ring finger protein 11	777.3							234
5300	PIN1	peptidylprolyl cis/trans isomerase, NIMA-interacting 1	771.7							n.s.
7314	UBB	ubiquitin B	771.7		x					3
7276	TTR	transthyretin	766		x		x			58
4287	ATXN3	ataxin 3	750	x		x				102
25894	PLEKHG4	pleckstrin homology domain containing, family G (with RhoGef domain) member 4	750			x				n.s.
1509	CTSD	cathepsin D	746.5	x			x		x	23
23621	BACE1	beta-site APP-cleaving enzyme 1	744.8				x			6
3315	HSPB1	heat shock 27kDa protein 1	739.7		x					212
2908	NR3C1	nuclear receptor subfamily 3, group C, member 1 (glucocorticoid receptor)	736.8				x			3
12	SERPINA3	serpin peptidase inhibitor, clade A (alpha-1 antiproteinase, antitrypsin), member 3	735.6			x				4
7422	VEGFA	vascular endothelial growth factor A	735.1			x	x			n.s.
22948	CCT5	chaperonin containing TCP1, subunit 5 (epsilon)	720.3		x			x	x	37
1410	CRYAB	crystallin, alpha B	719.5		x			x		10
7534	YWHAZ	tyrosine 3-monooxygenase/tryptophan 5-monooxygenase activation protein, zeta polypeptide	717				x	x	x	n.s.

GeneID	Gene Symbol	Gene name	Score	ND gene	Other disease gene	Pred. Risk factor	Drug target	Modulators of NDPs	Aggregation-prone	Interactions found
23400	ATP13A2	ATPase type 13A2	712.3	x				x		n.s.
5376	PMP22	peripheral myelin protein 22	710		x					171
3416	IDE	insulin-degrading enzyme	707.5			x	x			n.s.
51107	APH1A	anterior pharynx defective 1 homolog A (C. elegans)	706.7							3
3688	ITGB1	integrin, beta 1 (fibronectin receptor, beta polypeptide, antigen CD29 includes MDF2, MSK12)	705.5						x	2
23385	NCSTN	nicastrin	705			x				0
6571	SLC18A2	solute carrier family 18 (vesicular monoamine), member 2	700				x			1
538	ATP7A	ATPase, Cu++ transporting, alpha polypeptide	697.1	x				x		n.s.
5189	PEX1	peroxisomal biogenesis factor 1	690	x						43
55851	PSENEN	presenilin enhancer 2 homolog (C. elegans)	682.5							2
102	ADAM10	ADAM metallopeptidase domain 10	670.9			x				n.s.
367	AR	androgen receptor	662.6	x			x			n.s.
627	BDNF	brain-derived neurotrophic factor	660		x	x				46
4129	MAOB	monoamine oxidase B	660			x	x			0
6531	SLC6A3	solute carrier family 6 (neurotransmitter transporter, dopamine), member 3	660	x			x			n.s.
4803	NGF	nerve growth factor (beta polypeptide)	657.7		x		x			3
875	CBS	cystathionine-beta-synthase	656.9		x		x			8
5594	MAPK1	mitogen-activated protein kinase 1	655.7				x			n.s.
7804	LRP8	low density lipoprotein receptor-related protein 8, apolipoprotein e receptor	652.2							10
4133	MAP2	microtubule-associated	650.2				x			n.s

GeneID	Gene Symbol	Gene name	Score	ND gene	Other disease gene	Pred. Risk factor	Drug target	Modulators of NDPs	Aggregation-prone	Interactions found
		protein 2								.
23095	KIF1B	kinesin family member 1B	640.7		x					303
207	AKT1	v-akt murine thymoma viral oncogene homolog 1	632.5		x		x			13
4540	ND5	NADH dehydrogenase subunit 5	632.5	x						n.s.
2597	GAPDH	glyceraldehyde-3-phosphate dehydrogenase	632.3			x	x		x	16
1861	TOR1A	torsin family 1, member A (torsin A)	632.1		x			x		48
10273	STUB1	STIP1 homology and U-box containing protein 1, E3 ubiquitin protein ligase	628.8					x		11
2259	FGF14	fibroblast growth factor 14	628.7	x						2
1137	CHRNA4	cholinergic receptor, nicotinic, alpha 4 (neuronal)	627.5		x		x			5
540	ATP7B	ATPase, Cu++ transporting, beta polypeptide	621.4		x					n.s.
59269	HIVEP3	human immunodeficiency virus type I enhancer binding protein 3	620.3							n.s.
7466	WFS1	Wolfram syndrome 1 (wolframin)	617.9		x					497
22976	PAXIP1	PAX interacting (with transcription-activation domain) protein 1	617.9			x				1
7531	YWHAE	tyrosine 3-monooxygenase/tryptophan 5-monooxygenase activation protein, epsilon polypeptide	616.4					x		n.s.
4723	NDUFV1	NADH dehydrogenase (ubiquinone) flavoprotein 1, 51kDa	614	x			x			20
3320	HSP90AA1	heat shock protein 90kDa alpha (cytosolic), class A member 1	613.9				x	x		15
7018	TF	transferrin	609.2		x	x	x			n.s.

GeneID	Gene Symbol	Gene name	Score	ND gene	Other disease gene	Pred. Risk factor	Drug target	Modulators of NDPs	Aggregation-prone	Interactions found
8518	IKBKAP	inhibitor of kappa light polypeptide gene enhancer in B-cells, kinase complex-associated protein	600.7		x					n.s.
9479	MAPK8IP1	mitogen-activated protein kinase 8 interacting protein 1	600.4		x					n.s.
857	CAV1	caveolin 1, caveolae protein, 22kDa	595.7		x					1
22883	CLSTN1	calsyntenin 1	595.2							13
5631	PRPS1	phosphoribosyl pyrophosphate synthetase 1	591		x					125
3091	HIF1A	hypoxia inducible factor 1, alpha subunit (basic helix-loop-helix transcription factor)	590.3							n.s.
6383	SDC2	syndecan 2	588.8				x			6
79800	ALS2CR8	amyotrophic lateral sclerosis 2 (juvenile) chromosome region, candidate 8	587.3			x				5
5264	PHYH	phytanoyl-CoA 2-hydroxylase	586.9	x			x			16
2246	FGF1	fibroblast growth factor 1 (acidic)	580.1				x			n.s.
142	PARP1	poly (ADP-ribose) polymerase 1	577.8				x			n.s.
7248	TSC1	tuberous sclerosis 1	577.5		x					67
4000	LMNA	lamin A/C	576.3		x					74
498	ATP5A1	ATP synthase, H+ transporting, mitochondrial F1 complex, alpha subunit 1, cardiac muscle	574.7					x		3
1499	CTNNB1	catenin (cadherin-associated protein), beta 1, 88kDa	574.4		x		x	x		n.s.
5414	SEPT4	septin 4	570.8							n.s.
1272	CNTN1	contactin 1	569.6		x					n.s.
5579	PRKCB1	protein kinase C, beta	565.1				x			3
7317	UBA1	ubiquitin-like modifier activating enzyme 1	560	x				x	x	3
4771	NF2	neurofibromin 2 (merlin)	558.3		x					58

GeneID	Gene Symbol	Gene name	Score	ND gene	Other disease gene	Pred. Risk factor	Drug target	Modulators of NDPs	Aggregation-prone	Interactions found
443	ASPA	aspartoacylase	557.5	x			x			5
2629	GBA	glucosidase, beta, acid	550.1		x	x	x			13
120	ADD3	adducin 3 (gamma)	550					x		n.s.
9896	FIG4	FIG4 homolog, SAC1 lipid phosphatase domain containing (S. cerevisiae)	550	x						n.s.
10397	NDRG1	N-myc downstream regulated 1	550		x					15
56997	CABC1	aarF domain containing kinase 3	550	x						29
1576	CYP3A4	cytochrome P450, family 3, subfamily A, polypeptide 4	549.8				x			4
4524	MTHFR	methylenetetrahydrofolate reductase (NAD(P)H)	549.7		x		x			n.s.
6607	SMN2	survival of motor neuron 2, centromeric	549.4	x		x				37
5175	PECAM1	platelet/endothelial cell adhesion molecule 1	549							79
7431	VIM	vimentin	548.2							47
3706	ITPKA	inositol-trisphosphate 3-kinase A	547.9				x			n.s.
5337	PLD1	phospholipase D1, phosphatidylcholine-specific	545.6				x			9
3074	HEXB	hexosaminidase B (beta polypeptide)	545.5	x			x			25
7450	VWF	von Willebrand factor	543.7		x		x			4
58	ACTA1	actin, alpha 1, skeletal muscle	541.6		x		x			8
7249	TSC2	tuberous sclerosis 2	540.5		x					n.s.
9001	HAP1	huntingtin-associated protein 1	537.7			x				n.s.
4359	MPZ	myelin protein zero	537		x					7
3251	HPRT1	hypoxanthine phosphoribosyltransferase 1	535		x		x			0
25897	RNF19A	ring finger protein 19A	534.2							n.s.

GeneID	Gene Symbol	Gene name	Score	ND gene	Other disease gene	Pred. Risk factor	Drug target	Modulators of NDPs	Aggregation-prone	Interactions found
1161	ERCC8	excision repair cross-complementing rodent repair deficiency, complementation group 8	532.5		x					5
2074	ERCC6	excision repair cross-complementing rodent repair deficiency, complementation group 6	532.5		x					n.s.
8898	MTMR2	myotubularin related protein 2	532.5		x					n.s.
6843	VAMP1	vesicle-associated membrane protein 1 (synaptobrevin 1)	532.3				x			2
4741	NEFM	neurofilament, medium polypeptide	531.8							n.s.
1268	CNR1	cannabinoid receptor 1 (brain)	530.9				x			n.s.
9516	LITAF	lipopolysaccharide-induced TNF factor	530		x					24
6285	S100B	S100 calcium binding protein B	528.8				x			25
2099	ESR1	estrogen receptor 1	527.9				x			3
5868	RAB5A	RAB5A, member RAS oncogene family	526.6							17
3303	HSPA1A	heat shock 70kDa protein 1A	522.3				x	x		1
478	ATP1A3	ATPase, Na+/K+ transporting, alpha 3 polypeptide	519.4		x			x	x	17
6646	SOAT1	sterol O-acyltransferase 1	517.8				x			n.s.
3093	UBE2K	ubiquitin-conjugating enzyme E2K	517.6							61
3329	HSPD1	heat shock 60kDa protein 1 (chaperonin)	516.4		x				x	14
5590	PRKCZ	protein kinase C, zeta	515.9							n.s.
54205	CYCS	cytochrome c, somatic	515.1		x		x			23
6272	SORT1	sortilin 1	514.2							1
3028	HSD17B10	hydroxysteroid (17-beta) dehydrogenase 10	514		x		x		x	n.s.
2554	GABRA1	gamma-aminobutyric acid (GABA) A receptor, alpha	513.7				x			n.s.

GeneID	Gene Symbol	Gene name	Score	ND gene	Other disease gene	Pred. Risk factor	Drug target	Modulators of NDPs	Aggregation-prone	Interactions found
		1								
55660	PRPF40A	PRP40 pre-mRNA processing factor 40 homolog A (S. cerevisiae)	513							133
213	ALB	albumin	511.2				x			7
6750	SST	somatostatin	511				x			n.s.
1180	CLCN1	chloride channel 1, skeletal muscle	510		x					n.s.
1760	DMPK	dystrophia myotonica-protein kinase	510		x					n.s.
3092	HIP1	huntingtin interacting protein 1	510							76
4763	NF1	neurofibromin 1	510		x					n.s.
5191	PEX7	peroxisomal biogenesis factor 7	510	x						6
23636	NUP62	nucleoporin 62kDa	510	x				x		n.s.
55670	PEX26	peroxisomal biogenesis factor 26	510	x						36
1139	CHRNA7	cholinergic receptor, nicotinic, alpha 7 (neuronal)	509.5				x	x		10
3920	LAMP2	lysosomal-associated membrane protein 2	507.5							258
1644	DDC	dopa decarboxylase (aromatic L-amino acid decarboxylase)	505		x		x			n.s.
1114	CHGB	chromogranin B (secretogranin 1)	502.8							n.s.
3949	LDLR	low density lipoprotein receptor	501.7		x		x			n.s.
10915	TCERG1	transcription elongation regulator 1	501.1					x		n.s.
1785	DNM2	dynamin 2	500.8		x			x		124
839	CASP6	caspase 6, apoptosis-related cysteine peptidase	500							212
2263	FGFR2	fibroblast growth factor receptor 2	494.3		x		x			n.s.
84570	COL25A1	collagen, type XXV, alpha 1	491.7							5

GeneID	Gene Symbol	Gene name	Score	ND gene	Other disease gene	Pred. Risk factor	Drug target	Modulators of NDPs	Aggregation-prone	Interactions found
885	CCK	cholecystokinin	491.1				x			61
5901	RAN	RAN, member RAS oncogene family	490.4					x	x	135
51100	SH3GLB1	SH3-domain GRB2-like endophilin B1	488.8							130
3831	KLC1	kinesin light chain 1	487.7							n.s.
10963	STIP1	stress-induced-phosphoprotein 1	487.7					x	x	23
3163	HMOX2	heme oxygenase (decycling) 2	487.6				x			39
3309	HSPA5	heat shock 70kDa protein 5 (glucose-regulated protein, 78kDa)	485.2				x	x	x	9
5580	PRKCD	protein kinase C, delta	482.8							1
5520	PPP2R2A	protein phosphatase 2, regulatory subunit B, alpha	480.9							3
1471	CST3	cystatin C	478.4		x					n.s.
9973	CCS	copper chaperone for superoxide dismutase	478.3							n.s.
7529	YWHAB	tyrosine 3-monooxygenase/tryptophan 5-monooxygenase activation protein, beta polypeptide	477.7					x		143
5730	PTGDS	prostaglandin D2 synthase 21kDa (brain)	476.9					x		n.s.
3265	HRAS	v-Ha-ras Harvey rat sarcoma viral oncogene homolog	476		x		x			117
29979	UBQLN1	ubiquilin 1	475.3							139
2261	FGFR3	fibroblast growth factor receptor 3	475.2		x		x			331
2905	GRIN2C	glutamate receptor, ionotropic, N-methyl D-aspartate 2C	475				x			123
10558	SPTLC1	serine palmitoyltransferase, long chain base subunit 1	474.9		x		x			13
320	APBA1	amyloid beta (A4) precursor protein-binding, family	472.8							n.s.

GeneID	Gene Symbol	Gene name	Score	ND gene	Other disease gene	Pred. Risk factor	Drug target	Modulators of NDPs	Aggregation-prone	Interactions found
		A, member 1								
834	CASP1	caspase 1, apoptosis-related cysteine peptidase (interleukin 1, beta, convertase)	471				x			3
2247	FGF2	fibroblast growth factor 2 (basic)	470.4				x			n.s.
9093	DNAJA3	DnaJ (Hsp40) homolog, subfamily A, member 3	469							n.s.
821	CANX	calnexin	468				x			n.s.
1103	CHAT	choline O-acetyltransferase	467.5		x		x			113
4792	NFKBIA	nuclear factor of kappa light polypeptide gene enhancer in B-cells inhibitor, alpha	466.9		x					n.s.
154	ADRB2	adrenergic, beta-2, receptor, surface	466				x			26
6197	RPS6KA3	ribosomal protein S6 kinase, 90kDa, polypeptide 3	465.5		x					23
2776	GNAQ	guanine nucleotide binding protein (G protein), q polypeptide	462.3							n.s.
26092	TOR1AIP1	torsin A interacting protein 1	460.9							9
6950	TCP1	t-complex 1	460					x	x	8
10204	NUTF2	nuclear transport factor 2	460					x	x	n.s.
378465	HSN2	hereditary sensory neuropathy, type II	460							n.s.
2934	GSN	gelsolin	459.4		x					218
1191	CLU	clusterin	457.7			x				n.s.
4043	LRPAP1	low density lipoprotein receptor-related protein associated protein 1	456.8							n.s.
5045	FURIN	furin (paired basic amino acid cleaving enzyme)	455.8							n.s.

GeneID	Gene Symbol	Gene name	Score	ND gene	Other disease gene	Pred. Risk factor	Drug target	Modulators of NDPs	Aggregation-prone	Interactions found
1743	DLST	dihydrolipoamide S-succinyltransferase (E2 component of 2-oxo-glutarate complex)	455						x	77
5923	RASGRF1	Ras protein-specific guanine nucleotide-releasing factor 1	455							n.s.
811	CALR	calreticulin	454.1				x		x	77
3339	HSPG2	heparan sulfate proteoglycan 2	453.5		x		x			n.s.
7159	TP53BP2	tumor protein p53 binding protein, 2	453							7
1457	CSNK2A1	casein kinase 2, alpha 1 polypeptide	452.7				x	x	x	1
999	CDH1	cadherin 1, type 1, E-cadherin (epithelial)	451.7		x					30
1200	TPP1	tripeptidyl peptidase I	450	x						11
347	APOD	apolipoprotein D	450							n.s.
9976	CLEC2B	C-type lectin domain family 2, member B	450							1
114908	TMEM123	transmembrane protein 123	450							8
140609	NEK7	NIMA (never in mitosis gene a)-related kinase 7	450							78
2906	GRIN2D	glutamate receptor, ionotropic, N-methyl D-aspartate 2D	449				x			n.s.
7048	TGFBR2	transforming growth factor, beta receptor II (70/80kDa)	445.9		x		x			75
6261	RYR1	ryanodine receptor 1 (skeletal)	445.5		x		x			n.s.
10768	AHCYL1	adenosylhomocysteinase-like 1	444.8							15
475	ATOX1	ATX1 antioxidant protein 1 homolog (yeast)	444.5				x			47
9445	ITM2B	integral membrane protein 2B	441.2	x						2
7054	TH	tyrosine hydroxylase	440.8		x		x			n.s.
301	ANXA1	annexin A1	440.5				x			5
567	B2M	beta-2-microglobulin	440.2		x					4

GeneID	Gene Symbol	Gene name	Score	ND gene	Other disease gene	Pred. Risk factor	Drug target	Modulators of NDPs	Aggregation-prone	Interactions found
476	ATP1A1	ATPase, Na+/K+ transporting, alpha 1 polypeptide	439.2				x			n.s.
3362	HTR6	5-hydroxytryptamine (serotonin) receptor 6, G protein-coupled	439.1				x			n.s.
4478	MSN	moesin	438.6						x	n.s.
8851	CDK5R1	cyclin-dependent kinase 5, regulatory subunit 1 (p35)	437.5					x		20
983	CDC2	cyclin-dependent kinase 1	437.4				x			3
823	CAPN1	calpain 1, (mu/I) large subunit	436.7				x			1
5243	ABCB1	ATP-binding cassette, subfamily B (MDR/TAP), member 1	436.2				x			n.s.
2395	FXN	frataxin	435.5	x						11
3861	KRT14	keratin 14	435.5		x					n.s.
1392	CRH	corticotropin releasing hormone	434.6				x			1
908	CCT6A	chaperonin containing TCP1, subunit 6A (zeta 1)	434.2						x	6
22978	NT5C2	5'-nucleotidase, cytosolic II	433.4				x			n.s.
4131	MAP1B	microtubule-associated protein 1B	433.2							n.s.
1080	CFTR	cystic fibrosis transmembrane conductance regulator (ATP-binding cassette sub-family C, member 7)	432.9		x		x			n.s.
334	APLP2	amyloid beta (A4) precursor-like protein 2	432.5							3
5886	RAD23A	RAD23 homolog A (S. cerevisiae)	432.5					x	x	24
26003	GORASP2	golgi reassembly stacking protein 2, 55kDa	432.5							10
6812	STXBP1	syntaxin binding protein 1	432.1		x					n.s.
1996	ELAVL4	ELAV (embryonic lethal, abnormal vision, Drosophila)-like 4 (Hu antigen D)	431.8			x				35

GeneID	Gene Symbol	Gene name	Score	ND gene	Other disease gene	Pred. Risk factor	Drug target	Modulators of NDPs	Aggregation-prone	Interactions found
2902	GRIN1	glutamate receptor, ionotropic, N-methyl D-aspartate 1	430.9				x			n.s.
871	SERPINH1	serpin peptidase inhibitor, clade H (heat shock protein 47), member 1, (collagen binding protein 1)	430							38
6856	SYPL1	synaptophysin-like 1	430							n.s.
10134	BCAP31	B-cell receptor-associated protein 31	429.4							7
8601	RGS20	regulator of G-protein signaling 20	429.1							n.s.
321	APBA2	amyloid beta (A4) precursor protein-binding, family A, member 2	428.7							n.s.
1453	CSNK1D	casein kinase 1, delta	428.7							4
5870	RAB6A	RAB6A, member RAS oncogene family	427.9							3
5566	PRKACA	protein kinase, cAMP-dependent, catalytic, alpha	427.7							33
116444	GRIN3B	glutamate receptor, ionotropic, N-methyl-D-aspartate 3B	426.5				x			n.s.
2697	GJA1	gap junction protein, alpha 1, 43kDa	426		x		x			4
23468	CBX5	chromobox homolog 5	425.6							20
1141	CHRNB2	cholinergic receptor, nicotinic, beta 2 (neuronal)	424.9		x		x			n.s.
11140	CDC37	cell division cycle 37 homolog (S. cerevisiae)	424.9							n.s.
3350	HTR1A	5-hydroxytryptamine (serotonin) receptor 1A, G protein-coupled	424.3				x			n.s.
7415	VCP	valosin containing protein	424.2	x				x	x	2
79705	LRRK1	leucine-rich repeat kinase 1	424.2							1
780	DDR1	discoidin domain receptor tyrosine kinase 1	424				x			n.s.
8565	YARS	tyrosyl-tRNA synthetase	423.7		x		x			18
573	BAG1	BCL2-associated athanogene	423.5							n.s.

GeneID	Gene Symbol	Gene name	Score	ND gene	Other disease gene	Pred. Risk factor	Drug target	Modulators of NDPs	Aggregation-prone	Interactions found
1287	COL4A5	collagen, type IV, alpha 5	423.2		x			x	x	n.s.
5825	ABCD3	ATP-binding cassette, sub-family D (ALD), member 3	422.8	x						5
887	CCKBR	cholecystokinin B receptor	421.8				x			n.s.
2783	GNB2	guanine nucleotide binding protein (G protein), beta polypeptide 2	421.3							24
5950	RBP4	retinol binding protein 4, plasma	421				x			n.s.
9788	MTSS1	metastasis suppressor 1	420.5							n.s.
4217	MAP3K5	mitogen-activated protein kinase kinase kinase 5	419.9							2
4842	NOS1	nitric oxide synthase 1 (neuronal)	419.1			x	x			n.s.
203068	TUBB	tubulin, beta class I	418.7				x	x	x	4
60	ACTB	actin, beta	418.2		x			x		1
4843	NOS2A	nitric oxide synthase 2, inducible	417.8				x			n.s.
5538	PPT1	palmitoyl-protein thioeste-rase 1	417.4		x					8
6421	SFPQ	splicing factor proline/glutamine-rich	416.7							n.s.
5295	PIK3R1	phosphoinositide-3-kinase, regulatory subunit 1 (al-pha)	414.1				x			21
5728	PTEN	phosphatase and tensin homolog	413.8		x			x		n.s.
6850	SYK	spleen tyrosine kinase	412.9				x			17
10048	RANBP9	RAN binding protein 9	412.5							n.s.
841	CASP8	caspase 8, apoptosis-related cysteine peptidase	411.8		x					3
333	APLP1	amyloid beta (A4) precur-sor-like protein 1	410							1
1409	CRYAA	crystallin, alpha A	410		x					102
1654	DDX3X	DEAD (Asp-Glu-Ala-Asp) box polypeptide 3, X-linked	410							3

GeneID	Gene Symbol	Gene name	Score	ND gene	Other disease gene	Pred. Risk factor	Drug target	Modulators of NDPs	Aggregation-prone	Interactions found
1780	DYNC1I1	dynein, cytoplasmic 1, intermediate chain 1	410							2
1822	ATN1	atrophin 1	410	x						115
1993	ELAVL2	ELAV (embryonic lethal, abnormal vision, Drosophila)-like 2 (Hu antigen B)	410							2
3189	HNRNPH3	heterogeneous nuclear ribonucleoprotein H3 (2H9)	410							3
3337	DNAJB1	DnaJ (Hsp40) homolog, subfamily B, member 1	410							8
3707	ITPKB	inositol-trisphosphate 3-kinase B	410							0
3765	KCNJ9	potassium inwardly-rectifying channel, subfamily J, member 9	410							n.s.
4139	MARK1	MAP/microtubule affinity-regulating kinase 1	410							n.s.
5058	PAK1	p21 protein (Cdc42/Rac)-activated kinase 1	410							29
5260	PHKG1	phosphorylase kinase, gamma 1 (muscle)	410							n.s.
5962	RDX	radixin	410		x					35
6595	SMARCA2	SWI/SNF related, matrix associated, actin dependent regulator of chromatin, subfamily a, member 2	410							n.s.
6879	TAF7	TAF7 RNA polymerase II, TATA box binding protein (TBP)-associated factor, 55kDa	410							3
7050	TGIF1	TGFB-induced factor homeobox 1	410		x			x		3
7337	UBE3A	ubiquitin protein ligase E3A	410		x					1
8473	OGT	O-linked N-acetylglucosamine (GlcNAc) transferase (UDP-N-acetylglucosamine:polypeptide-N-acetylglucosaminyl transferase)	410							n.s.

GeneID	Gene Symbol	Gene name	Score	ND gene	Other disease gene	Pred. Risk factor	Drug target	Modulators of NDPs	Aggregation-prone	Interactions found
10418	SPON1	spondin 1, extracellular matrix protein	410							n.s.
10611	PDLIM5	PDZ and LIM domain 5	410							6
10755	GIPC1	GIPC PDZ domain containing family, member 1	410					x		37
10923	SUB1	SUB1 homolog (S. cerevisiae)	410					x		4
11051	NUDT21	nudix (nucleoside diphosphate linked moiety X)-type motif 21	410					x		n.s.
22882	ZHX2	zinc fingers and homeoboxes 2	410							3
25801	GCA	grancalcin, EF-hand calcium binding protein	410					x		n.s.
25825	BACE2	beta-site APP-cleaving enzyme 2	410							19
55062	WIPI1	WD repeat domain, phosphoinositide interacting 1	410							3
81628	TSC22D4	TSC22 domain family, member 4	410							n.s.
221037	JMJD1C	jumonji domain containing 1C	410							n.s.
9846	GAB2	GRB2-associated binding protein 2	409.6							5
2911	GRM1	glutamate receptor, metabotropic 1	409.4				x			n.s.
7157	TP53	tumor protein p53	409.1		x					n.s.
121512	FGD4	FYVE, RhoGEF and PH domain containing 4	409		x					n.s.
9927	MFN2	mitofusin 2	408.4		x					n.s.
80025	PANK2	pantothenate kinase 2	407.8	x						11
1778	DYNC1H1	dynein, cytoplasmic 1, heavy chain 1	407					x		48
4725	NDUFS5	NADH dehydrogenase (ubiquinone) Fe-S protein 5, 15kDa (NADH-coenzyme Q reductase)	407				x			4
87	ACTN1	actinin, alpha 1	406.4						x	n.s.
1278	COL1A2	collagen, type I, alpha 2	405.8		x		x			n.s.

GeneID	Gene Symbol	Gene name	Score	ND gene	Other disease gene	Pred. Risk factor	Drug target	Modulators of NDPs	Aggregation-prone	Interactions found
64374	SIL1	SIL1 homolog, endoplasmic reticulum chaperone (S. cerevisiae)	405.4		x					n.s.
5653	KLK6	kallikrein-related peptidase 6	404.9				x			166
30818	KCNIP3	Kv channel interacting protein 3, calsenilin	404.8							9
2162	F13A1	coagulation factor XIII, A1 polypeptide	404.5		x		x			26
3301	DNAJA1	DnaJ (Hsp40) homolog, subfamily A, member 1	404.4					x	x	n.s.
1387	CREBBP	CREB binding protein	402.5		x			x		n.s.
189	AGXT	alanine-glyoxylate aminotransferase	399.3		x		x			n.s.
23390	ZDHHC17	zinc finger, DHHC-type containing 17	399.3							2
5742	PTGS1	prostaglandin-endoperoxide synthase 1 (prostaglandin G/H synthase and cyclooxygenase)	397.5				x			4
6457	SH3GL3	SH3-domain GRB2-like 3	397.4					x		5
9588	PRDX6	peroxiredoxin 6	397.3							4
5327	PLAT	plasminogen activator, tissue	397.1		x		x			0
5354	PLP1	proteolipid protein 1	397.1		x					7
23358	USP24	ubiquitin specific peptidase 24	396.8							0
2805	GOT1	glutamic-oxaloacetic transaminase 1, soluble (aspartate aminotransferase 1)	396.6				x	x		0
6623	SNCG	synuclein, gamma (breast cancer-specific protein 1)	396.3							0
3737	KCNA2	potassium voltage-gated channel, shaker-related subfamily, member 2	396.1							0
5034	P4HB	prolyl 4-hydroxylase, beta polypeptide	395.7				x	x	x	20
7879	RAB7A	RAB7A, member RAS oncogene family	394.8		x			x		7

GeneID	Gene Symbol	Gene name	Score	ND gene	Other disease gene	Pred. Risk factor	Drug target	Modulators of NDPs	Aggregation-prone	Interactions found
10210	TOPORS	topoisomerase I binding, arginine/serine-rich, E3 ubiquitin protein ligase	392.7		x					n.s.
2617	GARS	glycyl-tRNA synthetase	392.5		x		x		x	6
7388	UQCRH	ubiquinol-cytochrome c reductase hinge protein	390.5							n.s.
7374	UNG	uracil-DNA glycosylase	390		x					1
10972	TMED10	transmembrane emp24-like trafficking protein 10 (yeast)	390							0
11069	RAPGEF4	Rap guanine nucleotide exchange factor (GEF) 4	390					x		5
11129	SFRS16	CLK4-associating serine/arginine rich protein	390							1
26471	NUPR1	nuclear protein, transcriptional regulator, 1	390							3
6767	ST13	suppression of tumorigenicity 13 (colon carcinoma) (Hsp70 interacting protein)	389.4						x	8
1956	EGFR	epidermal growth factor receptor	389.2				x			0
2035	EPB41	erythrocyte membrane protein band 4.1 (elliptocytosis 1, RH-linked)	388.8		x					2
57449	PLEKHG5	pleckstrin homology domain containing, family G (with RhoGef domain) member 5	388.1	x						n.s.
9611	NCOR1	nuclear receptor corepressor 1	387.3							7
840	CASP7	caspase 7, apoptosis-related cysteine peptidase	386.4				x			3
5828	PXMP3	peroxisomal biogenesis factor 2	386.2	x				x		n.s.
10574	CCT7	chaperonin containing TCP1, subunit 7 (eta)	386.2					x		5
6566	SLC16A1	solute carrier family 16, member 1 (monocarboxylic acid transporter 1)	385.9		x		x			4
4697	NDUFA4	NADH dehydrogenase (ubiquinone) 1 alpha sub-	384.8				x			3

GeneID	Gene Symbol	Gene name	Score	ND gene	Other disease gene	Pred. Risk factor	Drug target	Modulators of NDPs	Aggregation-prone	Interactions found
		complex, 4, 9kDa								
23268	DNMBP	dynamin binding protein	384.4					x		1
2931	GSK3A	glycogen synthase kinase 3 alpha	384.3							n.s.
6301	SARS	seryl-tRNA synthetase	383.9				x		x	27
10133	OPTN	optineurin	382.7	x						173
4535	ND1	NADH dehydrogenase subunit 1	382.5	x						n.s.
3306	HSPA2	heat shock 70kDa protein 2	381.2					x		57
4716	NDUFB10	NADH dehydrogenase (ubiquinone) 1 beta subcomplex, 10, 22kDa	379				x	x		4
2475	FRAP1	mechanistic target of rapamycin (serine/threonine kinase)	378				x	x		n.s.
7846	TUBA1A	tubulin, alpha 1a	377.8		x		x	x	x	2
2280	FKBP1A	FK506 binding protein 1A, 12kDa	377.3				x			73
4067	LYN	v-yes-1 Yamaguchi sarcoma viral related oncogene homolog	376.8							2
4204	MECP2	methyl CpG binding protein 2 (Rett syndrome)	376.7		x					34
2782	GNB1	guanine nucleotide binding protein (G protein), beta polypeptide 1	375.9							2
8878	SQSTM1	sequestosome 1	374.5		x					8
4071	TM4SF1	transmembrane 4 L six family member 1	374.4							3
2081	ERN1	endoplasmic reticulum to nucleus signaling 1	372.5							36
1968	EIF2S3	eukaryotic translation initiation factor 2, subunit 3 gamma, 52kDa	372.1					x		28
3297	HSF1	heat shock transcription factor 1	371.6					x		11
8766	RAB11A	RAB11A, member RAS oncogene family	370.1					x		4
5999	RGS4	regulator of G-protein signaling 4	370							0

GeneID	Gene Symbol	Gene name	Score	ND gene	Other disease gene	Pred. Risk factor	Drug target	Modulators of NDPs	Aggregation-prone	Interactions found
7153	TOP2A	topoisomerase (DNA) II alpha 170kDa	369.4				x	x		n.s.
5053	PAH	phenylalanine hydroxylase	369.2		x		x			0
335	APOA1	apolipoprotein A-I	368.7		x					n.s.
5530	PPP3CA	protein phosphatase 3, catalytic subunit, alpha isozyme	368.3							n.s.
10396	ATP8A1	ATPase, aminophospholipid transporter (APLT), class I, type 8A, member 1	368.2				x			n.s.
1565	CYP2D6	cytochrome P450, family 2, subfamily D, polypeptide 6	367.9				x			n.s.
29072	SETD2	SET domain containing 2	367.5							n.s.
6714	SRC	v-src sarcoma (Schmidt-Ruppin A-2) viral oncogene homolog (avian)	367.3							11
2885	GRB2	growth factor receptor-bound protein 2	367				x			21
5914	RARA	retinoic acid receptor, alpha	367		x		x			1
2890	GRIA1	glutamate receptor, ionotropic, AMPA 1	366.9				x			5
2628	GATM	glycine amidinotransferase (L-arginine:glycine amidinotransferase)	366.7		x		x			14
2353	FOS	FBJ murine osteosarcoma viral oncogene homolog	366.5							33
6915	TBXA2R	thromboxane A2 receptor	366				x			n.s.
9500	MAGED1	melanoma antigen family D, 1	365.5							1
9638	FEZ1	fasciculation and elongation protein zeta 1 (zygin I)	365.5					x		n.s.
3384	ICAM2	intercellular adhesion molecule 2	365.1							1
54332	GDAP1	ganglioside induced differentiation associated protein 1	364.9		x					33
672	BRCA1	breast cancer 1, early onset	364		x					1

GeneID	Gene Symbol	Gene name	Score	ND gene	Other disease gene	Pred. Risk factor	Drug target	Modulators of NDPs	Aggregation-prone	Interactions found
3725	JUN	jun proto-oncogene	363.9				x			10
7416	VDAC1	voltage-dependent anion channel 1	363.8				x			0
4057	LTF	lactotransferrin	363.2				x			1
5445	PON2	paraoxonase 2	363							0
7277	TUBA4A	tubulin, alpha 4a	360.6				x			0
51586	MED15	mediator complex subunit 15	360					x		n.s.
5879	RAC1	ras-related C3 botulinum toxin substrate 1 (rho family, small GTP binding protein Rac1)	359.9				x			9
3065	HDAC1	histone deacetylase 1	359.3				x	x		0
6804	STX1A	syntaxin 1A (brain)	359.1					x		n.s.
4715	NDUFB9	NADH dehydrogenase (ubiquinone) 1 beta subcomplex, 9, 22kDa	359				x		x	n.s.
51079	NDUFA13	NADH dehydrogenase (ubiquinone) 1 alpha subcomplex, 13	359		x		x			0
9063	PIAS2	protein inhibitor of activated STAT, 2	358.3							0
4804	NGFR	nerve growth factor receptor	357.9							1
3757	KCNH2	potassium voltage-gated channel, subfamily H (eag-related), member 2	357.8		x		x			n.s.
7384	UQCRC1	ubiquinol-cytochrome c reductase core protein I	357.5				x		x	32
7430	EZR	ezrin	357.5							4
5585	PKN1	protein kinase N1	357.4							11
177	AGER	advanced glycosylation end product-specific receptor	357							2
7411	VBP1	von Hippel-Lindau binding protein 1	356.6							9
9378	NRXN1	neurexin 1	356.2							n.s.
7280	TUBB2A	tubulin, beta 2A class IIa	355.6		x					2
7299	TYR	tyrosinase (oculocutaneous albinism IA)	355.3		x		x			4

GeneID	Gene Symbol	Gene name	Score	ND gene	Other disease gene	Pred. Risk factor	Drug target	Modulators of NDPs	Aggregation-prone	Interactions found
6897	TARS	threonyl-tRNA synthetase	355				x		x	1
5430	POLR2A	polymerase (RNA) II (DNA directed) polypeptide A, 220kDa	354.1					x		2
762	CA4	carbonic anhydrase IV	352.5		x		x			n.s.
25764	HYPK	chromosome 15 open reading frame 63	352.2							0
1201	CLN3	ceroid-lipofuscinosis, neuronal 3	350	x						3
1203	CLN5	ceroid-lipofuscinosis, neuronal 5	350	x						n.s.
1762	DMWD	dystrophia myotonica, WD repeat containing	350							230
1959	EGR2	early growth response 2	350		x					487
2055	CLN8	ceroid-lipofuscinosis, neuronal 8 (epilepsy, progressive with mental retardation)	350	x						0
2733	GLE1	GLE1 RNA export mediator homolog (yeast)	350		x					66
3236	HOXD10	homeobox D10	350		x					6
6726	SRP9	signal recognition particle 9kDa	350							3
6792	CDKL5	cyclin-dependent kinase-like 5	350		x					n.s.
7070	THY1	Thy-1 cell surface antigen	350							0
9938	ARHGAP25	Rho GTPase activating protein 25	350							4
10010	TANK	TRAF family member-associated NFKB activator	350							n.s.
26580	BSCL2	Berardinelli-Seip congenital lipodystrophy 2 (seipin)	350		x					9
54982	CLN6	ceroid-lipofuscinosis, neuronal 6, late infantile, variant	350		x					2
79628	SH3TC2	SH3 domain and tetratricopeptide repeats 2	350		x					n.s.
81846	SBF2	SET binding factor 2	350		x					n.s.

GeneID	Gene Symbol	Gene name	Score	ND gene	Other disease gene	Pred. Risk factor	Drug target	Modulators of NDPs	Aggregation-prone	Interactions found
114798	SLITRK1	SLIT and NTRK-like family, member 1	350		x					0
161742	SPRED1	sprouty-related, EVH1 domain containing 1	350		x					465
256471	MFSD8	major facilitator superfamily domain containing 8	350		x					n.s.
493856	CISD2	CDGSH iron sulfur domain 2	350		x					5
6487	ST3GAL3	ST3 beta-galactoside alpha-2,3-sialyltransferase 3	348.6							2
11076	TPPP	tubulin polymerization promoting protein	348.6							2
1795	DOCK3	dedicator of cytokinesis 3	348.4							n.s.
2332	FMR1	fragile X mental retardation 1	348.2	x						13
7447	VSNL1	visinin-like 1	347.9							n.s.
3326	HSP90AB1	heat shock protein 90kDa alpha (cytosolic), class B member 1	347.7				x		x	1
8843	GPR109B	hydroxycarboxylic acid receptor 3	347.5				x			n.s.
10	NAT2	N-acetyltransferase 2 (arylamine N-acetyltransferase)	347.3							n.s.
5265	SERPINA1	serpin peptidase inhibitor, clade A (alpha-1 antiproteinase, antitrypsin), member 1	347		x		x			1
5052	PRDX1	peroxiredoxin 1	346.7							2
10059	DNM1L	dynamin 1-like	346.1						x	4
10694	CCT8	chaperonin containing TCP1, subunit 8 (theta)	346.1						x	7
4318	MMP9	matrix metallopeptidase 9 (gelatinase B, 92kDa gelatinase, 92kDa type IV collagenase)	344.5		x		x			0
4537	ND3	NADH dehydrogenase subunit 3	344.4	x						n.s.
6898	TAT	tyrosine aminotransferase	344.2		x		x			n.s.
7428	VHL	von Hippel-Lindau tumor	343.5		x					87

GeneID	Gene Symbol	Gene name	Score	ND gene	Other disease gene	Pred. Risk factor	Drug target	Modulators of NDPs	Aggregation-prone	Interactions found
		suppressor								
185	AGTR1	angiotensin II receptor, type 1	342		x		x			3
1936	EEF1D	eukaryotic translation elongation factor 1 delta (guanine nucleotide exchange protein)	341.6						x	15
2157	F8	coagulation factor VIII, procoagulant component	341.6				x			2
2147	F2	coagulation factor II (thrombin)	341.5				x			1
3043	HBB	hemoglobin, beta	341.5		x					2
135138	PACRG	PARK2 co-regulated	341.2							0
4694	NDUFA1	NADH dehydrogenase (ubiquinone) 1 alpha subcomplex, 1, 7.5kDa	341		x		x			0
3162	HMOX1	heme oxygenase (decycling) 1	340.8				x			n.s.
667	DST	dystonin	340.5							n.s.
29993	PACSIN1	protein kinase C and casein kinase substrate in neurons 1	340.5							5
4790	NFKB1	nuclear factor of kappa light polypeptide gene enhancer in B-cells 1	339.8				x			n.s.
3839	KPNA3	karyopherin alpha 3 (importin alpha 4)	339.6							n.s.
1520	CTSS	cathepsin S	339.4				x			0
5154	PDGFA	platelet-derived growth factor alpha polypeptide	339.1							n.s.
4023	LPL	lipoprotein lipase	337.8		x		x			12
3304	HSPA1B	heat shock 70kDa protein 1B	336.9					x		n.s.
4704	NDUFA9	NADH dehydrogenase (ubiquinone) 1 alpha subcomplex, 9, 39kDa	336.5				x		x	0
4719	NDUFS1	NADH dehydrogenase (ubiquinone) Fe-S protein 1, 75kDa (NADH-coenzyme Q reductase)	336.5		x		x		x	16

GeneID	Gene Symbol	Gene name	Score	ND gene	Other disease gene	Pred. Risk factor	Drug target	Modulators of NDPs	Aggregation-prone	Interactions found
4722	NDUFS3	NADH dehydrogenase (ubiquinone) Fe-S protein 3, 30kDa (NADH-coenzyme Q reductase)	336.5	x			x		x	5
5471	PPAT	phosphoribosyl pyrophosphate amidotransferase	335				x			n.s.
183	AGT	angiotensinogen (serpin peptidase inhibitor, clade A, member 8)	334.8		x		x			11
6135	RPL11	ribosomal protein L11	334.8		x			x		0
3818	KLKB1	kallikrein B, plasma (Fletcher factor) 1	334.6		x					12
10576	CCT2	chaperonin containing TCP1, subunit 2 (beta)	334.2					x	x	7
3376	IARS	isoleucyl-tRNA synthetase	333.7				x		x	n.s.
9510	ADAMTS1	ADAM metallopeptidase with thrombospondin type 1 motif, 1	333.7							1
9249	DHRS3	dehydrogenase/reductase (SDR family) member 3	333.6				x			0
7409	VAV1	vav 1 guanine nucleotide exchange factor	332.6							0
1537	CYC1	cytochrome c-1	332.5							3
1759	DNM1	dynamin 1	332.5						x	n.s.
7385	UQCRC2	ubiquinol-cytochrome c reductase core protein II	332.5					x		4
10524	KAT5	K(lysine) acetyltransferase 5	332.3							122
1999	ELF3	E74-like factor 3 (ets domain transcription factor, epithelial-specific)	332.1							n.s.
3105	HLA-A	major histocompatibility complex, class I, A	332							22
4233	MET	met proto-oncogene (hepatocyte growth factor receptor)	332		x		x			1
338	APOB	apolipoprotein B (including Ag(x) antigen)	331.9		x		x			n.s.

GeneID	Gene Symbol	Gene name	Score	ND gene	Other disease gene	Pred. Risk factor	Drug target	Modulators of NDPs	Aggregation-prone	Interactions found
506	ATP5B	ATP synthase, H+ transporting, mitochondrial F1 complex, beta polypeptide	331.2					x	x	n.s.
25942	SIN3A	SIN3 transcription regulator homolog A (yeast)	331.2					x		n.s.
5479	PPIB	peptidylprolyl isomerase B (cyclophilin B)	330.6		x		x			12
161	AP2A2	adaptor-related protein complex 2, alpha 2 subunit	330.5					x		1
7532	YWHAG	tyrosine 3-monooxygenase/tryptophan 5-monooxygenase activation protein, gamma polypeptide	330.4							124
3316	HSPB2	heat shock 27kDa protein 2	330.1							n.s.
2746	GLUD1	glutamate dehydrogenase 1	330		x		x		x	n.s.
4502	MT2A	metallothionein 2A	329.9							n.s.
26578	OSTF1	osteoclast stimulating factor 1	329.9							n.s.
2260	FGFR1	fibroblast growth factor receptor 1	329.4		x		x			2
5478	PPIA	peptidylprolyl isomerase A (cyclophilin A)	329.4				x		x	25
2335	FN1	fibronectin 1	329.1		x		x			n.s.
9869	SETDB1	SET domain, bifurcated 1	329							124
6572	SLC18A3	solute carrier family 18 (vesicular acetylcholine), member 3	328.7							n.s.
7051	TGM1	transglutaminase 1 (K polypeptide epidermal type I, protein-glutamine-gamma-glutamyltransferase)	328.7		x		x			0
3383	ICAM1	intercellular adhesion molecule 1	328.6				x			2
55885	LMO3	LIM domain only 3 (rhombotin-like 2)	328.4							124

GeneID	Gene Symbol	Gene name	Score	ND gene	Other disease gene	Pred. Risk factor	Drug target	Modulators of NDPs	Aggregation-prone	Interactions found
5578	PRKCA	protein kinase C, alpha	328.2				x			70
51588	PIAS4	protein inhibitor of activated STAT, 4	327.8							33
4552	MTRR	5-methyltetrahydrofolate-homocysteine methyltransferase reductase	327.6		x		x			n.s.
51606	ATP6V1H	ATPase, H+ transporting, lysosomal 50/57kDa, V1 subunit H	327.4					x	x	1
5126	PCSK2	proprotein convertase subtilisin/kexin type 2	327.3				x			1
3912	LAMB1	laminin, beta 1	327.2				x			n.s.
4514	COX3	cytochrome c oxidase subunit III	327							n.s.
8659	ALDH4A1	aldehyde dehydrogenase 4 family, member A1	326.6		x		x			2
5824	PEX19	peroxisomal biogenesis factor 19	326.5	x						n.s.
7166	TPH1	tryptophan hydroxylase 1	326.1				x			3
6667	SP1	Sp1 transcription factor	325.3							5
7533	YWHAH	tyrosine 3-monooxygenase/tryptophan 5-monooxygenase activation protein, eta polypeptide	325.3							n.s.
9531	BAG3	BCL2-associated athanogene 3	325.3		x					7
4144	MAT2A	methionine adenosyltransferase II, alpha	325				x	x	x	18
1508	CTSB	cathepsin B	324.5				x			1
793	CALB1	calbindin 1, 28kDa	324.4							1
7436	VLDLR	very low density lipoprotein receptor	324.1						x	n.s.
5315	PKM2	pyruvate kinase, muscle	323.5				x	x	x	2
2316	FLNA	filamin A, alpha	323.1		x			x		40
2262	GPC5	glypican 5	323					x		4
3690	ITGB3	integrin, beta 3 (platelet glycoprotein IIIa, antigen CD61)	322.9		x		x			n.s.
1915	EEF1A1	eukaryotic translation elongation factor 1 alpha 1	322.8						x	2

GeneID	Gene Symbol	Gene name	Score	ND gene	Other disease gene	Pred. Risk factor	Drug target	Modulators of NDPs	Aggregation-prone	Interactions found
5340	PLG	plasminogen	322.8		x		x			2
6189	RPS3A	ribosomal protein S3A	322.8					x	x	2
1213	CLTC	clathrin, heavy chain (Hc)	322.7					x	x	n.s.
8502	PKP4	plakophilin 4	321.9							n.s.
1462	VCAN	versican	321.6		x					0
10519	CIB1	calcium and integrin binding 1 (calmyrin)	321.6							n.s.
4087	SMAD2	SMAD family member 2	321.3							n.s.
4089	SMAD4	SMAD family member 4	319.6		x					n.s.
384	ARG2	arginase, type II	319.4				x			1
8287	USP9Y	ubiquitin specific peptidase 9, Y-linked	319.4		x					n.s.
9322	TRIP10	thyroid hormone receptor interactor 10	319.4							n.s.
156	ADRBK1	adrenergic, beta, receptor kinase 1	319.1				x			3
4513	COX2	cytochrome c oxidase subunit II	318.7							n.s.
3915	LAMC1	laminin, gamma 1 (formerly LAMB2)	318.6				x		x	9
54541	DDIT4	DNA-damage-inducible transcript 4	318.3							10
6329	SCN4A	sodium channel, voltage-gated, type IV, alpha subunit	317.5		x		x			n.s.
5747	PTK2	PTK2 protein tyrosine kinase 2	317.2				x	x		n.s.
55791	C1orf103	ligand dependent nuclear receptor interacting factor 1	317							7
10971	YWHAQ	tyrosine 3-monooxygenase/tryptophan 5-monooxygenase activation protein, theta polypeptide	316.8							n.s.
148	ADRA1A	adrenergic, alpha-1A-, receptor	316.4				x			n.s.

GeneID	Gene Symbol	Gene name	Score	ND gene	Other disease gene	Pred. Risk factor	Drug target	Modulators of NDPs	Aggregation-prone	Interactions found
3689	ITGB2	integrin, beta 2 (complement component 3 receptor 3 and 4 subunit)	316.3		x		x			3
136227	EMID2	EMI domain containing 2	315.7							34
8764	TNFRSF14	tumor necrosis factor receptor superfamily, member 14	314.3							1
3728	JUP	junction plakoglobin	314.1		x					n.s.
50848	F11R	F11 receptor	313.8							4
633	BGN	biglycan	313.6							5
515	ATP5F1	ATP synthase, H+ transporting, mitochondrial Fo complex, subunit B1	313.6					x		5
6628	SNRPB	small nuclear ribonucleoprotein polypeptides B and B1	313.6					x		6
6422	SFRP1	secreted frizzled-related protein 1	313.5							n.s.
4036	LRP2	low density lipoprotein receptor-related protein 2	313.4		x		x			n.s.
9546	APBA3	amyloid beta (A4) precursor protein-binding, family A, member 3	313.3							n.s.
114928	GPRASP2	G protein-coupled receptor associated sorting protein 2	313.3							n.s.
7087	ICAM5	intercellular adhesion molecule 5, telencephalin	311.9							26
4851	NOTCH1	notch 1	311.4		x					n.s.
5595	MAPK3	mitogen-activated protein kinase 3	311.2				x			7
7381	UQCRB	ubiquinol-cytochrome c reductase binding protein	311		x			x		11
7917	BAT3	BCL2-associated athanogene 6	310.7					x		118
6774	STAT3	signal transducer and activator of transcription 3 (acute-phase response factor)	310.6		x					n.s.
10049	DNAJB6	DnaJ (Hsp40) homolog, subfamily B, member 6	310.6					x		68

GeneID	Gene Symbol	Gene name	Score	ND gene	Other disease gene	Pred. Risk factor	Drug target	Modulators of NDPs	Aggregation-prone	Interactions found
1329	COX5B	cytochrome c oxidase subunit Vb	310							n.s.
1642	DDB1	damage-specific DNA binding protein 1, 127kDa	310							n.s.
1810	DR1	down-regulator of transcription 1, TBP-binding (negative cofactor 2)	310							71
2959	GTF2B	general transcription factor IIB	310							43
4045	LSAMP	limbic system-associated membrane protein	310							16
4978	OPCML	opioid binding protein/cell adhesion molecule-like	310		x					n.s.
7704	ZBTB16	zinc finger and BTB domain containing 16	310		x					n.s.
7802	DNALI1	dynein, axonemal, light intermediate chain 1	310					x		74
8462	KLF11	Kruppel-like factor 11	310		x			x		251
9330	GTF3C3	general transcription factor IIIC, polypeptide 3, 102kDa	310							66
9818	NUPL1	nucleoporin like 1	310							106
10540	DCTN2	dynactin 2 (p50)	310							1
11331	PHB2	prohibitin 2	310						x	3

5.2 Interactions of identified connecting proteins with neurodegenerative disease proteins (NDPs)

Connecting protein	NDP	Type of NDP	Disease
APP	APP	Wild-type and K670N/M671L	AD
APP	Presenilin 1	Wild-type and A431E	AD
APP	Presenilin 2	Wild-type	AD
APP	Dynactin 1	Wild-type	ALS

Connecting protein	NDP	Type of NDP	Disease
APP	α-synuclein	Wild-type and A30P	PD
APP	Parkin	Wild-type	PD
APP	UCHL1	Wild-type	PD
APP	DJ-1	Wild-type	PD
APP	PINK1	Wild-type	PD
APP	Huntingtin	Wild-type and Q49	HD
APP	Ataxin-1	Wild-type and Q79	SCA1
IQSEC1	APP	Wild-type and K670N/M671L	AD
IQSEC1	Presenilin 1	Wild-type and A431E	AD
IQSEC1	TDP-43	Wild-type, Q331K and M337V	ALS
IQSEC1	SOD1	Wild-type, A4V, G85R and G93A	ALS
IQSEC1	Alsin	Wild-type	ALS
IQSEC1	α-synuclein	Wild-type, A30P and E46K	PD
IQSEC1	Parkin	Wild-type and Q311Stop	PD
IQSEC1	DJ-1	Wild-type	PD
IQSEC1	PINK1	Wild-type	PD
IQSEC1	UCHL1	Wild-type	PD
IQSEC1	Huntingtin	Wild-type, Q49, Q51 and Q68	HD
IQSEC1	Ataxin-1	Wild-type and Q79	SCA1
ZNF179	APP	Wild-type and K670N/M671L	AD
ZNF179	Presenilin 1	Wild-type and A431E	AD
ZNF179	TDP-43	Wild-type, Q331K and M337V	ALS
ZNF179	SOD1	Wild-type, A4V, G85R and G93A	ALS
ZNF179	Dynactin 1	Wild-type	ALS
ZNF179	Optineurin	Wild-type	ALS

Connecting protein	NDP	Type of NDP	Disease
ZNF179	α-synuclein	Wild-type, A30P and E46K	PD
ZNF179	Parkin	Wild-type and Q311Stop	PD
ZNF179	DJ-1	Wild-type	PD
ZNF179	UCHL1	Wild-type	PD
ZNF179	Huntingtin	Wild-type, Q49, Q51, Q68 and Q79	HD
ZNF179	Ataxin-1	Wild-type and Q79	SCA1
ZMAT2	Presenilin 1	Wild-type and A431E	AD
ZMAT2	SOD1	Wild-type, A4V, G85R and G93A	ALS
ZMAT2	α-synuclein	Wild-type, A30P and E46K	PD
ZMAT2	Huntingtin	Wild-type, Q49, Q51 and Q79	HD
ZMAT2	Ataxin-1	Wild-type and Q79	SCA1

6 Bibliography

1. Martin JB (1999): **Molecular basis of the neurodegenerative disorders**. *N Engl J Med*, **340**(25):1970-1980.
2. Ince PG, Highley JR, Kirby J, Wharton SB, Takahashi H, Strong MJ, Shaw PJ (2011): **Molecular pathology and genetic advances in amyotrophic lateral sclerosis: an emerging molecular pathway and the significance of glial pathology**. *Acta Neuropathol*, **122**(6):657-671.
3. Martin I, Dawson VL, Dawson TM (2011): **Recent advances in the genetics of Parkinson's disease**. *Annu Rev Genomics Hum Genet*, **12**:301-325.
4. Matilla-Duenas A, Corral-Juan M, Volpini V, Sanchez I (2012): **The spinocerebellar ataxias: clinical aspects and molecular genetics**. *Adv Exp Med Biol*, **724**:351-374.
5. Orr HT, Zoghbi HY (2007): **Trinucleotide repeat disorders**. *Annu Rev Neurosci*, **30**:575-621.
6. Selkoe DJ (1998): **The cell biology of beta-amyloid precursor protein and presenilin in Alzheimer's disease**. *Trends Cell Biol*, **8**(11):447-453.
7. Selkoe DJ (2001): **Alzheimer's disease: genes, proteins, and therapy**. *Physiol Rev*, **81**(2):741-766.
8. Moore DJ, West AB, Dawson VL, Dawson TM (2005): **Molecular pathophysiology of Parkinson's disease**. *Annu Rev Neurosci*, **28**:57-87.
9. Thomas B, Beal MF (2007): **Parkinson's disease**. *Hum Mol Genet*, **16 Spec No. 2**:R183-194.
10. Carrell RW, Lomas DA (1997): **Conformational disease**. *Lancet*, **350**(9071):134-138.
11. Dobson CM (1999): **Protein misfolding, evolution and disease**. *Trends Biochem Sci*, **24**(9):329-332.
12. Soto C (2001): **Protein misfolding and disease; protein refolding and therapy**. *FEBS Lett*, **498**(2-3):204-207.
13. Duyao M, Ambrose C, Myers R, Novelletto A, Persichetti F, Frontali M, Folstein S, Ross C, Franz M, Abbott M, et al. (1993): **Trinucleotide repeat length instability and age of onset in Huntington's disease**. *Nat Genet*, **4**(4):387-392.
14. Kruger R, Kuhn W, Muller T, Woitalla D, Graeber M, Kosel S, Przuntek H, Epplen JT, Schols L, Riess O (1998): **Ala30Pro mutation in the gene encoding alpha-synuclein in Parkinson's disease**. *Nat Genet*, **18**(2):106-108.
15. Sreedharan J, Blair IP, Tripathi VB, Hu X, Vance C, Rogelj B, Ackerley S, Durnall JC, Williams KL, Buratti E, Baralle F, de Belleroche J, Mitchell JD, Leigh PN, Al-Chalabi A, Miller CC, Nicholson G, Shaw CE (2008): **TDP-43 mutations in familial and sporadic amyotrophic lateral sclerosis**. *Science*, **319**(5870):1668-1672.
16. Ibanez P, Bonnet AM, Debarges B, Lohmann E, Tison F, Pollak P, Agid Y, Durr A, Brice A (2004): **Causal relation between alpha-synuclein gene duplication and familial Parkinson's disease**. *Lancet*, **364**(9440):1169-1171.
17. Ross CA, Poirier MA (2005): **Opinion: What is the role of protein aggregation in neurodegeneration?** *Nat Rev Mol Cell Biol*, **6**(11):891-898.
18. Wong PC, Cai H, Borchelt DR, Price DL (2002): **Genetically engineered mouse models of neurodegenerative diseases**. *Nat Neurosci*, **5**(7):633-639.
19. Furukawa Y, Kaneko K, Watanabe S, Yamanaka K, Nukina N (2011): **A seeding reaction recapitulates intracellular formation of Sarkosyl-insoluble transactivation re-**

sponse element (TAR) DNA-binding protein-43 inclusions. *J Biol Chem*, **286**(21):18664-18672.

20. Jarrett JT, Berger EP, Lansbury PT, Jr. (1993): **The carboxy terminus of the beta amyloid protein is critical for the seeding of amyloid formation: implications for the pathogenesis of Alzheimer's disease**. *Biochemistry*, **32**(18):4693-4697.

21. Jarrett JT, Lansbury PT, Jr. (1993): **Seeding "one-dimensional crystallization" of amyloid: a pathogenic mechanism in Alzheimer's disease and scrapie?** *Cell*, **73**(6):1055-1058.

22. Clarke G, Collins RA, Leavitt BR, Andrews DF, Hayden MR, Lumsden CJ, McInnes RR (2000): **A one-hit model of cell death in inherited neuronal degenerations**. *Nature*, **406**(6792):195-199.

23. Eigen M (1996): **Prionics or the kinetic basis of prion diseases**. *Biophys Chem*, **63**(1):A1-18.

24. Perutz MF, Windle AH (2001): **Cause of neural death in neurodegenerative diseases attributable to expansion of glutamine repeats**. *Nature*, **412**(6843):143-144.

25. Gutekunst CA, Li SH, Yi H, Mulroy JS, Kuemmerle S, Jones R, Rye D, Ferrante RJ, Hersch SM, Li XJ (1999): **Nuclear and neuropil aggregates in Huntington's disease: relationship to neuropathology**. *J Neurosci*, **19**(7):2522-2534.

26. Kuemmerle S, Gutekunst CA, Klein AM, Li XJ, Li SH, Beal MF, Hersch SM, Ferrante RJ (1999): **Huntington aggregates may not predict neuronal death in Huntington's disease**. *Ann Neurol*, **46**(6):842-849.

27. Terry RD, Masliah E, Salmon DP, Butters N, DeTeresa R, Hill R, Hansen LA, Katzman R (1991): **Physical basis of cognitive alterations in Alzheimer's disease: synapse loss is the major correlate of cognitive impairment**. *Ann Neurol*, **30**(4):572-580.

28. Tompkins MM, Hill WD (1997): **Contribution of somal Lewy bodies to neuronal death**. *Brain Res*, **775**(1-2):24-29.

29. Keller JN, Dimayuga E, Chen Q, Thorpe J, Gee J, Ding Q (2004): **Autophagy, proteasomes, lipofuscin, and oxidative stress in the aging brain**. *Int J Biochem Cell Biol*, **36**(12):2376-2391.

30. Takahashi T, Kikuchi S, Katada S, Nagai Y, Nishizawa M, Onodera O (2008): **Soluble polyglutamine oligomers formed prior to inclusion body formation are cytotoxic**. *Hum Mol Genet*, **17**(3):345-356.

31. Arima K, Hirai S, Sunohara N, Aoto K, Izumiyama Y, Ueda K, Ikeda K, Kawai M (1999): **Cellular co-localization of phosphorylated tau- and NACP/alpha-synuclein-epitopes in lewy bodies in sporadic Parkinson's disease and in dementia with Lewy bodies**. *Brain Res*, **843**(1-2):53-61.

32. Delacourte A, Defossez A (1986): **Alzheimer's disease: Tau proteins, the promoting factors of microtubule assembly, are major components of paired helical filaments**. *J Neurol Sci*, **76**(2-3):173-186.

33. Lippa CF, Zhukareva V, Kawarai T, Uryu K, Shafiq M, Nee LE, Grafman J, Liang Y, St George-Hyslop PH, Trojanowski JQ, Lee VM (2000): **Frontotemporal dementia with novel tau pathology and a Glu342Val tau mutation**. *Ann Neurol*, **48**(6):850-858.

34. Wood JG, Mirra SS, Pollock NJ, Binder LI (1986): **Neurofibrillary tangles of Alzheimer disease share antigenic determinants with the axonal microtubule-associated protein tau (tau)**. *Proc Natl Acad Sci U S A*, **83**(11):4040-4043.

35. Baba M, Nakajo S, Tu PH, Tomita T, Nakaya K, Lee VM, Trojanowski JQ, Iwatsubo T (1998): **Aggregation of alpha-synuclein in Lewy bodies of sporadic Parkinson's disease and dementia with Lewy bodies**. *Am J Pathol*, **152**(4):879-884.

36. Yoshimoto M, Iwai A, Kang D, Otero DA, Xia Y, Saitoh T (1995): **NACP, the precursor protein of the non-amyloid beta/A4 protein (A beta) component of Alzheimer disease amyloid, binds A beta and stimulates A beta aggregation**. *Proc Natl Acad Sci U S A*, **92**(20):9141-9145.

37. Arai T, Hasegawa M, Akiyama H, Ikeda K, Nonaka T, Mori H, Mann D, Tsuchiya K, Yoshida M, Hashizume Y, Oda T (2006): **TDP-43 is a component of ubiquitin-positive tau-negative inclusions in frontotemporal lobar degeneration and amyotrophic lateral sclerosis**. *Biochem Biophys Res Commun*, **351**(3):602-611.

38. Neumann M, Sampathu DM, Kwong LK, Truax AC, Micsenyi MC, Chou TT, Bruce J, Schuck T, Grossman M, Clark CM, McCluskey LF, Miller BL, Masliah E, Mackenzie IR, Feldman H, Feiden W, Kretzschmar HA, Trojanowski JQ, Lee VM (2006): **Ubiquitinated TDP-43 in frontotemporal lobar degeneration and amyotrophic lateral sclerosis**. *Science*, **314**(5796):130-133.

39. Amador-Ortiz C, Lin WL, Ahmed Z, Personett D, Davies P, Duara R, Graff-Radford NR, Hutton ML, Dickson DW (2007): **TDP-43 immunoreactivity in hippocampal sclerosis and Alzheimer's disease**. *Ann Neurol*, **61**(5):435-445.

40. Nakashima-Yasuda H, Uryu K, Robinson J, Xie SX, Hurtig H, Duda JE, Arnold SE, Siderowf A, Grossman M, Leverenz JB, Woltjer R, Lopez OL, Hamilton R, Tsuang DW, Galasko D, Masliah E, Kaye J, Clark CM, Montine TJ, Lee VM, Trojanowski JQ (2007): **Co-morbidity of TDP-43 proteinopathy in Lewy body related diseases**. *Acta Neuropathol*, **114**(3):221-229.

41. Schwab C, Arai T, Hasegawa M, Yu S, McGeer PL (2008): **Colocalization of transactivation-responsive DNA-binding protein 43 and huntingtin in inclusions of Huntington disease**. *J Neuropathol Exp Neurol*, **67**(12):1159-1165.

42. Tan CF, Yamada M, Toyoshima Y, Yokoseki A, Miki Y, Hoshi Y, Kaneko H, Ikeuchi T, Onodera O, Kakita A, Takahashi H (2009): **Selective occurrence of TDP-43-immunoreactive inclusions in the lower motor neurons in Machado-Joseph disease**. *Acta Neuropathol*, **118**(4):553-560.

43. Danial NN, Korsmeyer SJ (2004): **Cell death: critical control points**. *Cell*, **116**(2):205-219.

44. Andreyev AY, Kushnareva YE, Starkov AA (2005): **Mitochondrial metabolism of reactive oxygen species**. *Biochemistry (Mosc)*, **70**(2):200-214.

45. Nunomura A, Perry G, Aliev G, Hirai K, Takeda A, Balraj EK, Jones PK, Ghanbari H, Wataya T, Shimohama S, Chiba S, Atwood CS, Petersen RB, Smith MA (2001): **Oxidative damage is the earliest event in Alzheimer disease**. *J Neuropathol Exp Neurol*, **60**(8):759-767.

46. Ohyagi Y, Yamada T, Nishioka K, Clarke NJ, Tomlinson AJ, Naylor S, Nakabeppu Y, Kira J, Younkin SG (2000): **Selective increase in cellular A beta 42 is related to apoptosis but not necrosis**. *Neuroreport*, **11**(1):167-171.

47. Lovell MA, Xiong S, Xie C, Davies P, Markesbery WR (2004): **Induction of hyperphosphorylated tau in primary rat cortical neuron cultures mediated by oxidative stress and glycogen synthase kinase-3**. *J Alzheimers Dis*, **6**(6):659-671; discussion 673-681.

48. Tamagno E, Parola M, Bardini P, Piccini A, Borghi R, Guglielmotto M, Santoro G, Davit A, Danni O, Smith MA, Perry G, Tabaton M (2005): **Beta-site APP cleaving enzyme up-regulation induced by 4-hydroxynonenal is mediated by stress-activated protein kinases pathways**. *J Neurochem*, **92**(3):628-636.

49. Lustbader JW, Cirilli M, Lin C, Xu HW, Takuma K, Wang N, Caspersen C, Chen X, Pollak S, Chaney M, Trinchese F, Liu S, Gunn-Moore F, Lue LF, Walker DG, Kuppusamy P,

Zewier ZL, Arancio O, Stern D, Yan SS, Wu H (2004): **ABAD directly links Abeta to mitochondrial toxicity in Alzheimer's disease**. *Science*, **304**(5669):448-452.

50. Hansson CA, Frykman S, Farmery MR, Tjernberg LO, Nilsberth C, Pursglove SE, Ito A, Winblad B, Cowburn RF, Thyberg J, Ankarcrona M (2004): **Nicastrin, presenilin, APH-1, and PEN-2 form active gamma-secretase complexes in mitochondria**. *J Biol Chem*, **279**(49):51654-51660.

51. Martin LJ, Pan Y, Price AC, Sterling W, Copeland NG, Jenkins NA, Price DL, Lee MK (2006): **Parkinson's disease alpha-synuclein transgenic mice develop neuronal mitochondrial degeneration and cell death**. *J Neurosci*, **26**(1):41-50.

52. Song DD, Shults CW, Sisk A, Rockenstein E, Masliah E (2004): **Enhanced substantia nigra mitochondrial pathology in human alpha-synuclein transgenic mice after treatment with MPTP**. *Exp Neurol*, **186**(2):158-172.

53. Darios F, Corti O, Lucking CB, Hampe C, Muriel MP, Abbas N, Gu WJ, Hirsch EC, Rooney T, Ruberg M, Brice A (2003): **Parkin prevents mitochondrial swelling and cytochrome c release in mitochondria-dependent cell death**. *Hum Mol Genet*, **12**(5):517-526.

54. Vives-Bauza C, Zhou C, Huang Y, Cui M, de Vries RL, Kim J, May J, Tocilescu MA, Liu W, Ko HS, Magrane J, Moore DJ, Dawson VL, Grailhe R, Dawson TM, Li C, Tieu K, Przedborski S (2010): **PINK1-dependent recruitment of Parkin to mitochondria in mitophagy**. *Proc Natl Acad Sci U S A*, **107**(1):378-383.

55. Lin MT, Beal MF (2006): **Mitochondrial dysfunction and oxidative stress in neurodegenerative diseases**. *Nature*, **443**(7113):787-795.

56. Pasinelli P, Belford ME, Lennon N, Bacskai BJ, Hyman BT, Trotti D, Brown RH, Jr. (2004): **Amyotrophic lateral sclerosis-associated SOD1 mutant proteins bind and aggregate with Bcl-2 in spinal cord mitochondria**. *Neuron*, **43**(1):19-30.

57. Kong J, Xu Z (1998): **Massive mitochondrial degeneration in motor neurons triggers the onset of amyotrophic lateral sclerosis in mice expressing a mutant SOD1**. *J Neurosci*, **18**(9):3241-3250.

58. Mattiazzi M, D'Aurelio M, Gajewski CD, Martushova K, Kiaei M, Beal MF, Manfredi G (2002): **Mutated human SOD1 causes dysfunction of oxidative phosphorylation in mitochondria of transgenic mice**. *J Biol Chem*, **277**(33):29626-29633.

59. Jenkins BG, Koroshetz WJ, Beal MF, Rosen BR (1993): **Evidence for impairment of energy metabolism in vivo in Huntington's disease using localized 1H NMR spectroscopy**. *Neurology*, **43**(12):2689-2695.

60. Gu M, Gash MT, Mann VM, Javoy-Agid F, Cooper JM, Schapira AH (1996): **Mitochondrial defect in Huntington's disease caudate nucleus**. *Ann Neurol*, **39**(3):385-389.

61. Choo YS, Johnson GV, MacDonald M, Detloff PJ, Lesort M (2004): **Mutant huntingtin directly increases susceptibility of mitochondria to the calcium-induced permeability transition and cytochrome c release**. *Hum Mol Genet*, **13**(14):1407-1420.

62. Bae BI, Xu H, Igarashi S, Fujimuro M, Agrawal N, Taya Y, Hayward SD, Moran TH, Montell C, Ross CA, Snyder SH, Sawa A (2005): **p53 mediates cellular dysfunction and behavioral abnormalities in Huntington's disease**. *Neuron*, **47**(1):29-41.

63. Chipuk JE, Kuwana T, Bouchier-Hayes L, Droin NM, Newmeyer DD, Schuler M, Green DR (2004): **Direct activation of Bax by p53 mediates mitochondrial membrane permeabilization and apoptosis**. *Science*, **303**(5660):1010-1014.

64. Douglas PM, Dillin A (2010): **Protein homeostasis and aging in neurodegeneration**. *J Cell Biol*, **190**(5):719-729.

65. Balch WE, Morimoto RI, Dillin A, Kelly JW (2008): **Adapting proteostasis for disease intervention**. *Science*, **319**(5865):916-919.

66. Muchowski PJ, Wacker JL (2005): **Modulation of neurodegeneration by molecular chaperones**. *Nat Rev Neurosci*, **6**(1):11-22.

67. Barral JM, Broadley SA, Schaffar G, Hartl FU (2004): **Roles of molecular chaperones in protein misfolding diseases**. *Semin Cell Dev Biol*, **15**(1):17-29.

68. Fonte V, Kipp DR, Yerg J, 3rd, Merin D, Forrestal M, Wagner E, Roberts CM, Link CD (2008): **Suppression of in vivo beta-amyloid peptide toxicity by overexpression of the HSP-16.2 small chaperone protein**. *J Biol Chem*, **283**(2):784-791.

69. Fujimoto M, Takaki E, Hayashi T, Kitaura Y, Tanaka Y, Inouye S, Nakai A (2005): **Active HSF1 significantly suppresses polyglutamine aggregate formation in cellular and mouse models**. *J Biol Chem*, **280**(41):34908-34916.

70. Outeiro TF, Klucken J, Strathearn KE, Liu F, Nguyen P, Rochet JC, Hyman BT, McLean PJ (2006): **Small heat shock proteins protect against alpha-synuclein-induced toxicity and aggregation**. *Biochem Biophys Res Commun*, **351**(3):631-638.

71. Chai Y, Koppenhafer SL, Bonini NM, Paulson HL (1999): **Analysis of the role of heat shock protein (Hsp) molecular chaperones in polyglutamine disease**. *J Neurosci*, **19**(23):10338-10347.

72. McLean PJ, Kawamata H, Shariff S, Hewett J, Sharma N, Ueda K, Breakefield XO, Hyman BT (2002): **TorsinA and heat shock proteins act as molecular chaperones: suppression of alpha-synuclein aggregation**. *J Neurochem*, **83**(4):846-854.

73. Watanabe M, Dykes-Hoberg M, Culotta VC, Price DL, Wong PC, Rothstein JD (2001): **Histological evidence of protein aggregation in mutant SOD1 transgenic mice and in amyotrophic lateral sclerosis neural tissues**. *Neurobiol Dis*, **8**(6):933-941.

74. Wilhelmus MM, Otte-Holler I, Wesseling P, de Waal RM, Boelens WC, Verbeek MM (2006): **Specific association of small heat shock proteins with the pathological hallmarks of Alzheimer's disease brains**. *Neuropathol Appl Neurobiol*, **32**(2):119-130.

75. Olzscha H, Schermann SM, Woerner AC, Pinkert S, Hecht MH, Tartaglia GG, Vendruscolo M, Hayer-Hartl M, Hartl FU, Vabulas RM (2011): **Amyloid-like aggregates sequester numerous metastable proteins with essential cellular functions**. *Cell*, **144**(1):67-78.

76. Chung KK, Zhang Y, Lim KL, Tanaka Y, Huang H, Gao J, Ross CA, Dawson VL, Dawson TM (2001): **Parkin ubiquitinates the alpha-synuclein-interacting protein, synphilin-1: implications for Lewy-body formation in Parkinson disease**. *Nat Med*, **7**(10):1144-1150.

77. Ciechanover A (2005): **Proteolysis: from the lysosome to ubiquitin and the proteasome**. *Nat Rev Mol Cell Biol*, **6**(1):79-87.

78. Pickart CM (2001): **Mechanisms underlying ubiquitination**. *Annu Rev Biochem*, **70**:503-533.

79. Pickart CM, Cohen RE (2004): **Proteasomes and their kin: proteases in the machine age**. *Nat Rev Mol Cell Biol*, **5**(3):177-187.

80. Ciechanover A (1998): **The ubiquitin-proteasome pathway: on protein death and cell life**. *Embo J*, **17**(24):7151-7160.

81. Ciechanover A, Schwartz AL (1998): **The ubiquitin-proteasome pathway: the complexity and myriad functions of proteins death**. *Proc Natl Acad Sci U S A*, **95**(6):2727-2730.

82. Koegl M, Hoppe T, Schlenker S, Ulrich HD, Mayer TU, Jentsch S (1999): **A novel ubiquitination factor, E4, is involved in multiubiquitin chain assembly**. *Cell*, **96**(5):635-644.

83. Cole GM, Timiras PS (1987): **Ubiquitin-protein conjugates in Alzheimer's lesions**. *Neurosci Lett*, **79**(1-2):207-212.

84. Kuzuhara S, Mori H, Izumiyama N, Yoshimura M, Ihara Y (1988): **Lewy bodies are ubiquitinated. A light and electron microscopic immunocytochemical study**. *Acta Neuropathol*, **75**(4):345-353.

85. Wang J, Wang CE, Orr A, Tydlacka S, Li SH, Li XJ (2008): **Impaired ubiquitin-proteasome system activity in the synapses of Huntington's disease mice**. *J Cell Biol*, **180**(6):1177-1189.

86. Kamp F, Exner N, Lutz AK, Wender N, Hegermann J, Brunner B, Nuscher B, Bartels T, Giese A, Beyer K, Eimer S, Winklhofer KF, Haass C (2010): **Inhibition of mitochondrial fusion by alpha-synuclein is rescued by PINK1, Parkin and DJ-1**. *Embo J*, **29**(20):3571-3589.

87. Rosen KM, Moussa CE, Lee HK, Kumar P, Kitada T, Qin G, Fu Q, Querfurth HW (2010): **Parkin reverses intracellular beta-amyloid accumulation and its negative effects on proteasome function**. *J Neurosci Res*, **88**(1):167-178.

88. Jana NR, Dikshit P, Goswami A, Kotliarova S, Murata S, Tanaka K, Nukina N (2005): **Co-chaperone CHIP associates with expanded polyglutamine protein and promotes their degradation by proteasomes**. *J Biol Chem*, **280**(12):11635-11640.

89. Miller VM, Nelson RF, Gouvion CM, Williams A, Rodriguez-Lebron E, Harper SQ, Davidson BL, Rebagliati MR, Paulson HL (2005): **CHIP suppresses polyglutamine aggregation and toxicity in vitro and in vivo**. *J Neurosci*, **25**(40):9152-9161.

90. Hatakeyama S, Matsumoto M, Kamura T, Murayama M, Chui DH, Planel E, Takahashi R, Nakayama KI, Takashima A (2004): **U-box protein carboxyl terminus of Hsc70-interacting protein (CHIP) mediates poly-ubiquitylation preferentially on four-repeat Tau and is involved in neurodegeneration of tauopathy**. *J Neurochem*, **91**(2):299-307.

91. Urushitani M, Kurisu J, Tateno M, Hatakeyama S, Nakayama K, Kato S, Takahashi R (2004): **CHIP promotes proteasomal degradation of familial ALS-linked mutant SOD1 by ubiquitinating Hsp/Hsc70**. *J Neurochem*, **90**(1):231-244.

92. Shin Y, Klucken J, Patterson C, Hyman BT, McLean PJ (2005): **The co-chaperone carboxyl terminus of Hsp70-interacting protein (CHIP) mediates alpha-synuclein degradation decisions between proteasomal and lysosomal pathways**. *J Biol Chem*, **280**(25):23727-23734.

93. Bennett EJ, Bence NF, Jayakumar R, Kopito RR (2005): **Global impairment of the ubiquitin-proteasome system by nuclear or cytoplasmic protein aggregates precedes inclusion body formation**. *Mol Cell*, **17**(3):351-365.

94. Gregori L, Fuchs C, Figueiredo-Pereira ME, Van Nostrand WE, Goldgaber D (1995): **Amyloid beta-protein inhibits ubiquitin-dependent protein degradation in vitro**. *J Biol Chem*, **270**(34):19702-19708.

95. Cheung ZH, Ip NY (2011): **Autophagy deregulation in neurodegenerative diseases - recent advances and future perspectives**. *J Neurochem*, **118**(3):317-325.

96. Ravikumar B, Vacher C, Berger Z, Davies JE, Luo S, Oroz LG, Scaravilli F, Easton DF, Duden R, O'Kane CJ, Rubinsztein DC (2004): **Inhibition of mTOR induces autophagy and reduces toxicity of polyglutamine expansions in fly and mouse models of Huntington disease**. *Nat Genet*, **36**(6):585-595.

97. Tain LS, Mortiboys H, Tao RN, Ziviani E, Bandmann O, Whitworth AJ (2009): **Rapamycin activation of 4E-BP prevents parkinsonian dopaminergic neuron loss**. *Nat Neurosci*, **12**(9):1129-1135.

98. Martinez-Vicente M, Talloczy Z, Wong E, Tang G, Koga H, Kaushik S, de Vries R, Arias E, Harris S, Sulzer D, Cuervo AM (2010): **Cargo recognition failure is responsible for inefficient autophagy in Huntington's disease**. *Nat Neurosci*, **13**(5):567-576.

99. Li X, Wang CE, Huang S, Xu X, Li XJ, Li H, Li S (2010): **Inhibiting the ubiquitin-proteasome system leads to preferential accumulation of toxic N-terminal mutant huntingtin fragments**. *Hum Mol Genet*, **19**(12):2445-2455.

100. Nixon RA, Wegiel J, Kumar A, Yu WH, Peterhoff C, Cataldo A, Cuervo AM (2005): **Extensive involvement of autophagy in Alzheimer disease: an immuno-electron microscopy study**. *J Neuropathol Exp Neurol*, **64**(2):113-122.

101. Yu WH, Cuervo AM, Kumar A, Peterhoff CM, Schmidt SD, Lee JH, Mohan PS, Mercken M, Farmery MR, Tjernberg LO, Jiang Y, Duff K, Uchiyama Y, Naslund J, Mathews PM, Cataldo AM, Nixon RA (2005): **Macroautophagy--a novel Beta-amyloid peptide-generating pathway activated in Alzheimer's disease**. *J Cell Biol*, **171**(1):87-98.

102. Hung SY, Huang WP, Liou HC, Fu WM (2009): **Autophagy protects neuron from Abeta-induced cytotoxicity**. *Autophagy*, **5**(4):502-510.

103. Wang H, Ma J, Tan Y, Wang Z, Sheng C, Chen S, Ding J (2010): **Amyloid-beta1-42 induces reactive oxygen species-mediated autophagic cell death in U87 and SH-SY5Y cells**. *J Alzheimers Dis*, **21**(2):597-610.

104. Nixon RA (2007): **Autophagy, amyloidogenesis and Alzheimer disease**. *J Cell Sci*, **120**(Pt 23):4081-4091.

105. Boland B, Kumar A, Lee S, Platt FM, Wegiel J, Yu WH, Nixon RA (2008): **Autophagy induction and autophagosome clearance in neurons: relationship to autophagic pathology in Alzheimer's disease**. *J Neurosci*, **28**(27):6926-6937.

106. Vogiatzi T, Xilouri M, Vekrellis K, Stefanis L (2008): **Wild type alpha-synuclein is degraded by chaperone-mediated autophagy and macroautophagy in neuronal cells**. *J Biol Chem*, **283**(35):23542-23556.

107. Webb JL, Ravikumar B, Atkins J, Skepper JN, Rubinsztein DC (2003): **Alpha-Synuclein is degraded by both autophagy and the proteasome**. *J Biol Chem*, **278**(27):25009-25013.

108. Cuervo AM, Stefanis L, Fredenburg R, Lansbury PT, Sulzer D (2004): **Impaired degradation of mutant alpha-synuclein by chaperone-mediated autophagy**. *Science*, **305**(5688):1292-1295.

109. Xilouri M, Vogiatzi T, Vekrellis K, Park D, Stefanis L (2009): **Abberant alpha-synuclein confers toxicity to neurons in part through inhibition of chaperone-mediated autophagy**. *PLoS One*, **4**(5):e5515.

110. Winslow AR, Chen CW, Corrochano S, Acevedo-Arozena A, Gordon DE, Peden AA, Lichtenberg M, Menzies FM, Ravikumar B, Imarisio S, Brown S, O'Kane CJ, Rubinsztein DC (2010): **alpha-Synuclein impairs macroautophagy: implications for Parkinson's disease**. *J Cell Biol*, **190**(6):1023-1037.

111. Banerjee R, Beal MF, Thomas B (2010): **Autophagy in neurodegenerative disorders: pathogenic roles and therapeutic implications**. *Trends Neurosci*, **33**(12):541-549.

112. Zhang X, Li L, Chen S, Yang D, Wang Y, Zhang X, Wang Z, Le W (2011): **Rapamycin treatment augments motor neuron degeneration in SOD1(G93A) mouse model of amyotrophic lateral sclerosis**. *Autophagy*, **7**(4):412-425.

113. Zhang F, Strom AL, Fukada K, Lee S, Hayward LJ, Zhu H (2007): **Interaction between familial amyotrophic lateral sclerosis (ALS)-linked SOD1 mutants and the dynein complex**. *J Biol Chem*, **282**(22):16691-16699.

114. Bose JK, Huang CC, Shen CK (2011): **Regulation of autophagy by neuropathological protein TDP-43**. *J Biol Chem*, **286**(52):44441-44448.

115. Zhang H, Ma Q, Zhang YW, Xu H (2012): **Proteolytic processing of Alzheimer's beta-amyloid precursor protein**. *J Neurochem*, **120 Suppl 1**:9-21.

116. Campion D, Flaman JM, Brice A, Hannequin D, Dubois B, Martin C, Moreau V, Charbonnier F, Didierjean O, Tardieu S, et al. (1995): **Mutations of the presenilin I gene in families with early-onset Alzheimer's disease**. *Hum Mol Genet*, **4**(12):2373-2377.

117. Levy-Lahad E, Wasco W, Poorkaj P, Romano DM, Oshima J, Pettingell WH, Yu CE, Jondro PD, Schmidt SD, Wang K, et al. (1995): **Candidate gene for the chromosome 1 familial Alzheimer's disease locus**. *Science*, **269**(5226):973-977.

118. Mullan M, Crawford F, Axelman K, Houlden H, Lilius L, Winblad B, Lannfelt L (1992): **A pathogenic mutation for probable Alzheimer's disease in the APP gene at the N-terminus of beta-amyloid**. *Nat Genet*, **1**(5):345-347.

119. Rogaev EI, Sherrington R, Rogaeva EA, Levesque G, Ikeda M, Liang Y, Chi H, Lin C, Holman K, Tsuda T, et al. (1995): **Familial Alzheimer's disease in kindreds with missense mutations in a gene on chromosome 1 related to the Alzheimer's disease type 3 gene**. *Nature*, **376**(6543):775-778.

120. Masters CL, Simms G, Weinman NA, Multhaup G, McDonald BL, Beyreuther K (1985): **Amyloid plaque core protein in Alzheimer disease and Down syndrome**. *Proc Natl Acad Sci U S A*, **82**(12):4245-4249.

121. Buee L, Bussiere T, Buee-Scherrer V, Delacourte A, Hof PR (2000): **Tau protein isoforms, phosphorylation and role in neurodegenerative disorders**. *Brain Res Brain Res Rev*, **33**(1):95-130.

122. Markesbery WR (1997): **Oxidative stress hypothesis in Alzheimer's disease**. *Free Radic Biol Med*, **23**(1):134-147.

123. Rozemuller JM, Eikelenboom P, Stam FC (1986): **Role of microglia in plaque formation in senile dementia of the Alzheimer type. An immunohistochemical study**. *Virchows Arch B Cell Pathol Incl Mol Pathol*, **51**(3):247-254.

124. Wyss-Coray T (2006): **Inflammation in Alzheimer disease: driving force, bystander or beneficial response?** *Nat Med*, **12**(9):1005-1015.

125. LaFerla FM, Green KN, Oddo S (2007): **Intracellular amyloid-beta in Alzheimer's disease**. *Nat Rev Neurosci*, **8**(7):499-509.

126. Allinson TM, Parkin ET, Turner AJ, Hooper NM (2003): **ADAMs family members as amyloid precursor protein alpha-secretases**. *J Neurosci Res*, **74**(3):342-352.

127. Vassar R, Bennett BD, Babu-Khan S, Kahn S, Mendiaz EA, Denis P, Teplow DB, Ross S, Amarante P, Loeloff R, Luo Y, Fisher S, Fuller J, Edenson S, Lile J, Jarosinski MA, Biere AL, Curran E, Burgess T, Louis JC, Collins F, Treanor J, Rogers G, Citron M (1999): **Beta-secretase cleavage of Alzheimer's amyloid precursor protein by the transmembrane aspartic protease BACE**. *Science*, **286**(5440):735-741.

128. Kojro E, Fahrenholz F (2005): **The non-amyloidogenic pathway: structure and function of alpha-secretases**. *Subcell Biochem*, **38**:105-127.

129. Haass C, Selkoe DJ (1993): **Cellular processing of beta-amyloid precursor protein and the genesis of amyloid beta-peptide**. *Cell*, **75**(6):1039-1042.

130. O'Brien RJ, Wong PC (2011): **Amyloid precursor protein processing and Alzheimer's disease**. *Annu Rev Neurosci*, **34**:185-204.

131. Iwatsubo T, Odaka A, Suzuki N, Mizusawa H, Nukina N, Ihara Y (1994): **Visualization of A beta 42(43) and A beta 40 in senile plaques with end-specific A beta monoclonals: evidence that an initially deposited species is A beta 42(43)**. *Neuron*, **13**(1):45-53.

132. Avila J, Lucas JJ, Perez M, Hernandez F (2004): **Role of tau protein in both physiological and pathological conditions**. *Physiol Rev*, **84**(2):361-384.

133. Ittner LM, Gotz J (2011): **Amyloid-beta and tau--a toxic pas de deux in Alzheimer's disease**. *Nat Rev Neurosci*, **12**(2):65-72.

134. Vossel KA, Zhang K, Brodbeck J, Daub AC, Sharma P, Finkbeiner S, Cui B, Mucke L (2010): **Tau reduction prevents Abeta-induced defects in axonal transport**. *Science*, **330**(6001):198.

135. Amadoro G, Corsetti V, Atlante A, Florenzano F, Capsoni S, Bussani R, Mercanti D, Calissano P (2011): **Interaction between NH(2)-tau fragment and Abeta in Alzheimer's disease mitochondria contributes to the synaptic deterioration**. *Neurobiol Aging*, **33**(4):833 e831-825.

136. Atlante A, Amadoro G, Bobba A, de Bari L, Corsetti V, Pappalardo G, Marra E, Calissano P, Passarella S (2008): **A peptide containing residues 26-44 of tau protein impairs mitochondrial oxidative phosphorylation acting at the level of the adenine nucleotide translocator**. *Biochim Biophys Acta*, **1777**(10):1289-1300.

137. Garwood CJ, Pooler AM, Atherton J, Hanger DP, Noble W (2011): **Astrocytes are important mediators of Abeta-induced neurotoxicity and tau phosphorylation in primary culture**. *Cell Death Dis*, **2**:e167.

138. Melov S, Adlard PA, Morten K, Johnson F, Golden TR, Hinerfeld D, Schilling B, Mavros C, Masters CL, Volitakis I, Li QX, Laughton K, Hubbard A, Cherny RA, Gibson B, Bush AI (2007): **Mitochondrial oxidative stress causes hyperphosphorylation of tau**. *PLoS One*, **2**(6):e536.

139. Su B, Wang X, Lee HG, Tabaton M, Perry G, Smith MA, Zhu X (2010): **Chronic oxidative stress causes increased tau phosphorylation in M17 neuroblastoma cells**. *Neurosci Lett*, **468**(3):267-271.

140. Hernandez F, Avila J (2008): **The role of glycogen synthase kinase 3 in the early stages of Alzheimers' disease**. *FEBS Lett*, **582**(28):3848-3854.

141. Lee MS, Kwon YT, Li M, Peng J, Friedlander RM, Tsai LH (2000): **Neurotoxicity induces cleavage of p35 to p25 by calpain**. *Nature*, **405**(6784):360-364.

142. Cho JH, Johnson GV (2004): **Glycogen synthase kinase 3 beta induces caspase-cleaved tau aggregation in situ**. *J Biol Chem*, **279**(52):54716-54723.

143. Chung CW, Song YH, Kim IK, Yoon WJ, Ryu BR, Jo DG, Woo HN, Kwon YK, Kim HH, Gwag BJ, Mook-Jung IH, Jung YK (2001): **Proapoptotic effects of tau cleavage product generated by caspase-3**. *Neurobiol Dis*, **8**(1):162-172.

144. Oddo S, Caccamo A, Kitazawa M, Tseng BP, LaFerla FM (2003): **Amyloid deposition precedes tangle formation in a triple transgenic model of Alzheimer's disease**. *Neurobiol Aging*, **24**(8):1063-1070.

145. Oddo S, Vasilevko V, Caccamo A, Kitazawa M, Cribbs DH, LaFerla FM (2006): **Reduction of soluble Abeta and tau, but not soluble Abeta alone, ameliorates cognitive decline in transgenic mice with plaques and tangles**. *J Biol Chem*, **281**(51):39413-39423.

146. Roberson ED, Scearce-Levie K, Palop JJ, Yan F, Cheng IH, Wu T, Gerstein H, Yu GQ, Mucke L (2007): **Reducing endogenous tau ameliorates amyloid beta-induced deficits in an Alzheimer's disease mouse model**. *Science*, **316**(5825):750-754.

147. Mitchell JD, Borasio GD (2007): **Amyotrophic lateral sclerosis**. *Lancet*, **369**(9578):2031-2041.

148. Lillo P, Hodges JR (2009): **Frontotemporal dementia and motor neurone disease: overlapping clinic-pathological disorders**. *J Clin Neurosci*, **16**(9):1131-1135.

149. Geser F, Martinez-Lage M, Kwong LK, Lee VM, Trojanowski JQ (2009): **Amyotrophic lateral sclerosis, frontotemporal dementia and beyond: the TDP-43 diseases**. *J Neurol*, **256**(8):1205-1214.

150. Kwiatkowski TJ, Jr., Bosco DA, Leclerc AL, Tamrazian E, Vanderburg CR, Russ C, Davis A, Gilchrist J, Kasarskis EJ, Munsat T, Valdmanis P, Rouleau GA, Hosler BA, Cortelli P, de Jong PJ, Yoshinaga Y, Haines JL, Pericak-Vance MA, Yan J, Ticozzi N, Siddique T, McKenna-Yasek D, Sapp PC, Horvitz HR, Landers JE, Brown RH, Jr. (2009): **Mutations in the FUS/TLS gene on chromosome 16 cause familial amyotrophic lateral sclerosis**. *Science*, **323**(5918):1205-1208.

151. Mackenzie IR, Bigio EH, Ince PG, Geser F, Neumann M, Cairns NJ, Kwong LK, Forman MS, Ravits J, Stewart H, Eisen A, McClusky L, Kretzschmar HA, Monoranu CM, Highley JR, Kirby J, Siddique T, Shaw PJ, Lee VM, Trojanowski JQ (2007): **Pathological TDP-43 distinguishes sporadic amyotrophic lateral sclerosis from amyotrophic lateral sclerosis with SOD1 mutations**. *Ann Neurol*, **61**(5):427-434.

152. Maruyama H, Morino H, Ito H, Izumi Y, Kato H, Watanabe Y, Kinoshita Y, Kamada M, Nodera H, Suzuki H, Komure O, Matsuura S, Kobatake K, Morimoto N, Abe K, Suzuki N, Aoki M, Kawata A, Hirai T, Kato T, Ogasawara K, Hirano A, Takumi T, Kusaka H, Hagiwara K, Kaji R, Kawakami H (2010): **Mutations of optineurin in amyotrophic lateral sclerosis**. *Nature*, **465**(7295):223-226.

153. Vance C, Rogelj B, Hortobagyi T, De Vos KJ, Nishimura AL, Sreedharan J, Hu X, Smith B, Ruddy D, Wright P, Ganesalingam J, Williams KL, Tripathi V, Al-Saraj S, Al-Chalabi A, Leigh PN, Blair IP, Nicholson G, de Belleroche J, Gallo JM, Miller CC, Shaw CE (2009): **Mutations in FUS, an RNA processing protein, cause familial amyotrophic lateral sclerosis type 6**. *Science*, **323**(5918):1208-1211.

154. Fiesel FC, Kahle PJ (2011): **TDP-43 and FUS/TLS: cellular functions and implications for neurodegeneration**. *Febs J*, **278**(19):3550-3568.

155. Stallings NR, Puttaparthi K, Luther CM, Burns DK, Elliott JL (2010): **Progressive motor weakness in transgenic mice expressing human TDP-43**. *Neurobiol Dis*, **40**(2):404-414.

156. Voigt A, Herholz D, Fiesel FC, Kaur K, Muller D, Karsten P, Weber SS, Kahle PJ, Marquardt T, Schulz JB (2010): **TDP-43-mediated neuron loss in vivo requires RNA-binding activity**. *PLoS One*, **5**(8):e12247.

157. Lagier-Tourenne C, Polymenidou M, Cleveland DW (2010): **TDP-43 and FUS/TLS: emerging roles in RNA processing and neurodegeneration**. *Hum Mol Genet*, **19**(R1):R46-64.

158. Inukai Y, Nonaka T, Arai T, Yoshida M, Hashizume Y, Beach TG, Buratti E, Baralle FE, Akiyama H, Hisanaga S, Hasegawa M (2008): **Abnormal phosphorylation of Ser409/410 of TDP-43 in FTLD-U and ALS**. *FEBS Lett*, **582**(19):2899-2904.

159. Neumann M, Kwong LK, Lee EB, Kremmer E, Flatley A, Xu Y, Forman MS, Troost D, Kretzschmar HA, Trojanowski JQ, Lee VM (2009): **Phosphorylation of S409/410 of TDP-43 is a consistent feature in all sporadic and familial forms of TDP-43 proteinopathies**. *Acta Neuropathol*, **117**(2):137-149.

160. Zhang YJ, Xu YF, Dickey CA, Buratti E, Baralle F, Bailey R, Pickering-Brown S, Dickson D, Petrucelli L (2007): **Progranulin mediates caspase-dependent cleavage of TAR DNA binding protein-43**. *J Neurosci*, **27**(39):10530-10534.

161. Polymenidou M, Lagier-Tourenne C, Hutt KR, Huelga SC, Moran J, Liang TY, Ling SC, Sun E, Wancewicz E, Mazur C, Kordasiewicz H, Sedaghat Y, Donohue JP, Shiue L, Bennett CF, Yeo GW, Cleveland DW (2011): **Long pre-mRNA depletion and RNA missplicing contribute to neuronal vulnerability from loss of TDP-43**. *Nat Neurosci*, **14**(4):459-468.

162. Sephton CF, Cenik C, Kucukural A, Dammer EB, Cenik B, Han Y, Dewey CM, Roth FP, Herz J, Peng J, Moore MJ, Yu G (2010): **Identification of neuronal RNA targets of TDP-43-containing ribonucleoprotein complexes**. *J Biol Chem*, **286**(2):1204-1215.

163. Tollervey JR, Curk T, Rogelj B, Briese M, Cereda M, Kayikci M, Konig J, Hortobagyi T, Nishimura AL, Zupunski V, Patani R, Chandran S, Rot G, Zupan B, Shaw CE, Ule J (2011): **Characterizing the RNA targets and position-dependent splicing regulation by TDP-43**. *Nat Neurosci*, **14**(4):452-458.

164. Ayala YM, De Conti L, Avendano-Vazquez SE, Dhir A, Romano M, D'Ambrogio A, Tollervey J, Ule J, Baralle M, Buratti E, Baralle FE (2010): **TDP-43 regulates its mRNA levels through a negative feedback loop**. *Embo J*, **30**(2):277-288.

165. Nishimoto I, Okamoto T, Matsuura Y, Takahashi S, Okamoto T, Murayama Y, Ogata E (1993): **Alzheimer amyloid protein precursor complexes with brain GTP-binding protein G(o)**. *Nature*, **362**(6415):75-79.

166. Fiore F, Zambrano N, Minopoli G, Donini V, Duilio A, Russo T (1995): **The regions of the Fe65 protein homologous to the phosphotyrosine interaction/phosphotyrosine binding domain of Shc bind the intracellular domain of the Alzheimer's amyloid precursor protein**. *J Biol Chem*, **270**(52):30853-30856.

167. Borg JP, Ooi J, Levy E, Margolis B (1996): **The phosphotyrosine interaction domains of X11 and FE65 bind to distinct sites on the YENPTY motif of amyloid precursor protein**. *Mol Cell Biol*, **16**(11):6229-6241.

168. Goehler H, Lalowski M, Stelzl U, Waelter S, Stroedicke M, Worm U, Droege A, Lindenberg KS, Knoblich M, Haenig C, Herbst M, Suopanki J, Scherzinger E, Abraham C, Bauer B, Hasenbank R, Fritzsche A, Ludewig AH, Bussow K, Coleman SH, Gutekunst CA, Landwehrmeyer BG, Lehrach H, Wanker EE (2004): **A protein interaction network links GIT1, an enhancer of huntingtin aggregation, to Huntington's disease**. *Mol Cell*, **15**(6):853-865.

169. Kaltenbach LS, Romero E, Becklin RR, Chettier R, Bell R, Phansalkar A, Strand A, Torcassi C, Savage J, Hurlburt A, Cha GH, Ukani L, Chepanoske CL, Zhen Y, Sahasrabudhe S, Olson J, Kurschner C, Ellerby LM, Peltier JM, Botas J, Hughes RE (2007): **Huntingtin interacting proteins are genetic modifiers of neurodegeneration**. *PLoS Genet*, **3**(5):e82.

170. Freibaum BD, Chitta RK, High AA, Taylor JP (2010): **Global analysis of TDP-43 interacting proteins reveals strong association with RNA splicing and translation machinery**. *J Proteome Res*, **9**(2):1104-1120.

171. Ling SC, Albuquerque CP, Han JS, Lagier-Tourenne C, Tokunaga S, Zhou H, Cleveland DW (2010): **ALS-associated mutations in TDP-43 increase its stability and promote TDP-43 complexes with FUS/TLS**. *Proc Natl Acad Sci U S A*, **107**(30):13318-13323.

172. Chen-Plotkin AS, Sadri-Vakili G, Yohrling GJ, Braveman MW, Benn CL, Glajch KE, DiRocco DP, Farrell LA, Krainc D, Gines S, MacDonald ME, Cha JH (2006): **Decreased association of the transcription factor Sp1 with genes downregulated in Huntington's disease**. *Neurobiol Dis*, **22**(2):233-241.

173. Dunah AW, Jeong H, Griffin A, Kim YM, Standaert DG, Hersch SM, Mouradian MM, Young AB, Tanese N, Krainc D (2002): **Sp1 and TAFII130 transcriptional activity disrupted in early Huntington's disease**. *Science*, **296**(5576):2238-2243.

174. Gauthier LR, Charrin BC, Borrell-Pages M, Dompierre JP, Rangone H, Cordelieres FP, De Mey J, MacDonald ME, Lessmann V, Humbert S, Saudou F (2004): **Huntingtin controls neurotrophic support and survival of neurons by enhancing BDNF vesicular transport along microtubules**. *Cell*, **118**(1):127-138.

175. Kegel KB, Meloni AR, Yi Y, Kim YJ, Doyle E, Cuiffo BG, Sapp E, Wang Y, Qin ZH, Chen JD, Nevins JR, Aronin N, DiFiglia M (2002): **Huntingtin is present in the nucleus, interacts with the transcriptional corepressor C-terminal binding protein, and represses transcription**. *J Biol Chem*, **277**(9):7466-7476.

176. Li SH, Cheng AL, Zhou H, Lam S, Rao M, Li H, Li XJ (2002): **Interaction of Huntington disease protein with transcriptional activator Sp1**. *Mol Cell Biol*, **22**(5):1277-1287.

177. Schaffar G, Breuer P, Boteva R, Behrends C, Tzvetkov N, Strippel N, Sakahira H, Siegers K, Hayer-Hartl M, Hartl FU (2004): **Cellular toxicity of polyglutamine expansion proteins: mechanism of transcription factor deactivation**. *Mol Cell*, **15**(1):95-105.

178. Zhai W, Jeong H, Cui L, Krainc D, Tjian R (2005): **In vitro analysis of huntingtin-mediated transcriptional repression reveals multiple transcription factor targets**. *Cell*, **123**(7):1241-1253.

179. Zuccato C, Tartari M, Crotti A, Goffredo D, Valenza M, Conti L, Cataudella T, Leavitt BR, Hayden MR, Timmusk T, Rigamonti D, Cattaneo E (2003): **Huntingtin interacts with REST/NRSF to modulate the transcription of NRSE-controlled neuronal genes**. *Nat Genet*, **35**(1):76-83.

180. Lam YC, Bowman AB, Jafar-Nejad P, Lim J, Richman R, Fryer JD, Hyun ED, Duvick LA, Orr HT, Botas J, Zoghbi HY (2006): **ATAXIN-1 interacts with the repressor Capicua in its native complex to cause SCA1 neuropathology**. *Cell*, **127**(7):1335-1347.

181. Lim J, Crespo-Barreto J, Jafar-Nejad P, Bowman AB, Richman R, Hill DE, Orr HT, Zoghbi HY (2008): **Opposing effects of polyglutamine expansion on native protein complexes contribute to SCA1**. *Nature*, **452**(7188):713-718.

182. Lim J, Hao T, Shaw C, Patel AJ, Szabo G, Rual JF, Fisk CJ, Li N, Smolyar A, Hill DE, Barabasi AL, Vidal M, Zoghbi HY (2006): **A protein-protein interaction network for human inherited ataxias and disorders of Purkinje cell degeneration**. *Cell*, **125**(4):801-814.

183. Soler-Lopez M, Zanzoni A, Lluis R, Stelzl U, Aloy P (2011): **Interactome mapping suggests new mechanistic details underlying Alzheimer's disease**. *Genome Res*, **21**(3):364-376.

184. Limviphuvadh V, Tanaka S, Goto S, Ueda K, Kanehisa M (2007): **The commonality of protein interaction networks determined in neurodegenerative disorders (NDDs)**. *Bioinformatics*, **23**(16):2129-2138.

185. Menon R, Farina C (2011): **Shared molecular and functional frameworks among five complex human disorders: a comparative study on interactomes linked to susceptibility genes**. *PLoS One*, **6**(4):e18660.

186. Freude S, Schilbach K, Schubert M (2009): **The role of IGF-1 receptor and insulin receptor signaling for the pathogenesis of Alzheimer's disease: from model organisms to human disease**. *Curr Alzheimer Res*, **6**(3):213-223.

187. Jolivalt CG, Hurford R, Lee CA, Dumaop W, Rockenstein E, Masliah E (2010): **Type 1 diabetes exaggerates features of Alzheimer's disease in APP transgenic mice**. *Exp Neurol*, **223**(2):422-431.

188. Kim B, Backus C, Oh S, Hayes JM, Feldman EL (2009): **Increased tau phosphorylation and cleavage in mouse models of type 1 and type 2 diabetes**. *Endocrinology*, **150**(12):5294-5301.

189. Chen JY, Shen C, Sivachenko AY (2006): **Mining Alzheimer disease relevant proteins from integrated protein interactome data**. *Pac Symp Biocomput*:367-378.

190. Stelzl U, Worm U, Lalowski M, Haenig C, Brembeck FH, Goehler H, Stroedicke M, Zenkner M, Schoenherr A, Koeppen S, Timm J, Mintzlaff S, Abraham C, Bock N, Kietzmann S, Goedde A, Toksoz E, Droege A, Krobitsch S, Korn B, Birchmeier W, Lehrach H, Wanker EE (2005): **A human protein-protein interaction network: a resource for annotating the proteome**. *Cell*, **122**(6):957-968.

191. Polymeropoulos MH, Lavedan C, Leroy E, Ide SE, Dehejia A, Dutra A, Pike B, Root H, Rubenstein J, Boyer R, Stenroos ES, Chandrasekharappa S, Athanassiadou A, Papapetropoulos T, Johnson WG, Lazzarini AM, Duvoisin RC, Di Iorio G, Golbe LI, Nussbaum RL (1997): **Mutation in the alpha-synuclein gene identified in families with Parkinson's disease**. *Science*, **276**(5321):2045-2047.

192. St George-Hyslop PH, Tanzi RE, Polinsky RJ, Haines JL, Nee L, Watkins PC, Myers RH, Feldman RG, Pollen D, Drachman D, et al. (1987): **The genetic defect causing familial Alzheimer's disease maps on chromosome 21**. *Science*, **235**(4791):885-890.

193. Tanzi RE, Gusella JF, Watkins PC, Bruns GA, St George-Hyslop P, Van Keuren ML, Patterson D, Pagan S, Kurnit DM, Neve RL (1987): **Amyloid beta protein gene: cDNA, mRNA distribution, and genetic linkage near the Alzheimer locus**. *Science*, **235**(4791):880-884.

194. (1993): **A novel gene containing a trinucleotide repeat that is expanded and unstable on Huntington's disease chromosomes. The Huntington's Disease Collaborative Research Group**. *Cell*, **72**(6):971-983.

195. Conway KA, Harper JD, Lansbury PT (1998): **Accelerated in vitro fibril formation by a mutant alpha-synuclein linked to early-onset Parkinson disease**. *Nat Med*, **4**(11):1318-1320.

196. Zarranz JJ, Alegre J, Gomez-Esteban JC, Lezcano E, Ros R, Ampuero I, Vidal L, Hoenicka J, Rodriguez O, Atares B, Llorens V, Gomez Tortosa E, del Ser T, Munoz DG, de Yebenes JG (2004): **The new mutation, E46K, of alpha-synuclein causes Parkinson and Lewy body dementia**. *Ann Neurol*, **55**(2):164-173.

197. Choi W, Zibaee S, Jakes R, Serpell LC, Davletov B, Crowther RA, Goedert M (2004): **Mutation E46K increases phospholipid binding and assembly into filaments of human alpha-synuclein**. *FEBS Lett*, **576**(3):363-368.

198. Greenbaum EA, Graves CL, Mishizen-Eberz AJ, Lupoli MA, Lynch DR, Englander SW, Axelsen PH, Giasson BI (2005): **The E46K mutation in alpha-synuclein increases amyloid fibril formation**. *J Biol Chem*, **280**(9):7800-7807.

199. Kitada T, Asakawa S, Hattori N, Matsumine H, Yamamura Y, Minoshima S, Yokochi M, Mizuno Y, Shimizu N (1998): **Mutations in the parkin gene cause autosomal recessive juvenile parkinsonism**. *Nature*, **392**(6676):605-608.

200. Hattori N, Matsumine H, Asakawa S, Kitada T, Yoshino H, Elibol B, Brookes AJ, Yamamura Y, Kobayashi T, Wang M, Yoritaka A, Minoshima S, Shimizu N, Mizuno Y (1998): **Point mutations (Thr240Arg and Gln311Stop) [correction of Thr240Arg and Ala311Stop] in the Parkin gene**. *Biochem Biophys Res Commun*, **249**(3):754-758.

201. Sriram SR, Li X, Ko HS, Chung KK, Wong E, Lim KL, Dawson VL, Dawson TM (2005): **Familial-associated mutations differentially disrupt the solubility, localization, binding and ubiquitination properties of parkin**. *Hum Mol Genet*, **14**(17):2571-2586.

202. Gandhi PN, Wang X, Zhu X, Chen SG, Wilson-Delfosse AL (2008): **The Roc domain of leucine-rich repeat kinase 2 is sufficient for interaction with microtubules**. *J Neurosci Res*, **86**(8):1711-1720.

203. Mata IF, Wedemeyer WJ, Farrer MJ, Taylor JP, Gallo KA (2006): **LRRK2 in Parkinson's disease: protein domains and functional insights**. *Trends Neurosci*, **29**(5):286-293.

204. Mata IF, Kachergus JM, Taylor JP, Lincoln S, Aasly J, Lynch T, Hulihan MM, Cobb SA, Wu RM, Lu CS, Lahoz C, Wszolek ZK, Farrer MJ (2005): **Lrrk2 pathogenic substitutions in Parkinson's disease**. *Neurogenetics*, **6**(4):171-177.

205. Tan EK, Zhao Y, Skipper L, Tan MG, Di Fonzo A, Sun L, Fook-Chong S, Tang S, Chua E, Yuen Y, Tan L, Pavanni R, Wong MC, Kolatkar P, Lu CS, Bonifati V, Liu JJ (2007): **The LRRK2 Gly2385Arg variant is associated with Parkinson's disease: genetic and functional evidence**. *Hum Genet*, **120**(6):857-863.

206. Banfi S, Servadio A, Chung MY, Kwiatkowski TJ, Jr., McCall AE, Duvick LA, Shen Y, Roth EJ, Orr HT, Zoghbi HY (1994): **Identification and characterization of the gene causing type 1 spinocerebellar ataxia**. *Nat Genet*, **7**(4):513-520.

207. Orr HT, Chung MY, Banfi S, Kwiatkowski TJ, Jr., Servadio A, Beaudet AL, McCall AE, Duvick LA, Ranum LP, Zoghbi HY (1993): **Expansion of an unstable trinucleotide CAG repeat in spinocerebellar ataxia type 1**. *Nat Genet*, **4**(3):221-226.

208. Kawaguchi Y, Okamoto T, Taniwaki M, Aizawa M, Inoue M, Katayama S, Kawakami H, Nakamura S, Nishimura M, Akiguchi I, et al. (1994): **CAG expansions in a novel gene for Machado-Joseph disease at chromosome 14q32.1**. *Nat Genet*, **8**(3):221-228.

209. Tsai HF, Tsai HJ, Hsieh M (2004): **Full-length expanded ataxin-3 enhances mitochondrial-mediated cell death and decreases Bcl-2 expression in human neuroblastoma cells**. *Biochem Biophys Res Commun*, **324**(4):1274-1282.

210. Johnson CD, Davidson BL (2010): **Huntington's disease: progress toward effective disease-modifying treatments and a cure**. *Hum Mol Genet*, **19**(R1):R98-R102.

211. Lajoie P, Snapp EL (2010): **Formation and toxicity of soluble polyglutamine oligomers in living cells**. *PLoS One*, **5**(12):e15245.

212. Deng HX, Hentati A, Tainer JA, Iqbal Z, Cayabyab A, Hung WY, Getzoff ED, Hu P, Herzfeldt B, Roos RP, et al. (1993): **Amyotrophic lateral sclerosis and structural defects in Cu,Zn superoxide dismutase**. *Science*, **261**(5124):1047-1051.

213. Rosen DR, Siddique T, Patterson D, Figlewicz DA, Sapp P, Hentati A, Donaldson D, Goto J, O'Regan JP, Deng HX, et al. (1993): **Mutations in Cu/Zn superoxide dismutase gene are associated with familial amyotrophic lateral sclerosis**. *Nature*, **362**(6415):59-62.

214. Rosen DR, Bowling AC, Patterson D, Usdin TB, Sapp P, Mezey E, McKenna-Yasek D, O'Regan J, Rahmani Z, Ferrante RJ, et al. (1994): **A frequent ala 4 to val superoxide dismutase-1 mutation is associated with a rapidly progressive familial amyotrophic lateral sclerosis**. *Hum Mol Genet*, **3**(6):981-987.

215. Bruijn LI, Becher MW, Lee MK, Anderson KL, Jenkins NA, Copeland NG, Sisodia SS, Rothstein JD, Borchelt DR, Price DL, Cleveland DW (1997): **ALS-linked SOD1 mutant G85R mediates damage to astrocytes and promotes rapidly progressive disease with SOD1-containing inclusions**. *Neuron*, **18**(2):327-338.

216. Bruijn LI, Houseweart MK, Kato S, Anderson KL, Anderson SD, Ohama E, Reaume AG, Scott RW, Cleveland DW (1998): **Aggregation and motor neuron toxicity of an ALS-linked SOD1 mutant independent from wild-type SOD1**. *Science*, **281**(5384):1851-1854.

217. Kostic V, Jackson-Lewis V, de Bilbao F, Dubois-Dauphin M, Przedborski S (1997): **Bcl-2: prolonging life in a transgenic mouse model of familial amyotrophic lateral sclerosis**. *Science*, **277**(5325):559-562.

218. Wiedau-Pazos M, Goto JJ, Rabizadeh S, Gralla EB, Roe JA, Lee MK, Valentine JS, Bredesen DE (1996): **Altered reactivity of superoxide dismutase in familial amyotrophic lateral sclerosis**. *Science*, **271**(5248):515-518.

219. Johnson BS, Snead D, Lee JJ, McCaffery JM, Shorter J, Gitler AD (2009): **TDP-43 is intrinsically aggregation-prone, and amyotrophic lateral sclerosis-linked mutations accelerate aggregation and increase toxicity**. *J Biol Chem*, **284**(30):20329-20339.

220. Huang C, Zhou H, Tong J, Chen H, Liu YJ, Wang D, Wei X, Xia XG (2011): **FUS transgenic rats develop the phenotypes of amyotrophic lateral sclerosis and frontotemporal lobar degeneration**. *PLoS Genet*, **7**(3):e1002011.

221. Yescas P, Huertas-Vazquez A, Villarreal-Molina MT, Rasmussen A, Tusie-Luna MT, Lopez M, Canizales-Quinteros S, Alonso ME (2006): **Founder effect for the Ala431Glu mutation of the presenilin 1 gene causing early-onset Alzheimer's disease in Mexican families**. *Neurogenetics*, **7**(3):195-200.

222. Murrell J, Ghetti B, Cochran E, Macias-Islas MA, Medina L, Varpetian A, Cummings JL, Mendez MF, Kawas C, Chui H, Ringman JM (2006): **The A431E mutation in PSEN1 causing familial Alzheimer's disease originating in Jalisco State, Mexico: an additional fifteen families**. *Neurogenetics*, **7**(4):277-279.

223. Citron M, Oltersdorf T, Haass C, McConlogue L, Hung AY, Seubert P, Vigo-Pelfrey C, Lieberburg I, Selkoe DJ (1992): **Mutation of the beta-amyloid precursor protein in familial Alzheimer's disease increases beta-protein production**. *Nature*, **360**(6405):672-674.

224. Citron M, Vigo-Pelfrey C, Teplow DB, Miller C, Schenk D, Johnston J, Winblad B, Venizelos N, Lannfelt L, Selkoe DJ (1994): **Excessive production of amyloid beta-protein by peripheral cells of symptomatic and presymptomatic patients carrying the Swedish familial Alzheimer disease mutation**. *Proc Natl Acad Sci U S A*, **91**(25):11993-11997.

225. Felsenstein KM, Hunihan LW, Roberts SB (1994): **Altered cleavage and secretion of a recombinant beta-APP bearing the Swedish familial Alzheimer's disease mutation**. *Nat Genet*, **6**(3):251-255.

226. Haass C, Lemere CA, Capell A, Citron M, Seubert P, Schenk D, Lannfelt L, Selkoe DJ (1995): **The Swedish mutation causes early-onset Alzheimer's disease by beta-secretase cleavage within the secretory pathway**. *Nat Med*, **1**(12):1291-1296.

227. Portelius E, Andreasson U, Ringman JM, Buerger K, Daborg J, Buchhave P, Hansson O, Harmsen A, Gustavsson MK, Hanse E, Galasko D, Hampel H, Blennow K, Zetterberg H (2010): **Distinct cerebrospinal fluid amyloid beta peptide signatures in sporadic and PSEN1 A431E-associated familial Alzheimer's disease**. *Mol Neurodegener*, **5**:2.

228. Van Criekinge W, Beyaert R (1999): **Yeast Two-Hybrid: State of the Art**. *Biol Proced Online*, **2**:1-38.

229. Assenov Y, Ramirez F, Schelhorn SE, Lengauer T, Albrecht M (2008): **Computing topological parameters of biological networks**. *Bioinformatics*, **24**(2):282-284.

230. Strogatz SH (2001): **Exploring complex networks**. *Nature*, **410**(6825):268-276.

231. Newman ME (2001): **The structure of scientific collaboration networks**. *Proc Natl Acad Sci U S A*, **98**(2):404-409.

232. Wagner A (2001): **The yeast protein interaction network evolves rapidly and contains few redundant duplicate genes**. *Mol Biol Evol*, **18**(7):1283-1292.

233. Barabasi AL, Oltvai ZN (2004): **Network biology: understanding the cell's functional organization**. *Nat Rev Genet*, **5**(2):101-113.

234. Albert R (2005): **Scale-free networks in cell biology**. *J Cell Sci*, **118**(Pt 21):4947-4957.

235. Ravasz E, Barabasi AL (2003): **Hierarchical organization in complex networks**. *Phys Rev E Stat Nonlin Soft Matter Phys*, **67**(2 Pt 2):026112.

236. Shannon P, Markiel A, Ozier O, Baliga NS, Wang JT, Ramage D, Amin N, Schwikowski B, Ideker T (2003): **Cytoscape: a software environment for integrated models of biomolecular interaction networks**. *Genome Res*, **13**(11):2498-2504.

237. Barrios-Rodiles M, Brown KR, Ozdamar B, Bose R, Liu Z, Donovan RS, Shinjo F, Liu Y, Dembowy J, Taylor IW, Luga V, Przulj N, Robinson M, Suzuki H, Hayashizaki Y, Jurisica I, Wrana JL (2005): **High-throughput mapping of a dynamic signaling network in mammalian cells**. *Science*, **307**(5715):1621-1625.

238. Palidwor GA, Shcherbinin S, Huska MR, Rasko T, Stelzl U, Arumughan A, Foulle R, Porras P, Sanchez-Pulido L, Wanker EE, Andrade-Navarro MA (2009): **Detection of alpha-rod protein repeats using a neural network and application to huntingtin**. *PLoS Comput Biol*, **5**(3):e1000304.

239. Braun P, Tasan M, Dreze M, Barrios-Rodiles M, Lemmens I, Yu H, Sahalie JM, Murray RR, Roncari L, de Smet AS, Venkatesan K, Rual JF, Vandenhaute J, Cusick ME, Pawson T, Hill DE, Tavernier J, Wrana JL, Roth FP, Vidal M (2009): **An experimentally derived confidence score for binary protein-protein interactions**. *Nat Methods*, **6**(1):91-97.

240. Venkatesan K, Rual JF, Vazquez A, Stelzl U, Lemmens I, Hirozane-Kishikawa T, Hao T, Zenkner M, Xin X, Goh KI, Yildirim MA, Simonis N, Heinzmann K, Gebreab F, Sahalie JM, Cevik S, Simon C, de Smet AS, Dann E, Smolyar A, Vinayagam A, Yu H, Szeto D, Borick H, Dricot A, Klitgord N, Murray RR, Lin C, Lalowski M, Timm J, Rau K, Boone C, Braun P, Cusick ME, Roth FP, Hill DE, Tavernier J, Wanker EE, Barabasi AL, Vidal M (2009): **An empirical framework for binary interactome mapping**. *Nat Methods*, **6**(1):83-90.

241. Boulay G, Rosnoblet C, Guerardel C, Angrand PO, Leprince D (2011): **Functional characterization of human Polycomb-like 3 isoforms identifies them as components of distinct EZH2 protein complexes**. *Biochem J*, **434**(2):333-342.

242. Uhlen M, Oksvold P, Fagerberg L, Lundberg E, Jonasson K, Forsberg M, Zwahlen M, Kampf C, Wester K, Hober S, Wernerus H, Bjorling L, Ponten F (2010): **Towards a knowledge-based Human Protein Atlas**. *Nat Biotechnol*, **28**(12):1248-1250.

243. Wolffe AP, Urnov FD, Guschin D (2000): **Co-repressor complexes and remodelling chromatin for repression**. *Biochem Soc Trans*, **28**(4):379-386.

244. Zhang Y, Ng HH, Erdjument-Bromage H, Tempst P, Bird A, Reinberg D (1999): **Analysis of the NuRD subunits reveals a histone deacetylase core complex and a connection with DNA methylation**. *Genes Dev*, **13**(15):1924-1935.

245. Priller C, Bauer T, Mitteregger G, Krebs B, Kretzschmar HA, Herms J (2006): **Synapse formation and function is modulated by the amyloid precursor protein**. *J Neurosci*, **26**(27):7212-7221.

246. Zheng H, Koo EH (2006): **The amyloid precursor protein: beyond amyloid**. *Mol Neurodegener*, **1**:5.

247. Someya A, Sata M, Takeda K, Pacheco-Rodriguez G, Ferrans VJ, Moss J, Vaughan M (2001): **ARF-GEP(100), a guanine nucleotide-exchange protein for ADP-ribosylation factor 6**. *Proc Natl Acad Sci U S A*, **98**(5):2413-2418.

248. Hiroi T, Someya A, Thompson W, Moss J, Vaughan M (2006): **GEP100/BRAG2: activator of ADP-ribosylation factor 6 for regulation of cell adhesion and actin cytoskeleton via E-cadherin and alpha-catenin**. *Proc Natl Acad Sci U S A*, **103**(28):10672-10677.

249. Seki N, Hattori A, Muramatsu M, Saito T (1999): **cDNA cloning of a human brain finger protein, BFP/ZNF179, a member of the RING finger protein family**. *DNA Res*, **6**(5):353-356.

250. Pao PC, Huang NK, Liu YW, Yeh SH, Lin ST, Hsieh CP, Huang AM, Huang HS, Tseng JT, Chang WC, Lee YC (2011): **A novel RING finger protein, Znf179, modulates cell cycle exit and neuronal differentiation of P19 embryonal carcinoma cells**. *Cell Death Differ*, **18**(11):1791-1804.

251. Huang X, Beullens M, Zhang J, Zhou Y, Nicolaescu E, Lesage B, Hu Q, Wu J, Bollen M, Shi Y (2009): **Structure and function of the two tandem WW domains of the pre-mRNA splicing factor FBP21 (formin-binding protein 21)**. *J Biol Chem*, **284**(37):25375-25387.

252. Muto Y, Pomeranz Krummel D, Oubridge C, Hernandez H, Robinson CV, Neuhaus D, Nagai K (2004): **The structure and biochemical properties of the human spliceosomal protein U1C**. *J Mol Biol*, **341**(1):185-198.

253. Hodges A, Strand AD, Aragaki AK, Kuhn A, Sengstag T, Hughes G, Elliston LA, Hartog C, Goldstein DR, Thu D, Hollingsworth ZR, Collin F, Synek B, Holmans PA, Young AB, Wexler NS, Delorenzi M, Kooperberg C, Augood SJ, Faull RL, Olson JM, Jones L, Luthi-Carter R (2006): **Regional and cellular gene expression changes in human Huntington's disease brain**. *Hum Mol Genet*, **15**(6):965-977.

254. Kupershmidt I, Su QJ, Grewal A, Sundaresh S, Halperin I, Flynn J, Shekar M, Wang H, Park J, Cui W, Wall GD, Wisotzkey R, Alag S, Akhtari S, Ronaghi M (2010): **Ontology-based meta-analysis of global collections of high-throughput public data**. *PLoS One*, **5**(9).

255. Liang WS, Reiman EM, Valla J, Dunckley T, Beach TG, Grover A, Niedzielko TL, Schneider LE, Mastroeni D, Caselli R, Kukull W, Morris JC, Hulette CM, Schmechel D, Rogers J, Stephan DA (2008): **Alzheimer's disease is associated with reduced expression of energy metabolism genes in posterior cingulate neurons**. *Proc Natl Acad Sci U S A*, **105**(11):4441-4446.

256. Moran LB, Duke DC, Deprez M, Dexter DT, Pearce RK, Graeber MB (2006): **Whole genome expression profiling of the medial and lateral substantia nigra in Parkinson's disease**. *Neurogenetics*, **7**(1):1-11.

257. Zhang Y, James M, Middleton FA, Davis RL (2005): **Transcriptional analysis of multiple brain regions in Parkinson's disease supports the involvement of specific protein processing, energy metabolism, and signaling pathways, and suggests novel disease mechanisms**. *Am J Med Genet B Neuropsychiatr Genet*, **137B**(1):5-16.

258. Zheng B, Liao Z, Locascio JJ, Lesniak KA, Roderick SS, Watt ML, Eklund AC, Zhang-James Y, Kim PD, Hauser MA, Grunblatt E, Moran LB, Mandel SA, Riederer P, Miller RM, Federoff HJ, Wullner U, Papapetropoulos S, Youdim MB, Cantuti-Castelvetri I, Young AB, Vance JM, Davis RL, Hedreen JC, Adler CH, Beach TG, Graeber MB, Middleton FA, Rochet JC, Scherzer CR (2010): **PGC-1alpha, a potential therapeutic target for early intervention in Parkinson's disease**. *Sci Transl Med*, **2**(52):52ra73.

259. Dewji NN, Do C, Bayney RM (1995): **Transcriptional activation of Alzheimer's beta-amyloid precursor protein gene by stress**. *Brain Res Mol Brain Res*, **33**(2):245-253.

260. Chartier-Harlin MC, Kachergus J, Roumier C, Mouroux V, Douay X, Lincoln S, Levecque C, Larvor L, Andrieux J, Hulihan M, Waucquier N, Defebvre L, Amouyel P, Farrer M, Destee A (2004): **Alpha-synuclein locus duplication as a cause of familial Parkinson's disease**. *Lancet*, **364**(9440):1167-1169.

261. Gregory JM, Barros TP, Meehan S, Dobson CM, Luheshi LM (2012): **The Aggregation and Neurotoxicity of TDP-43 and Its ALS-Associated 25 kDa Fragment Are Differentially Affected by Molecular Chaperones in Drosophila**. *PLoS One*, **7**(2):e31899.

262. Matilla-Duenas A, Goold R, Giunti P (2008): **Clinical, genetic, molecular, and pathophysiological insights into spinocerebellar ataxia type 1**. *Cerebellum*, **7**(2):106-114.

263. Wang CE, Tydlacka S, Orr AL, Yang SH, Graham RK, Hayden MR, Li S, Chan AW, Li XJ (2008): **Accumulation of N-terminal mutant huntingtin in mouse and monkey models implicated as a pathogenic mechanism in Huntington's disease**. *Hum Mol Genet*, **17**(17):2738-2751.

264. Gendron TF, Petrucelli L (2009): **The role of tau in neurodegeneration**. *Mol Neurodegener*, **4**:13.

265. Pauwels K, Williams TL, Morris KL, Jonckheere W, Vandersteen A, Kelly G, Schymkowitz J, Rousseau F, Pastore A, Serpell LC, Broersen K (2012): **Structural basis for increased toxicity of pathological abeta42:abeta40 ratios in Alzheimer disease**. *J Biol Chem*, **287**(8):5650-5660.

266. Gravina SA, Ho L, Eckman CB, Long KE, Otvos L, Jr., Younkin LH, Suzuki N, Younkin SG (1995): **Amyloid beta protein (A beta) in Alzheimer's disease brain. Biochemical and immunocytochemical analysis with antibodies specific for forms ending at A beta 40 or A beta 42(43)**. *J Biol Chem*, **270**(13):7013-7016.

267. Goedert M (1996): **Tau protein and the neurofibrillary pathology of Alzheimer's disease**. *Ann N Y Acad Sci*, **777**:121-131.

268. Porzig R, Singer D, Hoffmann R (2007): **Epitope mapping of mAbs AT8 and Tau5 directed against hyperphosphorylated regions of the human tau protein**. *Biochem Biophys Res Commun*, **358**(2):644-649.

269. Johnson BS, McCaffery JM, Lindquist S, Gitler AD (2008): **A yeast TDP-43 proteinopathy model: Exploring the molecular determinants of TDP-43 aggregation and cellular toxicity**. *Proc Natl Acad Sci U S A*, **105**(17):6439-6444.

270. Zhang YJ, Xu YF, Cook C, Gendron TF, Roettges P, Link CD, Lin WL, Tong J, Castanedes-Casey M, Ash P, Gass J, Rangachari V, Buratti E, Baralle F, Golde TE, Dickson DW, Petrucelli L (2009): **Aberrant cleavage of TDP-43 enhances aggregation and cellular toxicity**. *Proc Natl Acad Sci U S A*, **106**(18):7607-7612.

271. Pollitt SK, Pallos J, Shao J, Desai UA, Ma AA, Thompson LM, Marsh JL, Diamond MI (2003): **A rapid cellular FRET assay of polyglutamine aggregation identifies a novel inhibitor**. *Neuron*, **40**(4):685-694.

272. Palla G, Derenyi I, Farkas I, Vicsek T (2005): **Uncovering the overlapping community structure of complex networks in nature and society**. *Nature*, **435**(7043):814-818.

273. Abhyankar MM, Urekar C, Reddi PP (2007): **A novel CpG-free vertebrate insulator silences the testis-specific SP-10 gene in somatic tissues: role for TDP-43 in insulator function**. *J Biol Chem*, **282**(50):36143-36154.

274. Brehm A, Miska EA, McCance DJ, Reid JL, Bannister AJ, Kouzarides T (1998): **Retinoblastoma protein recruits histone deacetylase to repress transcription**. *Nature*, **391**(6667):597-601.

275. Kingston RE, Baldwin AS, Jr., Sharp PA (1984): **Regulation of heat shock protein 70 gene expression by c-myc**. *Nature*, **312**(5991):280-282.

276. Magnaghi-Jaulin L, Groisman R, Naguibneva I, Robin P, Lorain S, Le Villain JP, Troalen F, Trouche D, Harel-Bellan A (1998): **Retinoblastoma protein represses transcription by recruiting a histone deacetylase**. *Nature*, **391**(6667):601-605.

277. Olave I, Wang W, Xue Y, Kuo A, Crabtree GR (2002): **Identification of a polymorphic, neuron-specific chromatin remodeling complex**. *Genes Dev*, **16**(19):2509-2517.

278. Qiu Z, Ghosh A (2008): **A calcium-dependent switch in a CREST-BRG1 complex regulates activity-dependent gene expression**. *Neuron*, **60**(5):775-787.

279. Seo S, Richardson GA, Kroll KL (2005): **The SWI/SNF chromatin remodeling protein Brg1 is required for vertebrate neurogenesis and mediates transactivation of Ngn and NeuroD**. *Development*, **132**(1):105-115.

280. Zeng W, Ball AR, Jr., Yokomori K (2010): **HP1: heterochromatin binding proteins working the genome**. *Epigenetics*, **5**(4):287-292.

281. Adhikary S, Eilers M (2005): **Transcriptional regulation and transformation by Myc proteins**. *Nat Rev Mol Cell Biol*, **6**(8):635-645.

282. Cole MD, Nikiforov MA (2006): **Transcriptional activation by the Myc oncoprotein**. *Curr Top Microbiol Immunol*, **302**:33-50.

283. Oskarsson T, Trumpp A (2005): **The Myc trilogy: lord of RNA polymerases**. *Nat Cell Biol*, **7**(3):215-217.

284. Laherty CD, Yang WM, Sun JM, Davie JR, Seto E, Eisenman RN (1997): **Histone deacetylases associated with the mSin3 corepressor mediate mad transcriptional repression**. *Cell*, **89**(3):349-356.

285. Fiesel FC, Voigt A, Weber SS, Van den Haute C, Waldenmaier A, Gorner K, Walter M, Anderson ML, Kern JV, Rasse TM, Schmidt T, Springer W, Kirchner R, Bonin M, Neumann M, Baekelandt V, Alunni-Fabbroni M, Schulz JB, Kahle PJ (2010): **Knockdown of transactive response DNA-binding protein (TDP-43) downregulates histone deacetylase 6**. *Embo J*, **29**(1):209-221.

286. Hubbert C, Guardiola A, Shao R, Kawaguchi Y, Ito A, Nixon A, Yoshida M, Wang XF, Yao TP (2002): **HDAC6 is a microtubule-associated deacetylase**. *Nature*, **417**(6887):455-458.

287. Seigneurin-Berny D, Verdel A, Curtet S, Lemercier C, Garin J, Rousseaux S, Khochbin S (2001): **Identification of components of the murine histone deacetylase 6 complex: link between acetylation and ubiquitination signaling pathways**. *Mol Cell Biol*, **21**(23):8035-8044.

288. Diaz-Hernandez M, Moreno-Herrero F, Gomez-Ramos P, Moran MA, Ferrer I, Baro AM, Avila J, Hernandez F, Lucas JJ (2004): **Biochemical, ultrastructural, and reversibility studies on huntingtin filaments isolated from mouse and human brain**. *J Neurosci*, **24**(42):9361-9371.

289. Noguchi A, Matsumura S, Dezawa M, Tada M, Yanazawa M, Ito A, Akioka M, Kikuchi S, Sato M, Ideno S, Noda M, Fukunari A, Muramatsu S, Itokazu Y, Sato K, Takahashi H, Teplow DB, Nabeshima Y, Kakita A, Imahori K, Hoshi M (2009): **Isolation and characterization of patient-derived, toxic, high mass amyloid beta-protein (Abeta) assembly from Alzheimer disease brains**. *J Biol Chem*, **284**(47):32895-32905.

290. Lee JY, Nagano Y, Taylor JP, Lim KL, Yao TP (2010): **Disease-causing mutations in parkin impair mitochondrial ubiquitination, aggregation, and HDAC6-dependent mitophagy**. *J Cell Biol*, **189**(4):671-679.

291. Thomas SN, Cripps D, Yang AJ (2009): **Proteomic analysis of protein phosphorylation and ubiquitination in Alzheimer's disease**. *Methods Mol Biol*, **566**:109-121.

292. Harris H, Rubinsztein DC (2011): **Control of autophagy as a therapy for neurodegenerative disease**. *Nat Rev Neurol*, **8**(2):108-117.

293. Salminen A, Ojala J, Kaarniranta K, Hiltunen M, Soininen H (2011): **Hsp90 regulates tau pathology through co-chaperone complexes in Alzheimer's disease**. *Prog Neurobiol*, **93**(1):99-110.

294. Wacker JL, Huang SY, Steele AD, Aron R, Lotz GP, Nguyen Q, Giorgini F, Roberson ED, Lindquist S, Masliah E, Muchowski PJ (2009): **Loss of Hsp70 exacerbates pathogenesis but not levels of fibrillar aggregates in a mouse model of Huntington's disease**. *J Neurosci*, **29**(28):9104-9114.

295. Graham RK, Deng Y, Slow EJ, Haigh B, Bissada N, Lu G, Pearson J, Shehadeh J, Bertram L, Murphy Z, Warby SC, Doty CN, Roy S, Wellington CL, Leavitt BR, Raymond LA, Nicholson DW, Hayden MR (2006): **Cleavage at the caspase-6 site is required for neuronal dysfunction and degeneration due to mutant huntingtin**. *Cell*, **125**(6):1179-1191.

296. Li M, Ona VO, Guegan C, Chen M, Jackson-Lewis V, Andrews LJ, Olszewski AJ, Stieg PE, Lee JP, Przedborski S, Friedlander RM (2000): **Functional role of caspase-1 and caspase-3 in an ALS transgenic mouse model**. *Science*, **288**(5464):335-339.

297. Goold R, Hubank M, Hunt A, Holton J, Menon RP, Revesz T, Pandolfo M, Matilla-Duenas A (2007): **Down-regulation of the dopamine receptor D2 in mice lacking ataxin 1**. *Hum Mol Genet*, **16**(17):2122-2134.

298. Matilla A, Koshy BT, Cummings CJ, Isobe T, Orr HT, Zoghbi HY (1997): **The cerebellar leucine-rich acidic nuclear protein interacts with ataxin-1**. *Nature*, **389**(6654):974-978.

299. Mizutani A, Wang L, Rajan H, Vig PJ, Alaynick WA, Thaler JP, Tsai CC (2005): **Boat, an AXH domain protein, suppresses the cytotoxicity of mutant ataxin-1**. *Embo J*, **24**(18):3339-3351.

300. Okuda T, Hattori H, Takeuchi S, Shimizu J, Ueda H, Palvimo JJ, Kanazawa I, Kawano H, Nakagawa M, Okazawa H (2003): **PQBP-1 transgenic mice show a late-onset motor neuron disease-like phenotype**. *Hum Mol Genet*, **12**(7):711-725.

301. Tsai CC, Kao HY, Mitzutani A, Banayo E, Rajan H, McKeown M, Evans RM (2004): **Ataxin 1, a SCA1 neurodegenerative disorder protein, is functionally linked to the silencing mediator of retinoid and thyroid hormone receptors**. *Proc Natl Acad Sci U S A*, **101**(12):4047-4052.

302. Tsuda H, Jafar-Nejad H, Patel AJ, Sun Y, Chen HK, Rose MF, Venken KJ, Botas J, Orr HT, Bellen HJ, Zoghbi HY (2005): **The AXH domain of Ataxin-1 mediates neurodegeneration through its interaction with Gfi-1/Senseless proteins**. *Cell*, **122**(4):633-644.

303. Guo W, Chen Y, Zhou X, Kar A, Ray P, Chen X, Rao EJ, Yang M, Ye H, Zhu L, Liu J, Xu M, Yang Y, Wang C, Zhang D, Bigio EH, Mesulam M, Shen Y, Xu Q, Fushimi K, Wu JY (2011): **An ALS-associated mutation affecting TDP-43 enhances protein aggregation, fibril formation and neurotoxicity**. *Nat Struct Mol Biol*, **18**(7):822-830.

304. Nonaka T, Kametani F, Arai T, Akiyama H, Hasegawa M (2009): **Truncation and pathogenic mutations facilitate the formation of intracellular aggregates of TDP-43**. *Hum Mol Genet*, **18**(18):3353-3364.

305. Liachko NF, Guthrie CR, Kraemer BC (2010): **Phosphorylation promotes neurotoxicity in a Caenorhabditis elegans model of TDP-43 proteinopathy**. *J Neurosci*, **30**(48):16208-16219.

306. Wegorzewska I, Bell S, Cairns NJ, Miller TM, Baloh RH (2009): **TDP-43 mutant transgenic mice develop features of ALS and frontotemporal lobar degeneration**. *Proc Natl Acad Sci U S A*, **106**(44):18809-18814.

307. Zhou H, Huang C, Chen H, Wang D, Landel CP, Xia PY, Bowser R, Liu YJ, Xia XG (2010): **Transgenic rat model of neurodegeneration caused by mutation in the TDP gene**. *PLoS Genet*, **6**(3):e1000887.

308. Urushitani M, Sato T, Bamba H, Hisa Y, Tooyama I (2010): **Synergistic effect between proteasome and autophagosome in the clearance of polyubiquitinated TDP-43**. *J Neurosci Res*, **88**(4):784-797.

309. Wang X, Fan H, Ying Z, Li B, Wang H, Wang G (2010): **Degradation of TDP-43 and its pathogenic form by autophagy and the ubiquitin-proteasome system**. *Neurosci Lett*, **469**(1):112-116.

310. Caccamo A, Majumder S, Deng JJ, Bai Y, Thornton FB, Oddo S (2009): **Rapamycin rescues TDP-43 mislocalization and the associated low molecular mass neurofilament instability**. *J Biol Chem*, **284**(40):27416-27424.

311. Gomes C, Escrevente C, Costa J (2010): **Mutant superoxide dismutase 1 overexpression in NSC-34 cells: effect of trehalose on aggregation, TDP-43 localization and levels of co-expressed glycoproteins**. *Neurosci Lett*, **475**(3):145-149.

312. Brady OA, Meng P, Zheng Y, Mao Y, Hu F (2010): **Regulation of TDP-43 aggregation by phosphorylation and p62/SQSTM1**. *J Neurochem*, **116**(2):248-259.

313. Nakamura M, Kaneko S, Wate R, Asayama S, Nakamura Y, Fujita K, Ito H, Kusaka H (2012): **Regionally different immunoreactivity for Smurf2 and pSmad2/3 in TDP-43-positive inclusions of amyotrophic lateral sclerosis**. *Neuropathol Appl Neurobiol*.

314. Kawaguchi Y, Kovacs JJ, McLaurin A, Vance JM, Ito A, Yao TP (2003): **The deacetylase HDAC6 regulates aggresome formation and cell viability in response to misfolded protein stress**. *Cell*, **115**(6):727-738.

315. Kopito RR (2000): **Aggresomes, inclusion bodies and protein aggregation**. *Trends Cell Biol*, **10**(12):524-530.

316. Garcia-Mata R, Gao YS, Sztul E (2002): **Hassles with taking out the garbage: aggravating aggresomes**. *Traffic*, **3**(6):388-396.

317. McNaught KS, Shashidharan P, Perl DP, Jenner P, Olanow CW (2002): **Aggresome-related biogenesis of Lewy bodies**. *Eur J Neurosci*, **16**(11):2136-2148.

318. Garcia-Mata R, Bebok Z, Sorscher EJ, Sztul ES (1999): **Characterization and dynamics of aggresome formation by a cytosolic GFP-chimera**. *J Cell Biol*, **146**(6):1239-1254.

319. Johnston JA, Ward CL, Kopito RR (1998): **Aggresomes: a cellular response to misfolded proteins**. *J Cell Biol*, **143**(7):1883-1898.

320. Fiesel FC, Schurr C, Weber SS, Kahle PJ (2011): **TDP-43 knockdown impairs neurite outgrowth dependent on its target histone deacetylase 6**. *Mol Neurodegener*, **6**:64.

321. Kim SH, Shanware NP, Bowler MJ, Tibbetts RS (2010): **Amyotrophic lateral sclerosis-associated proteins TDP-43 and FUS/TLS function in a common biochemical complex to co-regulate HDAC6 mRNA**. *J Biol Chem*, **285**(44):34097-34105.

322. McCullough J, Clague MJ, Urbe S (2004): **AMSH is an endosome-associated ubiquitin isopeptidase**. *J Cell Biol*, **166**(4):487-492.

323. Ishii N, Owada Y, Yamada M, Miura S, Murata K, Asao H, Kondo H, Sugamura K (2001): **Loss of neurons in the hippocampus and cerebral cortex of AMSH-deficient mice**. *Mol Cell Biol*, **21**(24):8626-8637.

324. Suzuki S, Tamai K, Watanabe M, Kyuuma M, Ono M, Sugamura K, Tanaka N (2011): **AMSH is required to degrade ubiquitinated proteins in the central nervous system**. *Biochem Biophys Res Commun*, **408**(4):582-588.

325. Tradewell ML, Yu Z, Tibshirani M, Boulanger MC, Durham HD, Richard S (2011): **Arginine methylation by PRMT1 regulates nuclear-cytoplasmic localization and toxicity of FUS/TLS harbouring ALS-linked mutations**. *Hum Mol Genet*, **21**(1):136-149.

326. Bedford MT, Clarke SG (2009): **Protein arginine methylation in mammals: who, what, and why**. *Mol Cell*, **33**(1):1-13.

327. Freemont PS (2000): **RING for destruction?** *Curr Biol*, **10**(2):R84-87.

328. Joazeiro CA, Weissman AM (2000): **RING finger proteins: mediators of ubiquitin ligase activity**. *Cell*, **102**(5):549-552.

329. Lorick KL, Jensen JP, Fang S, Ong AM, Hatakeyama S, Weissman AM (1999): **RING fingers mediate ubiquitin-conjugating enzyme (E2)-dependent ubiquitination**. *Proc Natl Acad Sci U S A*, **96**(20):11364-11369.

330. Sannerud R, Declerck I, Peric A, Raemaekers T, Menendez G, Zhou L, Veerle B, Coen K, Munck S, De Strooper B, Schiavo G, Annaert W (2011): **ADP ribosylation factor 6 (ARF6) controls amyloid precursor protein (APP) processing by mediating the endosomal sorting of BACE1**. *Proc Natl Acad Sci U S A*, **108**(34):E559-568.

331. Moreau K, Ravikumar B, Puri C, Rubinsztein DC (2012): **Arf6 promotes autophagosome formation via effects on phosphatidylinositol 4,5-bisphosphate and phospholipase D**. *J Cell Biol*, **196**(4):483-496.

332. Bilen J, Bonini NM (2007): **Genome-wide screen for modifiers of ataxin-3 neurodegeneration in Drosophila**. *PLoS Genet*, **3**(10):1950-1964.

333. Cooper AA, Gitler AD, Cashikar A, Haynes CM, Hill KJ, Bhullar B, Liu K, Xu K, Strathearn KE, Liu F, Cao S, Caldwell KA, Caldwell GA, Marsischky G, Kolodner RD, Labaer J, Rochet JC, Bonini NM, Lindquist S (2006): **Alpha-synuclein blocks ER-Golgi traffic and Rab1 rescues neuron loss in Parkinson's models**. *Science*, **313**(5785):324-328.

334. Fernandez-Funez P, Nino-Rosales ML, de Gouyon B, She WC, Luchak JM, Martinez P, Turiegano E, Benito J, Capovilla M, Skinner PJ, McCall A, Canal I, Orr HT, Zoghbi HY, Botas J (2000): **Identification of genes that modify ataxin-1-induced neurodegeneration**. *Nature*, **408**(6808):101-106.

335. Kraemer BC, Burgess JK, Chen JH, Thomas JH, Schellenberg GD (2006): **Molecular pathways that influence human tau-induced pathology in Caenorhabditis elegans**. *Hum Mol Genet*, **15**(9):1483-1496.

336. Latouche M, Lasbleiz C, Martin E, Monnier V, Debeir T, Mouatt-Prigent A, Muriel MP, Morel L, Ruberg M, Brice A, Stevanin G, Tricoire H (2007): **A conditional pan-neuronal Drosophila model of spinocerebellar ataxia 7 with a reversible adult phenotype suitable for identifying modifier genes**. *J Neurosci*, **27**(10):2483-2492.

337. Wang J, Farr GW, Hall DH, Li F, Furtak K, Dreier L, Horwich AL (2009): **An ALS-linked mutant SOD1 produces a locomotor defect associated with aggregation and synaptic dysfunction when expressed in neurons of Caenorhabditis elegans**. *PLoS Genet*, **5**(1):e1000350.

338. Teuling E, Bourgonje A, Veenje S, Thijssen K, de Boer J, van der Velde J, Swertz M, Nollen E (2011): **Modifiers of mutant huntingtin aggregation: functional conservation of C. elegans-modifiers of polyglutamine aggregation**. *PLoS Curr*, **3**:RRN1255.

339. Elden AC, Kim HJ, Hart MP, Chen-Plotkin AS, Johnson BS, Fang X, Armakola M, Geser F, Greene R, Lu MM, Padmanabhan A, Clay-Falcone D, McCluskey L, Elman L, Juhr D, Gruber PJ, Rub U, Auburger G, Trojanowski JQ, Lee VM, Van Deerlin VM, Bonini NM,

Gitler AD (2010): **Ataxin-2 intermediate-length polyglutamine expansions are associated with increased risk for ALS**. *Nature*, **466**(7310):1069-1075.

340. Glisovic T, Bachorik JL, Yong J, Dreyfuss G (2008): **RNA-binding proteins and post-transcriptional gene regulation**. *FEBS Lett*, **582**(14):1977-1986.

341. Feiguin F, Godena VK, Romano G, D'Ambrogio A, Klima R, Baralle FE (2009): **Depletion of TDP-43 affects Drosophila motoneurons terminal synapsis and locomotive behavior**. *FEBS Lett*, **583**(10):1586-1592.

342. Kraemer BC, Schuck T, Wheeler JM, Robinson LC, Trojanowski JQ, Lee VM, Schellenberg GD (2010): **Loss of murine TDP-43 disrupts motor function and plays an essential role in embryogenesis**. *Acta Neuropathol*, **119**(4):409-419.

343. Tsai KJ, Yang CH, Fang YH, Cho KH, Chien WL, Wang WT, Wu TW, Lin CP, Fu WM, Shen CK (2010): **Elevated expression of TDP-43 in the forebrain of mice is sufficient to cause neurological and pathological phenotypes mimicking FTLD-U**. *J Exp Med*, **207**(8):1661-1673.

344. Wils H, Kleinberger G, Janssens J, Pereson S, Joris G, Cuijt I, Smits V, Ceuterick-de Groote C, Van Broeckhoven C, Kumar-Singh S (2010): **TDP-43 transgenic mice develop spastic paralysis and neuronal inclusions characteristic of ALS and frontotemporal lobar degeneration**. *Proc Natl Acad Sci U S A*, **107**(8):3858-3863.

345. Xu YF, Gendron TF, Zhang YJ, Lin WL, D'Alton S, Sheng H, Casey MC, Tong J, Knight J, Yu X, Rademakers R, Boylan K, Hutton M, McGowan E, Dickson DW, Lewis J, Petrucelli L (2010): **Wild-type human TDP-43 expression causes TDP-43 phosphorylation, mitochondrial aggregation, motor deficits, and early mortality in transgenic mice**. *J Neurosci*, **30**(32):10851-10859.

346. Buratti E, Baralle FE (2009): **The molecular links between TDP-43 dysfunction and neurodegeneration**. *Adv Genet*, **66**:1-34.

347. Budini M, Buratti E (2011): **TDP-43 autoregulation: implications for disease**. *J Mol Neurosci*, **45**(3):473-479.

348. Chen-Plotkin AS, Geser F, Plotkin JB, Clark CM, Kwong LK, Yuan W, Grossman M, Van Deerlin VM, Trojanowski JQ, Lee VM (2008): **Variations in the progranulin gene affect global gene expression in frontotemporal lobar degeneration**. *Hum Mol Genet*, **17**(10):1349-1362.

349. Mishra M, Paunesku T, Woloschak GE, Siddique T, Zhu LJ, Lin S, Greco K, Bigio EH (2007): **Gene expression analysis of frontotemporal lobar degeneration of the motor neuron disease type with ubiquitinated inclusions**. *Acta Neuropathol*, **114**(1):81-94.

350. Gitcho MA, Bigio EH, Mishra M, Johnson N, Weintraub S, Mesulam M, Rademakers R, Chakraverty S, Cruchaga C, Morris JC, Goate AM, Cairns NJ (2009): **TARDBP 3'-UTR variant in autopsy-confirmed frontotemporal lobar degeneration with TDP-43 proteinopathy**. *Acta Neuropathol*, **118**(5):633-645.

351. Ayyanathan K, Lechner MS, Bell P, Maul GG, Schultz DC, Yamada Y, Tanaka K, Torigoe K, Rauscher FJ, 3rd (2003): **Regulated recruitment of HP1 to a euchromatic gene induces mitotically heritable, epigenetic gene silencing: a mammalian cell culture model of gene variegation**. *Genes Dev*, **17**(15):1855-1869.

352. Braunstein M, Rose AB, Holmes SG, Allis CD, Broach JR (1993): **Transcriptional silencing in yeast is associated with reduced nucleosome acetylation**. *Genes Dev*, **7**(4):592-604.

353. Li Y, Danzer JR, Alvarez P, Belmont AS, Wallrath LL (2003): **Effects of tethering HP1 to euchromatic regions of the Drosophila genome**. *Development*, **130**(9):1817-1824.

354. Zhang HS, Gavin M, Dahiya A, Postigo AA, Ma D, Luo RX, Harbour JW, Dean DC (2000): **Exit from G1 and S phase of the cell cycle is regulated by repressor complexes containing HDAC-Rb-hSWI/SNF and Rb-hSWI/SNF**. *Cell*, **101**(1):79-89.

355. Aiken CT, Tobin AJ, Schweitzer ES (2004): **A cell-based screen for drugs to treat Huntington's disease**. *Neurobiol Dis*, **16**(3):546-555.

356. Yang C, Tan W, Whittle C, Qiu L, Cao L, Akbarian S, Xu Z (2010): **The C-terminal TDP-43 fragments have a high aggregation propensity and harm neurons by a dominant-negative mechanism**. *PLoS One*, **5**(12):e15878.

357. Collas P (2010): **The current state of chromatin immunoprecipitation**. *Mol Biotechnol*, **45**(1):87-100.

358. Biedler JL, Roffler-Tarlov S, Schachner M, Freedman LS (1978): **Multiple neurotransmitter synthesis by human neuroblastoma cell lines and clones**. *Cancer Res*, **38**(11 Pt 1):3751-3757.

359. Schweigerer L, Breit S, Wenzel A, Tsunamoto K, Ludwig R, Schwab M (1990): **Augmented *MYCN* expression advances the malignant phenotype of human neuroblastoma cells: Evidence for induction of autocrine growth factor activity**. *Cancer Res*, **50**:4411-4416.

360. Grelle G, Kostka S, Otto A, Kersten B, Genser KF, Muller EC, Walter S, Boddrich A, Stelzl U, Hanig C, Volkmer-Engert R, Landgraf C, Alberti S, Hohfeld J, Strodicke M, Wanker EE (2006): **Identification of VCP/p97, carboxyl terminus of Hsp70-interacting protein (CHIP), and amphiphysin II interaction partners using membrane-based human proteome arrays**. *Mol Cell Proteomics*, **5**(2):234-244.

361. Simpson JC, Wellenreuther R, Poustka A, Pepperkok R, Wiemann S (2000): **Systematic subcellular localization of novel proteins identified by large-scale cDNA sequencing**. *EMBO Rep*, **1**(3):287-292.

362. Higuchi R, Dollinger G, Walsh PS, Griffith R (1992): **Simultaneous amplification and detection of specific DNA sequences**. *Biotechnology (N Y)*, **10**(4):413-417.

363. Lee LG, Connell CR, Bloch W (1993): **Allelic discrimination by nick-translation PCR with fluorogenic probes**. *Nucleic Acids Res*, **21**(16):3761-3766.

364. Laemmli UK (1970): **Cleavage of structural proteins during the assembly of the head of bacteriophage T4**. *Nature*, **227**(5259):680-685.

365. Abraham VC, Taylor DL, Haskins JR (2004): **High content screening applied to large-scale cell biology**. *Trends Biotechnol*, **22**(1):15-22.

366. Fields S, Song O (1989): **A novel genetic system to detect protein-protein interactions**. *Nature*, **340**(6230):245-246.

367. Perez-Iratxeta C, Wjst M, Bork P, Andrade MA (2005): **G2D: a tool for mining genes associated with disease**. *BMC Genet*, **6**:45.

368. Wishart DS, Knox C, Guo AC, Shrivastava S, Hassanali M, Stothard P, Chang Z, Woolsey J (2006): **DrugBank: a comprehensive resource for in silico drug discovery and exploration**. *Nucleic Acids Res*, **34**(Database issue):D668-672.

369. Campillos M, Kuhn M, Gavin AC, Jensen LJ, Bork P (2008): **Drug target identification using side-effect similarity**. *Science*, **321**(5886):263-266.

370. Fontaine JF, Priller F, Barbosa-Silva A, Andrade-Navarro MA (2011): **Genie: literature-based gene prioritization at multi genomic scale**. *Nucleic Acids Res*, **39**(Web Server issue):W455-461.

371. Chaurasia G, Futschik M (2012): **The integration and annotation of the human interactome in the UniHI Database**. *Methods Mol Biol*, **812**:175-188.

372. Chaurasia G, Iqbal Y, Hanig C, Herzel H, Wanker EE, Futschik ME (2007): **UniHI: an entry gate to the human protein interactome**. *Nucleic Acids Res*, **35**(Database issue):D590-594.

373. Chaurasia G, Malhotra S, Russ J, Schnoegl S, Hanig C, Wanker EE, Futschik ME (2009): **UniHI 4: new tools for query, analysis and visualization of the human protein-protein interactome**. *Nucleic Acids Res*, **37**(Database issue):D657-660.

374. Snel B, Lehmann G, Bork P, Huynen MA (2000): **STRING: a web-server to retrieve and display the repeatedly occurring neighbourhood of a gene**. *Nucleic Acids Res*, **28**(18):3442-3444.

375. Lu T, Pan Y, Kao SY, Li C, Kohane I, Chan J, Yankner BA (2004): **Gene regulation and DNA damage in the ageing human brain**. *Nature*, **429**(6994):883-891.

376. Schlicker A, Lengauer T, Albrecht M (2010): **Improving disease gene prioritization using the semantic similarity of Gene Ontology terms**. *Bioinformatics*, **26**(18):i561-567.

377. Raghavachari B, Tasneem A, Przytycka TM, Jothi R (2008): **DOMINE: a database of protein domain interactions**. *Nucleic Acids Res*, **36**(Database issue):D656-661.

378. Yellaboina S, Tasneem A, Zaykin DV, Raghavachari B, Jothi R (2011): **DOMINE: a comprehensive collection of known and predicted domain-domain interactions**. *Nucleic Acids Res*, **39**(Database issue):D730-735.

379. Su AI, Wiltshire T, Batalov S, Lapp H, Ching KA, Block D, Zhang J, Soden R, Hayakawa M, Kreiman G, Cooke MP, Walker JR, Hogenesch JB (2004): **A gene atlas of the mouse and human protein-encoding transcriptomes**. *Proc Natl Acad Sci U S A*, **101**(16):6062-6067.

380. Langfelder P, Horvath S (2008): **WGCNA: an R package for weighted correlation network analysis**. *BMC Bioinformatics*, **9**:559.

381. Zhang B, Horvath S (2005): **A general framework for weighted gene co-expression network analysis**. *Stat Appl Genet Mol Biol*, **4**:Article17.

382. Persico M, Ceol A, Gavrila C, Hoffmann R, Florio A, Cesareni G (2005): **HomoMINT: an inferred human network based on orthology mapping of protein interactions discovered in model organisms**. *BMC Bioinformatics*, **6 Suppl 4**:S21.

383. Brown KR, Jurisica I (2005): **Online predicted human interaction database**. *Bioinformatics*, **21**(9):2076-2082.

384. Lehner B, Fraser AG (2004): **A first-draft human protein-interaction map**. *Genome Biol*, **5**(9):R63.

385. Schaefer MH, Fontaine JF, Vinayagam A, Porras P, Wanker EE, Andrade-Navarro MA (2012): **HIPPIE: Integrating protein interaction networks with experiment based quality scores**. *PLoS One*, **In press**.

386. Hosack DA, Dennis G, Jr., Sherman BT, Lane HC, Lempicki RA (2003): **Identifying biological themes within lists of genes with EASE**. *Genome Biol*, **4**(10):R70.

387. Maere S, Heymans K, Kuiper M (2005): **BiNGO: a Cytoscape plugin to assess overrepresentation of gene ontology categories in biological networks**. *Bioinformatics*, **21**(16):3448-3449.

388. Lupas A, Van Dyke M, Stock J (1991): **Predicting coiled coils from protein sequences**. *Science*, **252**(5009):1162-1164.

389. Prilusky J, Felder CE, Zeev-Ben-Mordehai T, Rydberg EH, Man O, Beckmann JS, Silman I, Sussman JL (2005): **FoldIndex: a simple tool to predict whether a given protein sequence is intrinsically unfolded**. *Bioinformatics*, **21**(16):3435-3438.

390. Rebhan M, Chalifa-Caspi V, Prilusky J, Lancet D (1997): **GeneCards: integrating information about genes, proteins and diseases**. *Trends Genet*, **13**(4):163.

391. Bertram L, McQueen MB, Mullin K, Blacker D, Tanzi RE (2007): **Systematic meta-analyses of Alzheimer disease genetic association studies: the AlzGene database**. *Nat Genet*, **39**(1):17-23.

392. Wishart DS (2007): **Discovering drug targets through the web**. *Comp Biochem Physiol Part D Genomics Proteomics*, **2**(1):9-17.

393. David DC, Ollikainen N, Trinidad JC, Cary MP, Burlingame AL, Kenyon C (2010): **Widespread protein aggregation as an inherent part of aging in C. elegans**. *PLoS Biol*, **8**(8):e1000450.

Selbstständigkeitserklärung

Hiermit erkläre ich, die vorliegende Arbeit selbstständig ohne fremde Hilfe verfasst und nur die angegebene Literatur und Hilfsmittel verwendet zu haben.

Jenny Russ

8. Mai 2012